SYNTHESIS AND EVALUATION OF BIOACTIVABLE NITRIC OXIDE (NO) DONORS

A THESIS

SUBMITTED IN PARTIAL FULFILMENT OF THE

REQUIREMENTS

OF THE DEGREE OF

DOCTOR OF PHILOSOPHY

BY

KAVITA SHARMA

20103069

INDIAN INSTITUTE OF SCIENCE EDUCATION AND RESEARCH PUNE – 411 008

2015

भारतीयविज्ञानशिक्षाएवंअनुसंधानसंस्थान, पुणे
INDIAN INSTITUTE OF SCIENCE EDUCATION AND RESEARCH (IISER), PUNE
(An Autonomous Institution, Ministry of Human Resource Development, Govt. of India)
900 NCL Innovation Park Dr Homi Bhabha Road Pune 411008

Harinath Chakrapani, Ph.D.
Assistant Professor – Chemistry
www.iiserpune.ac.in/~harinath/

CERTIFICATE

Certified that, the work incorporated in the thesis entitled, "***Synthesis and Evaluation of Bioactivable Nitric Oxide (NO) Donors***" submitted by ***Kavita Sharma*** was carried out by the candidate, under my supervision. The work presented here or any part of it has not been included in any other thesis submitted previously for the award of any degree or diploma from any other University or institution.

Date: 28th October 2015 **Dr. Harinath Chakrapani**

Pune (MH), India.

DECLARATION

I declare that this written submission represents my ideas in my own words and where others' ideas have been included; I have adequately cited and referenced the original sources. I also declare that I have adhered to all principles of academic honesty and integrity and have not misrepresented or fabricated or falsified any idea/data/fact/source in my submission. I understand that violation of the above will be cause for disciplinary action by the Institute and can also evoke penal action from the sources which have thus not been properly cited or from whom proper permission has not been taken when needed.

Date: 28th October 2015 **Kavita Sharma**

Pune (MH), India. **20103069**

Table of Contents

General remarks

- ^{1}H NMR spectra were recorded on JEOL ECX 400 MHz spectrometer using tetramethylsilane (TMS) as an internal standard. Chemical shifts are expressed in ppm units downfield to TMS.
- ^{13}C NMR spectra were recorded on JEOL ECX 100 MHz spectrometer.
- Mass spectra were obtained using HRMS-ESI-Q-Time of Flight LC-MS (Synapt G2, Waters) or MALDI TOF/TOF Analyser (Applied Biosystems 4800 Plus).
- FT-IR spectra were obtained using NICOLET 6700 FT-IR spectrophotometer as KBr disc or Bruker Alpha-FT-IR spectrometer and reported in cm^{-1}.
- All reactions were monitored by Thin-Layer Chromatography carried out on precoated Merck silica plates (F254, 0.25 mm thickness); compounds were visualized by UV light.
- All reactions were carried out under nitrogen or argon atmosphere with freshly dried solvents under anhydrous conditions and yields refer to chromatographically homogenous materials unless otherwise stated.
- All evaporators were carried out under reduced pressure on Büchi and Heildoph rotary evaporator below 45 °C unless otherwise specified.
- Silica gel (60-120) and (100-200) mesh were used for column chromatography.
- Materials were obtained from commercial suppliers and were used without further purification.
- Semi-preparative HPLC purification was performed using high performance liquid chromatography (HPLC), Dionex ICS-3000 model.
- HPLC analysis data was obtained using Agilent Technologies 1260 Infinity, C18 (5 μm, 4.6 × 250 mm).
- NO was detected using Sievers Nitric Oxide Analyzer (NOA 280i).
- Spectrophotometric and fluorimetric measurements were performed using Thermo Scientific Varioscan microwell plate reader.
- Cyclic voltammetry (CV) analysis was performed using a Basi Epsilon-EC-Ver 2.00.71-USB Bioanalytical systems.
- Scheme, Figure and Compound numbers in abstract and individual chapters are different.

Abbreviations

ACN – Acetonitrile

AcOH – Acetic acid

Ac_2O – Acetic anhydride

ADEPT – Antibody Directed Enzyme Prodrug Therapy

alloc – Allyloxy carbonyl

au – Arbitrary unit

BH_4 – Biopterin

bs – Broad singlet

^tBuOH – Tertiary-butanol

Bu_3SnH – Tributyl tin hydride

Calcd – Calculated

CaM – Calmodulin

$CDCl_3$ – Chloroform-D

$CHCl_3$ – Chloroform

$Cu(OAc)_2$ – Copper acetate

CV – Cyclic voltammetry

DAPI – 4', 6-Diamidino-2-phenylindole

dd – Doublet of doublet

DCM – Dichloromethane

DEPT – Directed Enzyme Prodrug Therapy

DIAD – Diisopropyl diazodicarboxylate

DMAP – *N*, *N*-Dimethylaminopyridine

DMEM – Dulbecco's Modified Eagle's Medium

DMF – *N*, *N*'-Dimethyl formamide

DMSO – Dimethyl sulfoxide

DNA – Deoxyribonucleic acid

DPBS – Dulbecco's Phosphate-Buffered Saline

dt – Doublet of triplet

DT-D – DT-Diaphorase

δ – Delta (in ppm)

E. coli – Escherichia coli

eq. – Equivalents

E_{Red} – Reduction potential

ESI – Electron spray ionization

EtOH – Ethanol

FACS – Fluorescence Activated Cell Sorting

FAD – Flavin-adenine-dinucleotide

FMN – Flavin-mononucleotide

g – Gram

GDEPT – Gene Directed Enzyme Prodrug Therapy

GSH – Glutathione

GS-T – Glutathione S-Transferase

h – Hours

HCl – Hydrochloric acid

HIF – Hypoxia Inducible Factor

H_2O – Water

HNO_3 – Nitric acid

HPLC – High performance liquid chromatography

HRMS – High-resolution mass spectrometry

Hz – Hertz

IC_{50} – Half maximal inhibitory concentration

IR – Infrared

J – Coupling constant

K_2CO_3 – Potassium carbonate

LB – Luria-Bertani

λ_{ex} – Excitation wavelength

λ_{em} – Emission wavelength

m – Multiplet

Me – Methyl

MeOH – Methanol

mg – Milligram

MIC – Minimum inhibitory concentration

min. – Minutes

MHz – Megahertz

mL – Millilitre

MMC – Mitomycin C

mM – Millimolar

mmol – Millimoles

m.p. – Melting point

MRP – Multidrug resistant proteins

MALDI – Matrix-Assisted Laser Desorption Ionization

M. smeg – Mycobacterium smegmatis

Mtb – Mycobacterium tuberculosis

MTT – 3-(4,5-Dimethylthiazol-2-yl)-2,5-diphenyltetrazolium bromide

µM – Micromolar

$NaBH_4$ – Sodium borohydride

NADPH – Reduced nicotinamide-adenine-dinucleotide phosphate

NaH – Sodium hydride

$NaHCO_3$ – Sodium bicarbonate

NaI – Sodium iodide

$NaIO_4$ – Sodium periodate

$NaNO_2$ – Sodium nitrite

Na_2SO_4 – Sodium sulphate

NH_4Cl – Ammonium chloride

n-BuLi – *n*-Butyllithium

NMO – *N*-Methyl morpholine *N*-oxide

NMR – Nuclear magnetic resonances

NO – Nitric oxide

NO^{2-} – Nitrite

NO^{3-} – Nitrate

NOA – Nitric oxide analyser

NOS – Nitric oxide synthase

nM – Nanomolar

NTR – Nitroreductase

OD – Optical density

$^{\bullet}OH$ – Hydroxyl radical

$O_2^{\bullet-}$ – Superoxide radical

$ONOO^-$ – Peroxynitrite

OsO_4 – Osmium tetraoxide

PBr_3 – Phosphorous tribromide

PBS – Phosphate buffered saline

Pd – Palladium

$Pd(OAc)_2$ – Palladium acetate

$Pd(PPh_3)$ – Tetrakis(triphenylphosphine)palladium(0)

pH – Potential of hydrogen

Ph – Phenyl

$POCl_3$ – Phosphorous oxychloride

PPh_3 – Triphenyl phosphine

Py – Pyridine

ppm – Parts per million

% – Per cent

RNS − Reactive nitrogen species

ROS – Reactive oxygen species

RPMI Medium – Roswell Park Memorial Institute Medium

RT – Room temperature

s – Singlet

SA – *Staphylococcus aureus*

SiO_2 – Silica

Sn – Tin

SNAP – *S*-Nitroso-*N*-acetylpenicillamine

t – Triplet

TEA - Triethylamine

THF – Tetrahydrofuran

TLC – Thin layer chromatography

TMS – Tetramethylsilane

TRIS – Tris(hydroxymethyl)aminomethane

µg – Microgram

µmol– Micromolar

µL – Microliter

Zn – Zinc

Acknowledgements

Writing "Acknowledgement" has been the toughest part of this thesis. It is difficult to thank each and everyone who have been and are in my life with very few words of gratitude.

I am lucky to be part of Dr. Harinath Chakrapani's lab and my sincere thanks to him for his faith in me. It has been nice time with him to walk through the field of science and research, which I alone wouldn't have dared to. His guidance helped me in reaching a milestone of my life. Time spent with him, Dr. Leelavati (his wife) and his daughters Ahana and Roshini, will be cherished always. I thank him from bottom of my heart for bringing out the best of me.

I would like to express my gratitude to RAC members Dr. Nithyanandhan (NCL Pune), Dr. Sudipta Basu (IISER Pune) and Dr. Kundan Sengupta for their valuable suggestions and feedback during RAC evaluations. I learnt biology experiments in collaboration with Dr. Kundan Sengupta's lab. I thank Aishwarya and Devika for giving their time and teaching me biology. I remember the group meetings we used to have alongwith Dr. Pinaki Talukdar's group. I thank Dr. Pinaki Talukdar for critically evaluating my presentations and giving useful suggestions. Special thanks for Dr. Hotha for his cheerful nature and giving his precious time by coming to lab trips. I thank all chemistry faculty members for their constant support and encouragement.

Special thanks to my labmates: Dr. Satish Malwal, Dr. A. T. Dharmaraja, Vinayak, Kundan, Ravi, Amogh, Preeti, Ajay, Dr. Viraj, Vignesh, Sankar, Abhijeet, Komal, Sharath, Charu, Abhishek and Shreyas. They all have made my life in IISER simpler, happier and memorable. It was fun working with my labmates. In IISER, I was fortunate to make good friends and I express my gratitude to all of them. Special thanks to students of Dr. Hotha and Dr. RGB in Lab 102. We worked together in lab, celebrated parties, arranged trips and we fought too. I thank Pooja, Swati (MALDI), Swati (HRMS), Naina, Deepali, Chinmay and Ganesh (UG lab) for helping in collecting compound data. I thank my batchmates, Rajesh, Mothukuri Ganesh, Sharad, Bapu, Kiran and Biplab, with whom I have spent good time.

Ashutosh, Harita, Shweta and Sumit thank you for your support and encouragement. I feel great to have best friends Tanpreet, Swati and Hema. I have spent best time with them taking lunch and talking about anything and everything. I owe special thanks to Shivaji. A special thanks to my Alchemist team members, it was really exciting to be with you all on the field and watching all the matches and our victory in IPL'2015.

I thank my all teachers, especially Mr. Bhasker Iyer (Army School, Ahmednagar) and Dr. Vijay Khanna (Ahmednagar College) for motivating me at all times for pursuing science. I thank Dr Partha Mukhopadhyay, Mr. Rajesh Bonagiri, Dr. Anil Despande and Mr. Sachin Kandalkar (Advinus Therapeutics Pvt. Ltd.) inspiring me to join IISER for PhD.

All these years I enjoyed my stay in Pune with my brother Rahul and my roommate Neeta. The bestest time has been spent with them fighting, shopping, eating, doing nothing, watching movies and lot more. Thanks to all my friends in Pune who have been around and supporting me. And last but not the least I thank my parents and family members for all their support, patience, blessings and endless love for me.

Kavita Sharma

****

ABSTRACT

Nitric oxide (NO) is an endogenously produced important biomolecule that is involved in various physiological processes that range from vasodialation to immunoregulation. NO alongwith other reactive nitrogen species react with majority of biomolecules (DNA, proteins and lipids) that leads to nitrosative and oxidative stress in cells. The induction of nitrosative and oxidative stress is an important component of immunogenic role of NO. Though, the immunogenic role of NO in containing pathogens and in controlling growth of cancer cells have been studied for long time but yet not fully characterized. In order to precisely study the role of NO inside cells, reliable sources of NO that can selectively enhance intracellular NO levels are required. Although numerous methodologies for NO delivery have been reported, they are associated with certain limitations such as lack of specificity and tunability, poor cell permeability and lack of a reporter for intracellular NO release. The work in this thesis describes different approaches for reliably enhancing NO inside cells in a site specific manner and also monitoring intracellular NO with reporter based NO donor.

For selective delivery of NO inside cells, firstly the bioreductive environment existing in cancer cells was exploited and enzyme activated NO donors which are substrates for bioreductive enzymes were synthesized. DT-Diaphorase (DT-D) is a bioreductive enzyme known to be over-expressed in certain solid tumors. Using indolequinone scaffold, INDQ/NO was designed and synthesized as a possible substrate for DT-D. INDQ/NO was found to be activated by DT-D to generate NO. Cellular assays revealed the capability of this compound to permeate cells to generate NO and damage DNA. Secondly, nitroreductase (NTR), a bacterial enzyme was chosen as a possible enzyme to activate NO donors. NTR has been extensively used in designing prodrugs for the directed enzyme prodrug therapies and is thus of therapeutic interest. 4-Nitrobenzyl based NO donors, possible substrates for NTR were synthesized and studied. These compounds were found to produce NO in the presence of NTR. The suitability of this compound to enhance NO within bacteria including mycobacteria was demonstrated. Current techniques to monitor NO inside cells depend solely on secondary assays. To

eliminate the need for secondary assays for detecting NO, we have developed a NTR-activated NO donor with a fluorescence reporter for NO. Lastly, for studying the possibilities of tunability of release, a new indole-based scaffold was designed, synthesized and release rates were studied. Using palladium as a chemical trigger that rapidly deprotects allyloxy carbonyl (alloc) group on indole scaffold, we found that the release rate could be modulated by simple structural modifications.

In summary, the results address important problems associated with site-specific delivery of NO but may find use for directed and tunable drug delivery as well. Also, these approaches may be used as tools to study mechanisms of NO in cellular stress responses.

Chapter 1: Introduction

1.1. Nitric oxide: History

Nitric oxide (NO), a diatomic gaseous molecule is the simplest stable nitrogen oxide with bond order of 2.5. With odd number of electrons, its reactivity is high. Discovered by Joseph Priestley in 1772, it was considered to be an air pollutant and a toxic gas for almost two centuries. In late 1970's it was discovered that NO was intrinsically involved in contraction and relaxation of blood vessels thus establishing it as the first gaseous signalling molecule.[1] This remarkable discovery was honoured with the Nobel Prize in field of Medicine and Physiology to Ferid Murad, Loius J. Ignarro and Robert F. Furchgott for discovering NO as major signalling molecule in the cardiovascular system.[2] Subsequently, extensive research started in order to explore the role of NO in physiological processes other than cardiovascular system. NO was found to play critical role in many of the physiological processes including nervous and immune system.

1.2. Biosynthesis of NO

NO is produced in nearly all the living cells and mediates numerous physiological processes. It is endogenously synthesized by two pathways: nitric oxide synthase (NOS)-dependent and NOS-independent pathway.[3] The major enzymatic pathway for NO production is during turnover of L-arginine to L-citrulline by NOS (Scheme 1.1).[4]

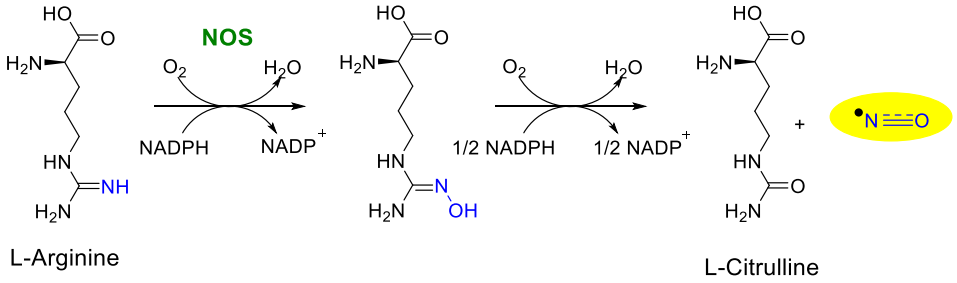

Scheme1.1. Biosynthesis of NO catalysed by NOS.

In mammalian cells, three different isoforms of NOS are present: endothelial NOS (*e*NOS), neuronal NOS (*n*NOS) and inducible NOS (*i*NOS).[5] The *e*NOS and *n*NOS are constitutively expressed in the endothelial cells and in the neuronal and peripheral cells,

respectively and release NO in nanomolar range. However, *i*NOS is expressed upon stimulation of immune cells and play important role in the immunity response. The NOS enzyme is a homodimer. Each monomer has two domains: a C-terminal reductase domain having binding sites for the cofactors: reduced nicotinamide-adenine-dinucleotide phosphate (NADPH), flavin-adenine-dinucleotide (FAD) and flavin-mononucleotide (FMN) and a *N*-terminal oxidase domain having binding site for the cofactors haem, biopterin (BH_4) and substrate L-arginine (Figure 1.1).[6] In a monomer, the flow of an electron starts from NADPH to FAD to FMN. The oxidase domain of unbound monomer is unable to bind to BH_4 and L-arginine and thus cannot generate NO alone. In the presence of haem, the two monomers dimerize and binding of sufficient amount of BH_4 and L-arginine leads to reduction of O_2 and generation of NO and L-citrulline as the by-product. For efficient flow of electrons between the inter-reductase domains of the dimer, binding of calmodulin (CaM) is necessary. One complete cycle of conversion of 1 mole of L-arginine to 1 mole of NO consumes 1.5 moles of NADPH and 2 moles of oxygen and generates one mole of L-citrulline.

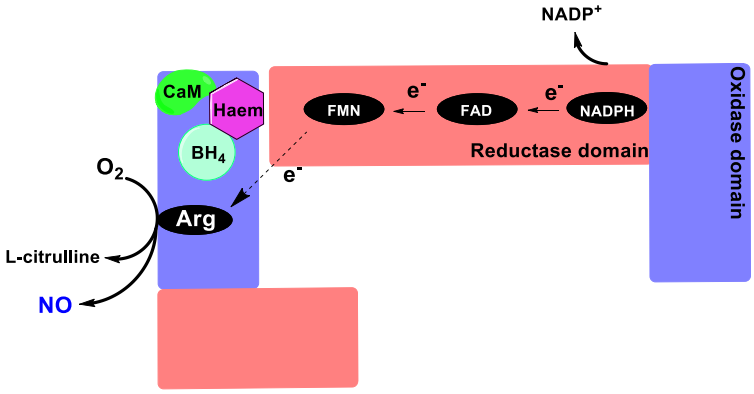

Figure 1.1. Structure of NOS and mechanism of NO release.

Alternatively, NO can also be produced from the nitrate-nitrite-nitric oxide pathway, independent of NOS. Nitrate (NO_3^-) being the ultimate oxidation product of NO is obtained either from the complete oxidation of NO or from dietary sources that are rich in nitrates. The major portion of nitrates is reduced to nitrites (NO_2^-) by the oral commensal bacteria and to minor extent by xanthine oxidoreductase and other enzymes in the tissue.

The nitrite is further reduced to NO by various enzymatic and non-enzymatic routes that are enhanced in hypoxic and acidic environment (Scheme 1.2).[7]

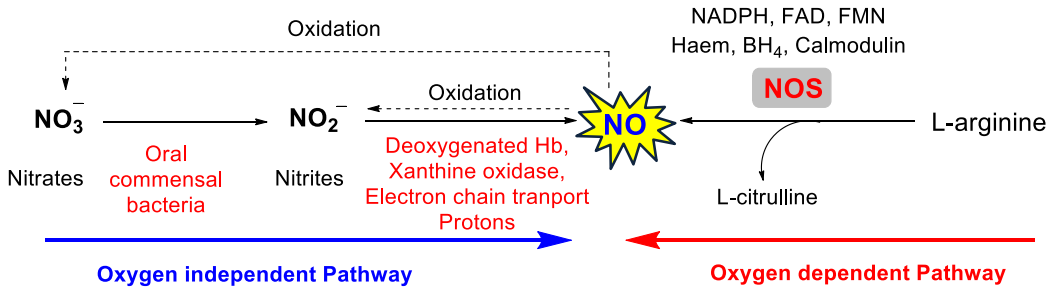

Scheme 1.2. Biosynthetic pathways of NO.

1.3. Biological effects of NO

NO is involved in numerous physiological functions that involve neurotransmission, regulation of blood pressure, respiration, cardiac functioning, platelet aggregation, regulating multiple functions in reproductive systems, signal transduction, antimicrobial defence, altering cellular redox status and anti-proliferative activity (Figure 1.2).[8] As NO is a multifaceted bio-effector molecule, it has become one of the most extensively studied molecules.

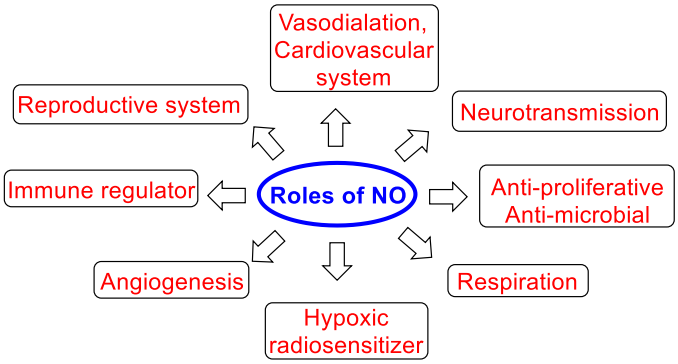

Figure 1.2. Physiological functions of NO.

NO can exhibit both cytotoxic and cytoprotective roles, largely influenced by the type of cell that is exposed, duration of exposure, its intracellular concentration and source of generation. When NO is produced in low concentration, it rapidly diffuses and reacts with biomolecules and predominantly have cell regulatory effects. In nanomolar (nM)

range, NO stimulates angiogenesis by inducing vascular endothelial growth factor (VEGF), fibroblast growth factor (FGF) and platelet derived growth factors (PDGF) that lead to tumor progression.[8h] Furthermore, it also plays important roles in neurotransmission, participation in vascular tone and inhibition of platelet aggregation. The fundamental mode of action for regulatory role exhibited by NO is by activation of soluble enzyme guanylate cyclase (sGC). NO, being a primary messenger, binds to the haem prosthetic group of sGC that brings about conformational change in the enzyme and enhances the conversion of GTP to 3′,5′-cyclic guanosine monophosphate (cGMP) about 100-200 times.[9] cGMP is a secondary messenger and increase in cGMP activates cGMP-based protein kinases, phosphodiesterases and cyclic nucleotide gated ion channels (Figure 1.3).[10] The various physiological processes controlled by cGMP activation include calcium homeostasis, platelet activation and adhesion, smooth muscle contraction, cardiac function, gene expression, feedback of the NO-signalling pathway and many other processes. Free NO is also known to react with proteins containing transition metals to form stable nitrosyls and then alter the protein activity. The nitrosylation modulates the protein behaviour which can either lead to inhibition of enzymes like cytochrome P450 or activation as in case of sGC.

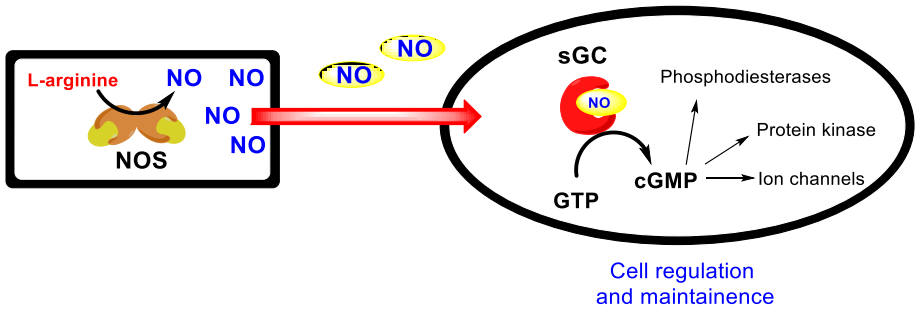

Figure 1.3. Activation of soluble guanylate cyclase by NO to trigger cascade of reactions via cGMP formation.

However, NO in micromolar (μM) concentration plays immunogenic and cytotoxic role. NO generated in the aerobic condition, reacts easily with oxygen and other oxygen species present within cells. The reaction of NO with molecular oxygen (O_2) forms nitrogen dioxide (NO_2) that further oxidizes NO to give unstable species dinitrogen

trioxide (N_2O_3). In physiological media N_2O_3 forms nitrosonium ion (NO^+) and nitrite (NO_2^-) (Figure 1.4.A).[11] Thus, N_2O_3 can nitrosylate nucleophiles in cells like thiols, secondary amines, phenols and can form oxidized species like S-nitrosothiols, metal-nitrosyl complexes, N-nitrosamines. Reactive oxygen species (ROS) are generally formed during mitochondrial respiration due to leakage of electrons to molecular oxygen from the electron transport chain.[12] One of the ROS, superoxide ($O_2^{\bullet-}$) when produced in the vicinity of NO can react in a diffusion-controlled manner to form a strong oxidant species, peroxynitrite ($ONOO^-$).[13] $ONOO^-$ is also short-lived molecule (<10 ms) that initiates cell damaging free radical reactions. Peroxynitrite in aqueous medium forms peroxynitrous acid (ONOOH) and is quickly oxidized to nitrite ($NO_2^{\bullet}$) and hydroxyl ($^{\bullet}OH$) radicals. The nitrite radical can lead to oxidation of biomolecules and formation of nitrated compounds. $^{\bullet}OH$ radical been a highly reactive oxygen species damages DNA, proteins and lipids by oxidation (Figure 1.4.B).[14]

The biomarker for $ONOO^-$ formation is the presence of oxidized and nitrated biomolecules, especially nitration of proteins that contain tyrosine. The formation of nitrosylated and nitrated species by NO and reactive nitrogen species (RNS) leads to nitrosative stress inside cells.[15] On the other hand, the formation of ROS ($^{\bullet}OH$) leads to hydroxylation, peroxidation of lipids, DNA damage and is termed as oxidative stress.[16] Higher levels of RNS and ROS lead to oxidative and nitrosative stress that impairs the cell machinery, inhibits respiration, enhances inflammatory response and leads to apoptosis.[17] Host cells generally adapt to this system in order to kill the invading pathogens and/or malignant cells. Therefore, the direct effects of NO are observed by NO diffusion and exert regulatory effects. However, the oxidation of NO to its congener RNS can result in indirect effects which include cytotoxic and immunogenic effects. Indirect effects are observed when there is high flux of NO, generally produced by *i*NOS for antimicrobial and anti-tumor effects.

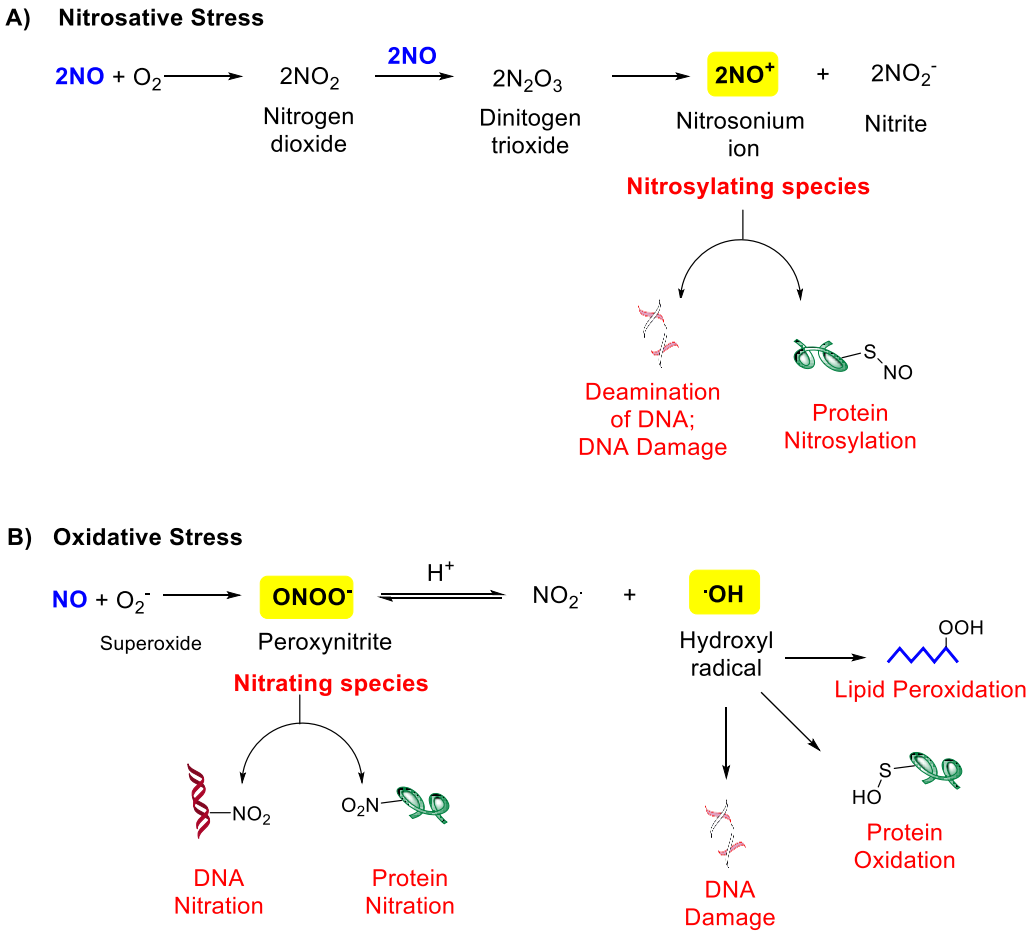

Figure 1.4. Cytotoxic effects mediated by reactive nitrogen species (RNS).

1.4. NO and cancer

The relationship between NO and cancer is complex and depends on NO's concentration, dosage, duration and its site of production.[18] A common phenotype associated with cancers is enhanced ROS in comparison with the paired normal tissue.[19] During episodes of oxidative stress, nitric oxide can react with superoxide, $O_2^{\bullet-}$, a reactive oxygen species (ROS), to produce peroxynitrite, which is highly toxic to cells.[13, 20] Thus, a synergy between ROS and RNS often leads to enhanced cytotoxicity (Figure 1.5). Hence, introduction of NO might result in greater inhibition of proliferation. At elevated concentrations, RNS can react spontaneously with metal ions and biomacromolecules possibly resulting in their inactivation. Some common RNS-induced modifications are nitration and nitrosylation of proteins, lipids and DNA, deamination of DNA leading to

mutations possibly causing loss in functions and triggering induction of necrosis and/or apoptosis; a favourable outcome in targeting cancers.[18, 21] NO is also known to reverse chemotherapy resistance in colon cancer cells.[22] Amongst the various mechanisms involved in the drug resistance, the important ones are the upregulation of efflux pumps in resistant cells that pump out the drugs out of the cell.[23] Due to diminished accumulation of cytotoxic drugs in cancer cells, desired anti-proliferative effects are not observed. The most common classes of efflux pumps include P-glycoprotein and multiple drug resistance-associated proteins (MRP) and are particularly relevant due to their broad spectrum of substrates. It has been found that NO inhibited the MRP-3 efflux pump by nitrating the tyrosine and thereby led to inversion of drug resistance.[22a, 24] Thus, it is likely that NO can be used in conjunction with traditional cancer drugs that have become ineffective due to such modes of efflux.

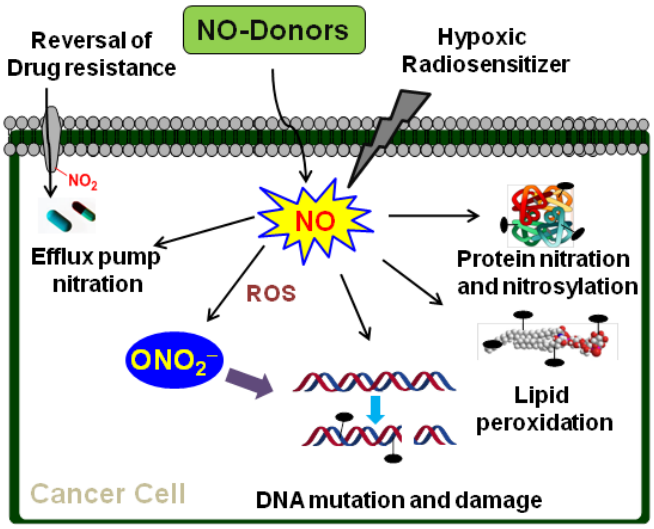

Figure 1.5. Cellular effects of increased exposure to nitric oxide.

A number of solid tumors are associated with extensive regions of low oxygen concentrations (hypoxia) and these cells are found to be resistant to most anticancer drugs.[21a, 25] Hypoxic cells are distant from blood vessels and as a result, are not adequately exposed to some types of anticancer drugs. The vasculature of tumours is chaotic and hence blood supply is not uniform to all regions. Also, hypoxia selects for cells that have lost sensitivity to p53-mediated apoptosis, and genes involved in drug resistance are upregulated, including genes encoding P-glycoprotein which might reduce

sensitivity to some anticancer agents.[15] Multidrug resistance has emerged as a major clinical problem and hypoxia contributes to drug resistance in solid cancers. Recent studies show that tumor hypoxia induces resistance to anticancer drugs by interfering with endogenous NO signalling and hence, introduction of low concentrations of NO might attenuate hypoxia-induced drug resistance in tumour cells.[24, 26] Furthermore, NO can also act as a hypoxic radiosensitizer[27] and this aspect is particularly useful as low oxygen concentrations in tumours result in diminished sensitivity to radiation therapy and poor prognosis. NO can accentuate radiation-induced DNA damage thus causing increased cell death. Another important adaption of hypoxic cells resulting in uncontrolled growth and recurrence of tumours post-surgery is the expression of the transcription factor hypoxia inducible factor (HIF-1).[28] HIF-1 has been reported to promote angiogenesis and promote metabolic adaptation through increase in glycolytic enzymes.[29] Increased expression of HIF in human cancer cells has been shown to increase tumour growth, angiogenesis, and metastasis, whereas genetic manipulations that decrease HIF expression result in decreased tumour growth, angiogenesis, and metastasis in animal models. This and other similar data supports inhibiting HIF-1 is an important strategy towards developing new drugs targeting hypoxic tumours. Under hypoxic conditions, nitric oxide blocks activation of HIF-1[30] by inhibition of an activation step of HIF-1α to a DNA-binding form. Since NO diffuses easily across the cell membranes, it can show its tumoristatic effects in neighbouring tumour cells as well through the bystander effect. Thus, selectively enhancing NO levels in tumours might have enormous therapeutic value.[21c, 31]

1.5. NO as an antimicrobial agent

NO is a key mediator for cytotoxicity against pathogens and thus is an important element of the innate immunity system (Figure 1.6).[8g, 32] In response to attack by pathogens, the immune cells like macrophages engulf the invading pathogen by endocytosis and try to either kill or inhibit the proliferation of pathogen inside host. The release of compounds like cytokines and interferon's after the pathogen attack induces expression of *i*NOS inside macrophages which releases NO in high concentrations. Macrophages also generate ROS to combat with the pathogen attack. NO and ROS inside macrophage

forms RNS, which causes an upsurge in nitrosative and oxidative stress within pathogens and induces cytotoxic effects. The main cellular targets of NO during host-pathogen interaction involve microbial DNA, proteins and lipids. NO can also interact with reactive thiols, proteins containing haem group, iron sulphur clusters, aromatic functionalities and other proteins as well and can inactivate or modify protein functioning.[33] RNS are known to oxidatively damage DNA by deaminating nucleobases to form abasic sites, alterations of DNA sequence and DNA strand breaks. Due to formation of peroxynitrite, lipid peroxidation is initiated in the pathogen that causes lipid damage.[13] Thus, the interplay of NO and ROS contributes to nitrosative and oxidative stress during host-pathogen interaction and potentially enhances cytotoxic effects for pathogen.

The important role of NO in immune system has been demonstrated by a series of key experiments that indicate NO production occurs in immune response to pathogens.[34] Firstly, significant increase in NO production in case of infection was detected (by measuring end products of NO oxidation in blood and urine samples).[35] Secondly, the concentration of NO in animal model was directly proportional to the ability to contain the infection.[36] Thirdly, it was also found that using NOS inhibitors like N^G-monomethyl-L-arginine, antimicrobial activity of NO was not observed.[37] Lastly, by using sources that deliver NO also showed inhibition or killing of the pathogens.[38]

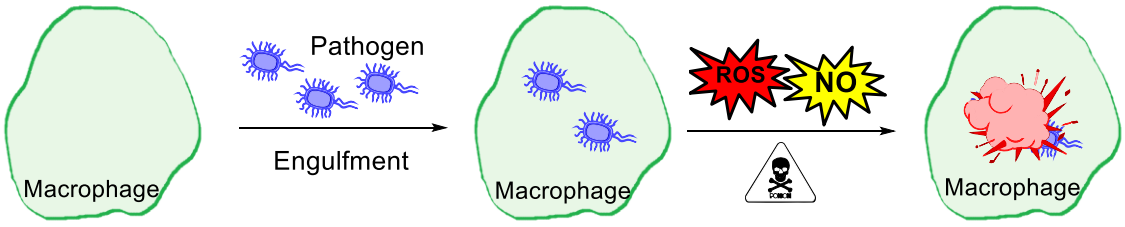

Figure 1.6. A pictorial representation of NO mediated immunogenic response in a macrophage.

In contrast, recent studies have shown that endogenously produced NO by bacteria have cytoprotective role possibly by attenuating the oxidative stress induced by class of antibiotics.[39] Bacterial NOS (*b*NOS) generate NO inside bacteria when exposed to

antibiotics and immune attack from the host cell. In case of *B. anthracis*, endogenous NO chemically detoxifies acriflavine by modifying it into less toxic form. In addition to this, NO also protects from the oxidative stress induced upon treatment with wide spectrum of antibiotics.[39a] Also in Methicillin resistant *Staphylococcus aureus* (MRSA), *b*NOS forms part of bacterial innate immunity and *b*NOS deficient MRSA mutant were less virulent and hyper-susceptible to ROS, human macrophages, antibiotics like vancomycin.[40] Further, bacteria have developed resistance to the exogenous NO by enzymatically detoxifying NO with help of haemoglobin, NO reductases and by repair mechanism that reverses the damage caused by NO.[41] However the mechanisms of detoxification in bacteria remain unclear. Thus, in order to study the precise antimicrobial role of NO, reliably enhancing the levels of NO inside bacteria and host immune cells is required.

1.6. NO delivery system

In order to study the precise roles of NO in cancer and immune response during infection, levels of NO within cells need to be reliably enhanced. As NO is a short-lived, highly diffusible and reactive gas that easily gets oxidized to inactive forms, namely, nitrate and nitrite, therefore delivering NO within cells is a challenging job. Furthermore, NO also forms a fundamental component of various physiological processes.

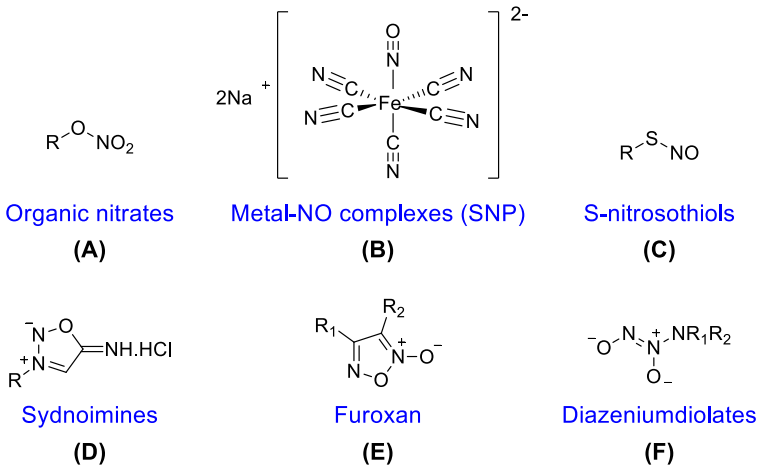

Figure 1.7. Structural representation of various classes of NO donors.

Hence, directed NO delivery to desired site in order to avoid the undesired side effects is necessary. So, in the interest of controlled and localised generation of NO, use of NO donors is a convenient strategy. NO donors are organic or inorganic compounds capable of releasing NO upon activation. NO donors have been used for the treatment of various ailments including cardiovascular diseases, inflammatory disorders and cancer.[42] Different classes of compounds that generate NO either spontaneously or with help of some external triggers have been used.[43] A brief overview of the major classes of NO donors is available in the following sections (Figure1.7).

1.6.1. Organic nitrates

Organic nitrates ($RONO_2$) are well known among the NO donors and are frequently used as vasodilators. They are nitric acid esters of alcohols (Figure 1.8).

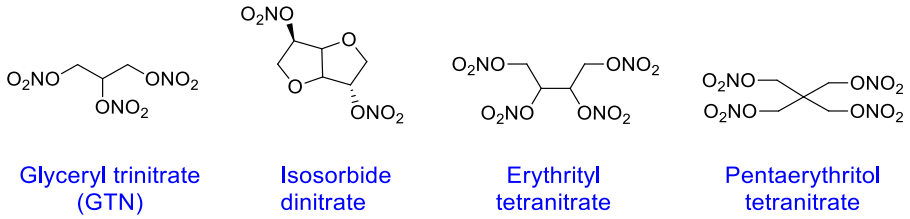

Figure1.8. Representative examples of organic nitrates.

The vasodialatory effects are exerted by the denitration of organic nitrates in the coronary and the systemic blood vessels to produce NO.[44] The breakdown of nitrates can occur either by enzymatic or non-enzymatic routes but involvement of thiols is suggested in both the cases (Scheme 1.3).

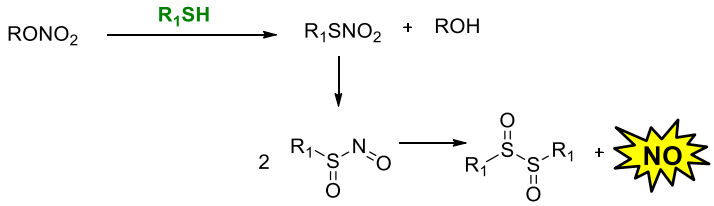

Scheme 1.3. Thiol mediated activation of organic nitrates to release NO.

1.6.2. Metal-NO complexes

Sodium nitroprusside (SNP) is one of most common example of metal-NO complexes and is used for vasodilation (Figure 1.7.B). During circulation, binding of SNP to

oxyhaemoglobin culminates in release of cyanide, methaemoglobin and nitric oxide. Release of NO from SNP is slow as it requires partial reduction by number of reducing agents inside the body to release NO.[45] The release of NO can be mediated by thiols or irradiation of light. Persistent use of SNP results in severe toxicity due to accumulation of toxic cyanide.

1.6.3. S-Nitrosothiols

S-nitrosothiols (RSNO) is another important class of NO donors (Figure 1.9), that decompose enzymatically, thermally, photochemically or some metal ions or by

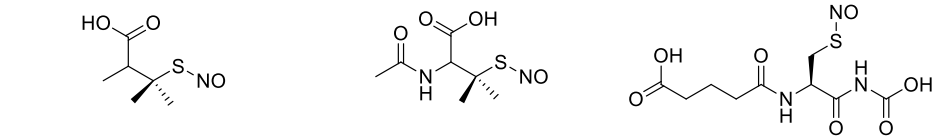

Figure 1.9. Representative examples of S-nitrosothiols.

superoxide and seleno compounds into NO and disulphide (Scheme 1.4).[46] SNAP is a potent vasodilator and low concentrations of GSNO shows protection to the myocardial ischemia.

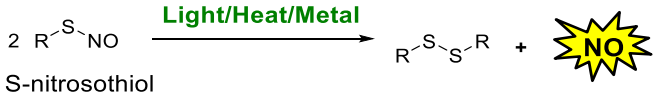

Scheme 1.4. Release of NO from S-nitrosothiols.

1.6.4. Sydnonimines

Derivatives of morpholine, these heterocyclic compounds release NO facilitated by the presence of alkaline pH and oxygen (Figure 1.7.D). The tandem release of superoxide radical combines with NO to generate peroxynitrite. Thus sydnoimines are better source for peroxynitrite.

1.6.5. Furoxans

Furoxans are yet another important class of NO donors that have shown anti-aggregatory and vasodialotory effects .The release of NO takes place by the attack of thiol on the heterocyclic ring (Scheme 1.5).

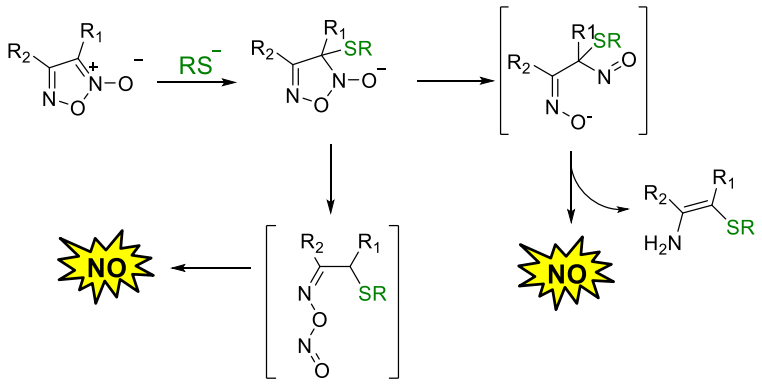

Scheme 1.5. Mechanism of thiol-mediated NO release from furoxan.

1.6.6. Diazeniumdialotes

Diazeniumdiolates belong to a class of NO donors that is been extensively used as a source to deliver NO. These organic salts are among the most reliable sources of NO that tend to undergo hydrolysis in aqueous solution to release upto two moles of NO in neutral and acidic solutions. The release of NO in aqueous media does not require any metabolic activation (Scheme 1.6).[47]

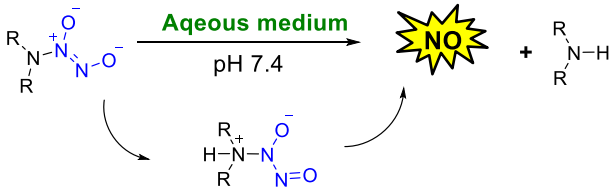

Scheme 1.6. Hydrolysis of a diazeniumdiolate anion in the aqueous solution to release an amine and two molecules of NO.

In the presence of aqueous solution, the diazeniumdiolate salt **F** gets protonated with three possible sites for protonation: a) at the terminal oxygen to form species **G**; b) at the second oxygen to form species **H**; c) at the amine nitrogen to form species **I** (Figure 1.7). The formation of species **G** and **H**, equilibrate back to diazeniumdiolate **F**, hence do not release NO. However, formation of **I** releases free amine and dimer of NO which undergoes homolytic cleavage to release 2 moles of NO (Scheme 1.7).[48]

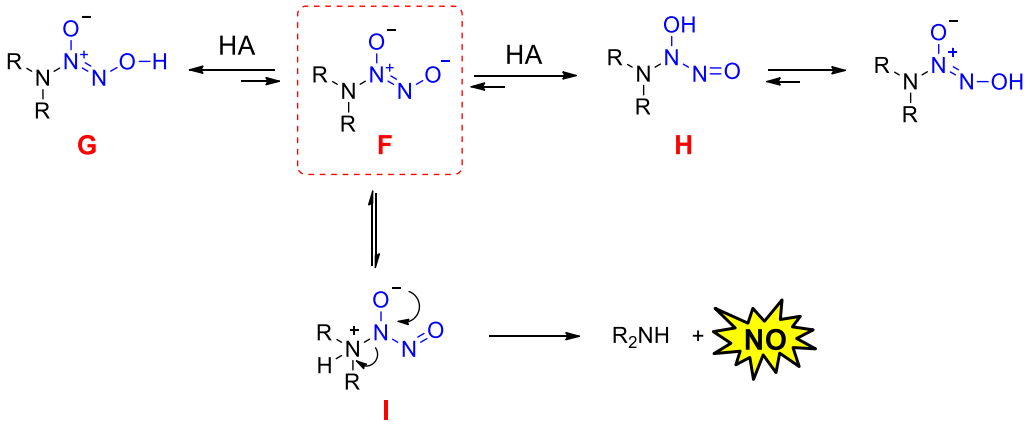

Scheme 1.7. Mechanism of hydrolysis of diazeniumdiolate salt in aqueous medium to release NO.

Depending on the bulk of alkyl groups on the amine nitrogen in species **I**, the half-lives of diazeniumdiolates range from 2 s to 20 h (Figure 1.10).[49] Thus, the amount of NO generated from diazeniumdiolates can be easily controlled in a predictive manner.

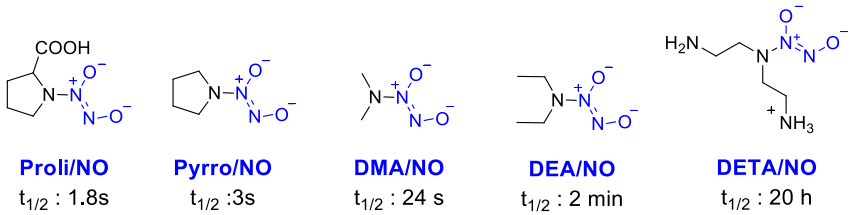

Figure 1.10. Examples of diazeniumdiolate salts with their respective $t_{1/2}$.

The strategies developed in the thesis for NO delivery focuses on the use of diazeniumdiolates as source of NO.

1.7. Bioactivated diazeniumdiolates for intracellular NO release

The diazeniumdiolate salts release NO in a non-specific manner in aqueous solution. Thus, diazeniumdiolates cannot be used to selectively deliver NO within tissues due to their non-specific activation which may result in systemic side-effects. In order to overcome this problem, the protected diazeniumdiolates are developed by derivatizing the terminal oxygen with a protecting group (Scheme 1.8). Generally, the protecting groups incorporated for derivatizing diazeniumdiolates are substrates for cellular enzymes. Thus, unlike free diazeniumdiolates, the protected diazeniumdiolates are modelled into a more stable form of NO-donor in physiological solutions. Further, the

protected diazeniumdiolates are metabolized into an active NO-donor by specific enzymes/biological triggers present within cells and thus ensure intracellular release of NO.

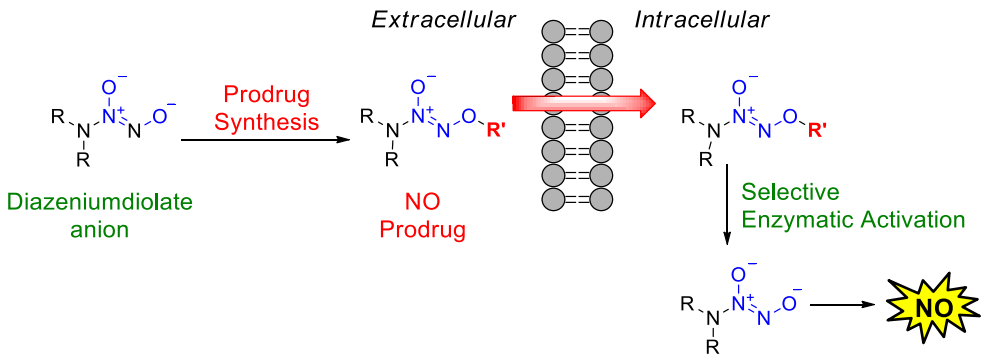

Scheme 1.8. Mechanism of activation of protected diazeniumdiolates by specific triggers for delivery of NO within cells.

JS-K, an arylated diazeniumdiolate, is an example of the thiol activated diazeniumdiolate which is highly toxic to cancer cells known to over-express glutathione (GSH) and glutathione-S-tranferase (GS-T) (Scheme 1.9).[50] The nucleophilic attack of GSH catalysed by GS-T on the aryl ring displaces diazeniumdiolate and releases NO within cells. JS-K effectively inhibits growth of a several cancer cells including gliomas, non-small lung cancer cells, hepatoma cells, prostate cancer cells and myeloma cells.

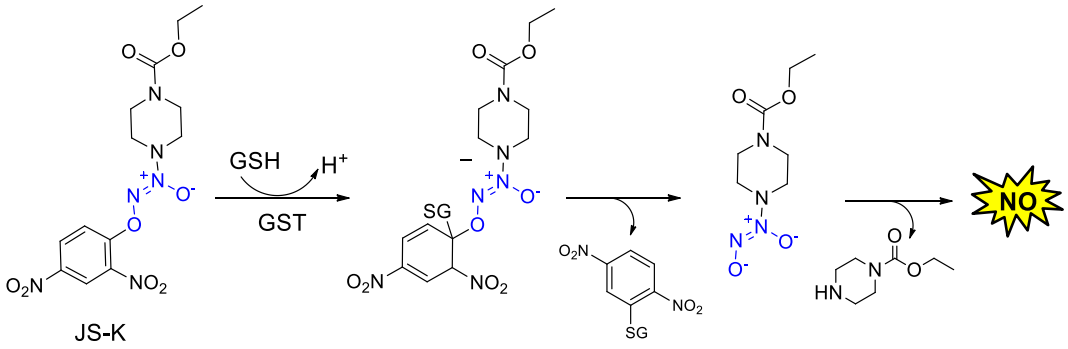

Scheme 1.9. Mechanism for GS-T catalysed GSH activation of 2, 4-dintrophenyl protected diazeniumdiolate, JS-K.

Saavedra *et. al* studied the nature of diazeniumdiolate as a leaving group in the arylated diazeniumdiolates. It was reported that the diazeniumdiolates were reasonably good leaving group and the rate constant for nucleophilic displacement was similar to that of a chloride in an aromatic nucleophilic substitution reaction.[51]

1.8. Challenges for intracellular NO delivery

So far, the reported bioactivated diazeniumdiolates are designed as substrates for esterases, glycosidases, and cellular thiols to deliver NO intracellularly (Figure 1.11).[50a, 52] Although these methodologies have been established for selective intracellular delivery of NO, however, aforementioned methodologies have the following limitations: a) the triggers like esterase and thiols that have been used for activation are present in normal cells as well; b) enzymes such as glycosidase do not efficiently catalyse activation to release NO; c) no scope for tunability of NO release; d) no reporter for monitoring intracellular NO release. So, an ideal NO delivery system should: a) be easily localized inside the desired target cell; b) be selectively activated by a specific trigger; c) have a provision for tuning the NO release; d) have a mechanism to report NO release within cells.

1.8.1. Selective delivery of NO to target

Although, the aforementioned bioactivated diazeniumdiolates as NO donors are useful (Figure 1.11) but the triggers that activate release of NO are generally present in normal cells as well. Hence these strategies cannot preclude the possibility of their activation in

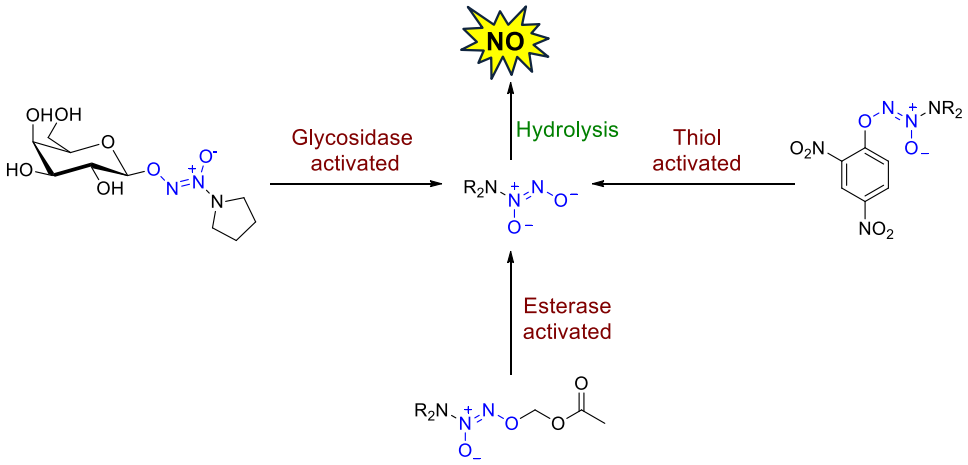

Figure 1.11. Bioactivated diazeniumdiolates for intracellular NO release.

normal cells also to generate NO. In order to avoid activation of NO donors at undesirable site, it is essential to design bioactivated diazeniumdiolates with protecting

groups that are highly specific for triggers which are explicitly present in the tissue of interest and not ubiquitous in nature (Path I, Figure 1.12).

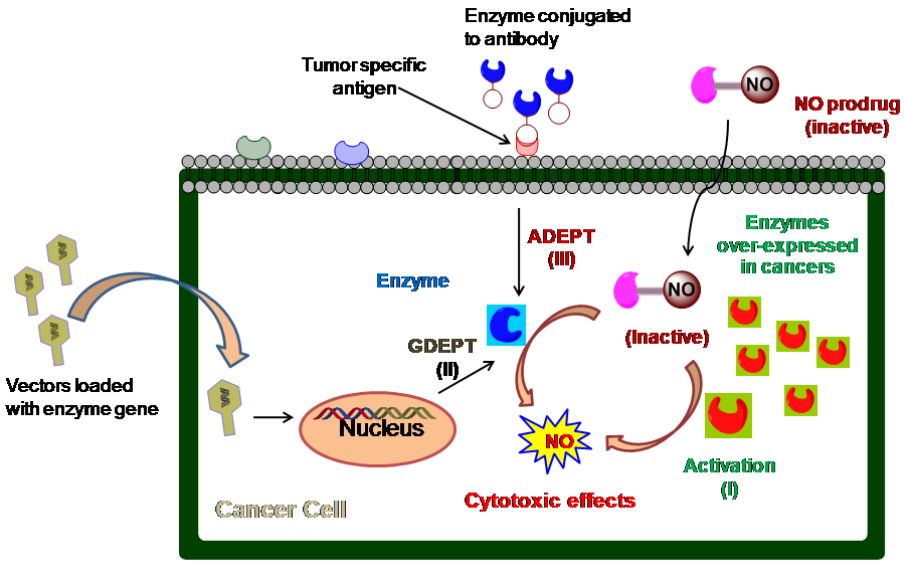

Figure 1.12. Some approaches for localized delivery of cytotoxic species including NO that are in development: (I) Enzymatic activation of NO prodrugs by enzymes over-expressed in tumors; (II) Gene directed enzyme prodrug therapy (GDEPT) and (III) Antibody directed enzyme prodrug therapy (ADEPT).

Furthermore, an alternate strategy that may be advantageous is directed enzyme prodrug therapy (DEPT) where an exogenous enzyme can be introduced for activating the NO donor (Path II and III, Figure 1.12). The levels of NO can be increased substantially inside desired cells and effects of NO can also be studied precisely.

To address the challenge of site-directed delivery of NO, a bioreductive enzyme DT-diaphorase (DT-D, EC 1.6.99.2) was selected. DT-D is a flavoprotein present in cytosol and is involved in the two-electron reduction of various quinones with the help of cofactor NADPH.[53] Bioreductive prodrugs are designed to exploit the reductive environment present in solid tumours. The inactive form of a drug gets metabolised into a cytotoxic drug in the presence of bioreductive enzymes.[54] Due to relatively higher levels of expression of DT-D in many solid tumours, mainly colon cancers, liver cancers, breast cancers, gastric carcinomas and lung cancers, it has gained lot of importance as a trigger in the field of bioreductive prodrugs.[55,56] Several indolequinone based prodrugs have been developed as chemotherapeutic agents based on the activation of indolequinone scaffold

by DT-D. Mitomycin C (MMC) and indoloquinone EO9 (Figure 1.13) are the examples of bioreductive prodrugs containing indolequinone that are metabolized into cytotoxic DNA alkylating species by DT-D.[57]

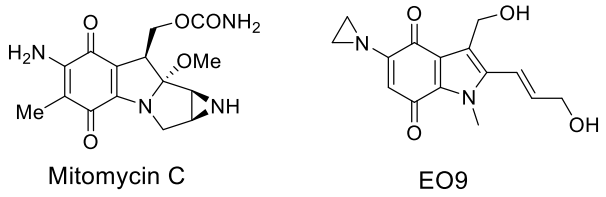

Figure 1.13. Examples of indolequinone based DT-D activated prodrugs.

The general mechanism for activation of indolequinone based prodrug involves two electron reduction of the indolequinone by DT-D to the dihydroxyindole intermediate **(J)** (Scheme 1.10). The dihydroxyindole intermediate has increased electron density on the indole nitrogen as a result of which electron rearrangement occurs that enables dispensing out the drug molecule attached to the quinone scaffold. Along with the release of cytotoxic drug, the electronic rearrangement results in the formation of a potentially cytotoxic DNA alkylating indolequinone iminium species **(K)**. Thus, using an indolequinone scaffold targets the cells by releasing two cytotoxic species upon bioreduction that are sufficiently toxic to kill cancer cells.

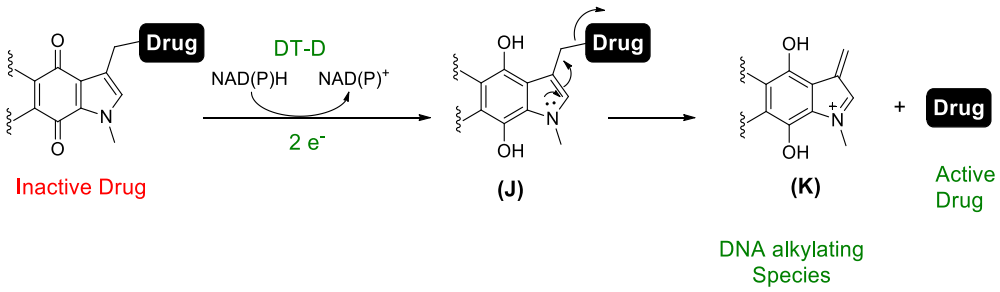

Scheme 1.10. Mechanism of activation of indolequinone-based prodrug by DT-D.

Thus, in Chapter 2, we propose to develop an indolequinone-based NO donor, using the concept of indolequinones as delivery vehicle for cancer cells over-expressing DT-D. This NO donor is expected to undergo activation by DT-D and can be used as a tool to deliver NO within cells that express this enzyme (Figure 1.14).

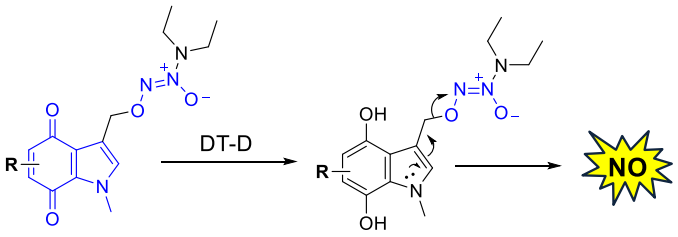

Figure 1.14. Proposed design of DT-D activated indolequinone based NO donor.

Next, directed enzyme prodrug therapy (DEPT) is one of the strategies for selective delivery of cytotoxin. In DEPT, an exogenous enzyme usually not present in host cell is expressed in target cell. This is followed by the administration of non-active prodrug and then selective activation of the prodrug in cytotoxic drug where the enzyme is expressed (Figure 1.15).

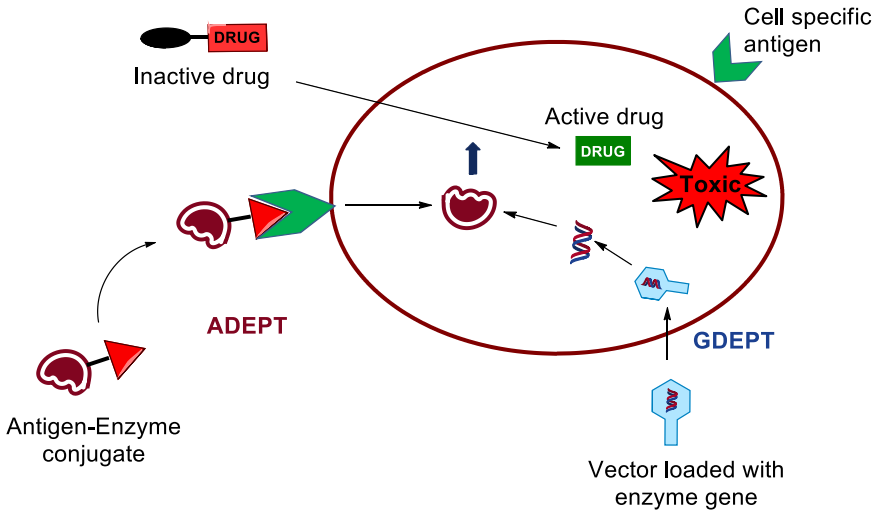

Figure 1.15. Directed enzyme prodrug therapies for localized delivery of toxic drug using two approaches: antibody-directed enzyme prodrug therapy (ADEPT) and gene-directed enzyme prodrug therapy (GDEPT).

Depending on the method by which enzyme is expressed in or on the host cell, DEPT is classified into gene-directed enzyme prodrug therapy (GDEPT) and antibody-directed enzyme prodrug therapy (ADEPT).[58] In the first case, the gene for the desired enzyme is loaded on a vector like virus or liposome and inserted into the host cell. The gene after entering the cell is decoded to produce desired enzyme intracellularly. Once the non-toxic prodrug reaches the transfected cell, it is activated into a toxin that kills the cells. In case of ADEPT, the enzyme is conjugated to the antibody that has high affinity for the

antigens present on the target cell. The enzyme-antibody conjugate is directed towards the cell with specific antigen and the enzyme is either released in the periphery of cell or by means of endocytosis delivered inside the cell.

Escherichia coli nitroreductase (NTR) is an enzyme that has been used as a metabolic trigger for directed prodrugs including ADEPT and GDEPT and is thus of therapeutic interest.[58a, 58c, 58d, 59] As NTR is not usually found in human cells, this enzyme is introduced either by transfection methodologies (for GDEPT) or by the use of antibody, highly specific for tumour-antigens, conjugated to the enzyme (for ADEPT). NTR-activated cancer drugs and cytotoxic species including DNA alkylating agents are previously reported.[58a, 59b, 60] A typical NTR-activated prodrug contains a 4-nitrobenzyl group which forms a substrate for NTR.[60a, 60c, 60e, 60f, 61] Several approaches for delivering cytotoxic species including DNA alkylating agents have been reported.

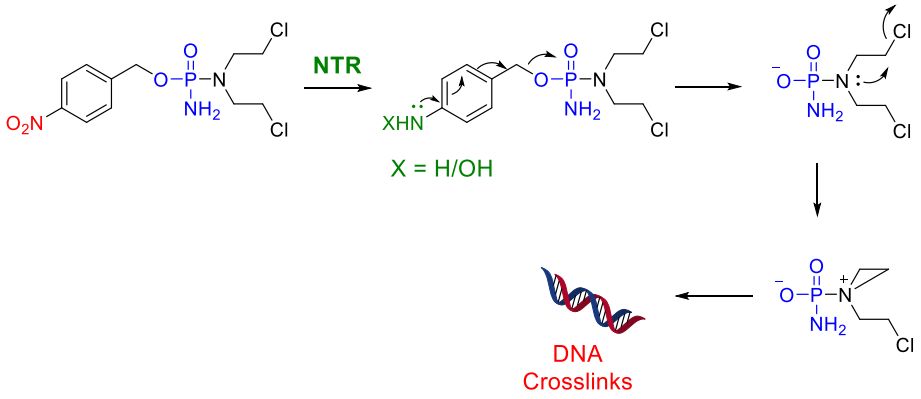

Scheme 1.11. An example of a rationally designed NTR-activated DNA alkylating agent.

For example, a phosphoramide mustard being masked by a 4-nitrobenzyl group was reported.[60f, 61a] This compound was metabolized by NTR to produce a DNA alkylating agent. NTR reduces the 4-nitrobenzyl group by two or four electron reduction using NADPH as the cofactor. Due to reduction, the electron withdrawing nitro group is converted into an electron donating hydroxylamine or amine group that pushes electron into the phenyl ring. As a result of this electronic rearrangement, the attached DNA alkylating species is released and cross-links the DNA (Scheme 1.11). A phosphoramide leaving group has been used, which then presumably irreversibly alkylates DNA through the generation of a cyclopropylaminium ion.

Therefore, in Chapter 3.1 we propose to synthesize NTR-activated NO donor which may have potential for applications in the directed or targeted prodrug therapy (Scheme 1.12).

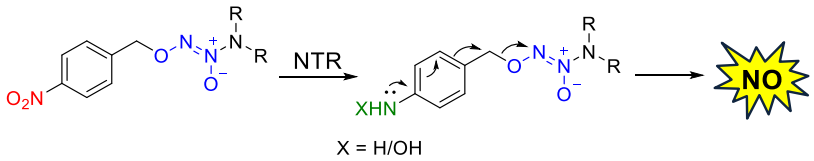

Scheme 1.12. Proposed design of NTR-activated NO donor.

1.8.2. Investigation into modulation of release rate

The biological effects of NO are mainly dictated by the concentration of NO present in the tissue. At times, lower concentration of NO is required and in some pathophysiological conditions burst of NO is necessary. But majority of NO delivery systems used are unable to modulate the release of NO upon activation. Therefore, the second challenge in the NO delivery system is modulation of release rate of NO from the delivery system. This challenge can be potentially addressed by selecting a delivery system that can be tuned by modifying the structure of the trigger.

Hay *et al*. studied the effects of substituent on the rate of reduction and release rate of leaving group upon reduction of the 4-nitrobenzyl group. It was reported that the 4 or 6 electron reduction of the 4-nitrobenzyl carbamate achieved radiolytically to release the attached group was improved[62] with electron donating groups at the C-2/C-3 of phenyl ring that stabilized the positive charge formed on the benzylic carbon and favoured the fragmentation. Also by placing an electron withdrawing group decelerates the fragmentation. The same study reported that the leaving group influenced the rate of fragmentation after reduction. But there were no such reports with NTR reduction of the 4-nitrobenzyl group. There are two important features that dictate the rate of NTR reduction: a) the efficiency of the enzyme to reduce the substrate; b) the fragmentation of the leaving group after reduction.

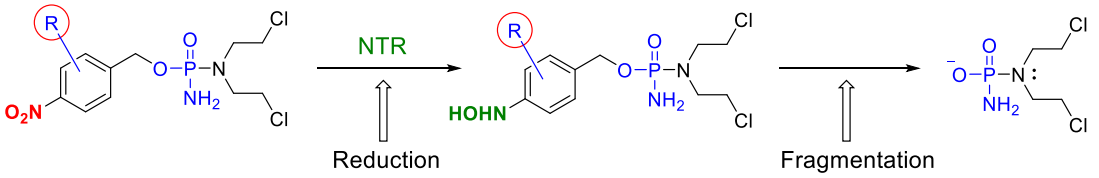

Figure 1.16. Schematic diagram for the reduction of 4-nitrobenzyl group with NTR followed by fragmentation to release free phosphoramide.

To further investigate the reduction in the presence *E. coli.* NTR, Hu *et al*. synthesized a series of substituted 4-nitrobenzyl phosphoramides and studied the structure activity relationship as substrate of NTR and effect on cytotoxicity in NTR transfected cells (Figure 1.16).[60f] It was found that substituting groups with different electronics affected the reduction by NTR and the cytotoxicity was also influenced. But the rate of reduction and cytotoxicity could not be correlated. So far, only the effects of substituents on the phenyl ring have been studied on the NTR reduction and release of leaving group. In order to further investigate the release profile, in Chapter 3.2, we propose the 4-nitrobenzyl based model with substitution at the benzylic position to study the release rate of leaving group using NTR activation (Scheme 1.13).

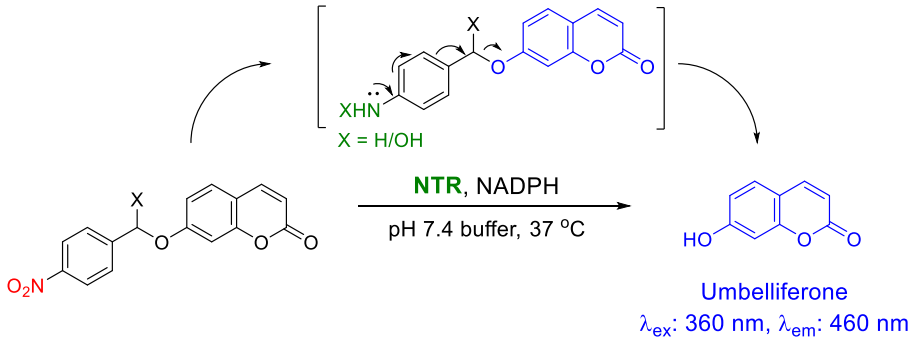

Scheme 1.13. NTR-activated model to study the effects of substituents at the benzylic position on the release of leaving group.

Indole scaffold has attracted significant attention as a pharmacophore as it forms the core for numerous naturally occurring compounds and also it is an active element for discovery of new drug molecules. Due to remarkable pharmacological bioactivities of indole containing molecules, indole has been termed as a privileged molecule.[63] Diverse synthetic routes have been established for efficiently synthesizing substituted indoles.[64] The indole molecule provides opportunities for modification that may assist in tunable

release (Figure 1.17). The indole nitrogen is a site for covalently linking different types of triggering group which may act as an activation site. The aromatic substituents may affect the total electron density on the indole ring. Due to the differences in the electron density of substituted indoles, the release of leaving group may be modulated. Therefore, indole may be an appropriate model to study for release tunability.

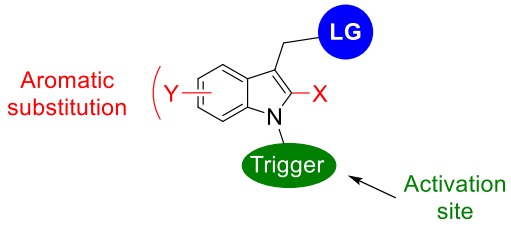

Figure 1.17. A versatile indole scaffold capable of tethering triggers at the indole nitrogen and also offers synthetic handle to tune the release of leaving group (LG) by aromatic substitutions, X and Y.

In order to study the tunability of leaving group release, we need to select a trigger that gets rapidly cleaved off from the scaffold and subsequently depending on the flow of the electrons, the leaving group departs. Allyloxy carbonyl (alloc) group is sensitive to cleavage by palladium (Pd).[65] The catalytic cycle of Pd starts with oxidative addition of the allyl bond to Pd(0) to form a Pd(II) π-allyl complex (A), which undergoes decarboxylation to form another Pd(II) π-allyl complex (B). Subsequently, reductive elimination affords deallylated product and regenerated Pd (0) (Scheme 1.14).

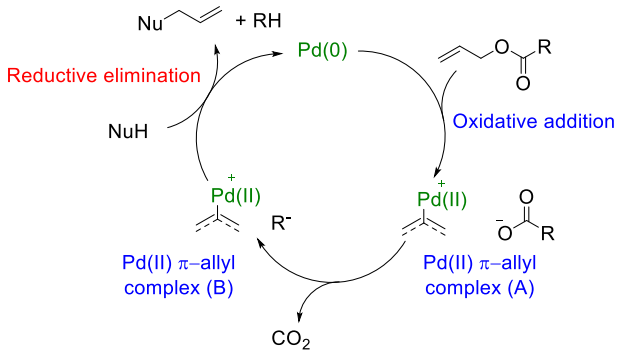

Scheme 1.14. Catalytic cycle for palladium mediated deallylation of alloc protected compounds.

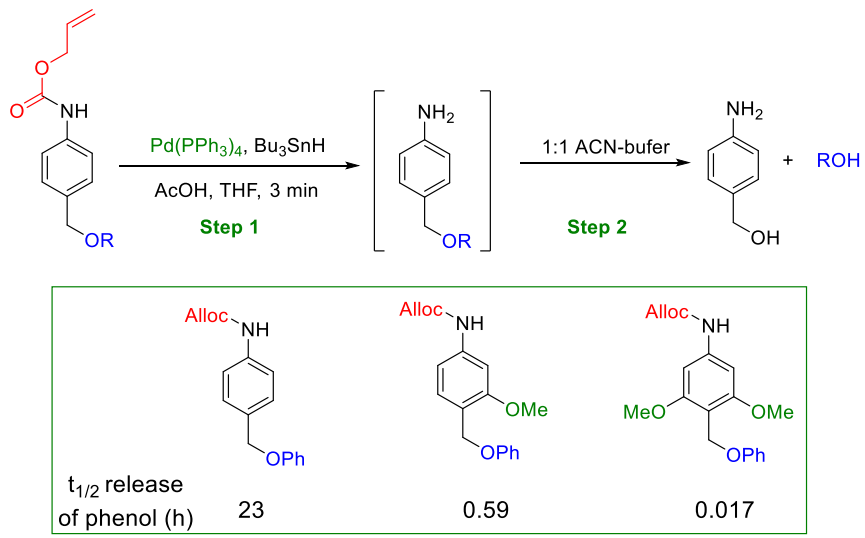

Figure 1.18. Molecular strategy designed by Schmid *et al.* for predictable and tunable release of phenols using palladium activated alloc group as trigger.

Schmid *et al*. developed a molecular strategy for tunable release of phenols using alloc as Pd activated trigger (Figure 1.18).[65a] In the presence of Pd catalyst, removal of the alloc group is accompanied by the release of phenol from the spacer molecule. Using the reported spacers, release of any type of phenols can be tuned. However the reported strategy has limitations: different spacers were used for modulating the release of phenol with different pKa's and modification of the benzyl based spacers synthetically would be cumbersome.

So, in order to have a synthetically accessible and more flexible scaffold, in Chapter 5, we propose a new indole based scaffold protected with alloc group and umbelliferone as the leaving group to study the tunability of the scaffold (Scheme 1.15).

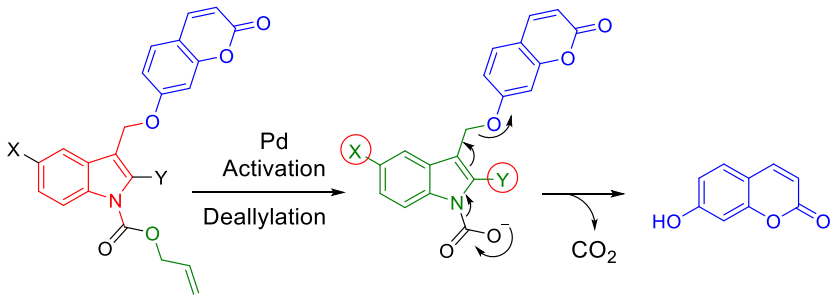

Scheme 1.15. A new indole based scaffold for studying the tunability of the release of umbelliferone from the scaffold. Alloc protected indole gets rapidly deprotected in the presence

of Pd catalyst and due to interplay of electronic and steric effects of substituents X and Y, the release of umbelliferone can be modulated.

1.8.3. Monitoring NO release inside cells

Physiological roles of NO are normally studied by using different classes of NO donors. The efficacy of the NO donor depends on its efficiency to enhance NO at the desired site. Due to high reactivity and diffusible nature, it is challenging to measure intracellular NO easily and accurately. DAF assay is a routinely used secondary assay for detection of intracellular NO.[66] In the assay, the cells are pre-treated with non-fluorescent DAF-2A dye, which gets hydrolysed upon its entry inside cells to form a non-fluorescent species DAF-2. DAF-2 does not react with NO directly. Intracellular NO undergoes auto-oxidation to form NO^+ species like N_2O_3 which reacts with DAF-2 and forms a fluorescent triazole moiety, DAF-2T.[67] By measuring fluorescence, a qualitative measurement of NO released from NO donor is achieved (Figure 1.19).

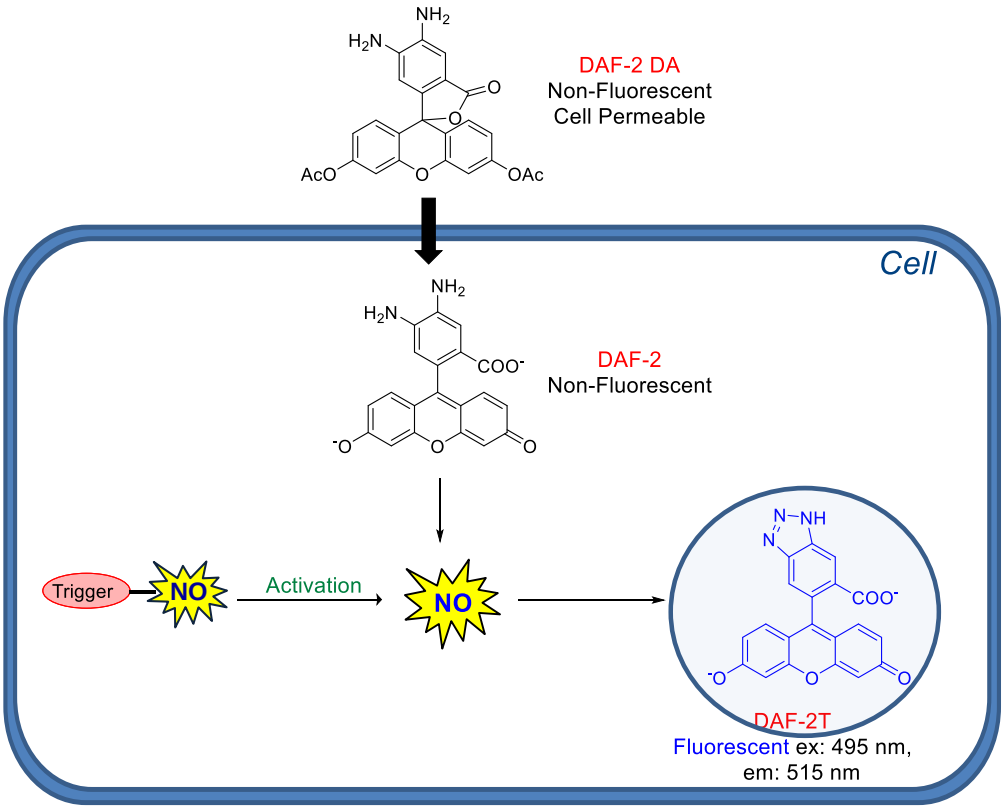

Figure 1.19. Intracellular NO measurement using a fluorescence based DAF assay.

However, once NO is released inside the cell, it can react with different molecules that are present inside cell, as a result of which measurement of NO might be imprecise. Thus, it is essential to monitor NO release as and when it is released. The secondary assays are typically destructive in nature and further cellular experiments are typically not possible. In other words, enhancement of NO within cells as well as simultaneous detection is cumbersome. It is therefore necessary to develop a reporter linked NO donor which would report NO release immediately without the need for secondary assays for detection.

Weinstein *et al*. reported real-time monitoring of drug release using a reporting drug delivery system (RDDS) where a 7-hydroxycoumarin linker was attached to the peptidase substrate to one end and to the drug molecule on the other end.[68] The activation of the RDDS by hydrolysis of amide bond by enzyme releases phenolate that undergoes 1,8-elimination to release the drug and turn-on fluorescent molecule 7-hydroxycoumarin as reporter molecule (Figure 1.20). Likewise few other reporter linked prodrugs have been synthesized for real-time monitoring of drug release[69] which enables real-time monitoring of the drug release with the help of a reporter molecule in a non-invasive manner.

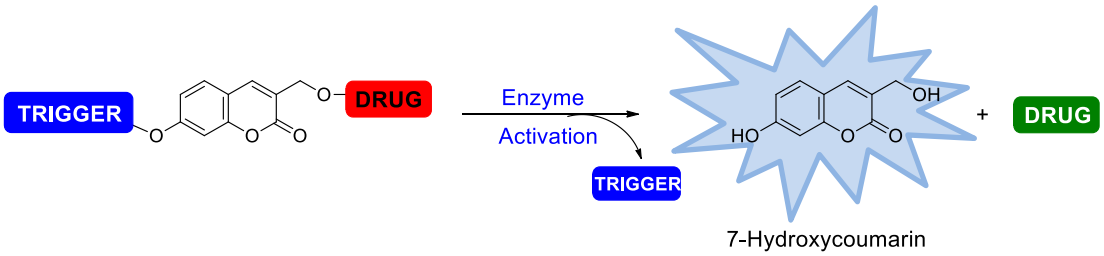

Figure 1.20. Reporting drug delivery system by Weinstein *et al*. for real-time monitoring of drug release using 7-hydroxycoumarin as the reporter molecule.

Therefore, based on the above strategy of real-time monitoring of drug release, in Chapter 4, we propose a reporter linked NTR-activated NO donor for bacterial system. The reporter linked NO donor is expected to undergo NTR reduction to release NO and simultaneously report the release of NO inside cells This will facilitate monitoring of NO-donor localisation, permeability and to study its activation mechanism *in vivo* (Scheme 1.16).

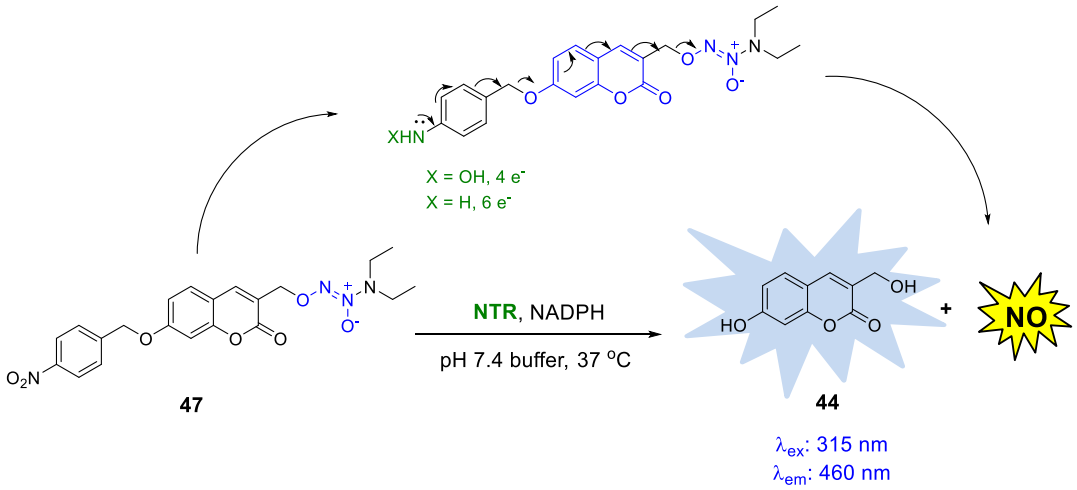

Scheme 1.16. Bioreductively activated NO donor with a fluorescence reporter: the turn-off reporter molecule inside bacteria gets reduced by NTR to form electron rich intermediate that spontaneously rearranges the electron and releases the turn-on fluorescent coumarin reporter molecule, **44** and NO.

Altogether, the results presented in this thesis address important problems associated with site-specific delivery of NO and may find use for directed and tuneable drug delivery as well. Also, these approaches may be used as tools to study mechanisms of NO in cellular stress responses.

1.9. References

1. Moncada, S.; Higgs, E. A., The discovery of nitric oxide and its role in vascular biology. *Br. J. Pharmacol.* **2006,** *147* (S1), S193-S201.

2. (a) SoRelle, R., Nobel Prize Awarded to Scientists for Nitric Oxide Discoveries. *Circulation* **1998,** *98* (22), 2365-2366; (b) Furchgott, R. F., Endothelium-Derived Relaxing Factor: Discovery, Early Studies, and Identifcation as Nitric Oxide (Nobel Lecture). *Angew. Chem. Int. Ed.* **1999,** *38* (13-14), 1870-1880.

3. Zweier, J. L.; Samouilov, A.; Kuppusamy, P., Non-enzymatic nitric oxide synthesis in biological systems. *BBA-Bioenergetics* **1999,** *1411* (2–3), 250-262.

4. O W Griffith, a.; Stuehr, D. J., Nitric Oxide Synthases: Properties and Catalytic Mechanism. *Annu. Rev. Physiol.* **1995,** *57* (1), 707-734.

5. Andrew, P. J.; Mayer, B., *Enzymatic function of nitric oxide synthases*. 1999; Vol. 43, p 521-531.

6. Förstermann, U.; Sessa, W. C., *Nitric oxide synthases: regulation and function*. 2012; Vol. 33, p 829-837.

7. Weitzberg, M. D. P. D. E.; Hezel, P. D. M.; Lundberg, M. D. P. D. J. O., Nitrate-Nitrite-Nitric Oxide PathwayImplications for Anesthesiology and Intensive Care. *The Journal of the American Society of Anesthesiologists* **2010,** *113* (6), 1460-1475-1460-1475.

8. (a) Dominiczak, A. F.; Bohr, D. F., Nitric Oxide and Its Putative Role in Hypertension. *Hypertension* **1995,** *25* (6), 1202-1211; (b) Brown, G. C., Nitric oxide and mitochondrial respiration. *Biochim. Biophys. Acta* **1999,** *1411* (2–3), 351-369; (c) Beltrán, B.; Mathur, A.; Duchen, M. R.; Erusalimsky, J. D.; Moncada, S., The effect of nitric oxide on cell respiration: A key to understanding its role in cell survival or death. *Proc. Natl. Acad. Sci.* **2000,** *97* (26), 14602-14607; (d) Massion, P. B.; Feron, O.; Dessy, C.; Balligand, J.-L., Nitric Oxide and Cardiac Function: Ten Years After, and Continuing. *Cir. Res.* **2003,** *93* (5), 388-398; (e) Rosselli, M.; Keller, R.; Dubey, R., Role of nitric oxide in the biology, physiology and pathophysiology of reproduction. *Hum. Reprod. Update* **1998,** *4* (1), 3-24; (f) Heinrich, T. A.; da Silva, R. S.; Miranda, K. M.; Switzer, C. H.; Wink, D. A.; Fukuto, J. M., Biological nitric oxide signalling: chemistry and terminology. *Br. J. Pharmacol.* **2013,** *169* (7), 1417-1429; (g) Bogdan, C., Nitric

oxide and the immune response. *Nat Immunol* **2001,** *2* (10), 907-916; (h) Wink, D. A.; Vodovotz, Y.; Laval, J.; Laval, F.; Dewhirst, M. W.; Mitchell, J. B., The multifaceted roles of nitric oxide in cancer. *Carcinogenesis* **1998,** *19* (5), 711-721.

9. Bellamy, T. C.; Wood, J.; Garthwaite, J., On the activation of soluble guanylyl cyclase by nitric oxide. *Proceedings of the National Academy of Sciences* **2002,** *99* (1), 507-510.

10. (a) Francis, S. H.; Busch, J. L.; Corbin, J. D., cGMP-Dependent Protein Kinases and cGMP Phosphodiesterases in Nitric Oxide and cGMP Action. *Pharmacological Reviews* **2010,** *62* (3), 525-563; (b) Mocellin, S.; Bronte, V.; Nitti, D., Nitric oxide, a double edged sword in cancer biology: Searching for therapeutic opportunities. *Medicinal Research Reviews* **2007,** *27* (3), 317-352.

11. Brown, G. C.; Borutaite, V., Interactions between nitric oxide, oxygen, reactive oxygen species and reactive nitrogen species. *Biochem. Soc. Trans.* **2006,** *34* (5), 953-956.

12. Sabharwal, S. S.; Schumacker, P. T., Mitochondrial ROS in cancer: initiators, amplifiers or an Achilles' heel? *Nat Rev Cancer* **2014,** *14* (11), 709-721.

13. Szabo, C.; Ischiropoulos, H.; Radi, R., Peroxynitrite: biochemistry, pathophysiology and development of therapeutics. *Nat Rev Drug Discov* **2007,** *6* (8), 662-680.

14. Pacher, P.; Beckman, J. S.; Liaudet, L., Nitric Oxide and Peroxynitrite in Health and Disease. *Physiol. Rev.* **2007,** *87* (1), 315-424.

15. Ridnour, L. A.; Thomas, D. D.; Mancardi, D.; Espey, M. G.; Miranda, K. M.; Paolocci, N.; Feelisch, M.; Fukuto, J.; Wink, D. A., The chemistry of nitrosative stress induced by nitric oxide and reactive nitrogen oxide species. Putting perspective on stressful biological situations. In *Biol Chem.*, 2004; Vol. 385, p 1.

16. Avery, Simon V., Molecular targets of oxidative stress. *Biochem. J.* **2011,** *434* (2), 201-210.

17. Wiseman, H.; Halliwell, B., Damage to DNA by reactive oxygen and nitrogen species: role in inflammatory disease and progression to cancer. *Biochem. J.* **1996,** *313* (1), 17-29.

18. (a) Heinrich, T. A.; da Silva, R. S.; Miranda, K. M.; Switzer, C. H.; Wink, D. A.; Fukuto, J. M., Biological nitric oxide signalling: chemistry and terminology. *Brit. J. Pharmacol.* **2013,** *169* (7), 1417-1429; (b) Ridnour, L. A.; Thomas, D. D.; Switzer, C.; Flores-Santana, W.; Isenberg, J. S.; Ambs, S.; Roberts, D. D.; Wink, D. A., Molecular mechanisms for discrete nitric oxide levels in cancer. *Nitric Oxide* **2008,** *19* (2), 73-76.

19. (a) Kuang, Y.; Balakrishnan, K.; Gandhi, V.; Peng, X., Hydrogen peroxide inducible DNA cross-linking agents: Targeted anticancer prodrugs. *J. Am. Chem. Soc.* **2011,** *133* (48), 19278-19281; (b) Miller, E. W.; Tulyanthan, O.; Isacoff, E. Y.; Chang, C. J., Molecular imaging of hydrogen peroxide produced for cell signaling. *Nat Chem Biol* **2007,** *3* (5), 263-267.

20. Szabó, C., Multiple pathways of peroxynitrite cytotoxicity. *Toxicol. Lett.* **2003,** *140–141* (0), 105-112.

21. (a) Wang, P. G.; Xian, M.; Tang, X.; Wu, X.; Wen, Z.; Cai, T.; Janczuk, A. J., Nitric Oxide Donors: Chemical Activities and Biological Applications. *Chem.Rev.* **2002,** *102* (4), 1091-1134; (b) Xu, W.; Liu, L. Z.; Loizidou, M.; Ahmed, M.; Charles, I. G., The role of nitric oxide in cancer. *Cell Res.* **2002,** *12* (5-6), 311-320; (c) Burke, A. J.; Sullivan, F. J.; Giles, F. J.; Glynn, S. A., The yin and yang of nitric oxide in cancer progression. *Carcinogen.* **2013,** *34* (3), 503-512.

22. (a) Riganti, C.; Miraglia, E.; Viarisio, D.; Costamagna, C.; Pescarmona, G.; Ghigo, D.; Bosia, A., Nitric Oxide Reverts the Resistance to Doxorubicin in Human Colon Cancer Cells by Inhibiting the Drug Efflux. *Cancer Res.* **2005,** *65* (2), 516-525; (b) Chegaev, K.; Riganti, C.; Lazzarato, L.; Rolando, B.; Guglielmo, S.; Campia, I.; Fruttero, R.; Bosia, A.; Gasco, A., Nitric Oxide Donor Doxorubicins Accumulate into Doxorubicin-Resistant Human Colon Cancer Cells Inducing Cytotoxicity. *ACS Med. Chem. Lett.* **2011,** *2* (7), 494-497.

23. (a) Gottesman, M. M., MECHANISMS OF CANCER DRUG RESISTANCE. *Annu. Rev. Med.* **2002,** *53* (1), 615-627; (b) Zaman, G. J.; Flens, M. J.; van Leusden, M. R.; de Haas, M.; Mülder, H. S.; Lankelma, J.; Pinedo, H. M.; Scheper, R. J.; Baas, F.; Broxterman, H. J., The human multidrug resistance-associated protein MRP is a plasma membrane drug-efflux pump. *Proc. Natl. Acad. Sci.* **1994,** *91* (19), 8822-8826; (c) Moitra, K.; Lou, H.; Dean, M., Multidrug Efflux Pumps and Cancer Stem Cells: Insights

Into Multidrug Resistance and Therapeutic Development. *Clin Pharmacol Ther* **2011,** *89* (4), 491-502.

24. (a) Fruttero, R.; Crosetti, M.; Chegaev, K.; Guglielmo, S.; Gasco, A.; Berardi, F.; Niso, M.; Perrone, R.; Panaro, M. A.; Colabufo, N. A., Phenylsulfonylfuroxans as Modulators of Multidrug-Resistance-Associated Protein-1 and P-Glycoprotein. *J. Med. Chem.* **2010,** *53* (15), 5467-5475; (b) Riganti, C.; Rolando, B.; Kopecka, J.; Campia, I.; Chegaev, K.; Lazzarato, L.; Federico, A.; Fruttero, R.; Ghigo, D., Mitochondrial-Targeting Nitrooxy-doxorubicin: A New Approach To Overcome Drug Resistance. *Mol. Pharm.* **2012,** *10* (1), 161-174.

25. (a) Brown, J. M.; Wilson, W. R., Exploiting tumour hypoxia in cancer treatment. *Nat Rev Cancer* **2004,** *4* (6), 437-447; (b) Shannon, A. M.; Bouchier-Hayes, D. J.; Condron, C. M.; Toomey, D., Tumour hypoxia, chemotherapeutic resistance and hypoxia-related therapies. *Cancer Treat. Rev.* **2003,** *29* (4), 297-307; (c) Sullivan, R.; Paré, G. C.; Frederiksen, L. J.; Semenza, G. L.; Graham, C. H., Hypoxia-induced resistance to anticancer drugs is associated with decreased senescence and requires hypoxia-inducible factor-1 activity. *Mol. Cancer Ther.* **2008,** *7* (7), 1961-1973.

26. (a) Frederiksen, L. J.; Sullivan, R.; Maxwell, L. R.; Macdonald-Goodfellow, S. K.; Adams, M. A.; Bennett, B. M.; Siemens, D. R.; Graham, C. H., Chemosensitization of Cancer In vitro and In vivo by Nitric Oxide Signaling. *Clin. Cancer Res.* **2007,** *13* (7), 2199-2206; (b) Bonavida, B.; Khineche, S.; Huerta-Yepez, S.; Garbán, H., Therapeutic potential of nitric oxide in cancer. *Drug resistance updates* **2006,** *9* (3), 157-173; (c) Wilson, W. R.; Hay, M. P., Targeting hypoxia in cancer therapy. *Nat. Rev. Cancer* **2011,** *11* (6), 393-410.

27. (a) Cowen, R. L.; Garside, E. J.; Fitzpatrick, B.; Papadopoulou, M. V.; Williams, K. J., Gene therapy approaches to enhance bioreductive drug treatment. *Brit. J. Radiol.* **2008,** *81* (special_issue_1), S45-S56; (b) De Ridder, M.; Verellen, D.; Verovski, V.; Storme, G., Hypoxic tumor cell radiosensitization through nitric oxide. *Nitric Oxide* **2008,** *19* (2), 164-169; (c) Mitchell, J. B.; Wink, D. A.; DeGraff, W.; Gamson, J.; Keefer, L. K.; Krishna, M. C., Hypoxic Mammalian Cell Radiosensitization by Nitric Oxide. *Cancer Res* **1993,** *53* (24), 5845-5848.

28. Yasuda, H., Solid tumor physiology and hypoxia-induced chemo/radio-resistance: Novel strategy for cancer therapy: Nitric oxide donor as a therapeutic enhancer. *Nitric Oxide* **2008,** *19* (2), 205-216.

29. (a) Talks, K. L.; Turley, H.; Gatter, K. C.; Maxwell, P. H.; Pugh, C. W.; Ratcliffe, P. J.; Harris, A. L., The Expression and Distribution of the Hypoxia-Inducible Factors HIF-1α and HIF-2α in Normal Human Tissues, Cancers, and Tumor-Associated Macrophages. *Amer.J.Path.* **2000,** *157* (2), 411-421; (b) Semenza, G. L., Targeting HIF-1 for cancer therapy. *Nat Rev Cancer* **2003,** *3* (10), 721-732.

30. (a) Sogawa, K.; Numayama-Tsuruta, K.; Ema, M.; Abe, M.; Abe, H.; Fujii-Kuriyama, Y., Inhibition of hypoxia-inducible factor 1 activity by nitric oxide donors in hypoxia. *Proc. Natl. Acad. Sci.* **1998,** *95* (13), 7368-7373; (b) *Role of nitric oxide in the regulation of HIF-1α expression during hypoxia*. 2002; Vol. 283, p C178-C186.

31. (a) Huerta, S.; Chilka, S.; Bonavida, B., Nitric oxide donors: Novel cancer therapeutics (review). *Int. J. Oncol.* **2008,** *33* (5), 909-927; (b) Sonveaux, P.; Jordan, B. F.; Gallez, B.; Feron, O., Nitric oxide delivery to cancer: Why and how? *Eur. J. Cancer* **2009,** *45* (8), 1352-1369; (c) Hirst, D.; Robson, T., Targeting nitric oxide for cancer therapy. *J. Pharm. Pharmacol.* **2007,** *59* (1), 3-13.

32. (a) Wink, D. A.; Hines, H. B.; Cheng, R. Y. S.; Switzer, C. H.; Flores-Santana, W.; Vitek, M. P.; Ridnour, L. A.; Colton, C. A., Nitric oxide and redox mechanisms in the immune response. *J. Leukoc. Biol.* **2011,** *89* (6), 873-891; (b) MacMicking, J.; Xie, Q.-w.; Nathan, C., Nitric oxide and macrophage function. *Annu. Rev. Immunol.* **1997,** *15* (1), 323-350.

33. (a) Habib, S.; Ali, A., Biochemistry of Nitric Oxide. *Ind. J. Clin. Biochem.* **2011,** *26* (1), 3-17; (b) Tamir, S.; Burney, S.; Tannenbaum, S. R., DNA Damage by Nitric Oxide. *Chem. Res. Toxicol.* **1996,** *9* (5), 821-827; (c) Wiseman, H.; Halliwell, B., Damage to DNA by reactive oxygen and nitrogen species: role in inflammatory disease and progression to cancer. *Biochem. J.* **1996,** *313* (Pt 1), 17-29; (d) Filomeni, G.; De Zio, D.; Cecconi, F., Oxidative stress and autophagy: the clash between damage and metabolic needs. *Cell Death Differ* **2015,** *22* (3), 377-388.

34. Fang, F. C., Perspectives series: host/pathogen interactions. Mechanisms of nitric oxide-related antimicrobial activity. *J. Clin. Invest.* **1997,** *99* (12), 2818-2825.

35. Evans, T. G.; Thai, L.; Granger, D. L.; Hibbs, J. B., Effect of in vivo inhibition of nitric oxide production in murine leishmaniasis. *J. Immunol.* **1993,** *151* (2), 907-15.

36. MacMicking, J. D.; North, R. J.; LaCourse, R.; Mudgett, J. S.; Shah, S. K.; Nathan, C. F., Identification of nitric oxide synthase as a protective locus against tuberculosis. *Proc. Natl. Acad. Sci.* **1997,** *94* (10), 5243-5248.

37. Adams, L. B.; Hibbs, J. B.; Taintor, R. R.; Krahenbuhl, J. L., Microbiostatic effect of murine-activated macrophages for Toxoplasma gondii. Role for synthesis of inorganic nitrogen oxides from L-arginine. *J. Immunol.* **1990,** *144* (7), 2725-9.

38. De Groote, M. A.; Fang, F. C., NO Inhibitions: Antimicrobial Properties of Nitric Oxide. *Clin. Infect. Dis.* **1995,** *21* (Supplement 2), S162-S165.

39. (a) Gusarov, I.; Shatalin, K.; Starodubtseva, M.; Nudler, E., Endogenous Nitric Oxide Protects Bacteria Against a Wide Spectrum of Antibiotics. *Science* **2009,** *325* (5946), 1380-1384; (b) Gusarov, I.; Nudler, E., NO-mediated cytoprotection: Instant adaptation to oxidative stress in bacteria. *Proc. Natl. Acad. Sci.* **2005,** *102* (39), 13855-13860.

40. van Sorge, N. M.; Beasley, F. C.; Gusarov, I.; Gonzalez, D. J.; von Köckritz-Blickwede, M.; Anik, S.; Borkowski, A. W.; Dorrestein, P. C.; Nudler, E.; Nizet, V., Methicillin-resistant Staphylococcus aureus Bacterial Nitric-oxide Synthase Affects Antibiotic Sensitivity and Skin Abscess Development. *J. Biol. Chem.* **2013,** *288* (9), 6417-6426.

41. (a) Laver, J. R.; Stevanin, T. M.; Messenger, S. L.; Lunn, A. D.; Lee, M. E.; Moir, J. W. B.; Poole, R. K.; Read, R. C., Bacterial nitric oxide detoxification prevents host cell S-nitrosothiol formation: a novel mechanism of bacterial pathogenesis. *FASEB J.* **2010,** *24* (1), 286-295; (b) Frey, A. D.; Kallio, P. T., Nitric oxide detoxification – a new era for bacterial globins in biotechnology? *Trends Biotechnol.* **2005,** *23* (2), 69-73; (c) Stevanin, T. M.; Moir, J. W. B.; Read, R. C., Nitric Oxide Detoxification Systems Enhance Survival of Neisseria meningitidis in Human Macrophages and in Nasopharyngeal Mucosa. *Infect. Immun.* **2005,** *73* (6), 3322-3329.

42. Carpenter, A. W.; Schoenfisch, M. H., Nitric oxide release: Part II. Therapeutic applications. *Chem. Soc. Rev.* **2012,** *41* (10), 3742-3752.

43. (a) Huerta, S.; Chilka, S.; Bonavida, B., Nitric oxide donors: novel cancer therapeutics (review). *Int J Oncol* **2008,** *33* (5), 909-27; (b) Wang, P. G.; Xian, M.; Tang, X.; Wu, X.; Wen, Z.; Cai, T.; Janczuk, A. J., Nitric Oxide Donors: Chemical Activities and Biological Applications. *Chemical Reviews* **2002,** *102* (4), 1091-1134.

44. Kukovetz, W. R.; Holzmann, S.; Romanin, C., Mechanism of Vasodilation by Nitrates: Role of Cyclic GMP. *Cardiology* **1987,** *74(suppl 1)* (Suppl. 1), 12-19.

45. Friederich, J. A.; Butterworth, J. F., Sodium Nitroprusside: Twenty Years and Counting. *Anesthesia & Analgesia* **1995,** *81* (1), 152-162.

46. Veleeparampil, M. M.; Aravind, U. K.; Aravindakumar, C. T., Decomposition of S-Nitrosothiols Induced by UV and Sunlight. *Advances in Physical Chemistry* **2009,** *2009*.

47. (a) Chakrapani, H.; Showalter, B. M.; Citro, M. L.; Keefer, L. K.; Saavedra, J. E., Nitric Oxide Prodrugs: Diazeniumdiolate Anions of Hindered Secondary Amines. *Organic Letters* **2007,** *9* (22), 4551-4554; (b) Keefer, L. K.; Flippen-Anderson, J. L.; George, C.; Shanklin, A. P.; Dunams, T. M.; Christodoulou, D.; Saavedra, J. E.; Sagan, E. S.; Bohle, D. S., Chemistry of the Diazeniumdiolates I. Structural and Spectral Characteristics of the [N(O)NO]− Functional Group. *Nitric Oxide* **2001,** *5* (4), 377-394.

48. (a) Dutton, A. S.; Fukuto, J. M.; Houk, K. N., The mechanism of NO formation from the decomposition of dialkylamino diazeniumdiolates: density functional theory and CBS-QB3 predictions. *Inorg. Chem.* **2004,** *43* (3), 1039-45; (b) Davies, K. M.; Wink, D. A.; Saavedra, J. E.; Keefer, L. K., Chemistry of the Diazeniumdiolates. 2. Kinetics and Mechanism of Dissociation to Nitric Oxide in Aqueous Solution. *J. Am. Chem. Soc.* **2001,** *123* (23), 5473-5481.

49. Fitzhugh, A. L.; Keefer, L. K., Diazeniumdiolates:: Pro- and antioxidant applications of the "NONOates"1. *Free Radical Bio. Med.* **2000,** *28* (10), 1463-1469.

50. (a) Shami, P. J.; Saavedra, J. E.; Wang, L. Y.; Bonifant, C. L.; Diwan, B. A.; Singh, S. V.; Gu, Y.; Fox, S. D.; Buzard, G. S.; Citro, M. L.; Waterhouse, D. J.; Davies, K. M.; Ji, X.; Keefer, L. K., JS-K, a Glutathione/Glutathione S-Transferase-activated Nitric Oxide Donor of the Diazeniumdiolate Class with Potent Antineoplastic Activity1. *Mol. Cancer Ther.* **2003,** *2* (4), 409-417; (b) Maciag, A. E.; Chakrapani, H.; Saavedra, J. E.; Morris, N. L.; Holland, R. J.; Kosak, K. M.; Shami, P. J.; Anderson, L. M.; Keefer, L.

K., The Nitric Oxide Prodrug JS-K Is Effective against Non–Small-Cell Lung Cancer Cells In Vitro and In Vivo: Involvement of Reactive Oxygen Species. *J. Pharmacol. Exp. Ther.* **2011,** *336* (2), 313-320; (c) Kiziltepe, T.; Hideshima, T.; Ishitsuka, K.; Ocio, E. M.; Raje, N.; Catley, L.; Li, C.-Q.; Trudel, L. J.; Yasui, H.; Vallet, S.; Kutok, J. L.; Chauhan, D.; Mitsiades, C. S.; Saavedra, J. E.; Wogan, G. N.; Keefer, L. K.; Shami, P. J.; Anderson, K. C., JS-K, a GST-activated nitric oxide generator, induces DNA double-strand breaks, activates DNA damage response pathways, and induces apoptosis in vitro and in vivo in human multiple myeloma cells. *Blood* **2007,** *110* (2), 709-718.

51. Saavedra, J. E.; Srinivasan, A.; Bonifant, C. L.; Chu, J.; Shanklin, A. P.; Flippen-Anderson, J. L.; Rice, W. G.; Turpin, J. A.; Davies, K. M.; Keefer, L. K., The Secondary Amine/Nitric Oxide Complex Ion R2N[N(O)NO]- as Nucleophile and Leaving Group in SNAr Reactions. *J. Org. Chem.* **2001,** *66* (9), 3090-3098.

52. (a) Wu, X.; Tang, X.; Xian, M.; Wang, P. G., Glycosylated diazeniumdiolates: a novel class of enzyme-activated nitric oxide donors. *Tetrahedron Lett.* **2001,** *42* (23), 3779-3782; (b) Saavedra, J. E.; Shami, P. J.; Wang, L. Y.; Davies, K. M.; Booth, M. N.; Citro, M. L.; Keefer, L. K., Esterase-Sensitive Nitric Oxide Donors of the Diazeniumdiolate Family: In Vitro Antileukemic Activity. *J. Med. Chem.* **2000,** *43* (2), 261-269.

53. (a) Tedeschi, G.; Chen, S.; Massey, V., DT-diaphorase: Redox potential, stead-state, and rapid reaction studies. *J. Biol. Chem.* **1995,** *270* (3), 1198-1204; (b) Chen, S.; Wu, K.; Knox, R., Structure-function studies of DT-diaphorase (NQO1) and NRH:quinone oxidoreductase (NQO2)1. *Free Radical Bio. Med.* **2000,** *29* (3–4), 276-284.

54. Phillips, R. M., Prospects for bioreductive drug development. *Expert Opin. Investig. Drugs* **1998,** *7* (6), 905-28.

55. (a) Marin, A.; Lopez de Cerain, A.; Hamilton, E.; Lewis, A. D.; Martinez-Penuela, J. M.; Idoate, M. A.; Bello, J., DT-diaphorase and cytochrome B5 reductase in human lung and breast tumours. *Br. J. Cancer* **1997,** *76* (7), 923-929; (b) Mikami, K.; Naito, M.; Tomida, A.; Yamada, M.; Sirakusa, T.; Tsuruo, T., DT-Diaphorase as a Critical Determinant of Sensitivity to Mitomycin C in Human Colon and Gastric Carcinoma Cell Lines. *Cancer Res.* **1996,** *56* (12), 2823-2826; (c) Smitskamp-Wilms, E.;

Giaccone, G.; Pinedo, H. M.; van der Laan, B. F.; Peters, G. J., DT-diaphorase activity in normal and neoplastic human tissues; an indicator for sensitivity to bioreductive agents? *Br. J. Cancer* **1995,** *72* (4), 917-921.

56. (a) Hernick, M.; Flader, C.; Borch, R. F., Design, Synthesis, and Biological Evaluation of Indolequinone Phosphoramidate Prodrugs Targeted to DT-diaphorase. *J. Med. Chem* **2002,** *45* (16), 3540-3548; (b) Huang, B.; Desai, A.; Tang, S.; Thomas, T. P.; Baker, J. R., The Synthesis of a c(RGDyK) Targeted SN38 Prodrug with an Indolequinone Structure for Bioreductive Drug Release. *Org. Lett.* **2010,** *12* (7), 1384-1387; (c) Jaffar, M.; Everett, S. A.; Naylor, M. A.; Moore, S. G.; Ulhaq, S.; Patel, K. B.; Stratford, M. R. L.; Nolan, J.; Wardman, P.; Stratford, I. J., Prodrugs for targeting hypoxic tissues: Regiospecific elimination of aspirin from reduced indolequinones. *Bioorg. Med. Chem. Lett* **1999,** *9* (1), 113-118; (d) Ross, D.; Beall, H. D.; Siegel, D.; Traver, R. D.; Gustafson, D. L., Enzymology of bioreductive drug activation. *Br. J. Canc. Suppl.*

1996, *27*, S1-8; (e) Zhang, Z.; Tanabe, K.; Hatta, H.; Nishimoto, S.-i., Bioreduction activated prodrugs of camptothecin: molecular design, synthesis, activation mechanism and hypoxia selective cytotoxicity. *Org. Bio. Chem.* **2005,** *3* (10), 1905-1910.

57. (a) Beall, H. D.; Winski, S. I., Mechanisms of action of quinone-containing alkylating agents. I: NQO1-directed drug development. *Front Biosci* **2000,** *5*, D639-648; (b) Andrez, J.-C., Mitomycins syntheses: a recent update. *Beilstein J. Org. Chem.* **2009,** *5*, 33.

58. (a) Friedlos, F.; Denny, W. A.; Palmer, B. D.; Springer, C. J., Mustard Prodrugs for Activation by Escherichia coli Nitroreductase in Gene-Directed Enzyme Prodrug Therapy. *J. Med. Chem.* **1997,** *40* (8), 1270-1275; (b) Xu, G.; McLeod, H. L., Strategies for Enzyme/Prodrug Cancer Therapy. *Clin. Cancer Res.* **2001,** *7* (11), 3314-3324; (c) Greco, O.; Dachs, G. U., Gene directed enzyme/prodrug therapy of cancer: Historical appraisal and future prospectives. *J. Cell. Physiol.* **2001,** *187* (1), 22-36; (d) Chung-Faye, G.; Palmer, D.; Anderson, D.; Clark, J.; Downes, M.; Baddeley, J.; Hussain, S.; Murray, P. I.; Searle, P.; Seymour, L.; Harris, P. A.; Ferry, D.; Kerr, D. J., Virus-directed, Enzyme Prodrug Therapy with Nitroimidazole Reductase: A Phase I and Pharmacokinetic Study of its Prodrug, CB1954. *Clin. Cancer Res.* **2001,** *7* (9), 2662-2668.

59. (a) Anlezark, G. M.; Melton, R. G.; Sherwood, R. F.; Coles, B.; Friedlos, F.; Knox, R. J., The bioactivation of 5-(aziridin-1-yl)-2,4-dinitrobenzamide (CB1954)--I. Purification and properties of a nitroreductase enzyme from Escherichia coli--a potential enzyme for antibody-directed enzyme prodrug therapy (ADEPT). *Biochem. Pharmacol.* **1992,** *44* (12), 2289-95; (b) Bridgewater, J. A.; Springer, C. J.; Knox, R. J.; Minton, N. P.; Michael, N. P.; Collins, M. K., Expression of the bacterial nitroreductase enzyme in mammalian cells renders them selectively sensitive to killing by the prodrug CB1954. *Eur. J. Cancer* **1995,** *31* (13–14), 2362-2370; (c) Mauger, A. B.; Burke, P. J.; Somani, H. H.; Friedlos, F.; Knox, R. J., Self-Immolative Prodrugs: Candidates for Antibody-Directed Enzyme Prodrug Therapy in Conjunction with a Nitroreductase Enzyme. *J. Med. Chem.*

1994, *37* (21), 3452-3458.

60. (a) Hay, M. P.; Wilson, W. R.; Denny, W. A., Nitrobenzyl carbamate prodrugs of enediynes for nitroreductase gene-directed enzyme prodrug therapy (GDEPT). *Bioorg. Med. Chem. Lett.* **1999,** *9* (24), 3417-3422; (b) Hay, M. P.; Anderson, R. F.; Ferry, D. M.; Wilson, W. R.; Denny, W. A., Synthesis and Evaluation of Nitroheterocyclic Carbamate Prodrugs for Use with Nitroreductase-Mediated Gene-Directed Enzyme Prodrug Therapy. *J. Med. Chem.* **2003,** *46* (25), 5533-5545; (c) Hay, M. P.; Atwell, G. J.; Wilson, W. R.; Pullen, S. M.; Denny, W. A., Structure−Activity Relationships for 4-Nitrobenzyl Carbamates of 5-Aminobenz[e]indoline Minor Groove Alkylating Agents as Prodrugs for GDEPT in Conjunction with E. coli Nitroreductase. *J. Med. Chem.* **2003,** *46* (12), 2456-2466; (d) Sykes, B. M.; Hay, M. P.; Bohinc-Herceg, D.; Helsby, N. A.; O'Connor, C. J.; Denny, W. A., Leaving group effects in reductively triggered fragmentation of 4-nitrobenzyl carbamates. *J. Chem. Soc., Perkin Trans.* **2000,** (10), 1601-1608; (e) Asche, C.; Dumy, P.; Carrez, D.; Croisy, A.; Demeunynck, M., Nitrobenzylcarbamate prodrugs of cytotoxic acridines for potential use with nitroreductase gene-directed enzyme prodrug therapy. *Bioorg. Med. Chem. Lett.* **2006,** *16* (7), 1990-1994; (f) Hu, L.; Wu, X.; Han, J.; Chen, L.; Vass, S. O.; Browne, P.; Hall, B. S.; Bot, C.; Gobalakrishnapillai, V.; Searle, P. F.; Knox, R. J.; Wilkinson, S. R., Synthesis and structure–activity relationships of nitrobenzyl phosphoramide mustards as nitroreductase-activated prodrugs. *Bioorg. Med. Chem. Lett.* **2011,** *21* (13), 3986-3991.

61. (a) Hu, L.; Yu, C.; Jiang, Y.; Han, J.; Li, Z.; Browne, P.; Race, P. R.; Knox, R. J.; Searle, P. F.; Hyde, E. I., Nitroaryl Phosphoramides as Novel Prodrugs for E. coli Nitroreductase Activation in Enzyme Prodrug Therapy. *J. Med. Chem.* **2003,** *46* (23), 4818-4821; (b) P. Hay, M.; M. Sykes, B.; A. Denny, W.; J. O'Connor, C., Substituent effects on the kinetics of reductively-initiated fragmentation of nitrobenzyl carbamates designed as triggers for bioreductive prodrugs. *J. Chem. Soc. , Perkin Trans. 1* **1999,** *0* (19), 2759-2770; (c) Zhu, R.; Liu, M.-C.; Luo, M.-Z.; Penketh, P. G.; Baumann, R. P.; Shyam, K.; Sartorelli, A. C., 4-Nitrobenzyloxycarbonyl Derivatives of O6-Benzylguanine as Hypoxia-Activated Prodrug Inhibitors of O6-Alkylguanine-DNA Alkyltransferase (AGT), Which Produces Resistance to Agents Targeting the O-6 Position of DNA Guanine. *J. Med. Chem.* **2011,** *54* (21), 7720-7728.

62. P. Hay, M.; M. Sykes, B.; A. Denny, W.; J. O'Connor, C., Substituent effects on the kinetics of reductively-initiated fragmentation of nitrobenzyl carbamates designed as triggers for bioreductive prodrugs. *J. Chem. Soc., Perkin Trans. 1* **1999,** (19), 2759-2770.

63. Klekota, J.; Roth, F. P., Chemical substructures that enrich for biological activity. *Bioinformatics* **2008,** *24* (21), 2518-2525.

64. (a) Gribble, G. W., Recent developments in indole ring synthesis-methodology and applications. *J. Chem. Soc., Perkin Trans. 1* **2000,** (7), 1045-1075; (b) Barluenga, J.; Jiménez-Aquino, A.; Aznar, F.; Valdés, C., Modular Synthesis of Indoles from Imines and o-Dihaloarenes or o-Chlorosulfonates by a Pd-Catalyzed Cascade Process. *J. Am. Chem. Soc.* **2009,** *131* (11), 4031-4041; (c) Schütznerová, E.; Krchňák, V., Solid-Phase Synthesis of 2-Aryl-3-alkylamino-1H-indoles from 2-Nitro-N-(2-oxo-2-arylethyl)benzenesulfonamides via Base-Mediated C-Arylation. *ACS Comb. Sci.* **2015,** *17* (2), 137-146.

65. (a) Schmid, K. M.; Jensen, L.; Phillips, S. T., A Self-Immolative Spacer That Enables Tunable Controlled Release of Phenols under Neutral Conditions. *J. Org. Chem.* **2012,** *77* (9), 4363-4374; (b) Song, F.; Garner, A. L.; Koide, K., A Highly Sensitive Fluorescent Sensor for Palladium Based on the Allylic Oxidative Insertion Mechanism. *J. Am. Chem. Soc.* **2007,** *129* (41), 12354-12355; (c) Li, J.; Yu, J.; Zhao, J.; Wang, J.; Zheng, S.; Lin, S.; Chen, L.; Yang, M.; Jia, S.; Zhang, X.; Chen, P. R., Palladium-

triggered deprotection chemistry for protein activation in living cells. *Nat Chem* **2014,** *6* (4), 352-361.

66. (a) Leikert, J. F.; Räthel, T. R.; Müller, C.; Vollmar, A. M.; Dirsch, V. M., Reliable in vitro measurement of nitric oxide released from endothelial cells using low concentrations of the fluorescent probe 4,5-diaminofluorescein. *FEBS Lett.* **2001,** *506* (2), 131-134; (b) Planchet, E.; Kaiser, W. M., Nitric oxide (NO) detection by DAF fluorescence and chemiluminescence: a comparison using abiotic and biotic NO sources. *J. Exp. Bot.* **2006,** *57* (12), 3043-3055; (c) Strijdom, H.; Muller, C.; Lochner, A., Direct intracellular nitric oxide detection in isolated adult cardiomyocytes: flow cytometric analysis using the fluorescent probe, diaminofluorescein. *J Mol. Cell Cardiol.* **2004,** *37* (4), 897-902.

67. Roche, C. J.; Friedman, J. M., NO reactions with sol-gel and solution phase samples of the ferric nitrite derivative of HbA. *Nitric oxide* **2010,** *22* (2), 180-190.

68. Weinstain, R.; Segal, E.; Satchi-Fainaro, R.; Shabat, D., Real-time monitoring of drug release. *Chem. Commun.* **2010,** *46* (4), 553-555.

69. (a) Cao, Y.; Pan, R.; Xuan, W.; Wei, Y.; Liu, K.; Zhou, J.; Wang, W., Photo-triggered fluorescent theranostic prodrugs as DNA alkylating agents for mechlorethamine release and spatiotemporal monitoring. *Org. Biomol. Chem.* **2015,** *13* (24), 6742-6748; (b) Liu, P.; Xu, J.; Yan, D.; Zhang, P.; Zeng, F.; Li, B.; Wu, S., A DT-diaphorase responsive theranostic prodrug for diagnosis, drug release monitoring and therapy. *Chem. Commun.* **2015,** *51* (46), 9567-9570; (c) Wu, J.; Huang, R.; Wang, C.; Liu, W.; Wang, J.; Weng, X.; Tian, T.; Zhou, X., Thiol-inducible direct fluorescence monitoring of drug release. *Org. Biomol. Chem.* **2013,** *11* (4), 580-585.

CHAPTER 2: INDQ/NO, A DT-Diaphorase activated NO donor

2.1. Introduction

In this chapter, in order to deliver NO in cancer cells, a bioreductive enzyme DT-Diaphorase (DT-D) was selected. DT-D is a two electron reductase enzyme involved in detoxification of quinone containing compounds. The enzyme uses the cofactors NADPH and FAD for bioreduction of quinones. The over-expression of DT-D in certain type of cancers has been exploited for activation of many quinone containing prodrugs in chemotherapy.[1] As normal cells have minimal levels of DT-D expression, the prodrug activation in normal cells to release cytotoxic species is considerably reduced and as a result the extent of side effects are also reduced remarkably. Mitomycin C (MMC), being a prototype for bioreductively activated chemotherapeutic agent, gets activated by DT-D to form cytotoxic DNA cross-linking species (Scheme 2.1).

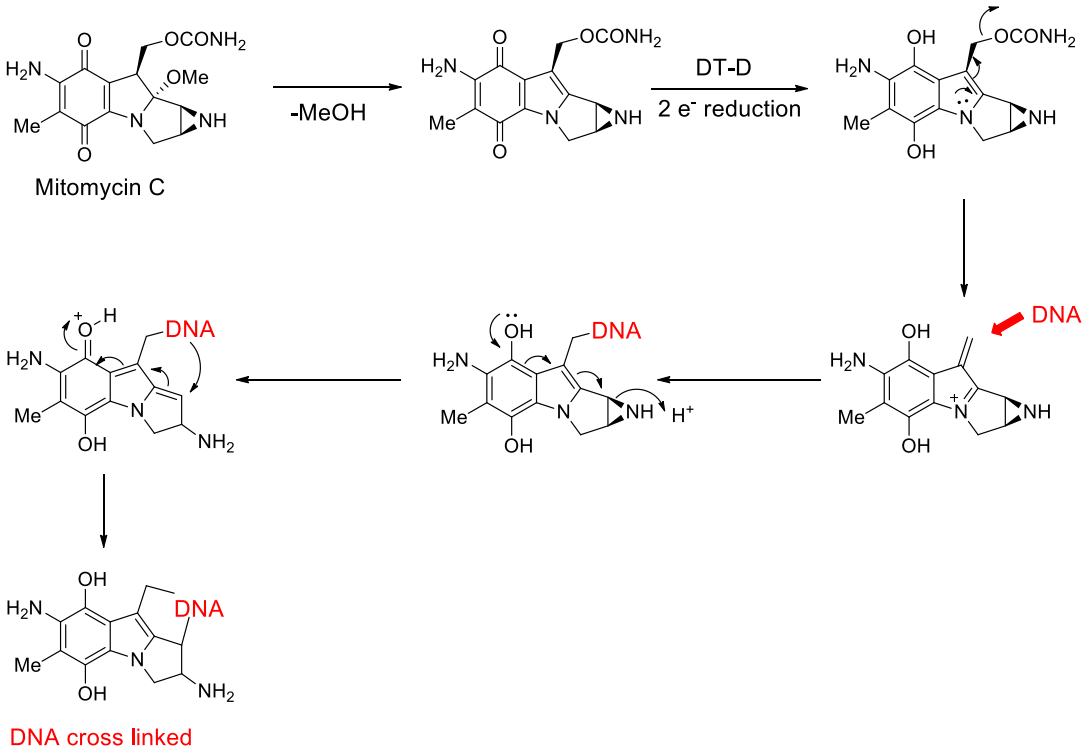

Scheme 2.1. Bioreduction of Mitomycin C by DT-D.

The activation of MMC begins with removal of methanol to form an indolequinone moiety that undergoes two electron reduction by DT-D and forms the electron rich dihydroxyindole capable of crosslinking nucleophilic sites of DNA.[2]

A number of indolequinone based prodrugs have been developed as bioreductive prodrugs activated by DT-D.[3] Indolequinones have been used as a delivery vehicle for cytotoxic species under bioreductive environment by covalently linking a cytotoxic species at the C-3 position.[1d, 4] Using the concept of indolequinones as delivery vehicle for cancer cells over-expressing DT-D, an indolequinone-based NO donor is proposed. This NO donor is expected to undergo activation by DT-D and can be used as a tool to deliver NO within cells that express this enzyme. Diazeniumdiolate is used as a source of NO in the design of novel DT-D activated NO donor. Thus, the proposed mechanism for bioreduction of indolequinone **A** is as follows: in the presence of DT-D enzyme, substrate **A** undergoes two electron reduction with the help of cofactors NADPH and FAD to form the dihydroxyindole intermediate **B** (Scheme 2.2). The reduction of indolequinone to the dihydroxyindole increases the electron density on the indole nitrogen and as a result, rearrangement of electrons take place to release the diazeniumdiolate and potentially cytotoxic DNA alkylating alkenyliminium species (C). The free diazeniumdiolate in physiological medium undergoes hydrolysis to release NO.

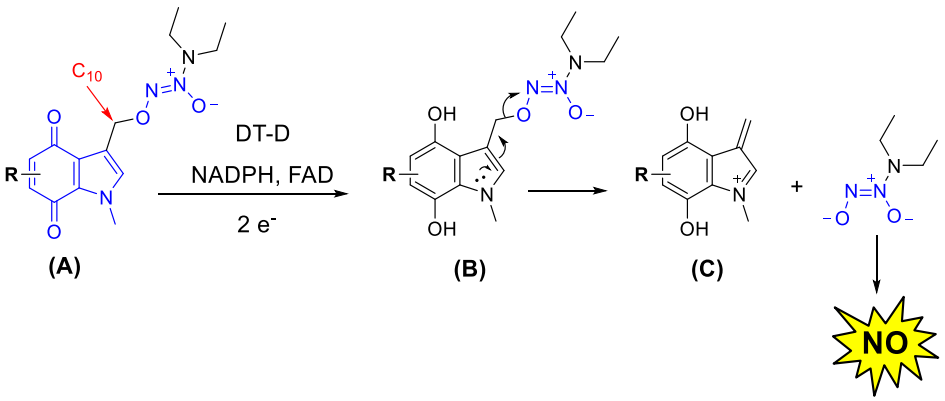

Scheme 2.2. Proposed model for bioreduction of indolequinone based NO donor.

2.2. Results and discussion

2.2.1. INDQ/NO: Synthesis and evaluation of NO generation in buffer

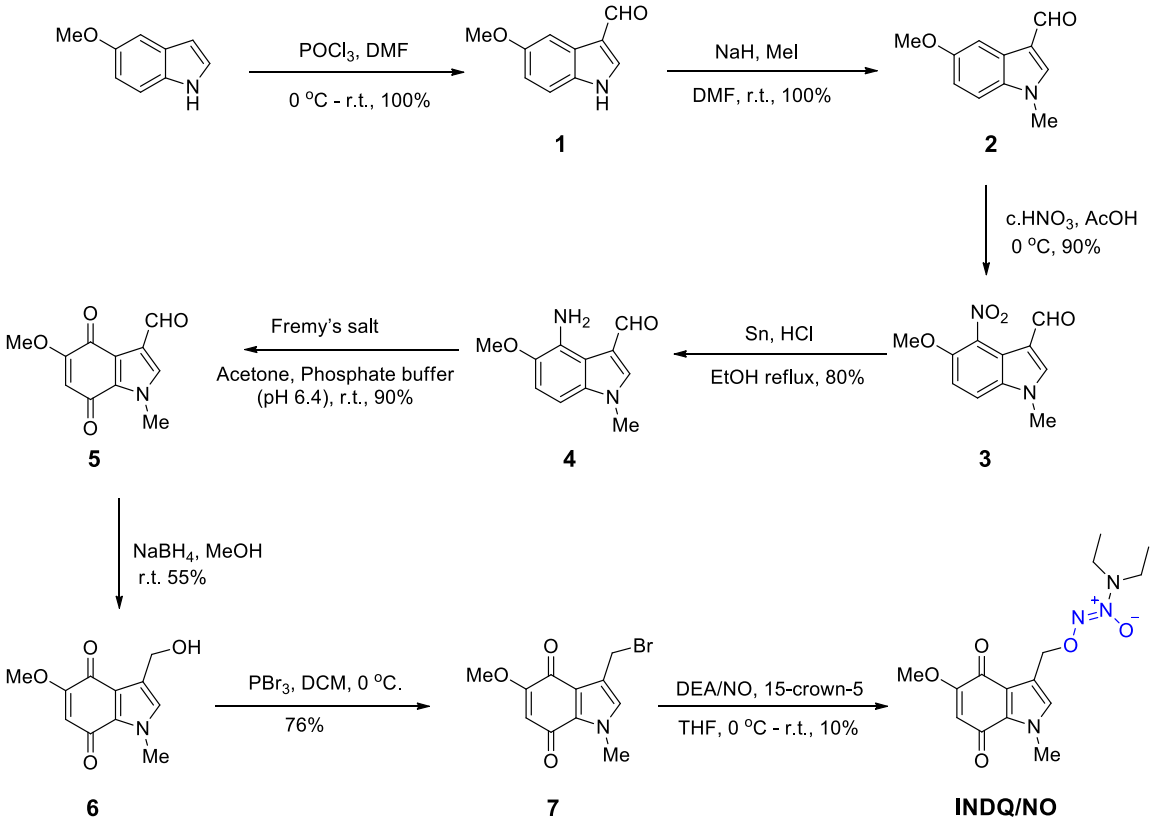

Scheme 2.3. Synthesis of **INDQ/NO**.

In order to test our hypothesis of DT-D activated NO donor, **INDQ/NO** was synthesized (Scheme 2.3). The synthesis of **INDQ/NO** was started with formylation of 5-methoxyindole to form compound **1** in quantitative yield. The indole nitrogen was protected with methyl group using methyl iodide in the presence of sodium hydride to obtain compound **2** in 100% yield. Nitration of compound **2** using concentrated nitric acid in acetic acid gave compound **3** in 90% yield. The nitro group was reduced using tin-hydrochloride to obtain compound **4** in 80% yield. The oxidation of amino indole **4** to indolequinone **5** was achieved using Fremy's salt in 90% yield. Compound **5** was subsequently reduced using $NaBH_4$ to afford **6** in 55% yield. The synthesis of compounds **1**-**6** were performed using reported procedures.[1d, 4b] In order to introduce a

diazeniumdiolate at the 10-position, the alcohol **6** was converted into the bromide **7** using PBr_3 in DCM. The bromide **7** (crude) was reacted soon after preparation with sodium N, N-(diethylamino)diazen-1-ium-1,2-diolate (DEA/NO) in THF in the presence of 15-crown-5 to afford **INDQ/NO**, in 10% yield.

In order to test whether **INDQ/NO** was a suitable substrate for DT-D, it was treated with DT-D in the presence of NADPH and FAD at 37 ^{o}C in pH 7.4 buffer. HPLC analysis was performed to study DT-D reduction of **INDQ/NO** by monitoring the disappearance of peak for **INDQ/NO**. Significant amount of **INDQ/NO** (~ 70%) was consumed within 5 min of DT-D addition and by the end of 3 h, 80% of **INDQ/NO** was consumed (Figure 2.1.A). The data indicated that **INDQ/NO** was a substrate for bioreduction by DT-D. As we found **INDQ/NO** was reduced by DT-D, we next estimated the amount of NO released upon reduction over time.

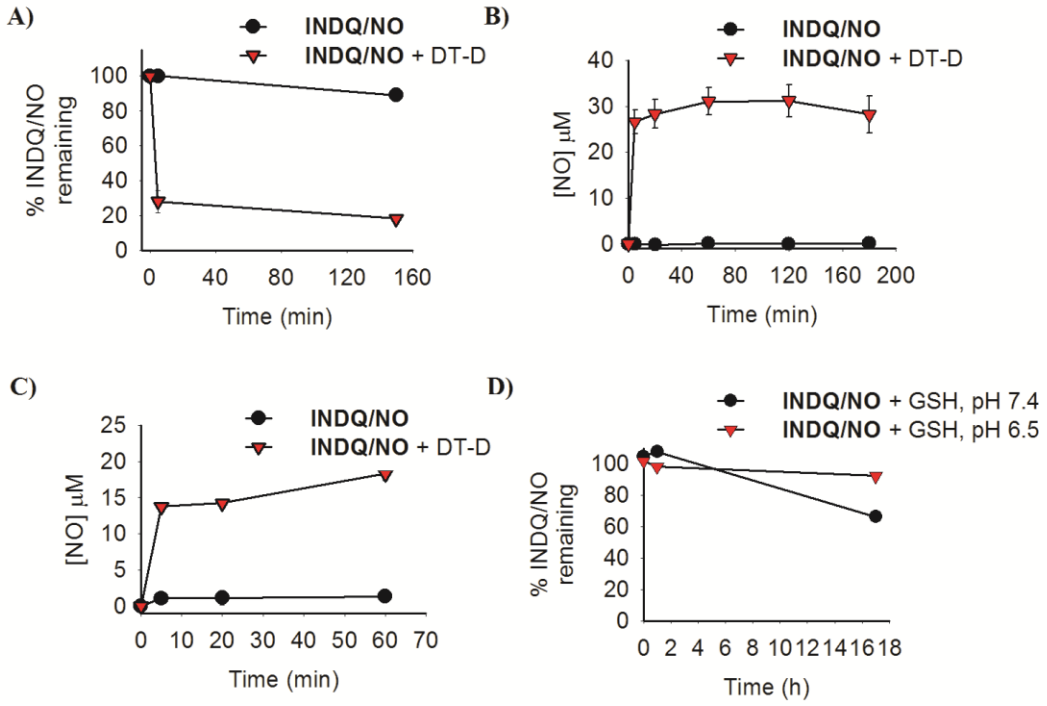

Figure 2.1. A) HPLC decompostion profiles of **INDQ/NO** (50 µM) in pH 7.4 buffer in the presence and absence of DT-D. **B)** NO release from **INDQ/NO** (50 µM) in the presence and absence of DT-D in pH 7.4 buffer detected using chemiluminesence based assay. **C)** NO release from **INDQ/NO** (50 µM) in the presence and absence of DT-D in pH 6.5 buffer detected using chemiluminesence based assay. **D)** Stablity of **INDQ/NO** (50 µM) in the presence of glutathione (20 eq.) in buffers with pH 7.4 and 6.5 at 37 ^{o}C.

In order to study the release of NO from **INDQ/NO**, a chemiluminescence based NO detection method was used. Incubation of **INDQ/NO** in the presence DT-D in pH 7.4 buffer released NO (~ 30 µM) within 5 min (Figure 2.1.B). However, incubation of **INDQ/NO** in pH 7.4 buffer in the absence of DT-D under similar conditions, did not release NO in the buffer. Thus, **INDQ/NO** was reduced in aqueous media in the presence of DT-D to release NO.

Solid tumor cells are characterised by low pH conditions in certain regions.[5] Thus, we investigated the metabolism of **INDQ/NO** by DT-D to release NO at low pH by incubation **INDQ/NO** in pH 6.5 buffer in the presence and absence of DT-D for 60 min. It was observed that at low pH condition, the amount of NO released was ~ 20 µM at the end of 60 min. In pH 7.4, however, the amount of NO released by DT-D was slightly more (~30 µM). Possibly due to acidic condition, the release of NO from the dihydroxyindole intermediate **(B)** had been delayed which resulted in low NO yield in pH 6.5 buffer (Scheme 2.1.C).

2.2.2. Stability of INDQ/NO in the presence of GSH

Glutathione (GSH) is an important anti-oxidant present in eukaryotic cells which protects the cell from damage caused by reactive species. In many cancers, the expression levels of GSH are elevated (approx. 10 mM) that protect cancer cells from xenobiotics, ionizing radiations, free radicals, etc.[6] GSH alongwith glutathione-S-transferase (GST) has been used in the activation of (2, 4-dinitrophenyl) diazeniumdiolates, due to its nucleophilic nature and high intracellular levels of GSH in differnet cancer cells (Scheme 2.4). GST catalyses the nucleophilic substituion of diazeniumdiolate by GSH that releases free diazeniumdioalte in physiological media to release NO.[7]

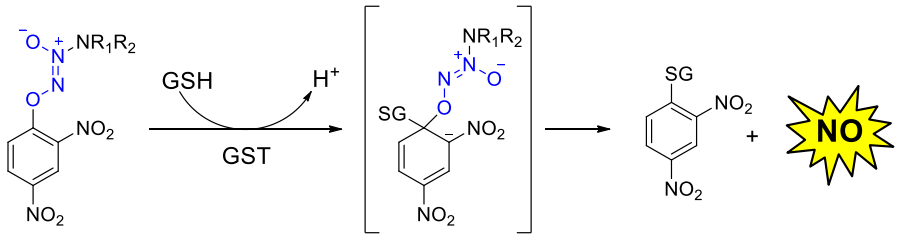

Scheme 2.4. Activation of (2, 4-dinitrophenyl) diazeniumdiolate by GSH catalysed by GST.

Therefore, **INDQ/NO** can probably react with GSH and get metabolised when treated with cells. In order to test the stability of **INDQ/NO** towards GSH, it was reacted with GSH (20 equivalents) in pH 7.4 buffer at 37 ^{o}C. HPLC analysis was performed to monitor decomposition of **INDQ/NO** during 1 h. It was found that **INDQ/NO** was inert to GSH over peroid of 1 h. However, approximately 70% of **INDQ/NO** remained in the pH 7.4 buffer after 17 h. The stability of **INDQ/NO** was also examined at pH 6.5. HPLC analysis data showed nearly 92% **INDQ/NO** remained in the pH 6.5 buffer even after 17 h. These results suggest that **INDQ/NO** was stable towards glutathione at pH 6.5 and it reacted sluggishly at pH 7.4 (Figure 2.1.D). Thus, **INDQ/NO** was found to be quite stable towards GSH, a predominant cellular thiol.

2.2.3. Cell-based studies with INDQ/NO

The activation of **INDQ/NO** in cellular environment was analysed by performing cell based assays. We selected three human cancer cell lines known to over express the bioreductive enzyme DT-D, namely, DLD-1 human colorectal adenocarcinoma,[8] T-24 human renal carcinoma and HeLa human cervical carcinoma cells.[1b, 9] To begin with, we performed a cell based experiment to check whether **INDQ/NO** gets activated by cells or not. We incubated **INDQ/NO** in DLD-1 cells and studied NO released in extracellular medium using NOA over 5 h. We found that DLD-1 cells in the presence of **INDQ/NO** release significant amount of NO (~18 μM). However, negligible amount of NO was produced by DLD-1 cells in the absence of **INDQ/NO** (Figure 2.2). Thus, this experiment suggested that **INDQ/NO** was activated within cells to generate NO.

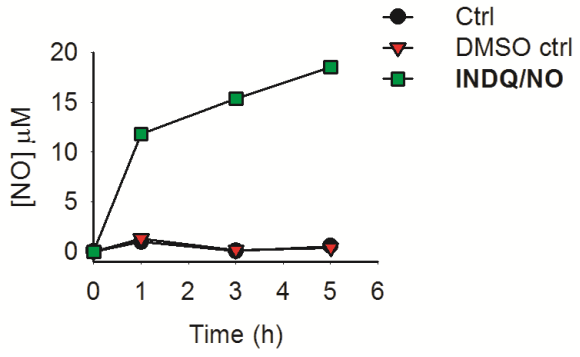

Figure 2.2. Estimation of NO generation in extracellular medium of DLD-1 upon incubation with **INDQ/NO** (25 μM) detected using a chemiluminesence based assay.

Next the efficiency of **INDQ/NO** to inhibit cell proliferation was examined using a standard cell viability assay and a half maximal inhibitory concentration, IC_{50}: concentration of test compound at which 50% of the cells are killed, was determined. Upon incubation of **INDQ/NO** in DLD-1 cells for 72 h, it effectively inhibited DLD-1 proliferation with calculated IC_{50} to be 0.25 µM. Similarly, **INDQ/NO** exhibited anti-proliferative effects in HeLa cells with an IC_{50} of 0.96 µM and in T-24 cells with an IC_{50} of 0.56 µM (Figure 2.3). We performed cell viability assay with compound **6** in DLD-1 cells and found it was killing 50% of cells at a concentration higher than IC_{50} of **INDQ/NO** in DLD-1 by a factor of fifty.

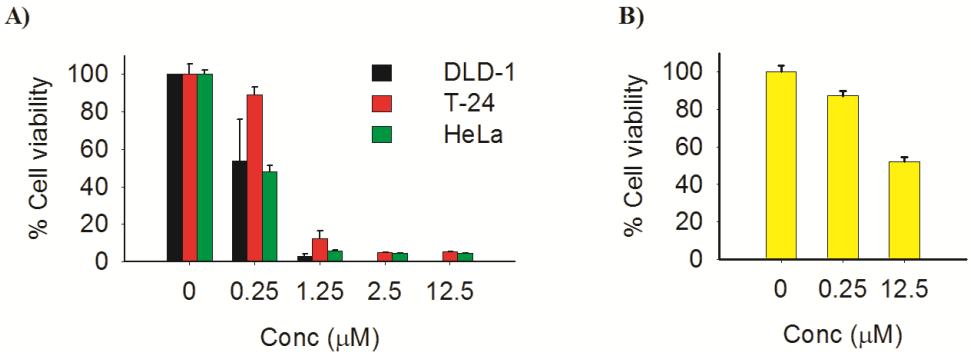

Figure 2.3. A) Cancer cell proliferation inhibition in DLD-1, T-24 and HeLa cells after 72 h of incubation with **INDQ/NO** using a standard cell viability assay. B**)** Cancer cell proliferation inhibition in DLD-1after 72 h of incubation with compound **6** using a standard cell viability assay.

Hernick *et. al* reported the 3-acetoxy indolequinone to be potent cell growth inhibitor cancer cells expressing DT-D.[1d] The observed cytotoxicity was attributed to the indolequinone moiety. An indolequinone vehicle used for delivery of cytotoxin exhibits growth inhibitory in two fold action: delivery of cytotoxic molecule and release of potentially cytotoxic DNA alkylating indolequinone iminium species within cell. Therefore, the cytotoxicity of **INDQ/NO** in the cancer cells over-expressing DT-D was, in part, due to NO released upon bioreduction.

RNS are well known to induce DNA damage, especially double strand breaks (DSBs).[10] The extent of DSBs induced by cytotoxic species is frequently investigated by using an immunofluorescence assay for detecting γ- H2AX.[11] DNA damage occurring either due to endogenous or exogenous factors, leads to phosphorylation of serine-139 of a histone

protein, H2AX in the nucleus. This phosphorylation acts as a signal to initiate detection of DNA damage sites followed by its repair. γ- H2AX formation is a biomarker for DNA DSBs. Using a fluorescently-labelled antibody for γ- H2AX, the damaged sites can be visualized using an immunofluorescence assay as fluorescent spots in nuclei called foci.

Therefore, in order to check whether NO released by **INDQ/NO** damaged DNA, we performed immunofluorescence assay for detecting γ- H2AX in HeLa cells. We incubated 10 μM of **INDQ/NO** in HeLa cells for 1.5 h. The immunofluorescence studies indicated that **INDQ/NO** induced a significant dose-dependent formation of DSBs (seen as foci) as early as 1.5 h of **INDQ/NO** treatment (Figure 2.4). This observation is consistent with an earlier report where NO release from JS-K, glutathione/glutathione-S-transferase activated NO induced apoptosis by damaging DNA by DSBs both in *in vitro* and *in vivo* human multiple myeloma cells.[10a]

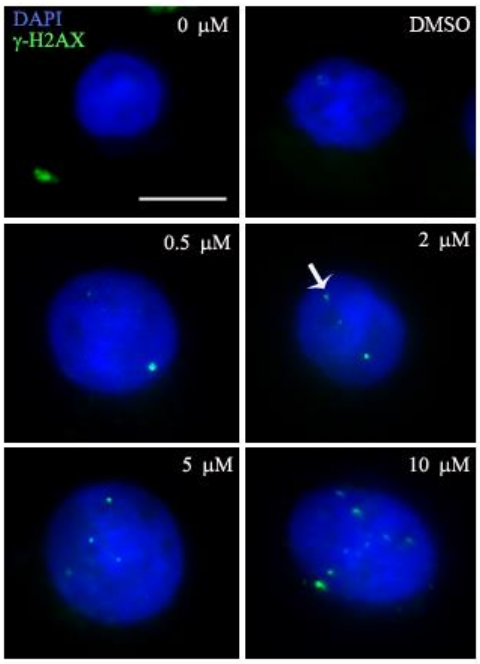

Figure 2.4. Representative images of HeLa cells labelled with anti-γ-H2AX antibody in immunofluorescence assays after treatment with **INDQ/NO** for 1.5 h. Nuclei were counterstained with DAPI. Arrow indicates γ-H2AX foci (Scale bar: ~5 μm).

2.2.4. 2-Me INDQ/NO: Synthesis and evaluation of NO generation

The metabolism of the indolequinone by DT-D has been found to be affected by introducing a substituent at the C-2 position. It has been reported that increasing the steric bulk at the C-2 of indolequinone, not only diminished the rate of its metabolism by DT-D, but also reduced the cytotoxicity of the C-2 substituted indolequinone-based prodrugs.[1c, 12] Using the concept, we proposed to synthesize **2-Me INDQ/NO,** C-2 substituted analogue of **INDQ/NO** and study the effects of DT-D metabolism on the release of NO. Using a similar synthetic route as for **INDQ/NO**, we synthesized **2-Me INDQ/NO** starting from 5-methoxy-2-methylindole (Scheme 2.5).

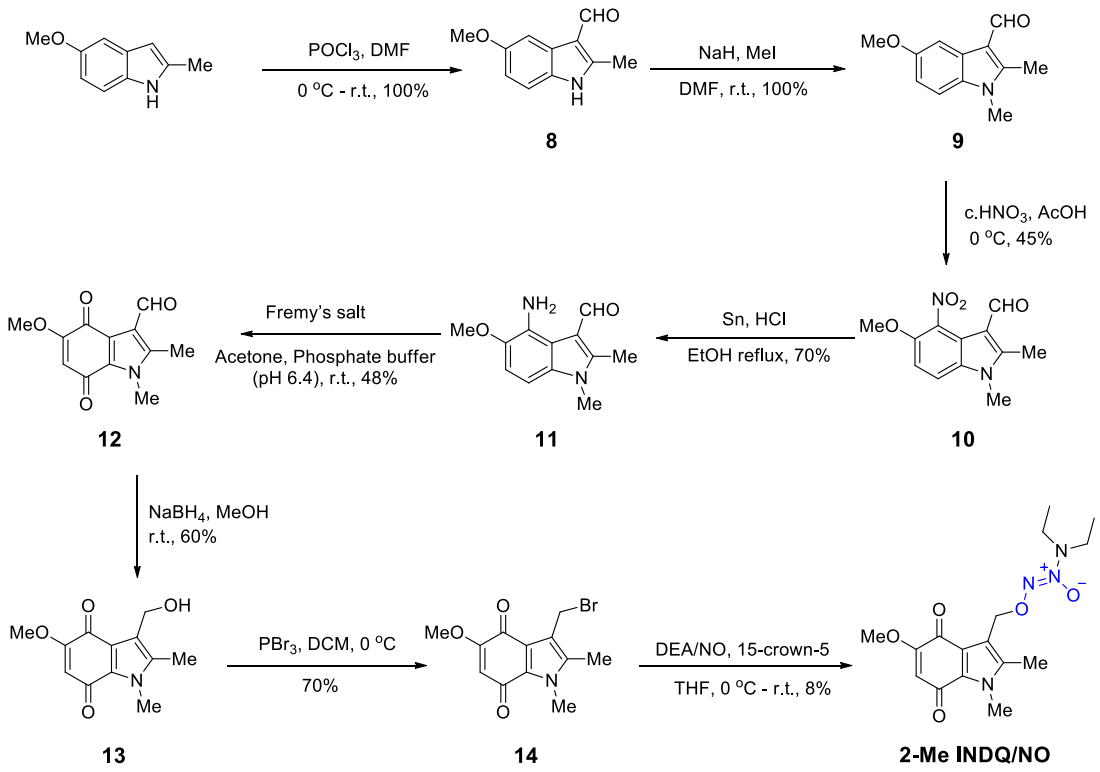

Scheme 2.5. Synthesis of **2-Me INDQ/NO**.

In order to study the metabolism of **2-Me INDQ/NO** by DT-D, it was incubated with DT-D in presence of NADPH and FAD at 37 °C in pH 7.4 buffer under conditions similar for **INDQ/NO**. HPLC analysis was performed to study the enzymatic reduction of **2-Me INDQ/NO** by DT-D. **2-MeINDQ/NO** was found to be barely reduced by DT-D even after 3 h. (Figure 2.5.A) and negligible amount of NO was released during

incubation of **2-Me INDQ/NO** with DT-D in pH 7.4 buffer (Figure 2.5.B). Thus we observed that the methyl substituent at C-2 position diminished the metabolism by DT-D in comparison with unsubstituted analogue, **INDQ/NO**.

To assess the effect of substitution on indolequinone in cellular assay, **2-Me INDQ/NO** was treated with cells and the cytotoxicity of the compound was evaluated. The cell viability assay was performed to study the cytotoxicity effect of **2-Me INDQ/NO** in DLD-1 and T-24. Although, **2-Me INDQ/NO** was also a good inhibitor of cancer cells but the IC_{50} values were higher compared to **INDQ/NO** (Table 2.1) indicating that due to slow DT-D metabolism, the cytotoxicity was also reduced. Indeed, C-2 methyl substitution diminished the activity of **INDQ/NO** due to hindered interaction with DT-D and also impedes NO release both in cell-free systems as well in cells.

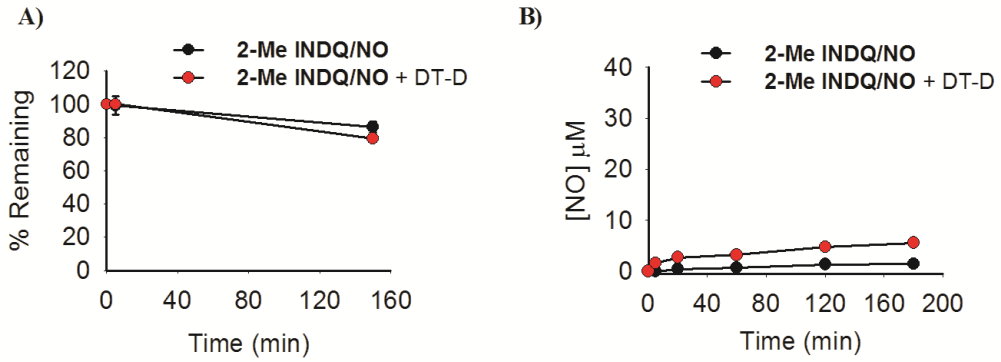

Figure 2.5. A) HPLC decompostion profiles of **2-Me INDQ/NO** (50 µM) in pH 7.4 buffer in the presence and absence of DT-D. **B)** NO release from **2-Me INDQ/NO** (50 µM) in presence and absence of DT-D detected using chemiluminisence based assay using NOA.

	INDQ/NO IC_{50} (µM)	**2-Me INDQ/NO** IC_{50} (µM)
DLD-1	0.25	3.0
T-24	0.56	9.4

Table 2.1. IC_{50} comparison for **INDQ/NO** and **2-Me INDQ/NO**.

2.3. Conclusion

In this chapter, we presented the design and synthesis of a new indolequinone based NO donor, **INDQ/NO**. The proposed mechanism for activation is as follows, the indolequinone scaffold undergoes two electron reduction in the presence of DT-D to form the electron rich dihydroxyindole intermediate. The electronic rearrangement leads to expulsion of the diazeniumdiolate, which then hydrolyze to release NO. **INDQ/NO** was found to release NO in the presence of DT-D at physiological conditions. From the cell-based experiments, it was shown that **INDQ/NO** was bioreductively activated by DLD-1 human colorectal adenomacarcinoma cells to release NO in extracellular media. The cytotoxicity assays performed in the three human cancer cell lines known to over-express DT-D implied **INDQ/NO** was a potent inhibitor of proliferation with good IC_{50} values. We also showed using immunofluorescence assay for detecting γ-H2AX that NO released from **INDQ/NO** led to cellular DNA damage. Further, we also demonstrated that by increasing the steric bulk at C-2 position of indolequinone with introduction of methyl, the release of NO was slowed down due to reduced metabolism of **2-Me INDQ/NO** by DT-D.

2.4. Experimental and characterization data

2.4.1. Experimental section

Compounds 1[13], 2 – 6[1d], 8[13], and 9 – 14[14] have been previously reported and analytical data that we collected were consistent with the reported values.

Synthesis of 3-(bromomethyl)-5-methoxy-1-methyl-1H–indole-4,7-dione, 7.

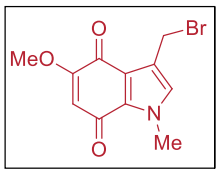

To an ice cold solution of **6** (0.31 g, 1.40 mmol) in dry DCM (15 mL), PBr_3 (0.26 mL, 2.80 mmol) was added under a nitrogen atmosphere and the reaction mixture was stirred at 0 ^oC for 15 min. The reaction mixture was quenched with saturated $NaHCO_3$ solution (10 mL) and extracted using DCM (3×10 mL). The combined organic layer was washed with brine, dried (Na_2SO_4), filtered and the filtrate was concentrated to give a crude orange solid which was used without further purification (0.32 g, 84%): FT-IR (ν_{max}, cm^{-1}): 1666, 1645, 1596, 1517, 1215, 1031; ^1H NMR ($CDCl_3$, 400 MHz): δ 6.87 (s, 1H), 5.68 (s, 1H), 4.69 (s, 2H), 3.93 (s, 3H), 3.82 (s, 3H); ^{13}C NMR ($CDCl_3$, 100 MHz): δ 179.0, 177.5, 160.4, 130.2, 130.0, 121.7, 120.8, 106.9, 56.7, 36.5, 23.6; MALDI for $C_{11}H_{10}{}^{79}BrNO_3[M+K]^+$: Calcd., 321.948, Found, 321.920.

Synthesis of 3-(bromomethyl)-5-methoxy-1, 2-dimethyl-1H-indole-4,7-dione, 15.

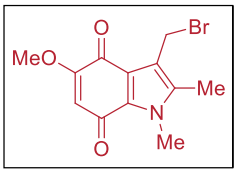

A procedure similar to the synthesis of **7** was used. Starting from **14** (0.13 g, 0.55 mmol) and PBr_3 (0.10 mL, 1.12 mmol), an orange colored crude compound was obtained (0.15 g, 90%): FT-IR (ν_{max}, cm^{-1}): 1671, 1634, 1597, 1509, 1460, 1336, 1183, 1065; ^1H NMR ($CDCl_3$, 400 MHz): δ 5.62 (s, 1H), 4.77 (s, 2H), 3.89 (s, 3H), 3.80 (s, 3H), 2.25 (s, 3H); MALDI for $C_{12}H_{12}{}^{79}BrNO_3[M+K]^+$: Calcd., 335.9638, Found, 335.9079.

Synthesis of (Z)-3, 3-diethyl-1-(2-(5-methoxy-1-methyl-4, 7-dioxo-4,7-dihydro-1H-indol-3-yl)ethyl)triaz-1-ene 2-oxide, INDQ/NO.

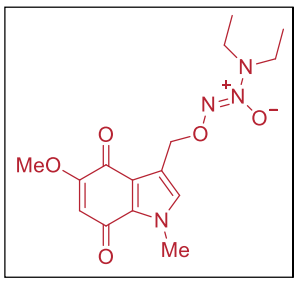

To an ice cold solution of DEA/NO (0.11g, 0.70 mmol) in THF (10 mL), 15-crown-5 (0.05 mL) was added and the reaction mixture was stirred at 0 ^oC for 15 min under a nitrogen atmosphere. Compound **7** (0.10 g, 0.35 mmol) was added to the

reaction mixture at 0 ^{o}C and allowed to stir at room temperature for 6 h. The solvent was evaporated, diluted with water (25 mL) and aqueous solution was extracted with DCM (3×15 mL). The combined organic layer was washed with brine, dried (Na_2SO_4), filtered and the filtrate was concentrated to give a crude compound, which was purified using semi preparative HPLC to obtain a yellow solid (15 mg, 10%): FT-IR (ν_{max}, cm^{-1}): 2360, 2341, 1672, 1646, 1597, 1508, 1189, 1003; ^{1}H NMR ($CDCl_3$, 400 MHz): δ 6.84 (s, 1H), 5.66 (s, 1H), 5.49 (s, 2H), 3.92 (s, 3H), 3.81 (s, 3H), 3.11 (q, *J* = 7.0 Hz, 4H), 1.09 (t, *J* = 6.9 Hz, 6H); ^{13}C NMR ($CDCl_3$, 100 MHz): δ 179.1, 177.5, 160.4, 129.9, 129.1, 121.4, 119.7, 106.9, 67.7, 56.6, 48.7, 36.4, 11.6; MALDI for $C_{15}H_{20}N_4O_5[M+Na]^+$: Calcd., 359.1331, Found,359.07; Anal. Calcd. for $C_{15}H_{20}N_4O_5$: C, 53.56; H, 5.99; N, 16.66. Found: C, 53.72; H, 5.068; N, 16.17.

Synthesis of (Z)-3,3-diethyl-1-(2-(5-methoxy-1,2-dimethyl-4,7-dioxo-4,7-dihydro-1H-indol-3-yl)ethyl)triaz-1-ene 2-oxide, 2-Me INDQ/NO.

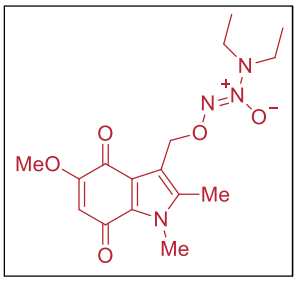

A procedure similar to synthesis of **INDQ/NO** was followed. **14** (0.12 g, 0.5 mmol) was reacted with DEA/NO (0.09, 0.75 mmol). The crude reaction mixture was purified using semi-preparative HPLC to obtain an orange solid (15 mg, 8%): FT-IR (ν_{max}, cm^{-1}): 2921, 2853, 1675, 1639, 1510, 1464, 1224, 1152, 996; ^{1}H NMR ($CDCl_3$, 400 MHz): δ 5.61 (s, 1H), 5.49 (s, 2H), 3.88 (s, 3H), 3.79 (s, 3H), 3.09 (q, *J* = 7.1 Hz, 4H), 2.29 (s, 3H), 1.07 (t, *J* = 7.1 Hz, 6H); ^{13}C NMR ($CDCl_3$, 100 MHz): δ 178.9, 177.8, 159.7, 138.7, 128.9, 121.8, 115.1, 106.7, 65.8, 56.5, 48.6, 32.4, 11.6, 9.9; MALDI for $C_{16}H_{22}N_4O_5[M+K]^+$: Calcd., 389.1227, Found, 389.0968.

2.4.2. Stability of INDQ/NO in glutathione

A 10 mM stock solution of **INDQ/NO** was prepared in DMSO and 10 mM stock solution of GSH was prepared in tris(hydroxymethyl)aminomethane (TRIS) buffer pH 7.4. The reaction mixture was prepared by dissolving 5 µL of **INDQ/NO** and 100 µL of GSH stock solution in 895 µL of TRIS buffer pH 7.4. The corresponding blank solution was prepared by dissolving 5 µL of **INDQ/NO** in 995 µL of TRIS buffer pH 7.4. The reaction mixtures were stirred at 37 ^{o}C and the decomposition of starting material was monitored

by HPLC. Similar reaction conditions were used for determining the stability of **INDQ/NO** in TRIS buffer pH 6.5.

2.4.3. DT-Diaphorase mediated reduction

A 10 mM stock solution of **INDQ/NO** was prepared in DMSO and stock solutions of 10 mM NADPH and 1 mM FAD were prepared in TRIS buffer pH 7.4. The enzyme stock solution was prepared by dissolving 1.5 mg of the lyophilized human DT-Diaphorase (Sigma) in TRIS buffer pH 7.4. 20 μL of this enzyme solution was further diluted to 100 μL and was used in the subsequent reactions. The reaction mixture was prepared by dissolving 10 μL of **INDQ/NO**, 10 μL of FAD solution, 40 μL of NADPH solution and 2 μL of the enzyme solution in 1938 μL of TRIS buffer. The corresponding blank solution was prepared by dissolving 10 μL of test compound in 1990 μL of TRIS buffer. The reaction mixture and blank solution were stirred at 37 ^{o}C and monitored by HPLC. A similar methodology for the study of decomposition of **2-Me INDQ/NO** was used. **INDQ/NO** was similarly reduced using DT-diaphorase in pH 6.5. The decomposition of **INDQ/NO** was monitored using HPLC.

2.4.4. NO detection

A Sievers Nitric Oxide Analyzer (NOA 280i) was used to determine amount of NO being produced during decomposition. The reservoir contained NaI (50 mg) dissolved in 2 ml deionised water and acetic acid (5 mL) and was bubbled with argon, the carrier gas. A 10 mM stock solution of $NaNO_2$ was prepared in TRIS buffer pH 7.4. The standard calibration curve was obtained by using a concentration range varying from 0-50μM of $NaNO_2$ solutions. 10 μL of each varying concentrations were injected in Sievers Nitric Oxide Analyzer (NOA 280i). For quantifying amount of NO release, the area under the peak of each signal was quantified and a standard calibration curve was obtained (Figure 2.6). The reading for each concentration was average of three readings.

For quantifying amount of NO release from enzymatic reduction of **INDQ/NO**, the reaction mixtures were prepared as mentioned in section 2.4.3 for both pH 6.5 and 7.4 buffers and 10 μL of the reaction mixture and blank solution were injected at the specified time points into Sievers Nitric Oxide Analyzer (NOA 280i). The amount of NO

released was measured using the $NaNO_2$ standard calibration curve; (Figure 2.6, y = 40.86x + 30.24, R^2 = 0.997). A similar method was used for quantifying NO release from DT-D mediated reduction of **2-Me INDQ/NO**.

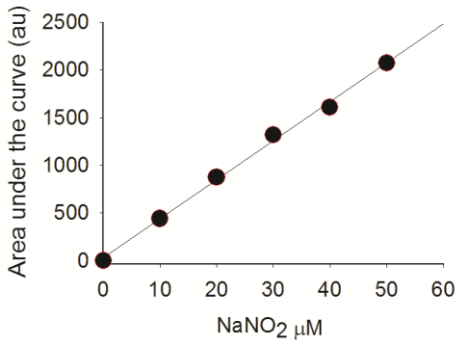

Figure 2.6. The standard calibration curve for $NaNO_2$ generated using chemiluminescence based NOA 280i.

2.4.5. Extracellular NO release in DLD-1 cells

DLD-1 human colorectal adenocarcinoma cells were seeded at a concentration of 1.0×10^6 cells/well in a 6-well plate in complete RPMI 1640 overnight at 37 ^oC. 5 μL of **INDQ/NO** (20 mM stock solution) was dissolved in 4 mL RPMI media to obtain 25 μM **INDQ/NO** solution. 2mL of this solution was added into two wells. Similarly, DMSO blank solution was prepared by dissolving 5μL DMSO in 4 mL of RPMI solution and 2mL was added into other two wells. The remaining two wells were incubated with media only. The culture media was aliquot at mentioned time intervals and injected in NOA 280i for quantification of released NO.

2.4.6. Cell viability assay

DLD-1 cells were seeded at a concentration of 3×10^4 cells/well overnight in a 96-well plate in complete RPMI 1640 media. Cells were exposed to varying concentrations of the test compounds prepared as a DMSO stock solution so that the final concentration of DMSO was 1%. The cells were incubated for 72 h at 37 ^oC. A stock solution of 3-(4, 5-dimethylthiazol-2-yl)-2, 5-diphenyl tetrazolium bromide (MTT) was prepared by dissolving 3.5 mg of MTT in 700 μL DPBS. This stock was diluted with 6.3 mL DPBS and 100 μL of the resulting solution was added to each well. After 4 h incubation, the media was removed carefully and 100 μL of DMSO was added. Spectrophotometric

analysis of each well using a microplate reader (Thermo Scientific Varioscan) at 570 nm was carried out to estimate cell viability. Similar MTT assays were performed with HeLa, human cervical adenocarcinoma cells and T24, human urinary bladder carcinoma. These cells were grown at a concentration of 1×10^4 cells/well overnight in a 96-well plate in complete DMEM media followed by test compound treatments at varying concentrations.

2.4.7. H2AX phosphorylation

HeLa cells were seeded at 0.2×10^6 cells/well in a 6-well plate overnight in complete DMEM at 37 ^oC. **INDQ/NO** treatment was done at a concentration range of 0.5 μM, 2 μM, 5 μM and 10 μM for 1.5 h at 37 ^oC with 0.1% DMSO. At the end of 1.5 h, **INDQ/NO** was removed and each well was washed three times with phosphate buffered saline (1×PBS) for 5 min each. 1 mL of cytoskeleton buffer (CSK) pH 7.5 was added to each well and incubated for 4 min. The cells were then fixed with 4% paraformaldehyde (PFA) for 10 min followed by washing with 0.1 M TRIS-HCl pH 7.4 for 5 min. The cells were again washed two times for 5 min each with 1×PBS. The cells were permealised by incubating with 0.2% triton-100 in PBS for 10 min. Cells were then washed three times with 1×PBS for 5 min each. The cells were treated with 1% bovine serum albumin (BSA) in phosphate buffered saline with tween-20 (PBST) for 30 min for blocking and were then washed three times with 1×PBS. The primary antibody of H2AX (Anti-phospho-Histone H2A.X (Ser139) Antibody, clone JBW301, FITC conjugate; 16-202A; Upstate) was diluted in ratio1:200. The cells were incubated with 50 μL of the diluted primary antibody solution for 1 h in dark and then washed three times with 1×PBS. The cells were stained with 1 mL of DAPI in 2xSSC solution for 3 min, washed with 1×PBS for 1 min and mounted on the slide. The fluorescent images were obtained using Zeiss Axio Imager.Z2 software. The slides were observed under the SKY microscope using FITC filter. For each concentration around 30 nuclei were viewed randomly for each set of experiment. The result shown is an average of two experiments performed on two different days.

2.5. Spectral charts:

^{1}H NMR Spectrum (400 MHz, $CDCl_3$) of compound **7**

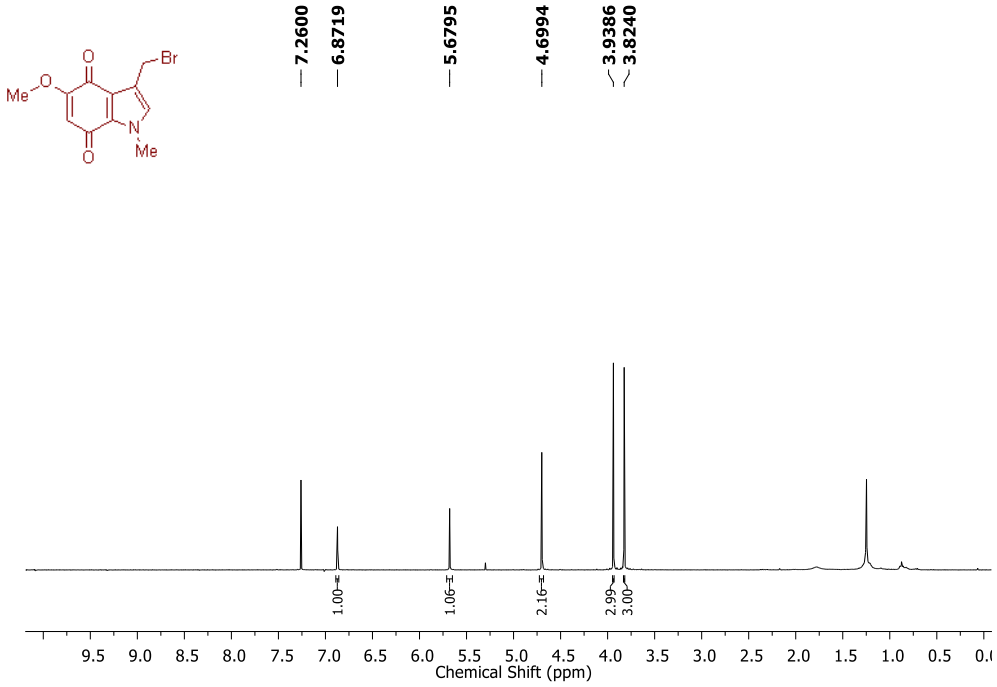

^{13}C NMR Spectrum (100 MHz, $CDCl_3$) of compound **7**

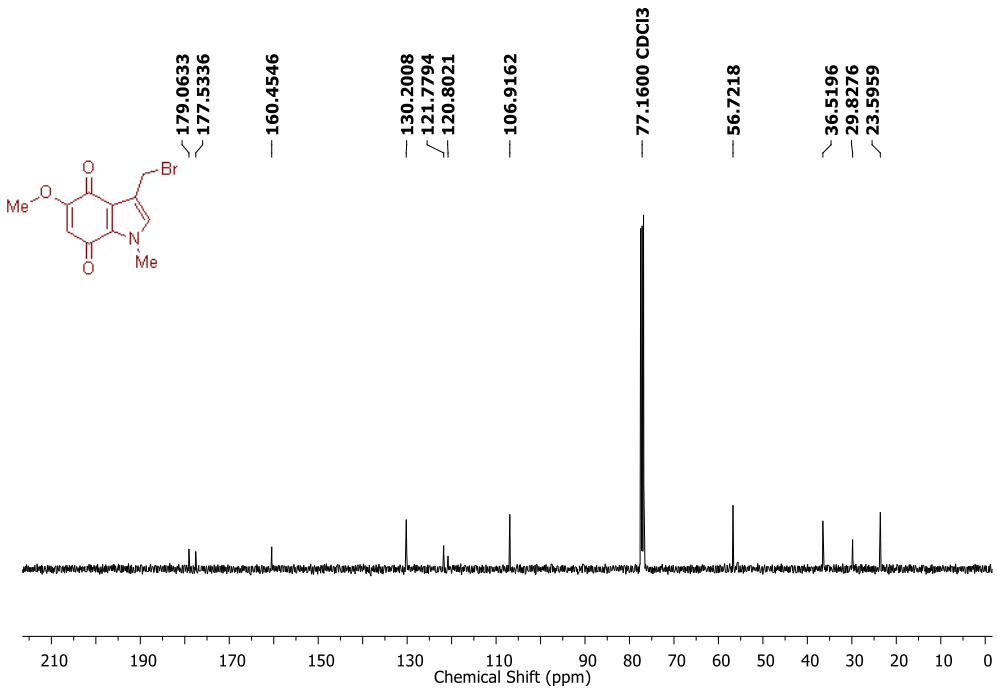

^{1}H NMR Spectrum (400 MHz, $CDCl_3$) of **INDQ/NO**

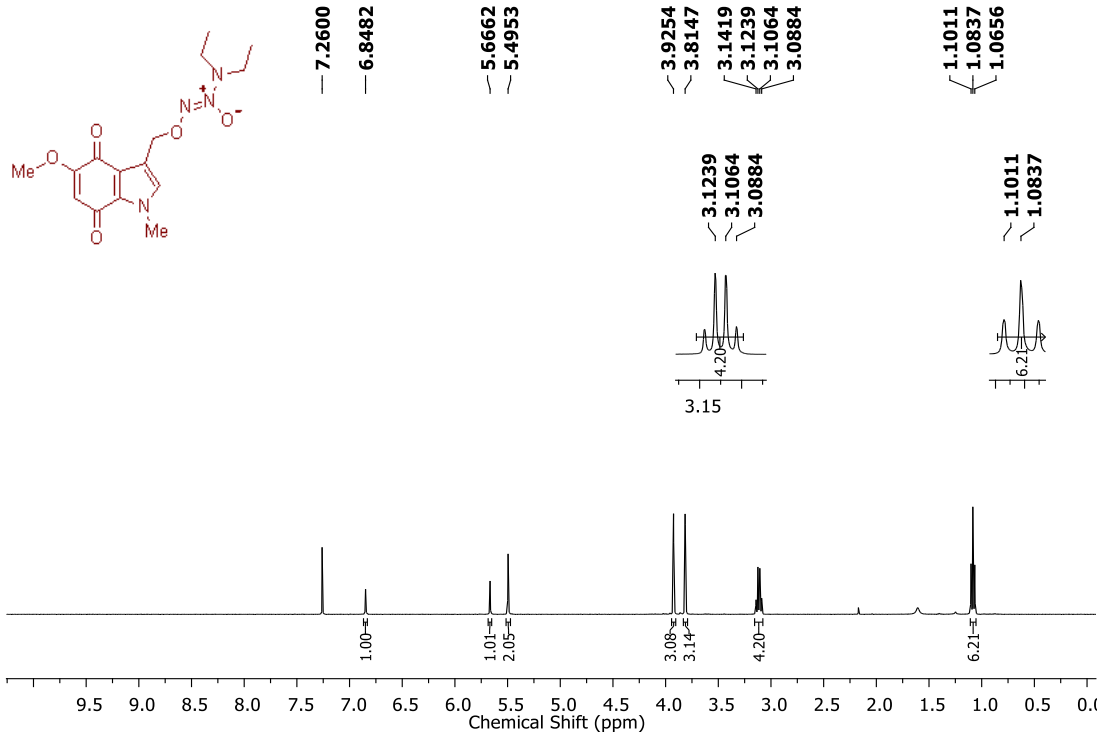

^{13}C NMR Spectrum (100 MHz, $CDCl_3$) of **INDQ/NO**

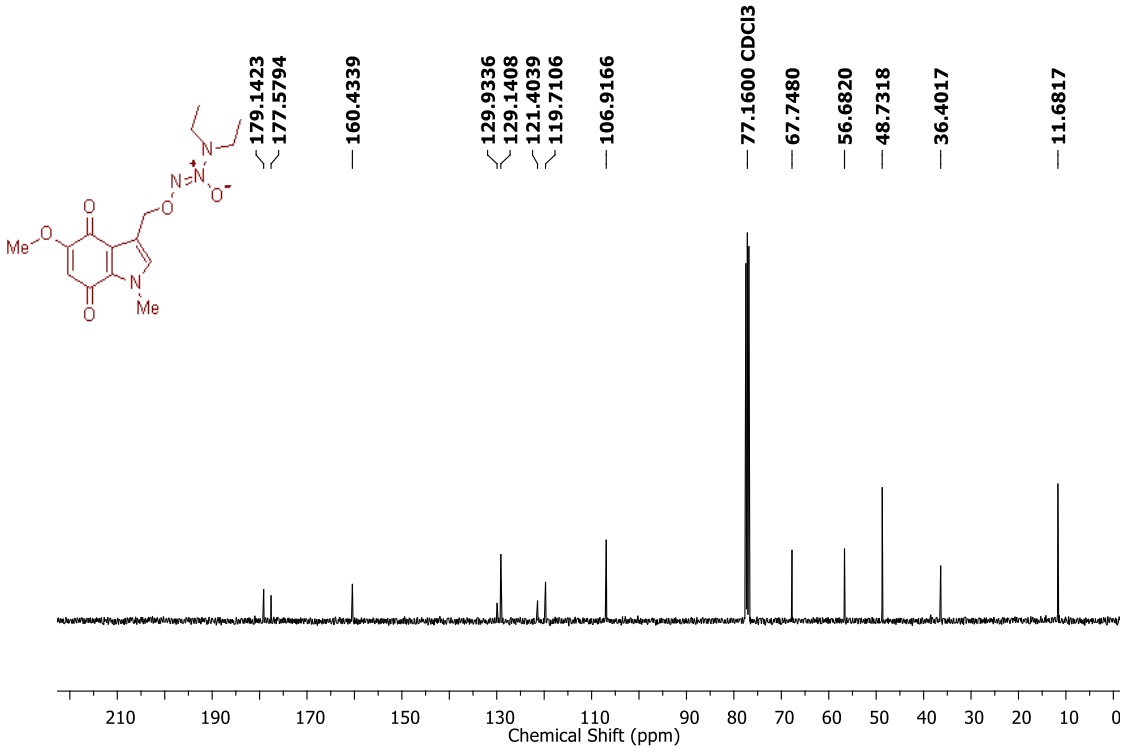

^{1}H NMR Spectrum (400 MHz, $CDCl_3$) of compound **14**

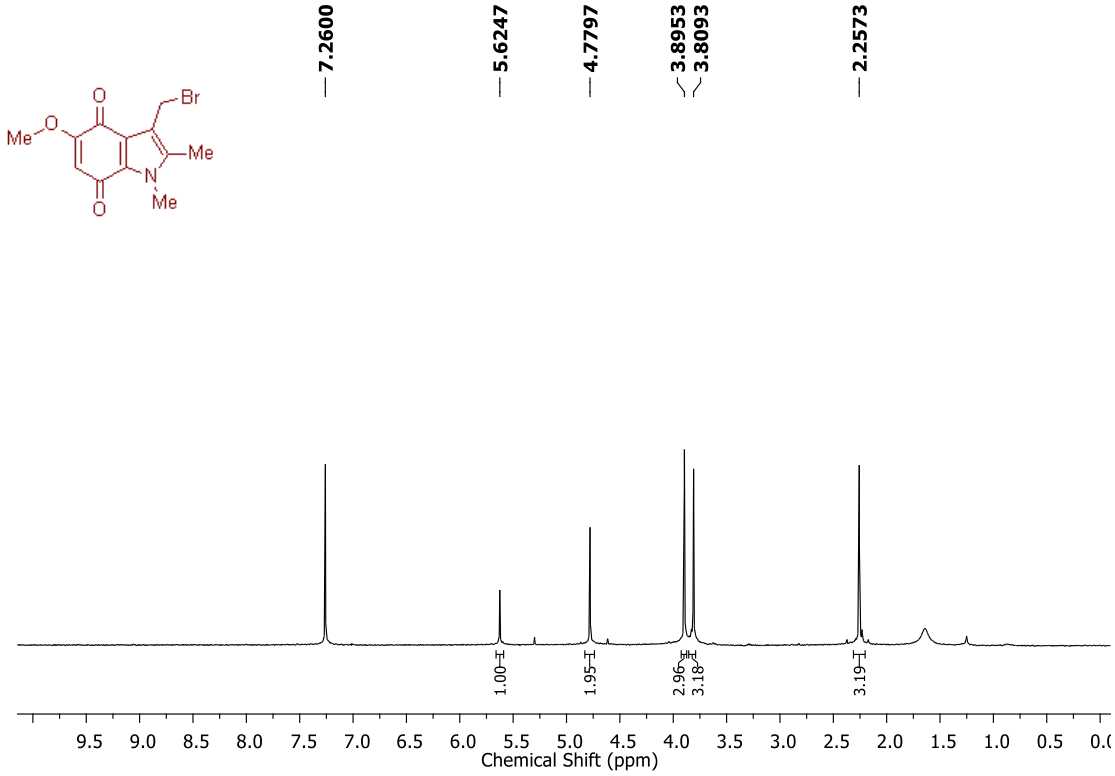

^{1}H NMR Spectrum (400 MHz, $CDCl_3$) of **2- Me INDQ/NO**

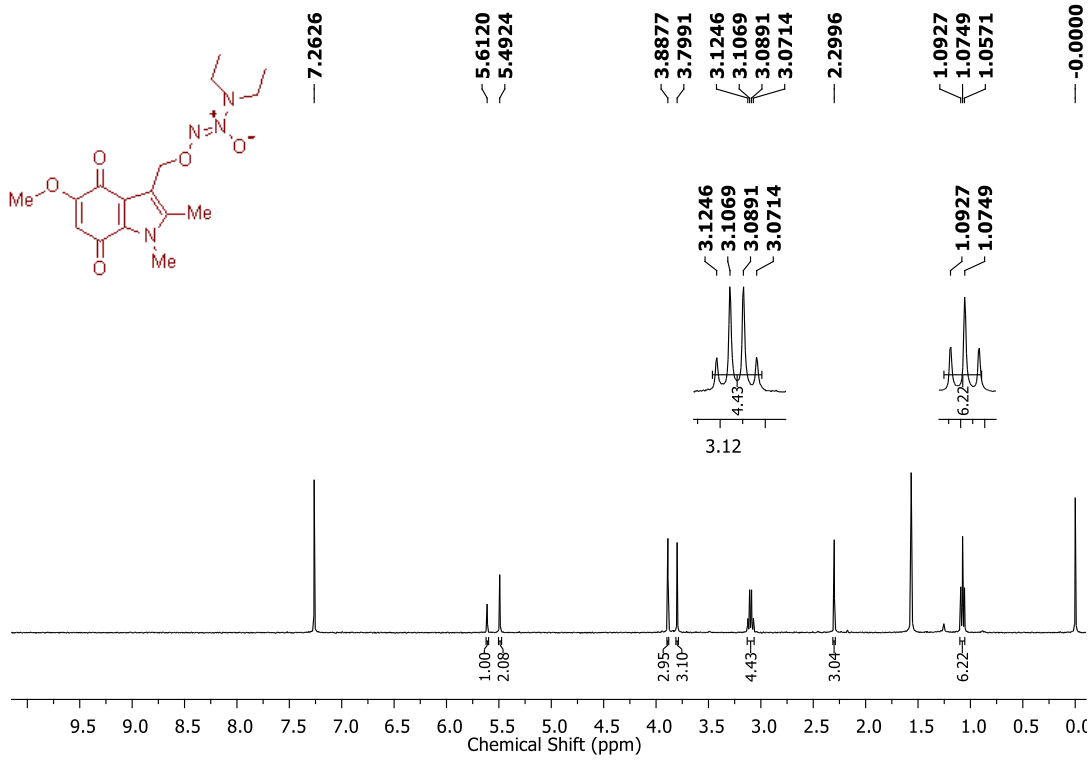

^{13}C NMR Spectrum (100 MHz, $CDCl_3$) of **2-Me INDQ/NO**

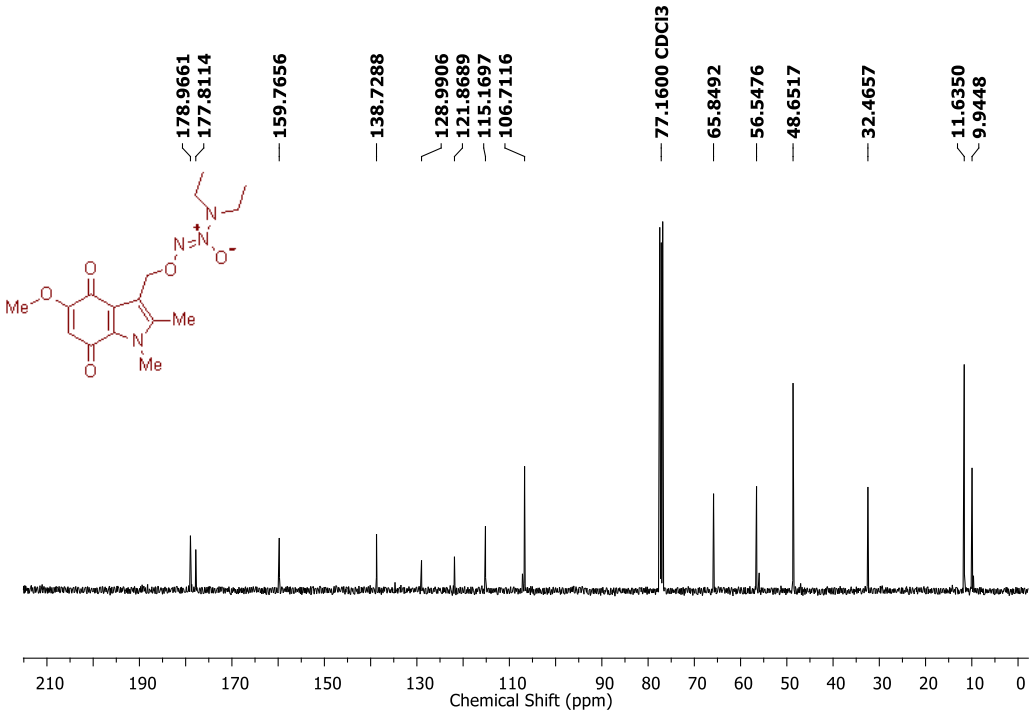

2.6. References:

1. (a) Brown, J. M.; Wilson, W. R., Exploiting tumour hypoxia in cancer treatment. *Nat Rev Cancer* **2004,***4* (6), 437-447; (b) Choudry, G. A.; Stewart, P. A. H.; Double, J. A.; Krul, M. R. L.; Naylor, B.; Flannigan, G. M.; Shah, T. K.; Brown, J. E.; Phillips, R. M., A novel strategy for NQO1 (NAD(P)H:quinone oxidoreductase, EC 1.6.99.2) mediated therapy of bladder cancer based on the pharmacological properties of EO9. *Br. J. Cancer* **2001,***85* (8), 1137-1146; (c) Colucci, M. A.; Couch, G. D.; Moody, C. J., Natural and synthetic quinones and their reduction by the quinone reductase enzyme NQO1: from synthetic organic chemistry to compounds with anticancer potential. *Org. Biomol. Chem.* **2008,***6* (4), 637-656; (d) Hernick, M.; Flader, C.; Borch, R. F., Design, Synthesis, and Biological Evaluation of Indolequinone Phosphoramidate Prodrugs Targeted to DT-diaphorase. *J. Med. Chem.* **2002,***45* (16), 3540-3548.

2. (a) Volpato, M.; Seargent, J.; Loadman, P. M.; Phillips, R. M., Formation of DNA interstrand cross-links as a marker of Mitomycin C bioreductive activation and chemosensitivity. *Eur. J. Cancer* **2005,***41* (9), 1331-1338; (b) He, Q.-Y.; Maruenda, H.; Tomasz, M., Novel Bioreductive Activation Mechanism of Mitomycin C Derivatives Bearing a Disulfide Substituent in Their Quinone. *J. Am. Chem. Soc.* **1994,***116* (20), 9349-9350; (c) Siegel, D.; Beall, H.; Senekowitsch, C.; Kasai, M.; Arai, H.; Gibson, N. W.; Ross, D., Bioreductive activation of mitomycin C by DT-diaphorase. *Biochemistry* **1992,***31* (34), 7879-7885.

3. (a) Huang, B.; Desai, A.; Tang, S.; Thomas, T. P.; Baker, J. R., The Synthesis of a c(RGDyK) Targeted SN38 Prodrug with an Indolequinone Structure for Bioreductive Drug Release. *Org. Lett.* **2010,***12* (7), 1384-1387; (b) Huang, B.; Tang, S.; Desai, A.; Cheng, X.-m.; Kotlyar, A.; Spek, A. V. D.; Thomas, T. P.; Baker Jr, J. R., Human plasma-mediated hypoxic activation of indolequinone-based naloxone pro-drugs. *Bioorg. Med. Chem. Lett.* **2009,***19* (17), 5016-5020; (c) Zhang, Z.; Tanabe, K.; Hatta, H.; Nishimoto, S.-i., Bioreduction activated prodrugs of camptothecin: molecular design, synthesis, activation mechanism and hypoxia selective cytotoxicity. *Org. Biomol. Chem.* **2005,***3* (10), 1905-1910; (d) Phillips, R. M.; Naylor, M. A.; Jaffar, M.; Doughty, S. W.; Everett, S. A.; Breen, A. G.; Choudry, G. A.; Stratford, I. J., Bioreductive Activation of a

Series of Indolequinones by Human DT-Diaphorase: Structure−Activity Relationships. *J. Med. Chem.* **1999,***42* (20), 4071-4080.

4. (a) Colucci, M. A.; Reigan, P.; Siegel, D.; Chilloux, A.; Ross, D.; Moody, C. J., Synthesis and Evaluation of 3-Aryloxymethyl-1,2-dimethylindole-4,7-diones as Mechanism-Based Inhibitors of NAD(P)H:Quinone Oxidoreductase 1 (NQO1) Activity. *J. Med. Chem.* **2007,***50* (23), 5780-5789; (b) Hernick, M.; Borch, R. F., Studies on the Mechanisms of Activation of Indolequinone Phosphoramidate Prodrugs. *J. Med. Chem.* **2003,***46* (1), 148-154.

5. (a) Tannock, I. F.; Rotin, D., Acid pH in Tumors and Its Potential for Therapeutic Exploitation. *Cancer Res.* **1989,***49* (16), 4373-4384; (b) Trédan, O.; Galmarini, C. M.; Patel, K.; Tannock, I. F., Drug Resistance and the Solid Tumor Microenvironment. *J. Natl. Cancer Inst.* **2007,***99* (19), 1441-1454.

6. (a) Traverso, N.; Ricciarelli, R.; Nitti, M.; Marengo, B.; Furfaro, A. L.; Pronzato, M. A.; Marinari, U. M.; Domenicotti, C., Role of Glutathione in Cancer Progression and Chemoresistance. *Oxid. Med. Cell. Longev.* **2013,***2013*, 10; (b) Ortega, A. L.; Mena, S.; Estrela, J. M., Glutathione in Cancer Cell Death. *Cancers* **2011,***3* (1), 1285.

7. (a) Shami, P. J.; Saavedra, J. E.; Wang, L. Y.; Bonifant, C. L.; Diwan, B. A.; Singh, S. V.; Gu, Y.; Fox, S. D.; Buzard, G. S.; Citro, M. L.; Waterhouse, D. J.; Davies, K. M.; Ji, X.; Keefer, L. K., JS-K, a Glutathione/Glutathione S-Transferase-activated Nitric Oxide Donor of the Diazeniumdiolate Class with Potent Antineoplastic Activity1. *Mol. Cancer Ther.* **2003,***2* (4), 409-417; (b) Maciag, A. E.; Chakrapani, H.; Saavedra, J. E.; Morris, N. L.; Holland, R. J.; Kosak, K. M.; Shami, P. J.; Anderson, L. M.; Keefer, L. K., The Nitric Oxide Prodrug JS-K Is Effective against Non–Small-Cell Lung Cancer Cells In Vitro and In Vivo: Involvement of Reactive Oxygen Species. *J. Pharmacol. Exp. Ther.* **2011,***336* (2), 313-320.

8. (a) Collard, J.; Matthew, A. M.; Double, J. A.; Bibby, M. C., EO9: relationship between DT-diaphorase levels and response in vitro and in vivo. *Br. J. Cancer* **1995,***71* (6), 1199-1203; (b) Kelland, L. R.; Sharp, S. Y.; Rogers, P. M.; Myers, T. G.; Workman, P., DT-Diaphorase Expression and Tumor Cell Sensitivity to 17-Allylamino,17-demethoxygeldanamycin, an Inhibitor of Heat Shock Protein 90. *J. Natl. Cancer Inst.* **1999,***91* (22), 1940-1949.

9. (a) Bello, R. I.; Gómez-Díaz, C.; Navarro, F.; Alcaín, F. J.; Villalba, J. M., Expression of NAD(P)H:Quinone Oxidoreductase 1 in HeLa Cells: Role of Hydrogen Peroxide and Growth Phase. *J. Biol. Chem.* **2001,***276* (48), 44379-44384; (b) Li, D.; Gan, Y.; Wientjes, M. G.; Badalament, R. A.; Au, J. L. S., Distribution of DT-Diaphorase And Reduced Niotinamide Adenine Dinucleotide Phosphate: Cytochrome P450 Oxidoreductase in Bladder Tissues And Tumors. *J. Urol.* **2001,***166* (6), 2500-2505.

10. (a) Kiziltepe, T.; Hideshima, T.; Ishitsuka, K.; Ocio, E. M.; Raje, N.; Catley, L.; Li, C.-Q.; Trudel, L. J.; Yasui, H.; Vallet, S.; Kutok, J. L.; Chauhan, D.; Mitsiades, C. S.; Saavedra, J. E.; Wogan, G. N.; Keefer, L. K.; Shami, P. J.; Anderson, K. C., JS-K, a GST-activated nitric oxide generator, induces DNA double-strand breaks, activates DNA damage response pathways, and induces apoptosis in vitro and in vivo in human multiple myeloma cells. *Blood* **2007,***110* (2), 709-718; (b) Dickey, J. S.; Baird, B. J.; Redon, C. E.; Sokolov, M. V.; Sedelnikova, O. A.; Bonner, W. M., Intercellular communication of cellular stress monitored by γ-H2AX induction. *Carcinogenesis* **2009,***30* (10), 1686-1695.

11. (a) KUO, L. J.; YANG, L.-X., γ-H2AX - A Novel Biomarker for DNA Double-strand Breaks. *In Vivo* **2008,***22* (3), 305-309; (b) Ivashkevich, A.; Redon, C. E.; Nakamura, A. J.; Martin, R. F.; Martin, O. A., Use of the γ-H2AX assay to monitor DNA damage and repair in translational cancer research. *Cancer Lett.* **2012,***327* (1–2), 123-133.

12. Hodges, J. C.; Remers, W. A.; Bradner, W. T., Synthesis and antineoplastic activity of mitosene analogs of the mitomycins. *J. Med. Chem.* **1981,***24* (10), 1184-1191.

13. Diana, P.; Carbone, A.; Barraja, P.; Montalbano, A.; Martorana, A.; Dattolo, G.; Gia, O.; Via, L. D.; Cirrincione, G., Synthesis and antitumor properties of 2,5-bis(3′-indolyl)thiophenes: Analogues of marine alkaloid nortopsentin. *Bioorg. Med. Chem. Lett.* **2007,***17* (8), 2342-2346.

14. Naylor, M. A.; Jaffar, M.; Nolan, J.; Stephens, M. A.; Butler, S.; Patel, K. B.; Everett, S. A.; Adams, G. E.; Stratford, I. J., 2-Cyclopropylindoloquinones and Their Analogues as Bioreductively Activated Antitumor Agents: Structure−Activity in Vitro and Efficacy in Vivo. *J. Med. Chem.* **1997,***40* (15), 2335-2346.

CHAPTER 3.1: Nitroreductase-activated NO donors

3.1.1. Introduction

Enzyme activated prodrug strategy is employed for selective delivery and activation NO donor to tumours (Scheme 3.1.1).[1] The enzymes used as trigger are generally over-expressed in particular cell type. However, a shortcoming in such strategies for localized delivery of NO and other similar cytotoxic species is the presence of the trigger enzymes in normal tissues as well. In order to overcome this potential drawback of unwanted side-effects, targeted prodrug therapies have been developed that include gene-directed enzyme prodrug therapy (GDEPT) and antibody-directed enzyme prodrug therapy (ADEPT).[2]

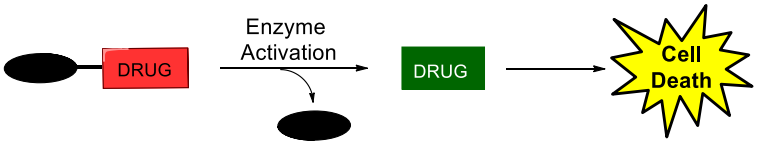

Scheme 3.1.1. Schematic diagram for enzyme prodrug therapy.

Escherichia coli nitroreductase (NTR) is a bacterial enzyme which has been used as a metabolic trigger for ADEPT and GDEPT.[2a, b, 2f, 3] Although there are several reported strategies for localizing cytotoxic species including DNA alkylating agents, but targeted prodrug therapy using nitric oxide was unreported. Therefore, in order to develop new NO-based cancer therapeutics, we propose 4-nitrobenzyl protected diazeniumdiolates, O^2-(4-nitrobenzyl) diazeniumdiolates as NTR activated NO donor which may have potential for applications in directed or targeted prodrug therapy. NTR activated NO donor was designed by linking a typical NTR substrate, 4-nitrobenzyl group with diazeniumdiolate as NO source. The proposed mechanism of activation of O^2-(4-nitrobenzyl) diazeniumdiolates is as follows. The 4-nitrobenzyl group is expected to undergo two or four electron reduction in the presence of NTR. As a result of reduction, the strong electron withdrawing nitro group is converted into an electron donating hydroxylamine or amine group. The lone pair of electrons on the amine nitrogen thus formed is pushed into the phenyl ring to release the diazeniumdiolate and the

benzyliminium species. The diazeniumdiolate is hydrolysed to give upto two moles of NO (Scheme 3.1.2).

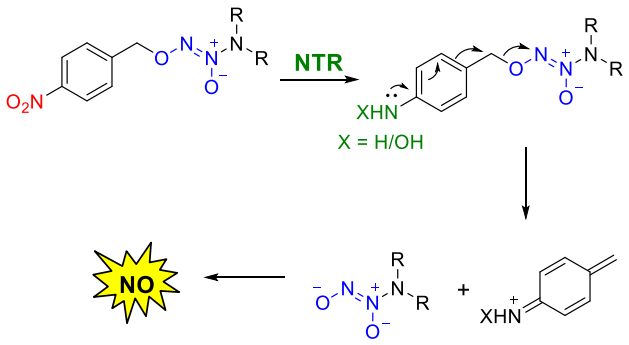

Scheme 3.1.2. Proposed mechanism of activation of NTR-activated NO donor.

3.1.2. Results and discussion

3.1.2.1. Synthesis

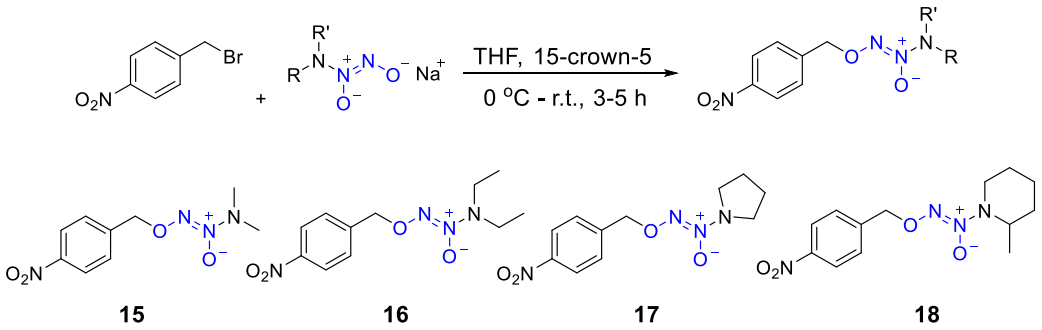

Scheme 3.1.3. Synthesis of O^2-(4-nitrobenzyl) diazeniumdiolates, **15-18**.

To test our hypothesis of NTR-activated NO donor, four different O^2-(4-nitrobenzyl) diazeniumdiolates were synthesized. The compounds, **15-18** in the series were prepared by reacting 4-nitrobenzyl bromide with the corresponding diazeniumdiolates (Scheme 3.1.3). The diazeniumdiolates selected for synthesis of O^2-(4-nitrobenzyl) diazeniumdiolates had a structural variability and the half-lives of NO release varied from 2 s to 8.3 min (Table 3.1.1).[4] A negative control **19**, which was a substrate for NTR but not a source of NO, was synthesized by reacting 4-nitrobenzyl alcohol with benzoic acid (Scheme 3.1.4).

R^1NR^2	Diazeniumdiolate	$t_{1/2}$	Product	Yield
Me_2N	DMA/NO	24 s	**15**	9
Et_2N	DEA/NO	2 min	**16**	15
Pyrrolidine	PYRRO/NO	2 s	**17**	16
2-Me- piperidine	2-Me Piperidi/NO	8.3 min	**18**	25

Table 3.1.1. Reported half-lives of diazeniumdiolates and synthetic yields of O^2-(4-nitrobenzyl) diazeniumdiolates.

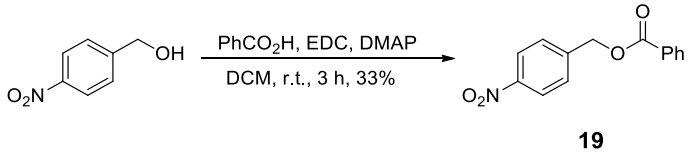

19

Scheme 3.1.4. Synthesis of **19**.

3.1.2.2. Chemoreduction

In order to test the ability of the nitro group to undergo reduction, the chemical reduction of the O^2-(4-nitrobenzyl) diazeniumdiolates was performed using a reported protocol.[5] The nitro group was reduced using Zn-ammonium formate and the reduction of the test compound was analyzed using HPLC by monitoring disappearance of the peak for the test compound. It was observed that all the compounds were completely reduced within 3 h (Figure 3.1.1), suggesting the nitro group of O^2-(4-nitrobenzyl) diazeniumdiolates was capable of getting reduced.

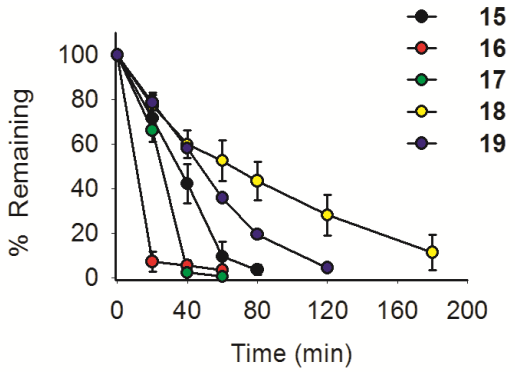

Figure 3.1.1. HPLC decompostion profiles of chemoreduction of compounds **15-19** using Zn-ammonium formate.

The reduction potentials of the nitro group of the O^2-(4-nitrobenzyl) diazeniumdiolates were calculated using cyclic voltammetric (CV) analysis (Table 3.1.2). p-Nitrotoluene was used as a reference for nitro-group reduction and one electron reduction potential (E_{red}) of -0.11 V was recorded. The E_{red} values from CV data analysis were almost similar for all the compounds **15-19**, indicating the diazeniumdiolate was not affecting the rate of nitro group reduction (Figure 3.1.2).

Entry	Compound	E_{Red} (V)[a]	% Remaining[b]	NO (µM)[c]
1	**15**	-0.09	60	13.6
2	**16**	-0.106	60	6.8
3	**17**	-0.11	28	18.3
4	**18**	-0.11	31	19.7
5	**19**	-0.139	68	1.1

Table 3.1.2. Cyclic voltammetric analysis and NTR-mediated decomposition and nitric oxide release profiles. [a]One electron reduction potential of compounds **15-19**. [b]Decomposition of **15-19** (50 µM) in the presence of NTR in pH 7.0 buffer after 1 h was estimated by HPLC. [c]NO released during decomposition of **15**–**19** (50 µM) in the presence of NTR in pH 7.0 buffer after 1 h measured using a chemiluminescence assay.

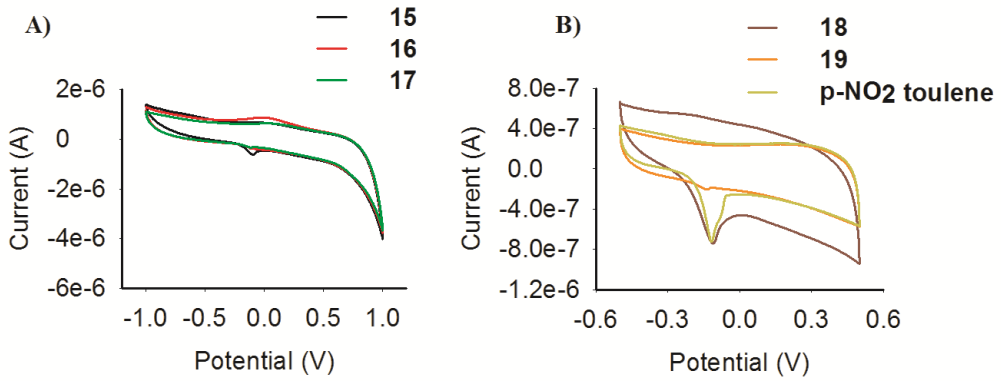

Figure 3.1.2. A) Cyclic voltammetric curve recorded for compounds **15-17**. **B)** Cyclic voltammetric curve recorded for compounds **18**, **19** and p-nitrotoulene. Conditions: Pt disc working electrode; Pt wire auxiliary electrode; $Ag/AgNO_3$ reference electrode; scan rate = 25 mV/s; NBu_4PF_6 = 100 mM as the background electrolyte in acetonitrile.

3.1.2.3. NTR reduction and evaluation of NO generation

Next, in order to assess whether the compounds were substrates for NTR, the compounds were individually reacted with NTR alongwith the cofactor NADPH in pH 7.0 buffer for

1 h. HPLC analysis was performed to study the NTR reduction of the test compound by monitoring the disappearance of the compound peak. From the HPLC data it was observed that the compounds **15-18** were substrate for NTR (Figure 3.1.3.A). During this time period, no significant decomposition of **15-18** was observed in the absence of NTR suggesting that these compounds were not candidates for hydrolysis in pH 7.0 buffer and the decomposition must be due to metabolism by NTR. During 1 h nearly 60% of **15** and **16** remained while in the cases of cyclic derivatives **17** and **18**, 28 and 31 % remained after NTR treatment, respectively (Table 3.1.2).

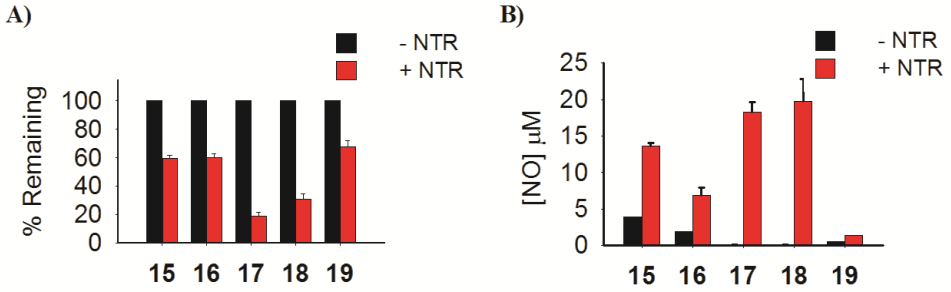

Figure 3.1.3. A) Decompostion data of O^2-(4-nitrobenzyl) diazeniumdiolates **15-18** (50 µM) and **19** (50 µM) in pH 7.0 buffer in the presence and absence of NTR monitored by HPLC. **B)** NO release from O^2-(4-nitrobenzyl) diazeniumdiolates **15-18** and **19** in the presence and absence of NTR in pH 7.0 buffer detected using chemiluminesence based assay.

The amount NO released from the NTR reduction of the compounds was measured using the chemiluminescence based assay using NOA 280i. It was observed that the compounds **15-18** were reduced by NTR to release NO (Figure 3.1.3.B). The amount of NO released for compounds **17** and **18** was higher (~ 19 µM) in accordance with decomposition rates. We observe a discrepancy in the reduction of compounds **17** and **18** (~70% reduction) and the amount of NO released after reduction (~20% release). So, probably the compound undergoes reduction by NTR reduction and forms intermediate which then slowly fragments to release the diazeniumdiolate, as a result low yields of NO were estimated.

Although the negative control **19** was metabolized by NTR (68% remaining after 1 h) but the analysis of reaction mixtures of **19** in the presence NTR showed negligible NO release (Figure 3.1.2.A and 3.1.2.B). Nitroreductases are known to mediate generation of NO from nitro aromatic compounds.[6] However, negligible NO generation from

incubation of **19** in the presence and absence of NTR, eliminates the possibility of the nitro group on the aromatic ring as a significant source of NO upon NTR reduction in case of O^2-(4-nitrobenzyl) diazeniumdiolates.

3.1.2.4. Cell based assays

As O^2-(4-nitrobenzyl) diazeniumdiolates were activated by NTR in buffer to release NO, next we studied the effects of these compounds in cells in the presence of NTR. Generally, a cell transfected with NTR protein is used as a model for studying NTR activated bioreductive prodrugs. However, we used a reported experiment setup in which cells were treated with compound and NTR enzyme and cofactor NADPH were added externally.[7] An initial cell viability assay was performed with a concentration of 75 μM of the compounds in DLD-1 human colorectal adenocarcinoma cells, in the presence and absence of NTR. All compounds **15-18** showed moderate cell inhibitory activity in absence of NTR and compound **19** was not effective in killing cells (Figure 3.1.4). However, when NTR and NADPH were added to compound treated cells, there was an increase in the inhibitory activity by compounds **15-18**. Also, only 25% inhibition was noticed for the negative control **19**. As less inhibition was observed in case of **19**, this indicated that the enhanced cytotoxic effects seen in O^2-(4-nitrobenzyl) diazeniumdiolates upon addition of NTR were due to NO release alongwith cytotoxic of effects of the by-products of the bioreduction.

Although in aqueous media compound **17** and **18** were found to be better source of NO in the presence of NTR, but in cell based assay compound **18** was better in inhibiting growth of cancer cells in the presence of NTR in comparison with **17**. The origin of this difference is unclear. However, a recent study on NTR-activated DNA alkylating agents indicated that the anti-proliferative activity of the NTR substrate did not always correlate with propensity for its metabolism by NTR.[8] Based on these results, O^2-(4-nitrobenzyl) 1-(2-methylpiperidin-1-yl)diazen-1-ium-1,2-diolate, **18** was identified as the best NTR-activated NO donor with enhanced cytotoxicity in the presence of exogenously added NTR and was chosen for further evaluation.

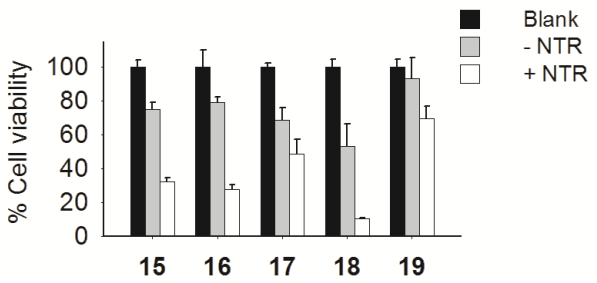

Figure 3.1.4. Cell viability assay to assess anti-proliferative activity of **15-19** at 75 µM in the presence and absence of NTR conducted with DLD-1 human colorectal adenocarcinoma cells. Blank is untreated cells.

Next, a detailed concentration based cytotoxicity assay was performed in DLD-1 cells to assess the difference in cytotoxicity in the presence and absence of NTR. Enhancement in the cytotoxicity of **18** was observed in the presence of NTR (Figure 3.1.5 A). A similar concentration dependent cytotoxicity assay was performed in HeLa human cervical cancer cells with compound **18** in the presence and absence of NTR. Again it was found that the anti-proliferative effects of **18** was increased in the presence of NTR (Figure 3.1.5 B).

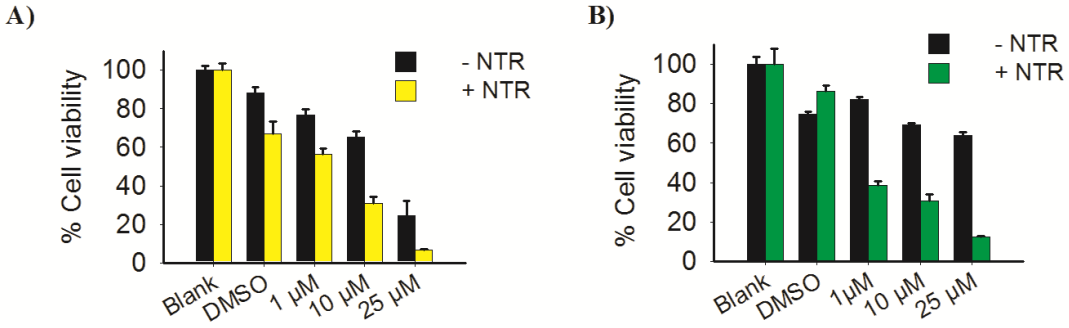

Figure 3.1.5. A) A concentration dependent cell viability assay to assess anti-proliferative activity of **18** in the presence and absence of NTR conducted with DLD-1 human adenocarcinoma cells. **B)** A concentration dependent cell viability assay to assess anti-proliferative activity of **18** in the presence and absence of NTR conducted with HeLa human cervical cancer cells. Blank is untreated cells.

As the pH varies across the tumour, we monitored release of NO from O^2-(4-nitrobenzyl) diazeniumdiolate **18** by NTR in different aqueous solutions: phosphate buffer saline (PBS) and phosphate buffers with pH 7.4, pH 7.0 and pH 6.5 during 1 h. Compound **18** (50 µM) was independently incubated in aqueous solutions with different pH with NTR

and NADPH for 1 h and the release of NO was detected using a chemiluminescence based assay. It was found that in PBS, buffers with pH 7.4 and 7.0, **18** released ~20 µM of NO was released after 1 h of incubation with NTR (Figure 3.1.6). However, in buffer of pH 6.5, it was found that **18** released ~10 µM after 1 h of incubation with NTR. The low amount of NO released in acidic pH may be due to protonation of the amine or hydroxylamine intermediate formed after the nitro group reduction. As a result of protonation, the release of diazeniumdiolate was probably slowed down and low amount of NO was observed. Despite low NO release, this data suggested that **18** might be useful for NO delivery to hypoxic tumors as well.

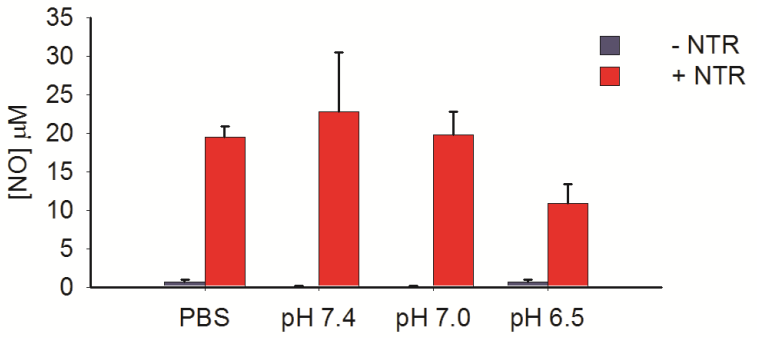

Figure 3.1.6. Estimation of NO released during reduction of **18** (50 µM) in the presence of NTR in phosphate buffer saline (PBS) and in phosphate buffers with pH 7.4, 7.0 and 6.5 after 1 h of incubation at 37 ^{o}C.

3.1.2.5. Bioreduction in bacteria

NTR is an enzyme which is present bacteria and 4-nitrobenzyl is well known substrate for NTR. Thus in order to check, whether O^2-(4-nitrobenzyl) diazeniumdiolates is activated within bacteria to release NO, a frequently used diaminofluorescein based secondary assay was used for intracellular NO measurement in *Mycobacterium smegmatis* (*M. smeg*). For measuring intracellular NO, compound **17** was used as a representative of O^2-(4-nitrobenzyl) diazeniumdiolates. In this assay, a 4,5-diaminofluorescein diacetate (DAF-2DA) dye was treated with *M. smeg*. The dye permeates the cells and the diester gets hydrolysed to form DAF. Next bacteria was treated with compound **17** which is bioreductively activated to release NO. DAF reacts with NO^+ formed by oxidation of NO, to form a flourescent dye DAF-2T. By measuring

the fluorescence for DAF-2T at λ_{ex}: 495 nm and λ_{em}: 515 nm, we monitored NO release inside bacteria. Two different concentrations of compound **17** were incubated in *M. smeg* for 12 h and the fluorescence for DAF-2T was measured. A concentration dependent increase in fluorescence of DAF-2T in *M. smeg* was observed, indicating **17** was reduced within bacteria to generate NO intracellularly (Figure 3.1.7).

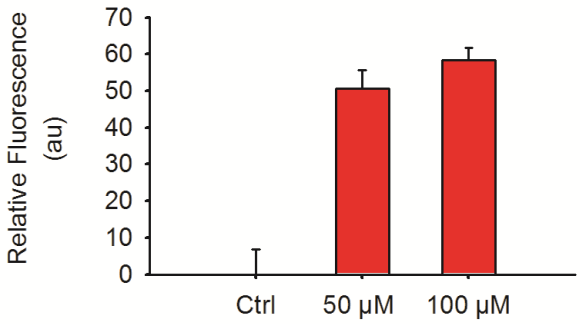

Figure 3.1.7. Levels of intracellular NO measured in *M. smeg* upon incubation with 50 and 100 µM of **17** using DAF assay.

3.1.3. Conclusion

In this chapter, a series of O^2-(4-nitrobenzyl) diazeniumdiolates were designed as substrates for *E. coli* nitroreductase (NTR), an enzyme that has been used to facilitate site-directed delivery of cytotoxic species to cancers. These compounds were found to be stable in pH 7.4 but were reduced in the presence of NTR to generate NO. Among the four O^2-(4-nitrobenzyl) diazeniumdiolates, the study revealed that O^2-(4-nitrobenzyl) 1-(2-methylpiperidin-1-yl)diazen-1-ium-1,2-diolate (**18**) was selectively activated by NTR to produce NO. Finally, a cell viability assay revealed that cytotoxic effects of O^2-(4-nitrobenzyl) 1-(2-methylpiperidin-1-yl)diazen-1-ium-1,2-diolate (**18**) towards two cancer cell lines was significantly enhanced in the presence of NTR suggesting the potential for use of this compound in nitric oxide-based antibody or gene-directed prodrug therapy. We also developed that O^2-(4-nitrobenzyl) diazeniumdiolates can be potentially used to enhance NO inside bacterial cells to study the effects of NO.

3.1.4. Experimental and characterization data

3.1.4.1. General procedure for synthesis of O^2-(4-nitrobenzyl) diazeniumdiolates

To an ice cold solution of diazeniumdiolate salt (1.04 mmol) in THF (10 mL), 15-crown-5 (25 µL) was added. After 15 min of stirring at 0 ^{o}C, 4-nitrobenzyl bromide (0.69 mmol) was added. The reaction mixture was warmed to room temperature and stirred for 3-5 h. The reaction mixture was concentrated under reduced pressure and the resulting crude was chromatographed using silica gel support to isolate pure product.

Synthesis of O^2-(4-nitrobenzyl) 1-(N,N-dimethyl)diazen-1-ium-1,2-diolate, 15.

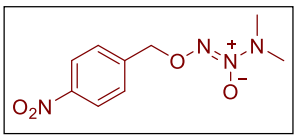

Pale yellow solid (15 mg, 9%): FT-IR (ν_{max}, cm^{-1}): 2933, 1605, 1518, 1495, 1383, 1349, 1271, 1071; ^{1}H NMR (400 MHz, $CDCl_3$) δ: 8.23 (d, *J* = 8.7 Hz, 2H), 7.55 (d, *J* = 8.8 Hz, 2H), 5.30 (s, 2H), 3.00 (s, 6H); ^{13}C NMR (100 MHz, $CDCl_3$) δ: 148.0, 143.3, 128.7, 123.9, 73.8, 42.7; HRMS (ESI) for $C_9H_{12}N_4O_4$ $[M+Na]^+$: Calcd., 263.0756, Found, 263.0779.

Synthesis of O^2-(4-nitrobenzyl) 1-(N,N-diethyl)diazen-1-ium-1,2-diolate, 16.

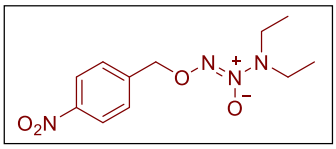

Light brown solid (27 mg, 15%): FT-IR (ν_{max}, cm^{-1}): 2359, 2341, 1606, 1520, 1384, 1355, 1018; ^{1}H NMR (400 MHz, $CDCl_3$) δ: 8.23 (d, *J* = 8.7 Hz, 2H), 7.55 (d, *J* = 8.6 Hz, 2H), 5.35 (s, 2H), 3.10 (q, *J* = 7.1 Hz, 4H), 1.02 (t, *J* = 7.1 Hz, 6H); ^{13}C NMR (100 MHz, $CDCl_3$) δ: 148.0, 143.2, 128.7, 123.9, 73.9, 48.7, 11.6; HRMS (ESI) for $C_{11}H_{16}N_4O_4$ $[M+Na]^+$: Calcd., 291.1069, Found, 291.1069.

Synthesis of O^2-(4-nitrobenzyl) 1-(pyrrolidin-1-yl)diazen-1-ium-1,2-diolate, 17.

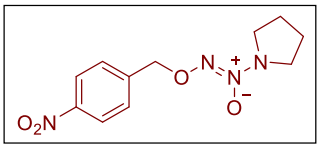

Pale yellow solid (15 mg, 16%): FT-IR (ν_{max}, cm^{-1}): 2360, 1652, 1540, 1521, 1507, 1343; ^{1}H NMR (400 MHz, $CDCl_3$) δ: 8.22 (d, *J* = 8.8 Hz, 2H), 7.55 (d, *J* = 8.6 Hz, 2H), 5.26 (s, 2H), 3.49-3.53 (m, 4H), 1.91-1.95 (m, 4H); ^{13}C NMR (100 MHz, $CDCl_3$) δ: 147.9, 143.7, 128.7, 123.8, 73.5, 50.9, 22.9; HRMS (ESI) for $C_{11}H_{14}N_4O_4$ $[M+Na]^+$: Calcd., 289.0913, Found, 289.0922.

Synthesis of O^2-(4-nitrobenzyl) 1-(2-methylpiperidin-1-yl)diazen-1-ium-1,2-diolate, 18.

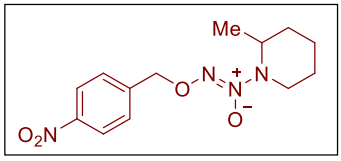

Pale yellow solid (50 mg, 25%): FT-IR (ν_{max}, cm^{-1}): 2934, 2857, 1521, 1505, 1383, 1344, 1020; ^{1}H NMR (400 MHz, $CDCl_3$) δ: 8.22 (d, *J* = 8.6, 2H), 7.54 (d, *J* = 8.6 Hz, 2H), 5.36 (s, 2H), 3.16-3.23 (m, 3H), 1.70-1.81 (m, 4H), 1.37-1.45 (m, 2H), 0.94 (d, *J* = 6.1 Hz, 3H); ^{13}C NMR (100 MHz, $CDCl_3$) δ: 148.0, 143.1, 128.6, 123.9, 73.9, 56.7, 54.1, 32.8, 25.1, 23.1, 18.2; HRMS (ESI) for $C_{13}H_{18}N_4O_4$ $[M+Na]^+$: Calcd., 317.1226, Found, 317.1245.

Synthesis of 4-nitrobenzyl benzoate, 19.

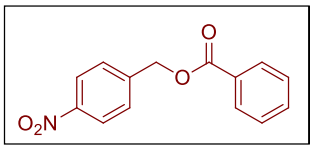

The compound has been previously reported[9] but we synthesized using a different reaction condition as follows. To an ice cooled solution of 4-nitrobenzyl alcohol (0.1 g, 0.652 mmol), benzoic acid (0.12 g, 0.98 mmol) and DMAP (0.16 g, 1.30 mmol) in dry DCM (10 mL), EDC (0.25 g, 1.30 mmol) was added. The reaction mixture was stirred at room temperature for 3 h. The reaction mixture was diluted with water and extracted in DCM (3×10 mL). The combined organic layer was washed with brine, dried (Na_2SO_4), filtered and the filtrate was evaporated under reduced pressure. The resulting crude was chromatographed using silica gel support to isolate pure product as a white solid (55 mg, 33%): ^{1}H NMR (400 MHz, $CDCl_3$) δ: 8.24-8.26 (m, 2H), 8.08-8.10 (m, 2H), 7.58-7.62 (m, 3H), 7.45-7.49 (m, 2H), 5.46 (s, 2H); ^{13}C NMR (100 MHz, $CDCl_3$) δ: 166.2, 147.8, 143.4, 133.6, 129.8, 129.5, 128.7, 128.4, 124.0, 65.3.

3.1.4.2. Zinc-mediated chemoreduction

Zinc mediated chemoreduction was performed using a reported protocol.[5a, 10] A solution of the test compound (20 µL, 10 mM stock) was diluted in a methanol-water solution (1:1; 1970 µL) so that the final concentration of compound in the solution was 100 µM. To this 10 µL of ammonium formate (10 mM stock in deionised water) was added and stirred at 37 ^{o}C. This served as blank solution. The zinc-mediated decomposition was carried out by preparing the reaction mixture as mentioned for blank followed by addition

of zinc powder (15 mg). At different time points, the reaction mixture was aliquot, centrifuged and the supernatant was filtered (10 micron, PTFE) and decomposition of test compound was analysed using HPLC (Eclipse Plus C18, 5 μm, 4.6 × 250 mm; flow rate: 1 mL/min; eluent 70% ACN: H_2O). The results reported are averages of three independent runs.

3.1.4.3. Cyclic voltammetry (CV)

Cyclic voltammetric analysis was performed using a Basi Epsilon-EC-Ver 2.00.71-USB Bioanalytical systems. A three-electrode setup was used: Pt wire auxiliary electrode, platinum disc working electrode, and $Ag/AgNO_3$ reference electrode. All potential values were calibrated against the saturated calomel electrode (SCE) by measuring the oxidation of ferrocene as a reference ($E°$ (Fc^+/Fc) = 0.19 V vs SCE). The working electrode was polished with 0.05 μM alumina (Basi polishing solution) on a felt pad and washed with de-ionized water and rinsed using acetonitrile. All electrochemical samples were purged with nitrogen for 5 min and were measured under a nitrogen atmosphere. The supporting electrolyte of 0.1 M tetrabutyl ammonium hexafluorophosphate ($TBAPF_6$) and a 10 mM stock solution of the compound in DMSO was used and the analysis was carried out in acetonitrile.

3.1.4.4. Nitroreductase-catalyzed decomposition and nitric oxide release

Enzyme stock solution was prepared by dissolving 1.5 mg of lyophilized NTR powder in phosphate buffer pH 7.0 (100 μL). 10 mM stock solutions of the compounds were prepared in DMSO. 50 μL of the freshly prepared enzyme stock was added to a reaction solution consisting of 10 μL of the test compound (10 mM stock in DMSO) and 400 μL NADPH (1 mM stock in phosphate buffer pH 7.0) and 1540 μL of phosphate buffer pH 7.0. The blank consisted of 10 μL of the test compound (10 mM stock in DMSO) and 1990 μL of phosphate buffer pH 7.0. Data reported are averages of three independent runs. These reaction mixtures were stirred at 37 °C and after 1 h an aliquot was analysed for decomposition and NO generation. The reduction of starting compounds was monitored using HPLC (Eclipse Plus C-18, 5 μm, 4.6 × 250 mm; flow rate: 1 mL/min; eluent 70% ACN: H_2O). For quantifying amount of NO release from enzymatic decomposition, the reaction mixtures were prepared in pH 6.5, pH 7.0, and 7.4. 10 μL of

the reaction mixture and blank solution were injected at the specified time points into NOA using argon as the carrier gas. Using a standard calibration curve of $NaNO_2$, NO generated during enzymatic assay was quantified using the chemiluminescence detector.

3.1.4.5. Cell viability assay

DLD-1 human colorectal adenocarcinoma cells were seeded at 3 $\times 10^4$ cells/well overnight in a 96-well plate in complete RPMI 1640 media. A NTR (lyophilized powder) stock solution containing 6 mg in Dulbecco's phosphate buffered saline (DPBS) 2 mL was prepared. A 1 mM NADPH stock solution was prepared in DPBS. Cells were incubated with varying concentrations of the test compound prepared as a DMSO stock solution so that the final concentration of DMSO was 1%. The cells were incubated for 72 h at 37 ^oC. A stock solution of 3-(4,5-dimethylthiazol-2-yl)-2,5-diphenyl tetrazolium bromide (MTT) was prepared 3.5 mg in 7mL DPBS and 100 µL of this solution was added to each well. After 4 h incubation, the media was removed carefully and 100 µL of DMSO was added. Spectrophotometric analysis of each well using a microwell plate reader at 570 nm was carried out to estimate cell viability. A similar assay was conducted in the presence of NTR (5 µL stock) and NADPH (10 µL stock) to analyze the effect of addition of NTR on cell viability.

3.1.4.6. DAF assay-Intracellular NO release in *Mycobacterium smegmatis*

Using a reported protocol[11] with slight modification, intracellular NO release was detected as follows: a 5 mM stock solution of diaminofluorescein-2 diacetate (DAF-2DA) was prepared in DMSO. Using a 10 mM DMSO stock solution of **17**, 2 mL solutions of concentration 100 and 200 µM were prepared in middle brook M7H9 medium. *Mycobacterium smegmatis* [*M. smeg* (mc^2155)] was inoculated in 10 mL M7H9 for 16 h. The bacterial culture was suspended to apsirate out the medium and then resuspended in fresh medium to make bacterial solution of O.D 1.0. To 2 mL of this bacterial culture, 4 µL of DAF-2DA solution was added so as to obtain a final concentration of 10 µM. The bacterial suspension was incubated at 37 ^oC for 2 h. The bacterial cells were suspended to aspirate media and washed with fresh media twice. The cell pellet was resuspended in 1 mL fresh media and again incubated at 37 ^oC for 1 h. A diluted bacterial suspension with O.D 0.5 was prepared. In a 96-well plate, 100 µL of

bacterial suspension treated with DAF was added. For control set, 100 µL of bacterial suspension was diluted with 100 µL of medium. For obtaining 50 µM of **17**, the 100 µL of bacterial suspension was diluted with 100 µL of 100 µM solution of **17**. Likewise, for obtaining 100 µM of **17**, the 100 µL of bacterial suspension was diluted with 100 µL of 200 µM solution of **17**. Each concentration three reading were taken. The 96-well plate was incubated at 37 ^{o}C for 12 h. Fluorimetric reading was recorded in a microwell plate reader with excitation wavelength of 490 nm and emission wavelength of 530 nm.

3.1.5. Spectral charts

^{1}H NMR Spectrum (400 MHz, $CDCl_3$) of compound **15**

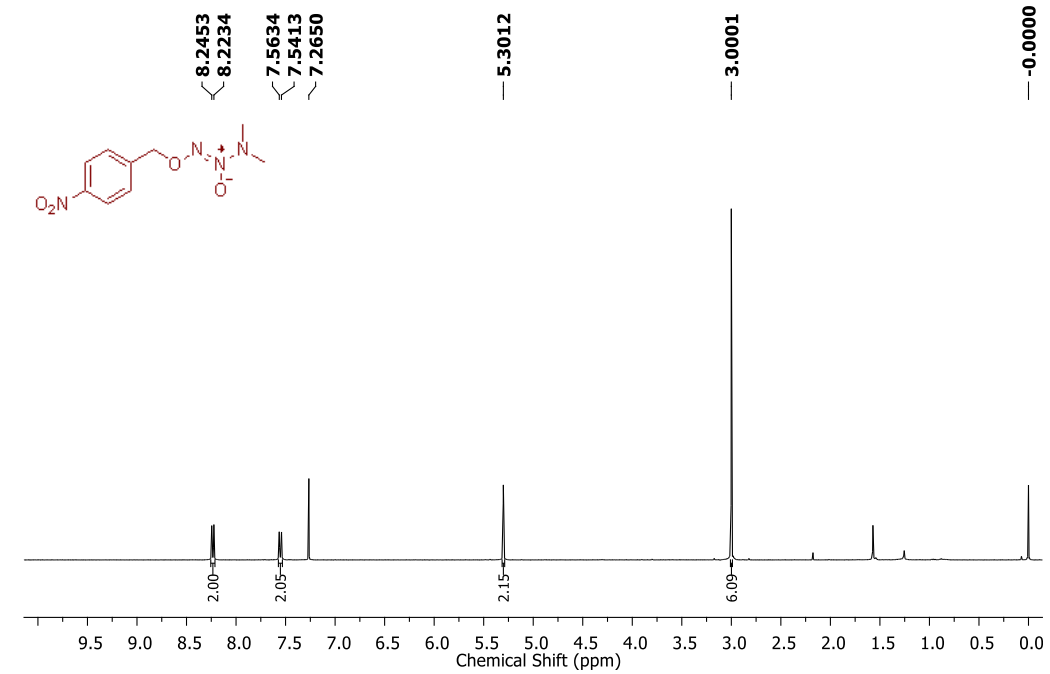

^{13}C NMR Spectrum (100 MHz, $CDCl_3$) of compound **15**

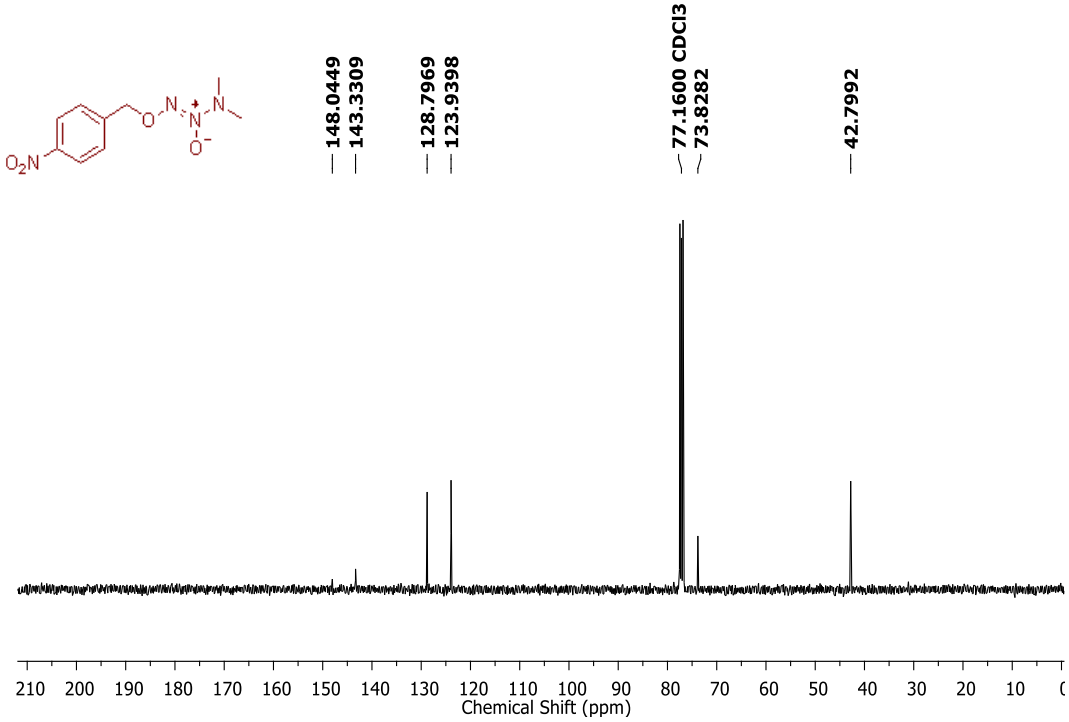

^{1}H NMR Spectrum (400 MHz, $CDCl_3$) of compound **16**

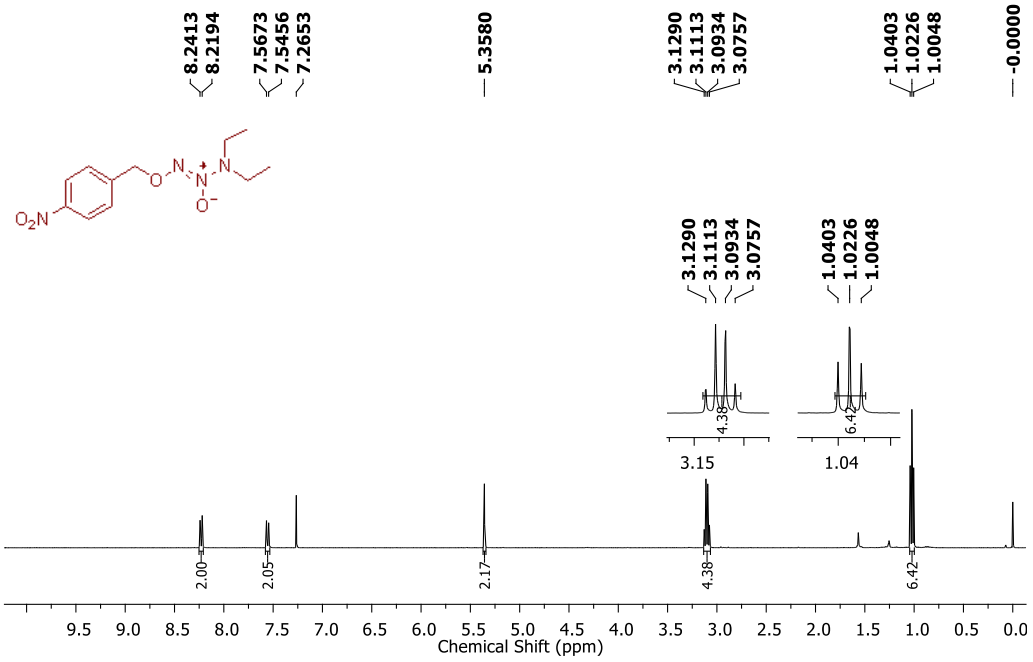

^{13}C NMR Spectrum (100 MHz, $CDCl_3$) of compound **16**

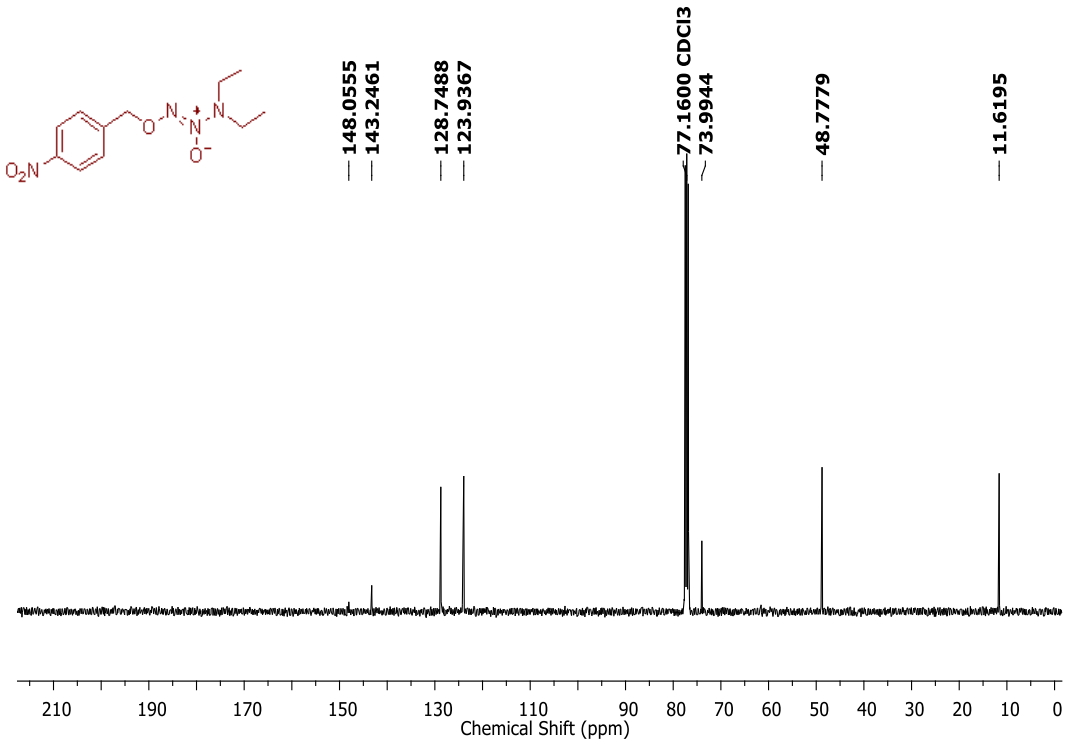

^{1}H NMR Spectrum (400 MHz, $CDCl_3$) of compound **17**

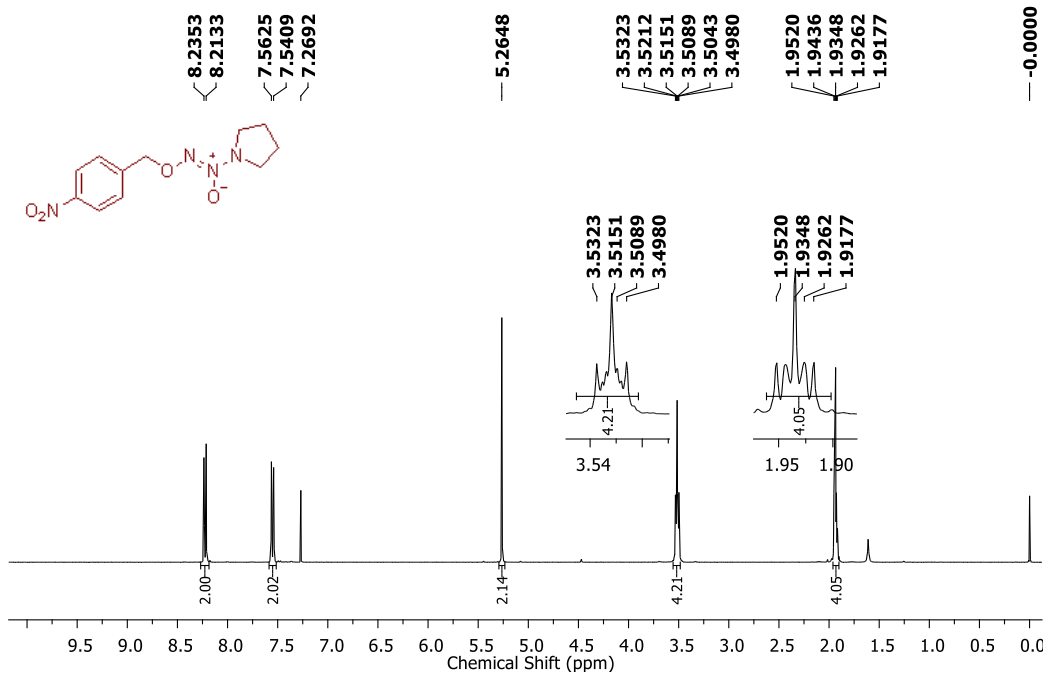

^{13}C NMR Spectrum (100 MHz, $CDCl_3$) of compound **17**

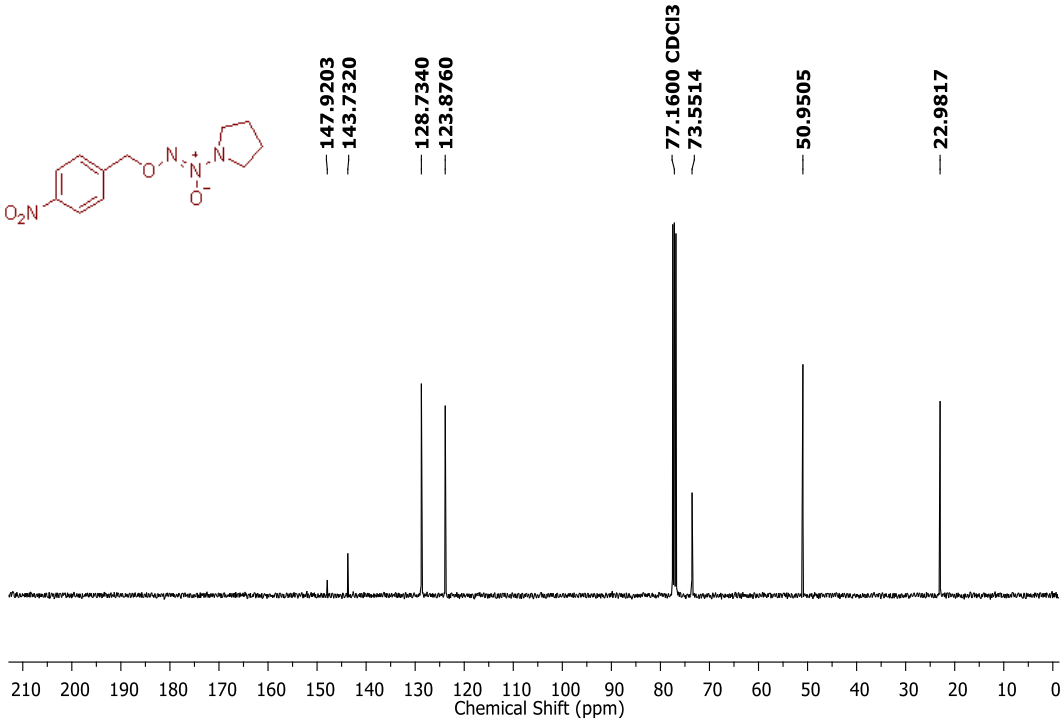

^{1}H NMR Spectrum (400 MHz, $CDCl_3$) of compound **18**

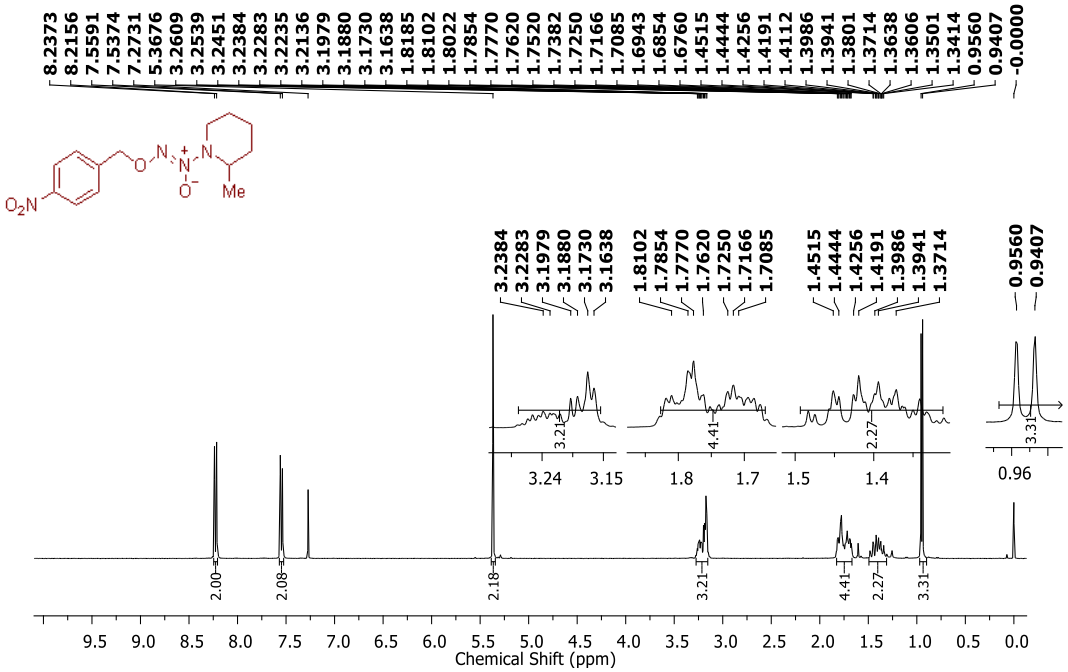

^{13}C NMR Spectrum (100 MHz, $CDCl_3$) of compound **18**

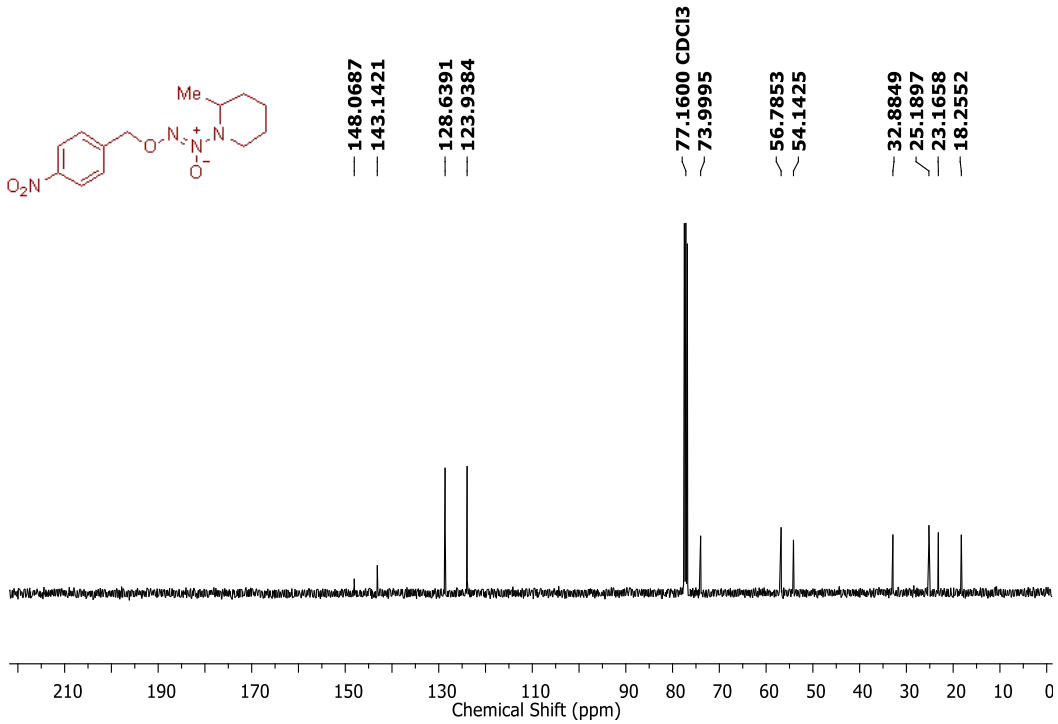

^{1}H NMR Spectrum (400 MHz, $CDCl_3$) of compound **19**

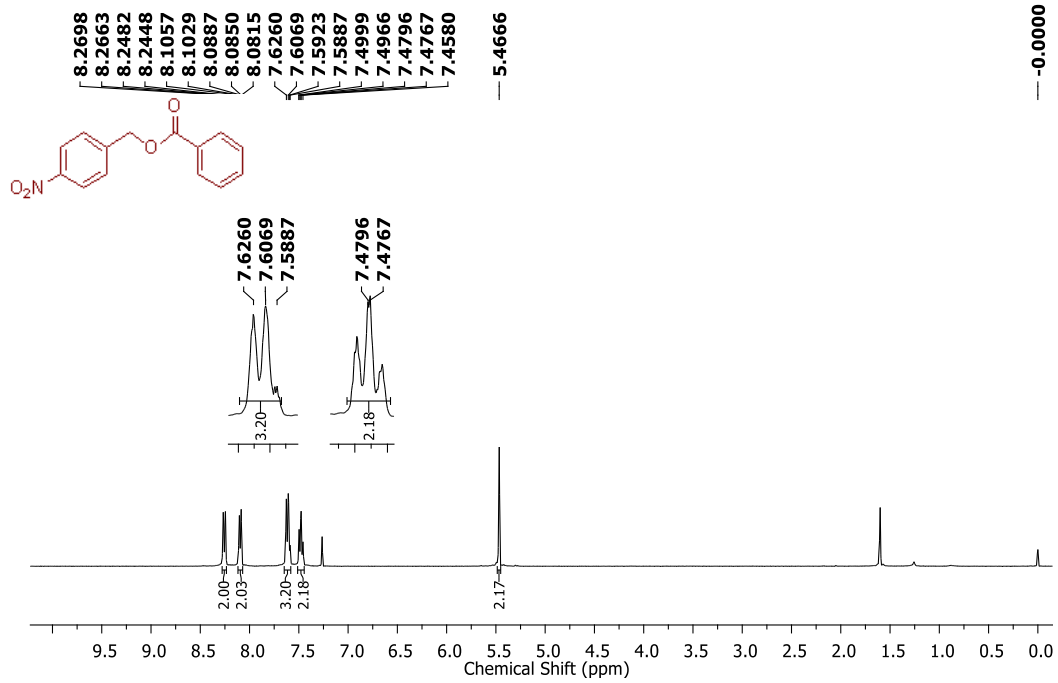

^{13}C NMR Spectrum (100 MHz, $CDCl_3$) of compound **19**

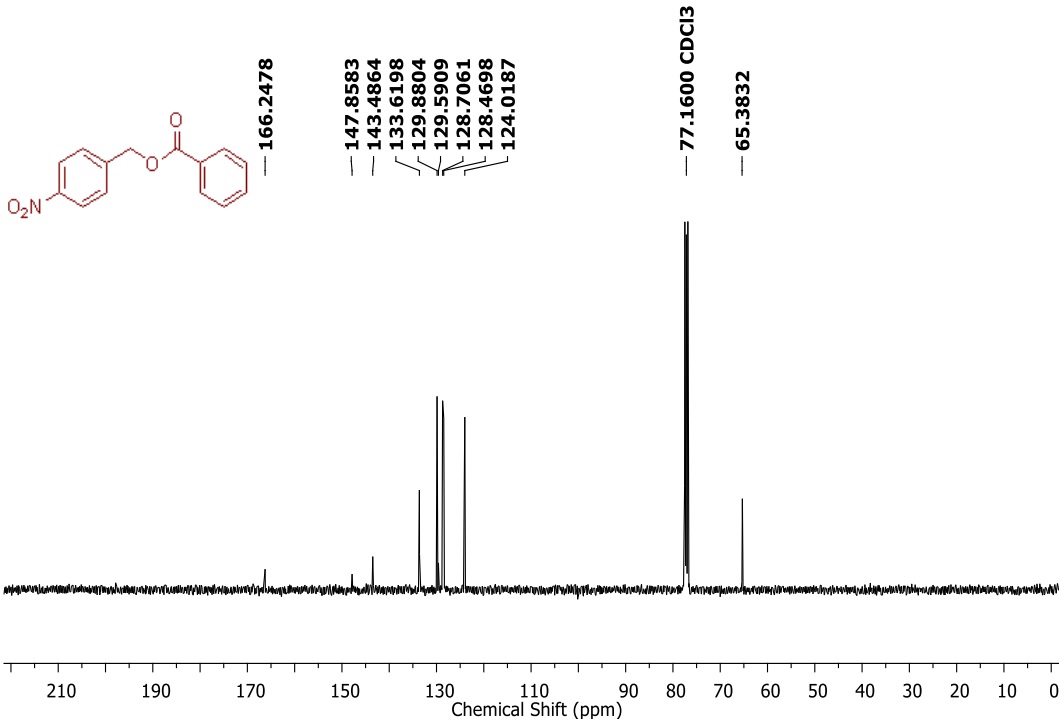

3.1.6. References.

1. (a) Chakrapani, H.; Maciag, A. E.; Citro, M. L.; Keefer, L. K.; Saavedra, J. E., Cell-Permeable Esters of Diazeniumdiolate-Based Nitric Oxide Prodrugs. *Org. Lett.* **2008,***10* (22), 5155-5158; (b) Nandurdikar, R. S.; Maciag, A. E.; Hong, S. Y.; Chakrapani, H.; Citro, M. L.; Keefer, L. K.; Saavedra, J. E., Glycosylated PROLI/NO Derivatives as Nitric Oxide Prodrugs. *Org. Lett.* **2010,***12* (1), 56-59; (c) Saavedra, J. E.; Shami, P. J.; Wang, L. Y.; Davies, K. M.; Booth, M. N.; Citro, M. L.; Keefer, L. K., Esterase-Sensitive Nitric Oxide Donors of the Diazeniumdiolate Family: In Vitro Antileukemic Activity. *J. Med. Chem.* **2000,***43* (2), 261-269; (d) Shami, P. J.; Saavedra, J. E.; Wang, L. Y.; Bonifant, C. L.; Diwan, B. A.; Singh, S. V.; Gu, Y.; Fox, S. D.; Buzard, G. S.; Citro, M. L.; Waterhouse, D. J.; Davies, K. M.; Ji, X.; Keefer, L. K., JS-K, a Glutathione/Glutathione S-Transferase-activated Nitric Oxide Donor of the Diazeniumdiolate Class with Potent Antineoplastic Activity1. *Mol. Cancer Ther.* **2003,***2* (4), 409-417.

2. (a) Xu, G.; McLeod, H. L., Strategies for Enzyme/Prodrug Cancer Therapy. *Clin. Cancer Res.* **2001,***7* (11), 3314-3324; (b) Greco, O.; Dachs, G. U., Gene directed enzyme/prodrug therapy of cancer: Historical appraisal and future prospectives. *J. Cell. Physiol.* **2001,***187* (1), 22-36; (c) Hay, M. P.; Anderson, R. F.; Ferry, D. M.; Wilson, W. R.; Denny, W. A., Synthesis and Evaluation of Nitroheterocyclic Carbamate Prodrugs for Use with Nitroreductase-Mediated Gene-Directed Enzyme Prodrug Therapy. *J. Med. Chem.* **2003,***46* (25), 5533-5545; (d) Hay, M. P.; Atwell, G. J.; Wilson, W. R.; Pullen, S. M.; Denny, W. A., Structure−Activity Relationships for 4-Nitrobenzyl Carbamates of 5-Aminobenz[e]indoline Minor Groove Alkylating Agents as Prodrugs for GDEPT in Conjunction with E. coli Nitroreductase. *J. Med. Chem.* **2003,***46* (12), 2456-2466; (e) Hay, M. P.; Wilson, W. R.; Denny, W. A., Nitrobenzyl carbamate prodrugs of enediynes for nitroreductase gene-directed enzyme prodrug therapy (GDEPT). *Bioorg. Med. Chem. Lett.* **1999,***9* (24), 3417-3422; (f) Mauger, A. B.; Burke, P. J.; Somani, H. H.; Friedlos, F.; Knox, R. J., Self-Immolative Prodrugs: Candidates for Antibody-Directed Enzyme Prodrug Therapy in Conjunction with a Nitroreductase Enzyme. *J. Med. Chem.* **1994,***37* (21), 3452-3458.

3. Tietze, L. F.; Schuster, H. J.; Krewer, B.; Schuberth, I., Synthesis and Biological Studies of Different Duocarmycin Based Glycosidic Prodrugs for Their

Use in the Antibody-Directed Enzyme Prodrug Therapy. *J. Med. Chem.* **2009,***52* (2), 537-543.

4. (a) Keefer, L. K., Fifty Years of Diazeniumdiolate Research. From Laboratory Curiosity to Broad-Spectrum Biomedical Advances. *ACS Chem. Biol.* **2011,***6* (11), 1147-1155; (b) Chakrapani, H.; Goodblatt, M. M.; Udupi, V.; Malaviya, S.; Shami, P. J.; Keefer, L. K.; Saavedra, J. E., Synthesis and in vitro anti-leukemic activity of structural analogues of JS-K, an anti-cancer lead compound. *Bioorg. Med. Chem. Lett.* **2008,***18* (3), 950-953.

5. (a) Ferrer, S.; Naughton, D. P.; Threadgill, M. D., Studies on the reductively triggered release of heterocyclic and steroid drugs from 5-nitrothien-2-ylmethyl prodrugs. *Tetrahedron* **2003,***59* (19), 3437-3444; (b) Sykes, B. M.; Hay, M. P.; Bohinc-Herceg, D.; Helsby, N. A.; O'Connor, C. J.; Denny, W. A., Leaving group effects in reductively triggered fragmentation of 4-nitrobenzyl carbamates. *J. Chem. Soc., Perkin Trans.* **2000,** (10), 1601-1608.

6. Gurumurthy, M.; Mukherjee, T.; Dowd, C. S.; Singh, R.; Niyomrattanakit, P.; Tay, J. A.; Nayyar, A.; Lee, Y. S.; Cherian, J.; Boshoff, H. I.; Dick, T.; Barry, C. E.; Manjunatha, U. H., Substrate specificity of the deazaflavin-dependent nitroreductase from Mycobacterium tuberculosis responsible for the bioreductive activation of bicyclic nitroimidazoles. *FEBS J.* **2012,***279* (1), 113-125.

7. Asche, C.; Dumy, P.; Carrez, D.; Croisy, A.; Demeunynck, M., Nitrobenzylcarbamate prodrugs of cytotoxic acridines for potential use with nitroreductase gene-directed enzyme prodrug therapy. *Bioorg. Med. Chem. Lett.* **2006,***16* (7), 1990-1994.

8. Hu, L.; Wu, X.; Han, J.; Chen, L.; Vass, S. O.; Browne, P.; Hall, B. S.; Bot, C.; Gobalakrishnapillai, V.; Searle, P. F.; Knox, R. J.; Wilkinson, S. R., Synthesis and structure–activity relationships of nitrobenzyl phosphoramide mustards as nitroreductase-activated prodrugs. *Bioorg. Med. Chem. Lett.* **2011,***21* (13), 3986-3991.

9. Ohno, O.; Ye, M.; Koyama, T.; Yazawa, K.; Mura, E.; Matsumoto, H.; Ichino, T.; Yamada, K.; Nakamura, K.; Ohno, T.; Yamaguchi, K.; Ishida, J.; Fukamizu, A.; Uemura, D., Inhibitory effects of benzyl benzoate and its derivatives on angiotensin II-induced hypertension. *Bioorg. Med. Chem.* **2008,***16* (16), 7843-7852.

10. Sykes, B. M.; Hay, M. P.; Bohinc-Herceg, D.; Helsby, N. A.; O'Connor, C. J.; Denny, W. A., Leaving group effects in reductively triggered fragmentation of 4-nitrobenzyl carbamates. *J. Chem. Soc., Perkin Trans. 1* **2000,** (10), 1601-1608.

11. Singh, R.; Manjunatha, U.; Boshoff, H. I. M.; Ha, Y. H.; Niyomrattanakit, P.; Ledwidge, R.; Dowd, C. S.; Lee, I. Y.; Kim, P.; Zhang, L.; Kang, S.; Keller, T. H.; Jiricek, J.; Barry, C. E., PA-824 Kills Nonreplicating Mycobacterium tuberculosis by Intracellular NO Release. *Science* **2008,***322* (5906), 1392-1395.

CHAPTER 3.2: Investigation into modulation of release rate

3.2.1. Introduction

In Chapter 3.1, we presented O^2-(4-nitrobenzyl) diazeniumdiolates as nitroreductase (NTR) activated NO donor which can be potential candidates for delivery of cytotoxic NO in cancer cells in enzyme directed prodrug therapy (Figure 3.2.1). The release of NO from O^2-(4-nitrobenzyl) diazeniumdiolates takes place after reduction of nitro group to hydroxyl amine or amine group which undergoes electronic rearrangement to expel the diazeniumdiolate.

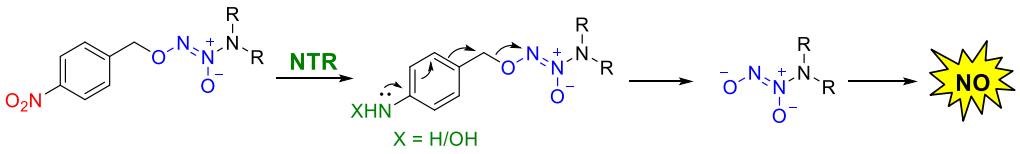

Figure 3.2.1. Proposed mechanism of activation of O^2-(4-nitrobenzyl) diazeniumdiolates by NTR.

There are two important features that dictate the rate of NTR reduction: a) the efficiency of the enzyme to reduce the substrate; and b) the fragmentation of the leaving group after reduction. In a study by Hu *et al.*, it was reported that substituents on the phenyl ring not only affected the reduction by NTR but the cytotoxicity was also influenced. However, the rate of reduction and cytotoxicity could not be correlated.[1] So far, the effects of substitution on the phenyl ring have been studied on NTR reduction and release of leaving group. The effect of benzylic substitution on NTR reduction has not been yet explored. As flow of electrons dictate release, substituting groups with different electron density at the benzylic position, may influence the release of the leaving group from the scaffold. Therefore, we propose the substituents on the benzylic position of 4-nitrobenzyl group may affect the release of NO or any other leaving group (Scheme 3.2.1).

In order to investigate the effects of benzylic substituent variation on the release of leaving group, several 4-nitrobenzyl umbelliferone ethers were synthesized as model compounds. In the presence of NTR with cofactor NADPH, the nitro group of 4-nitrobenzyl umbelliferone ethers gets reduced by NTR to form the electron rich hydroxylamine or amine species that releases umbelliferone. Using umbelliferone as

the fluorescence readout for NTR activation, the release profile of different benzylic-substituted compounds can be monitored conveniently.

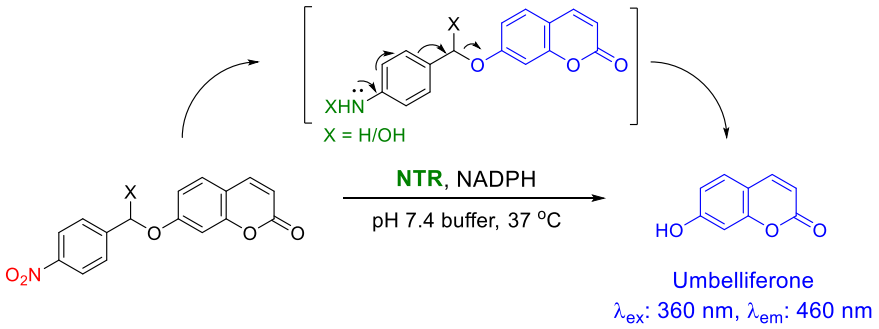

Scheme 3.2.1. NTR-activated model to study the effects of substituents at the benzylic position on the release of leaving group.

3.2.2. Results and discussion

3.2.2.1. Synthesis

In order to test our hypothesis, we synthesized nine compounds **20**, **21**, **24**, **27**, **30**, **32**, **34**, **36** and **38** to study the effects of benzylic substituents on the release of leaving group upon NTR reduction (Figure 3.2.2).

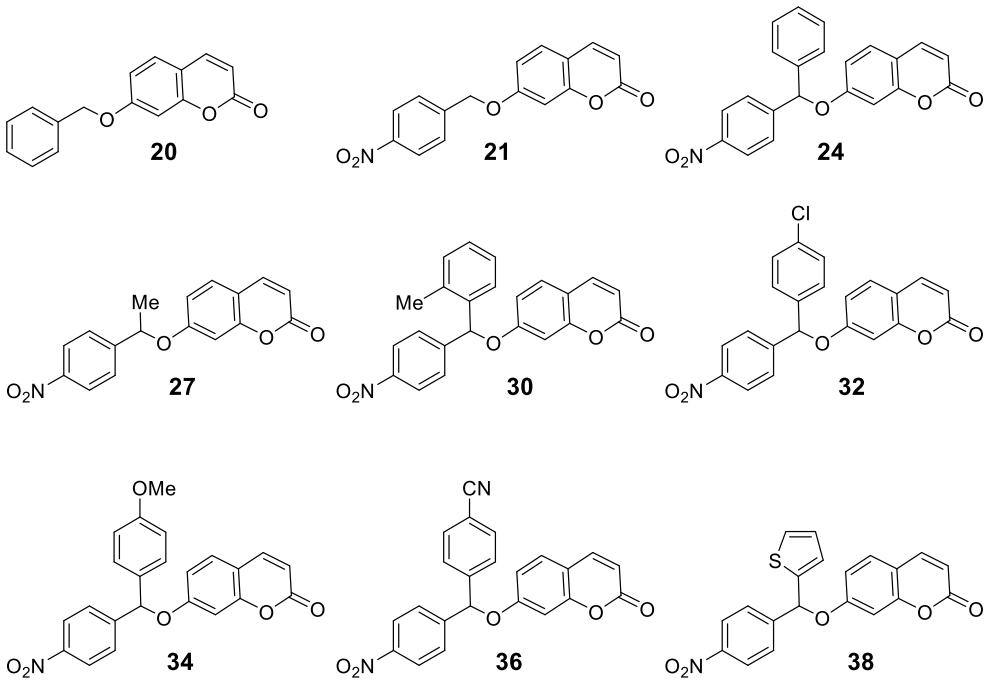

Figure 3.2.2. Substituted 4-nitrobenzyl umbelliferone ethers synthesized to study the modulation on release of umbelliferone from 4-nitrobenzyl group.

A negative control **20**, which is not a substrate for NTR, was synthesized by reacting benzyl bromide with umbelliferone in the presence of K_2CO_3 to obtain **20** in 66% yield. Due to the absence of nitro group on the phenyl ring, compound **20** cannot be reduced by NTR to release umbelliferone. Using similar reaction conditions, compound **21** was synthesized with 88% yield by reacting 4-nitrobenzyl bromide with umbelliferone in the presence of K_2CO_3 (Scheme 3.2.2).

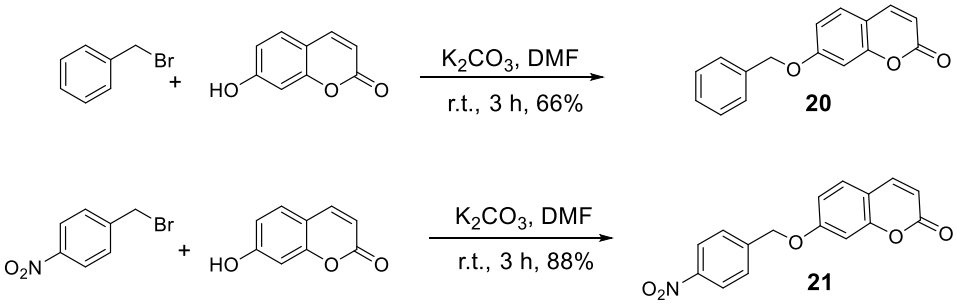

Scheme 3.2.2. Synthesis of **20** and **21**.

In order to derivatize the benzylic position, 4-nitrobenzaldehyde was reacted with different Grignard reagents at -78 ^oC to afford benzyl substituted 4-nitrobenzyl alcohols in yields ranging from 21-72% (Table 3.2.1).

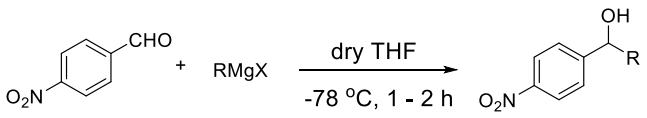

Entry	Compound	Substituent, R	% Yield
1	**22**	Phenyl	65
2	**25**	Methyl	21
3	**28**	2-Me phenyl	72
4	**31**	4-Cl phenyl	62

Table 3.2.1. Synthesis of benzyl substituted 4-nitrobenzyl alcohols.

The alcohols were then converted into bromides by treating with PBr_3 in dry DCM with yields ranging from 36-87% (Table 3.2.2).

The bromides were displaced with umbelliferone in the presence of K_2CO_3 to obtain the benzyl substituted 4-nitrobenzyl umbelliferone ethers in yields ranging from 37-65% (Table 3.2.3).

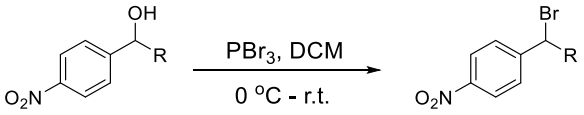

Entry	Compound	Substituent, R	% Yield
1	**23**	Phenyl	47
2	**26**	Methyl	36
3	**29**	2-Me phenyl	49

Table 3.2.2. Synthesis of benzyl substituted 4-nitrobenzyl bromides using PBr_3.

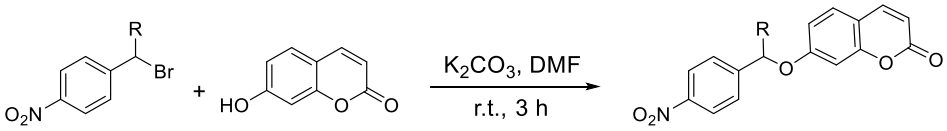

Entry	Compound	Substituent, R	% Yield
1	**24**	Phenyl	37
2	**27**	Methyl	45
3	**30**	2-Me phenyl	65

Table 3.2.3. Synthesis of 4-nitrobenzyl umbelliferone ethers **24**, **27** and **30**.

In order to synthesize benzhydrol **33**, 4-methoxyphenyl magnesium bromide was generated *in situ* using 4-bromo anisole, magnesium and dibromoethane by refluxing in dry THF. The Grignard reagent thus generated was reacted with 4-nitrobenzaldehyde in the same reaction flask to obtain **33** in 86% yield (Scheme 3.2.3).

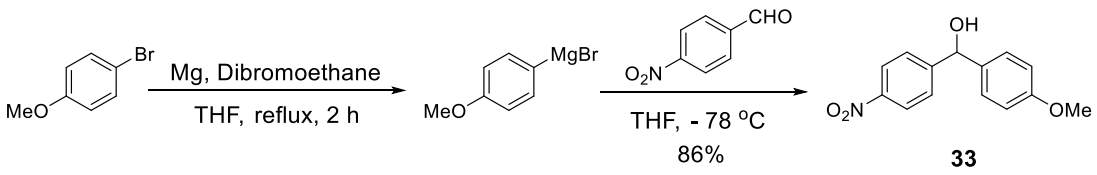

Scheme 3.2.3. *In situ* generation of 4-methoxy phenyl magnesium bromide followed by reaction with 4-nitrobenzaldehyde to form **33**.

Next, 4-bromobenzonitrile was reacted with n-BuLi to generate lithiated benzonitrile which was then reacted with 4-nitrobenzaldehyde to obtain compound **35** in 57% yield (Scheme 3.2.4).

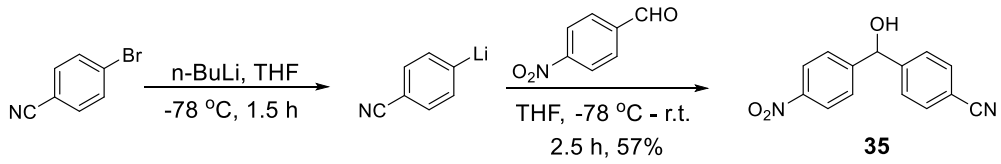

Scheme 3.2.4. *In situ* generation of lithiated benzonitrile followed by reaction with 4-nitrobenzaldehyde to form **35**.

Similarly, compound **37** was synthesized by treating 2-bromo thiophene with *n*-BuLi in THF at -78 °C. The lithiated thiophene formed *in situ* was reacted with 4-nitrobenzaldehyde to obtain compound **37** in 47% yield (Scheme 3.2.5).

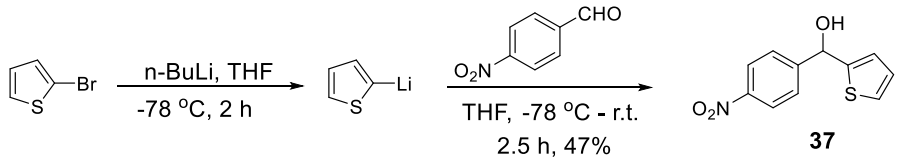

Scheme 3.2.5. *In situ* generation of lithiated thiophene followed by reaction with 4-nitrobenzaldehyde to form **37**.

The benzhydrols **33**, **35** and **37** were then reacted with umbelliferone to form 4-nitrobenzyl umbelliferone ethers using Mitsunobu reaction condition to form compounds **34**, **36** and **38**, respectively (Table 3.2.4).

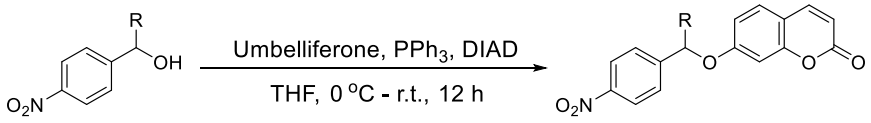

Entry	Compound	Substituent, R	% Yield
1	**32**	4-Cl phenyl	65
2	**34**	4-OMe phenyl	6
3	**36**	4-CN phenyl	73
4	**38**	2-Thiophenyl	29

Table 3.2.4. Synthesis of substituted 4-nitrobenzyl umbelliferone ethers **32**, **34**, **36** and **38**.

3.2.2.2. Evaluation of NTR reduction

To evaluate NTR activation and umbelliferone release, compound **21** (50 µM) was incubated with NTR in the presence of NADPH in pH 7.4 buffer at 37 ^{o}C and an increase in umbelliferone fluorescence was monitored over 3 h using a microwell plate reader (λ_{ex}: 360 nm; λ_{em}: 460 nm). Compound **21** was reduced by NTR to release umbelliferone as measured by increase in fluorescence (Figure 3.2.3). Next, the negative control **20** was incubated with NTR under similar reaction condition and an increase in fluorescence was monitored over 3 h. Due to absence of 4-nitro group, **20** was not a substrate for NTR and hence, it was not metabolised to release umbelliferone in buffer (Figure 3.2.3).

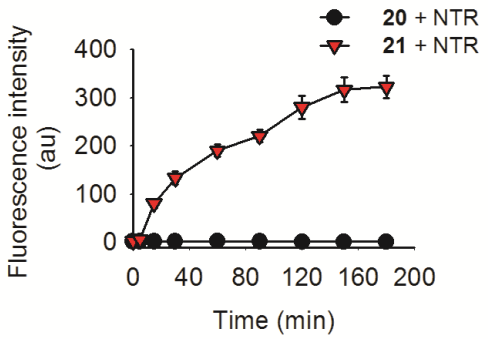

Figure 3.2.3. Fluorescence measurement due to umbelliferone release upon NTR reduction of **20** and **21** (50 µM) using NADPH as cofactor (λ_{ex}: 360 nm; λ_{em}: 460 nm).

Next, compounds **24**, **27**, **30**, **32**, **34**, **36** and **38** (50 µM) were independently incubated with NTR and cofactor NADPH in pH 7.4 buffer in a 96-well plate and the release of umbelliferone over 3 h was monitored. Altogether, we found an increase in fluorescence for 4-nitrobenzyl umbelliferone ethers **20**, **24**, **27**, **30**, **32**, **34**, **36** and **38** when incubated with NTR, suggesting these model compounds were reduced by NTR to release umbelliferone. However, **20** was not reduced by NTR to release umbelliferone (Figure 3.2.4). Comparing the fluorescence intensity of umbelliferone (50 µM) under similar buffer conditions, it was found that none of the 4-nitrobenzyl umbelliferone ethers were able to generate 100% umbelliferone upon incubation with NTR (Table 3.2.5). In case of the unsubstituted compound **21**, the umbelliferone release was found to be 27%. Compound **38** with thiophene substituent was slightly better in releasing umbelliferone (~ 7% more) compared to **21**. Compounds **24** (phenyl substituent) and **36** (4-CN phenyl substituent) released similar amount of

umbelliferone as compound **21**. Compounds **30** (2-Me phenyl substituent) and **34** (4-OMe phenyl substituent) released ~20% umbelliferone. However, compounds **27** (methyl substituent) and **32** (4-Cl phenyl substituent) were found to release very less, ~10% umbelliferone after 3 h of NTR incubation.

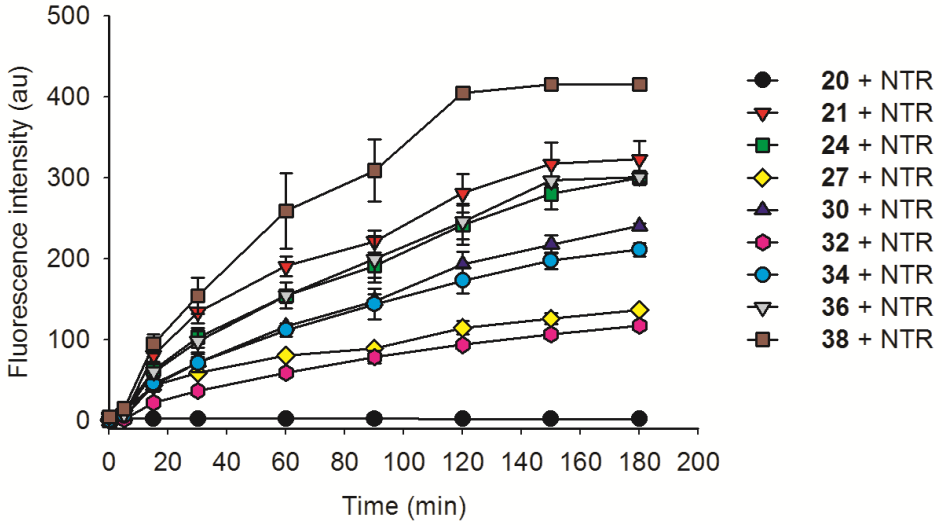

Figure 3.2.4. Fluorescence measurement due to umbelliferone release upon NTR reduction of **20** and 4-nitrobenzyl umbelliferone ethers by NTR (λ_{ex}: 360 nm; λ_{em}: 460 nm).

Entry	Compound	%Fluorescence
1	**20**	0.1
2	**21**	27.5
3	**24**	25.5
4	**27**	11.5
5	**30**	20.4
6	**32**	9.9
7	**34**	17.9
8	**36**	25.5
9	**38**	35.3
10	Umbelliferone	100.0

Table 3.2.5. Estimation of umbelliferone released from incubation of 50 µM of **20** and 4-nitrobenzyl umbelliferone ethers with NTR and NADPH in pH 7.4 buffer at 37 ^{o}C after 3 h. Fluorescence intensity (λ_{ex}: 360 nm; λ_{em}: 460 nm) from 50 µM of umbelliferone was considered to be 100%.

Thus, we found 4-nitrobenzyl umbelliferone ethers were reduced by NTR to release umbelliferone in different amounts. During HPLC based experiment to monitor the decomposition of 4-nitrobenzyl umbelliferone ethers in the presence of NTR, it was found that some compounds were precipitating out in buffer. Therefore, due to solubility issues, the results of enzymatic reduction of 4-nitrobenzyl umbelliferone ethers in buffer may not be conclusive and it would be difficult to explain the effects of benzylic substituent on the release profile.

3.2.2.3. Bioreduction in bacteria

As NTR is a bacterial enzyme and 4-nitrobenzyl is well known substrate for bacterial NTR so, it is expected that the 4-nitrobenzyl umbelliferone ethers undergo bioreduction when incubated in bacteria to release umbelliferone. In order to study the bioreduction of the 4-nitrobenzyl umbelliferone ethers, we selected *Escherichia coli* (*E. coli*), a gram negative bacteria and *Staphylococcus aureus* (SA), a gram positive bacteria, that express NTR.[2]

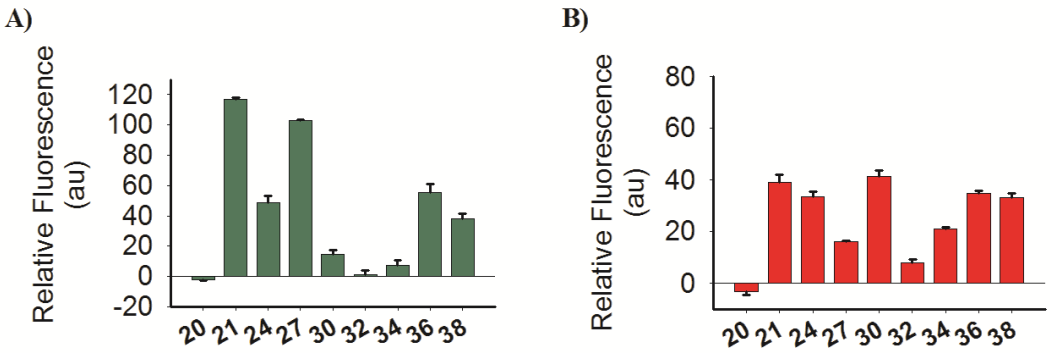

Figure 3.2.5. Bioreduction of 4-nitrobenzyl umbelliferone ethers (5 µM) in bacteria. **A)** Fluorescence measurement due to umbelliferone release (λ_{ex}: 360 nm; λ_{em}: 460 nm) upon incubation of different 4-nitrobenzyl umbelliferone ethers and **20** in *E. coli*. for 12 h at 37 ^{o}C. **B)** Fluorescence measurement due to umbelliferone release (λ_{ex}: 360 nm; λ_{em}: 460 nm) upon incubation of different 4-nitrobenzyl umbelliferone ethers and **20** in SA for 12 h at 37 ^{o}C.

5 µM of the 4-nitrobenzyl umbelliferone ethers were independently incubated in *E. coli* at 37 ^{o}C for 12 h in a 96-well plate and increase in umbelliferone fluorescence was monitored (λ_{ex}: 360 nm; λ_{em}: 460 nm). An increase in fluorescence for 4-nitrobenzyl umbelliferone ethers treated *E. coli* was observed as compared to compound untreated *E. coli*. A similar bioreduction experiment performed by independently incubating 5 µM of the 4-nitrobenzyl umbelliferone ethers in SA resulted in increase in fluorescence. Thus, an increase in fluorescence for both *E. coli*

and SA cultures treated independently with **21**, suggested that **21** was bioreductively activated by bacterial NTR to release umbelliferone. On the contrary, negligible increase in fluorescence was seen with the negative control **20** when incubated in both bacteria. However, here also we noticed that the compounds were precipitating out to some extent in media. In *E. coli*, it was found that aromatic substituents reduced the rate of bioreduction presumably due to increased steric bulk that hinders NTR reduction and subsequently reduces umbelliferone release (Figure 3.2.5.A). However, methyl substituent at the benzylic position in **27** is sterically less bulkier group and therefore fluorescence increase was similar to **21**. In SA, aromatic substituted compounds showed almost similar umbelliferone release as **21** (Figure 3.2.5.B). We found that compound **32** (4-Cl phenyl substituent) was found to be reduced slowly in both bacteria to release umbelliferone.

3.2.3. Conclusion

In this chapter, we synthesized benzylic substituted 4-nitrobenzyl umbelliferone ethers to study substituent effect on NTR reduction. There are two main aspects of NTR reduction: the selectivity of enzyme for substrates and fragmentation of leaving group after NTR reduction. With the help of 4-nitrobenzyl umbelliferone ethers, we attempted to study the effects of benzylic substituent of the 4-nitrobenzyl group on NTR reduction. The enzymatic reduction of the model compounds, led to an increase in fluorescence indicating that 4-nitrobenzyl umbelliferone ethers were reduced to release umbelliferone. Bioreduction of the compounds was performed in *E. coli* and SA. It was observed that the 4-nitrobenzyl umbelliferone ethers were reduced inside bacteria to generate umbelliferone as well. However, solubility issue of the model compounds may complicate interpretation during enzymatic reduction in buffer and also in culture media during bioreduction. Thus due to solubility issue of the compounds, no correlation between substituent effect and umbelliferone release could be inferred.

3.2.4. Experimental Section

3.2.4.1. General procedure for synthesis of benzhydrols 22, 25, 28 and 31

A solution of dry THF was cooled to -78 ^{o}C under nitrogen atmosphere. The Grignard reagent (1.2 eq.) was added and stirred at -78 ^{o}C for 30 min. To the reaction mixture, a solution of 4-nitrobenzaldehyde (1 eq.) in dry THF was added drop wise and reaction mixture was stirred at -78 ^{o}C for 1 to 2 h. The reaction mixture was quenched using saturated NH_4Cl solution and the aqueous solution was extracted using ethyl acetate. The combined organic layer was washed with brine, dried (Na_2SO_4), filtered and the filtrate was evaporated to give crude product. The crude product was purified using silica gel column chromatography.

Compounds **22**, **25**, **28** and **31** have been previously reported and the analytical data that we obtained were consistent with reported data.[3]

3.2.4.2. General procedure for bromination of benzhydrols 23, 26 and 29

The solution of benzhydrol (1 eq.) in dry DCM under nitrogen atmosphere was cooled to 0 ^{o}C. To the reaction mixture PBr_3 (1.2 eq) was added and the reaction mixture was stirred at 0 ^{o}C with gradual warming to room temperature for 1 to 2 h. The reaction mixture was quenched using saturated $NaHCO_3$ solution. The aqueous solution was extracted in DCM. The combined organic layer was washed with brine, dried (Na_2SO_4), filtered and the filtrate was evaporated to give crude product. Purification was done using silica gel column chromatography to obtain pure product.

Compounds **23**[4] and **26**[5] have been previously reported and the analytical data that we obtained were consistent with the reported data.

Synthesis of 1-(bromo(4-nitrophenyl)methyl)-2-methylbenzene, 29.

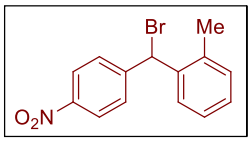

Brown liquid (0.26 g, 49%); FT-IR (ν_{max}, cm^{-1}): 1599, 1519, 1345, 701; ^{1}H NMR ($CDCl_3$, 400 MHz) δ: 8.17 (d, *J* = 8.8 Hz, 2H), 7.59 (d, *J* = 8.7 Hz, 2H), 7.39-7.43 (m, 1H), 7.16-7.25 (m, 3H), 6.47 (s, 1H); ^{13}C NMR ($CDCl_3$, 100 MHz) δ: 147.6, 147.4, 137.7, 135.5, 131.1, 129.6, 129.5, 128.9, 126.9, 123.8, 50.7, 19.6; HRMS (ESI) for $C_{14}H_{12}BrNO_2$ $[M+H]^+$: Calcd., 306.0129, Found, 306.0107.

3.2.4.3. General procedure for synthesis of umbelliferone ethers from bromides 20, 21, 24, 27 and 30

To a stirred solution umbelliferone (1 eq.) in dry DMF under nitrogen atmosphere at room temperature, K_2CO_3 (1 eq.) was added and stirred for 10 min. To this solution, substituted bromide (1.2 eq.) was added and the reaction mixture was stirred at room temperature for 3-8 h. Ice cold water was added and the reaction mixture was extracted in ethyl acetate. The combined organic layer was washed with brine, dried (Na_2SO_4), filtered and the filtrate was evaporated to give crude product. Purification was done using silica gel column chromatography to obtain pure product.

Compound **20** has been previously reported and the analytical data that we obtained was consistent with the reported data.[6]

Synthesis of 7-((4-nitrobenzyl)oxy)-2H-chromen-2-one, 21.

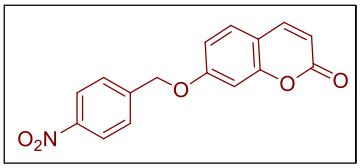

White solid (0.24 g, 88%); m.p. 181-182 ^{o}C; FT-IR (ν_{max}, cm^{-1}): 1728, 1614, 1516, 1346, 1127; ^{1}H NMR ($CDCl_3$, 400 MHz) δ: 8.27 (d, *J* = 8.7 Hz, 2H), 7.61-7.66 (m, 3H), 7.41 (d, *J* = 8.6 Hz, 1H), 6.93 (dd, *J* = 8.6, 2.4 Hz, 1H), 6.86 (d, *J* = 2.2 Hz, 1H), 6.28 (d, *J* = 9.5 Hz, 1H), 5.23 (s, 2H); ^{13}C NMR ($CDCl_3$, 400 MHz) δ: 161.1, 161.0, 155.8, 147.9, 143.3, 143.2, 129.1, 127.8, 124.1, 113.8, 113.3, 113.1, 102.0, 69.1; HRMS (ESI) for $C_{16}H_{11}NO_5$ $[M+H]^+$: Calcd., 298.0715, Found, 298.0685.

Synthesis of 7-((4-nitrophenyl)(phenyl)methoxy)-2H-chromen-2-one, 24.

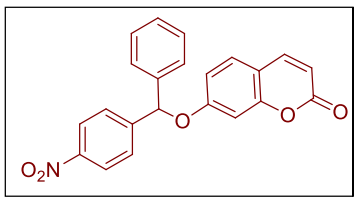

White solid (0.10 g, 37%), m.p. 210-211 ^{o}C; FT-IR (ν_{max}, cm^{-1}): 1724, 1611, 1513, 1342, 1124; ^{1}H NMR ($CDCl_3$, 400 MHz) δ: 8.22 (d, *J* = 8.8 Hz, 2H), 7.60-7.63 (m, 3H), 7.35-7.41 (m, 1H), 6.95 (dd, *J* = 8.6, 2.5 Hz, 1H), 6.82 (d, *J* = 2.4 Hz, 1H), 6.25 (d, *J* = 9.4 Hz, 1H); ^{13}C NMR ($CDCl_3$, 400 MHz) δ: 161.0 ,160.4, 155.6, 147.6, 147.4, 143.3, 138.8, 129.3, 129.0, 129.0, 127.5, 126.8, 124.2, 114.0, 113.8, 113.3, 103.3, 81.3; HRMS (ESI) for $C_{22}H_{15}NO_5$ $[M+H]^+$: Calcd., 374.1028, Found, 374.1033.

Synthesis of 7-(1-(4-nitrophenyl)ethoxy)-2H-chromen-2-one, 27.

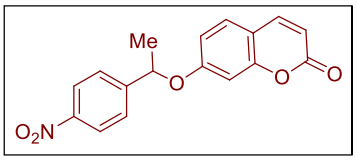

White solid (72 mg, 45%), m.p. 172-173 ^{o}C; FT-IR (ν_{max}, cm^{-1}): 1712, 1610, 1514, 1343, 1125; ^{1}H NMR ($CDCl_3$, 400 MHz) δ: 8.21 (d, *J* = 8.7 Hz, 2H), 7.59 (d, *J* = 9.4 Hz, 1H), 7.53 (d, *J* = 8.7 Hz, 2H), 7.33 (d, *J* = 8.6 Hz, 1H), 6.82 (dd, *J* = 8.5, 2.4 Hz, 1H), 6.66 (d, *J* = 2.4 Hz, 1H), 6.22 (d, *J* = 9.4 Hz, 1H), 5.46 (q, *J* = 6.4 Hz, 1H), 1.69 (d, *J* = 6.4 Hz, 3H); ^{13}C NMR ($CDCl_3$, 400 MHz) δ: 161.0, 160.4, 155.6, 149.3, 147.6, 143.3, 129.0, 126.4, 124.3, 113.7, 113.6, 113.0, 102.9, 75.8, 24.3; HRMS (ESI) for $C_{17}H_{13}NO_5$ $[M+H]^+$: Calcd., 312.0872, Found, 312.0836.

Synthesis of 7-((4-nitrophenyl)(o-tolyl)methoxy)-2H-chromen-2-one, 30.

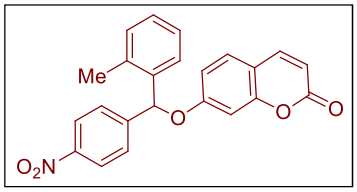

White solid (58 mg, 65%), m.p 154-155 ^{o}C; FT-IR (ν_{max}, cm^{-1}): 1728, 1610, 1517, 1344, 1123; ^{1}H NMR ($CDCl_3$, 400 MHz) δ: 8.23 (d, *J* = 8.8 Hz, 2H), 7.61 (d, *J* = 9.5 Hz, 1H), 7.55 (d, *J* = 8.5 Hz, 2H), 7.37 (d, *J* = 8.6 Hz, 1H), 7.23-7.29 (m, 4H), 6.91 (dd, *J* = 8.6, 2.4 Hz, 1H), 6.74 (d, *J* = 2.4 Hz, 1H), 6.48 (s, 1H), 6.25 (d, *J* = 9.5 Hz, 1H), 2.36 (s, 3H); ^{13}C NMR ($CDCl_3$, 400 MHz) δ: 161.0, 160.6, 155.7, 147.7, 146.2, 143.3, 136.2, 135.8, 131.5, 129.1, 128.4, 127.2, 126.9, 124.0, 113.9, 113.7, 113.2, 103.0, 78.9, 19.6; HRMS (ESI) for $C_{23}H_{17}NO_5$ $[M+H]^+$: Calcd., 388.1185, Found, 388.1162.

Synthesis of (4-methoxyphenyl)(4-nitrophenyl)methanol, 33.

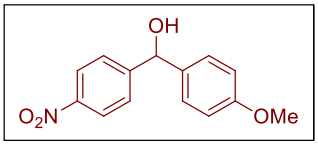

To a stirred solution of 4-bromo anisole (10.7 mmol) in dry THF (20 mL) under nitrogen atmosphere, activated magnesium (10.7 mmol) and dibromoethane (2.07 mmol) were added and the reaction mixture was refluxed until a grey coloured precipitate was seen. The reaction mixture was cooled to room temperature and then to -78 ^{o}C under nitrogen atmosphere. To this reaction mixture, a solution of 4-nitrobenzaldehyde (6.42 mmol) in dry THF (15 mL) was added dropwise and the reaction mixture was stirred at -78 ^{o}C with gradually warming to 0 ^{o}C (1.5 h). The reaction mixture was quenched using saturated NH_4Cl solution and the aqueous solution as extracted using ethyl acetate. The combined organic layer was washed with brine, dried (Na_2SO_4), filtered and the filtrate was evaporated to give crude product. Purification was done using silica gel column chromatography using 20%

ethyl acetate: pet ether as eluent to obtain pure product. This compound has been previously reported and the analytical data that we obtained was consistent with the reported data.[7]

Synthesis of 4-(hydroxy(4-nitrophenyl)methyl)benzonitrile, 35.

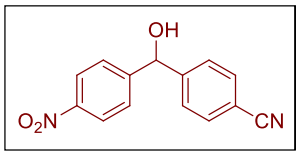

A solution of isopropyl magnesium chloride (1.1 mmol) in dry THF (5 mL) was cooled to 0 ^{o}C under nitrogen atmosphere. To the reaction mixture *n*-BuLi (1.1 mmol.) was added and the reaction mixture was stirred at 0 ^{o}C for 30 min. The reaction mixture was then cooled to -78 ^{o}C and stirred at the same temperature for 1 h. To this reaction mixture, a solution of 4-bromo benzonitrile (0.88 mmol) in dry THF (5 mL) was added dropwise and the reaction mixture was stirred -78 ^{o}C for an additional one hour. The reaction mixture was quenched using saturated NH_4Cl solution and the aqueous solution was extracted using ethyl acetate. The combined organic layer was washed with brine, dried (Na_2SO_4), filtered and the filtrate was evaporated to give crude product. Purification was done using silica gel column chromatography and by using 20-25% ethyl acetate: pet ether as eluent, pure product was obtained as a yellow solid (0.4 g, 57%), m.p. 152-153 ^{o}C; FT-IR (ν_{max}, cm^{-1}): 3424, 2231, 1676, 1516, 1344; ^{1}H NMR ($CDCl_3$, 400 MHz) δ: 8.19 (d, *J* = 8.8 Hz, 2H), 7.64 (d, *J* = 8.2 Hz, 2H), 7.55 (d, *J* = 8.7 Hz, 2H), 7.50 (d, *J* = 8.2 Hz, 2H), 5.97 (s, 1H), 2.91 (s, 1H); ^{13}C NMR ($CDCl_3$, 400 MHz) δ: 149.6, 147.7, 147.6, 132.7, 127.3, 127.2, 124.1, 118.5, 112.0, 74.7; HRMS (ESI) for $C_{24}H_{10}N_2O_3$ $[M+H]^+$: Calcd., 255.0769, Found, 255.0773.

Synthesis of (4-nitrophenyl)(thiophen-2-yl)methanol, 37.

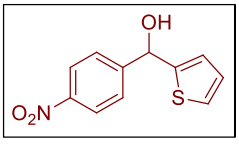

A solution of 2-bromo thiophene (2.69 mmol) in dry THF (5 mL) was cooled to -78 ^{o}C under nitrogen atmosphere. To the reaction mixture *n*-BuLi (2.69 mmol) was added dropwise and the reaction mixture was stirred at -78 ^{o}C for 1 h. To the reaction mixture, a solution of 4-nitrobenzadehyde (2.40 mmol) in dry THF (5 mL) was added dropwise and the reaction mixture was stirred at -78 ^{o}C for an additional 1 h. The reaction mixture was quenched using saturated NH_4Cl solution and aqueous solution was extracted using ethyl acetate. The combined organic layer was washed with brine, dried (Na_2SO_4), filtered and the filtrate was evaporated to give crude product. Purification was done

using silica gel column chromatography, 15% ethyl acetate: pet ether was used as eluent to obtain pure product. This compound has been previously reported and the analytical data that we obtained was consistent with the reported data.[8]

3.2.4.4. General procedure for Mitsunobu reaction 32, 34, 36 and 38

A solution of benzhydrol (1 eq.), umbelliferone (1 eq.) and PPh_3 (2 eq.) in dry THF was cooled to 0 ^oC under nitrogen atmosphere. To the reaction mixture, DIAD (2 eq.) was added and the reaction mixture was gradually warmed to room temperature and stirred for 12 h. The reaction mixture was diluted with water and the aqueous solution was extracted using DCM. The combined organic layer was washed with brine, dried (Na_2SO_4), filtered and the filtrate was evaporated to obtain crude product. Purification was done using silica gel column chromatography to afford pure product.

Synthesis of 7-((4-chlorophenyl)(4-nitrophenyl)methoxy)-2H-chromen-2-one, 32.

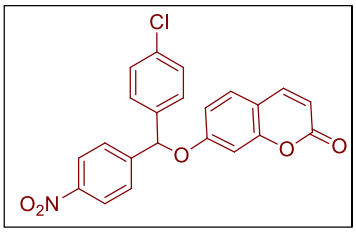

White solid (0.155 g, 65%), m.p. 185-186 ^oC; FT-IR (ν_{max}, cm^{-1}): 1728, 1611, 1519, 1345, 1125; ^1H NMR ($CDCl_3$, 400 MHz) δ: 8.22 (d, *J* = 8.7 Hz, 2H), 7.61 (d, *J* = 8.3 Hz, 3H), 7.36-7.39 (m, 5H), 6.93 (dd, *J* = 8.6, 2.3 Hz, 1H), 6.80 (d, *J* = 2.2 Hz, 1H), 6.34 (s, 1H), 6.25 (d, *J* = 9.5 Hz, 1H); ^{13}C NMR ($CDCl_3$, 400 MHz) δ: 160.9, 160.0, 155.6, 147.8, 146.8, 143.2, 137.3, 134.9, 129.5, 129.1, 128.2, 127.5, 124.3, 114.0, 113.9, 113.4, 103.3, 80.6; HRMS (ESI) for $C_{22}H_{14}ClNO_5$ $[M+H]^+$: Calcd., 408.0639, Found, 408.0618.

Synthesis of 7-((4-methoxyphenyl)(4-nitrophenyl)methoxy)-2H-chromen-2-one, 34.

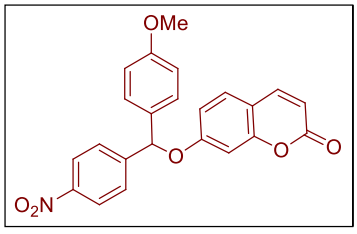

White solid (30 mg, 6%), m.p. 215-216 ^oC; FT-IR (ν_{max}, cm^{-1}): 1720, 1610, 1510, 1343, 1124, 1021; ^1H NMR ($CDCl_3$, 400 MHz) δ: 8.22 (d, *J* = 8.8 Hz, 2H), 7.58-7.61 (m, 3H), 7.35 (d, *J* = 8.6 Hz, 1H), 7.31 (d, *J* = 8.7 Hz, 2H), 6.89-6.95 (m, 3H), 6.81 (d, *J* = 2.4 Hz, 1H), 6.30 (s, 1H), 6.24 (d, *J* = 9.5 Hz, 1H), 3.79 (s, 3H); ^{13}C NMR ($CDCl_3$, 400 MHz) δ: 161.0, 160.5, 160.0, 155.7, 147.7, 147.6, 143.3, 130.8, 129.0, 128.4, 127.4, 124.1, 114.7, 114.1, 113.8, 113.2, 103.4, 81.1, 55.4; HRMS (ESI) for $C_{23}H_{17}NO_6$ $[M+H]^+$: Calcd., 404.1134, Found, 404.1113.

Synthesis of 4-((4-nitrophenyl)((2-oxo-2H-chromen-7-yl)oxy)methyl)benzonitrile, 36.

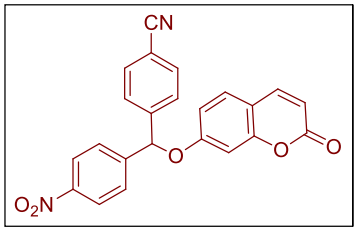

White solid (180 mg, 73%), m.p. 123-124 ^{o}C; FT-IR (ν_{max}, cm^{-1}): 2230, 1719, 1610, 1518, 1345, 1227, 1126; ^{1}H NMR ($CDCl_3$, 400 MHz) δ: 8.22 (d, *J* = 8.5 Hz, 2H), 7.68 (d, *J* = 8.1 Hz, 2H), 7.60-7.64 (m, 3H), 7.58 (d, *J* = 8.2 Hz, 2H), 7.38 (d, *J* = 8.6 Hz, 1H), 6.93 (dd, *J* = 8.5, 2.1 Hz, 1H), 6.68 (d, *J* = 2.1 Hz, 1H), 6.42 (s, 1H), 6.24 (d, *J* = 9.5 Hz, 1H); ^{13} C NMR ($CDCl_3$, 400 MHz) δ: 160.8, 159.7, 155.5, 147.9, 146.0, 144.0, 143.2, 133.0, 129.3, 127.5, 127.4, 124.4, 118.2, 114.1, 113.8, 113.6, 112.7, 103.3, 80.3; HRMS (ESI) for $C_{23}H_{14}N_2O_5$ $[M+H]^+$: Calcd., 399.0981, Found, 399.0984.

Synthesis of 7-((4-nitrophenyl)(thiophen-2-yl)methoxy)-2H-chromen-2-one, 38.

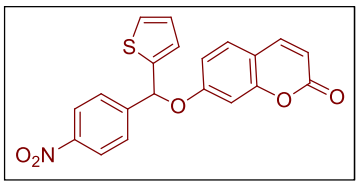

White solid (70 mg, 29 %), m.p. 197-198 ^{o}C; FT-IR (ν_{max}, cm^{-1}): 1718, 1161, 1510, 1339, 1123; ^{1}H NMR ($CDCl_3$, 400 MHz) δ: 8.24 (d, *J* = 8.8 Hz, 2H), 7.66 (d, *J* = 8.6 Hz, 2H), 7.60 (d, *J* = 9.5 Hz, 1H), 7.36 (d, *J* = 8.6 Hz, 1H), 7.34 (dd, *J* = 5.1, 1.4 Hz, 1H), 7.00-7.01 (m, 1H), 6.96-6.98 (m, 1H), 6.93 (dd, *J* = 8.6, 2.4 Hz, 1H), 6.83 (d, *J* = 2.4 Hz, 1H), 6.58 (s, 1H), 6.24 (d, *J* = 9.4 Hz, 1H); ^{13}C NMR ($CDCl_3$, 100 MHz) δ: 160.9, 160.0, 155.5, 147.9, 146.7, 143.3, 142.0, 129.1, 127.4, 127.3, 127.1, 126.9, 124.3, 114.0, 114.0, 113.5, 103.3; HRMS (ESI) for $C_{20}H_{13}NO_5S$ $[M+H]^+$: Calcd., 380.0592, Found, 380.0597.

3.2.4.5. Nitroreductase reduction

A 10 mM stock solution of the test compound was prepared in DMSO. Enzyme stock solution was prepared by dissolving 1.5 mg of NTR in phosphate buffer pH 7.4 (100 µL). A 210 µM stock solution of NADPH was prepared in phosphate buffer pH 7.4. A typical reaction mixture in a 96 well plate consisted of 50 µL of test compound (from 50 µM solution of test compound in buffer), 95 µL of NADPH and 5 µL of NTR enzyme. The control set was prepared by dissolving 50 µL of test compound (from 50 µM solution of test compound in buffer), 95 µL of NADPH and 5 µL of buffer. The 96-well plate was then incubated at 37 ^{o}C for 3 h. Fluorescence was measured using a Thermo Scientific Varioscan microwell plate reader (λ_{ex}: 360 nm and λ_{em}: 460 nm). The fluorescence reading for mentioned time point was average of four readings.

3.2.4.6. Bioreduction in bacteria

A stock solution of the test compound was prepared in DMSO. *Escherichia Coli* (EC2065) was cultured in 10 mL of Luria Bertani (LB) medium at 37 ºC for 16 h. *Staphylococcus aureus* (SA5021) was cultured in 10 mL of LB medium at 37 ºC for 16 h. The cultured *E. coli* bacterial suspension was centrifuged to aspirate out the medium and resuspended in fresh medium to obtain bacterial suspension of O.D 0.5. The experiment was performed in a 96 well plate. In control set, 100 µL of bacterial suspension was diluted with 100 µL LB. In another set serving as bioreductively activated set, 100 µL of bacterial suspension was diluted with 100 µL of test compound solution (final concentration of test compound: 5 µM). The 96-well plate was incubated at 37 ^{o}C for 12 h. Fluorescence was measured using a Thermo Scientific Varioscan microwell plate reader (λ_{ex}: 360 nm and λ_{em}: 460 nm). The fluorescence reading for mentioned time point was average of four readings. Same protocol was followed for monitoring bioreduction in *Staphylococcus aureus.*

3.2.5. Spectral charts

^{1}H NMR Spectrum (400 MHz, $CDCl_3$) of compound **21**

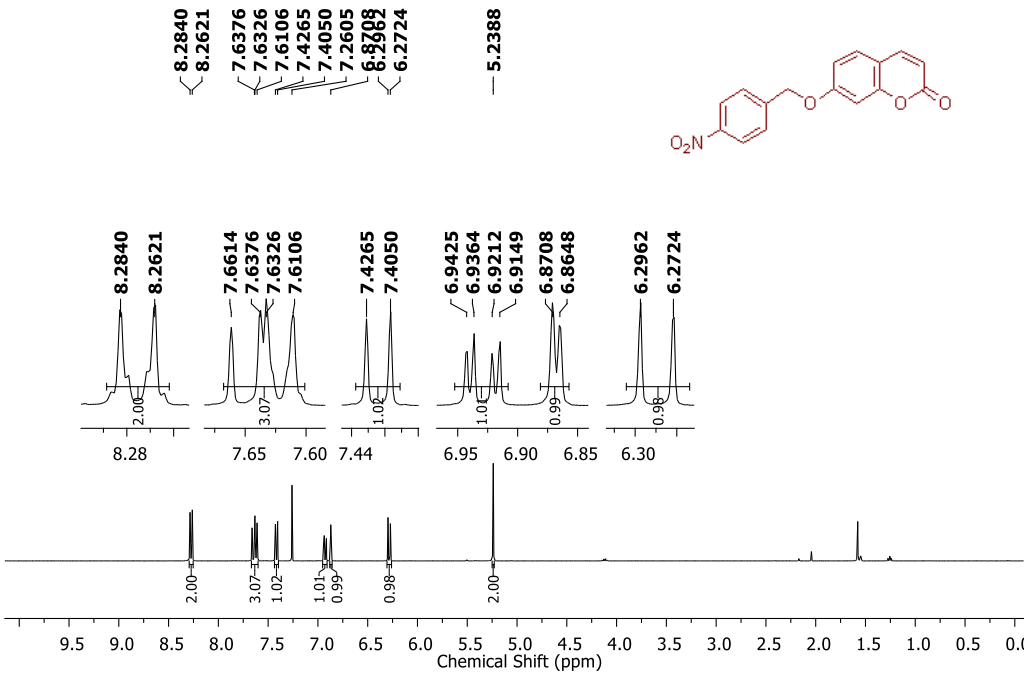

^{13}C NMR Spectrum (100 MHz, $CDCl_3$) of compound **21**

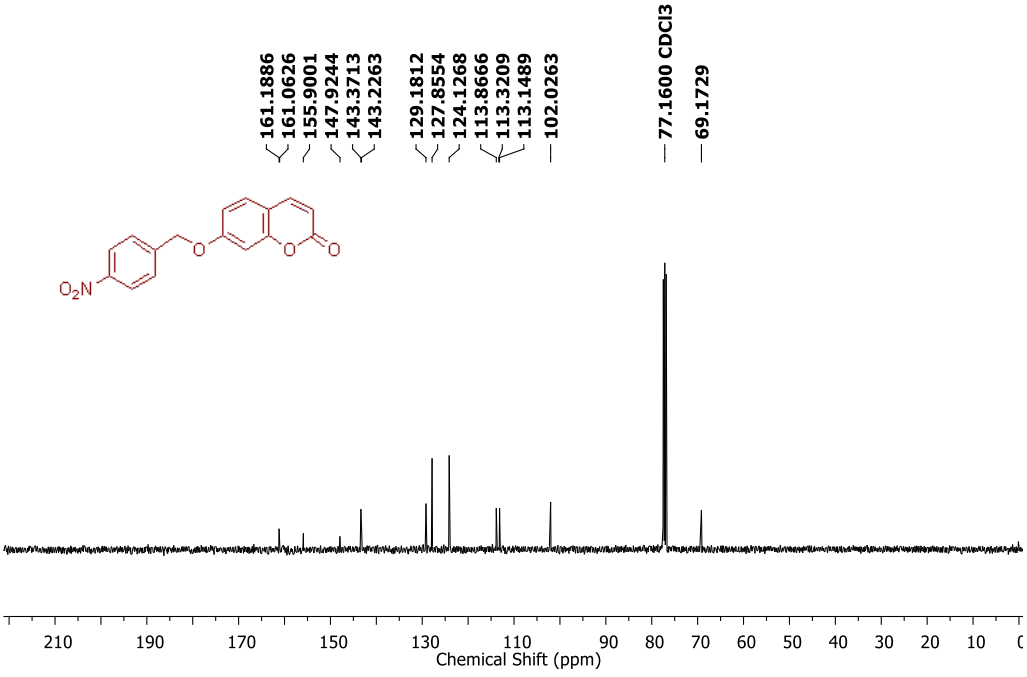

^{1}H NMR Spectrum (400 MHz, $CDCl_3$) of compound **24**

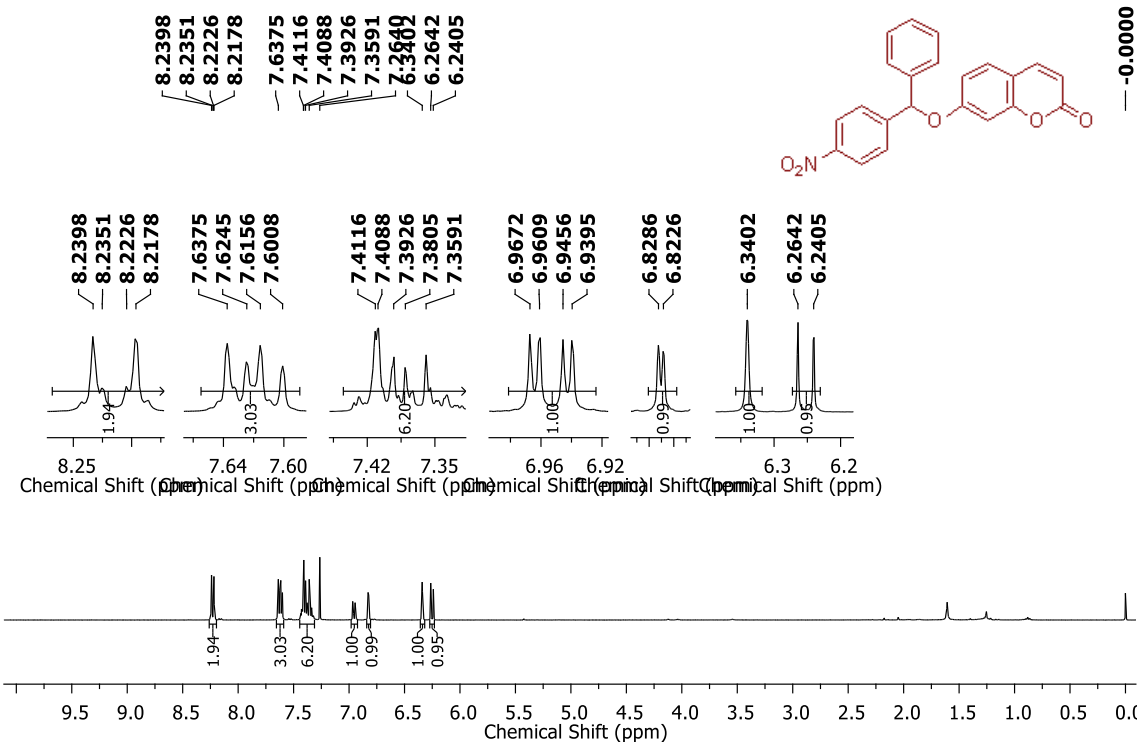

^{13}C NMR Spectrum (100 MHz, $CDCl_3$) of compound **24**

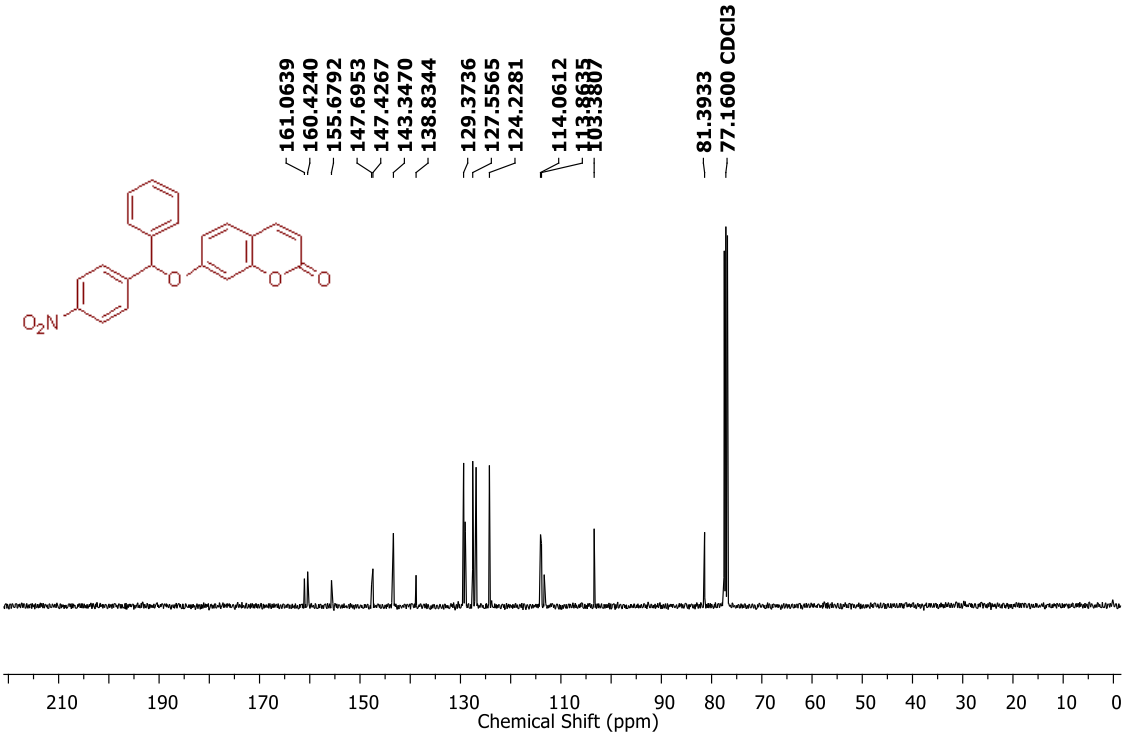

^{1}H NMR Spectrum (400 MHz, $CDCl_3$) of compound **27**

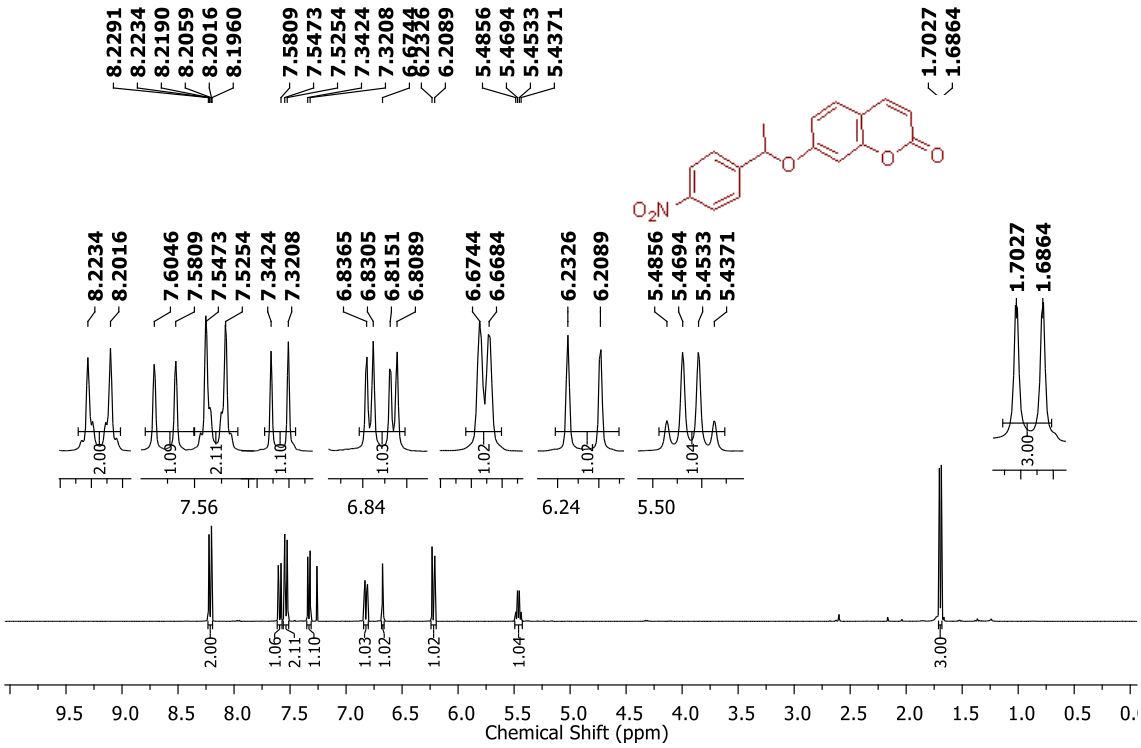

^{13}C NMR Spectrum (100 MHz, $CDCl_3$) of compound **27**

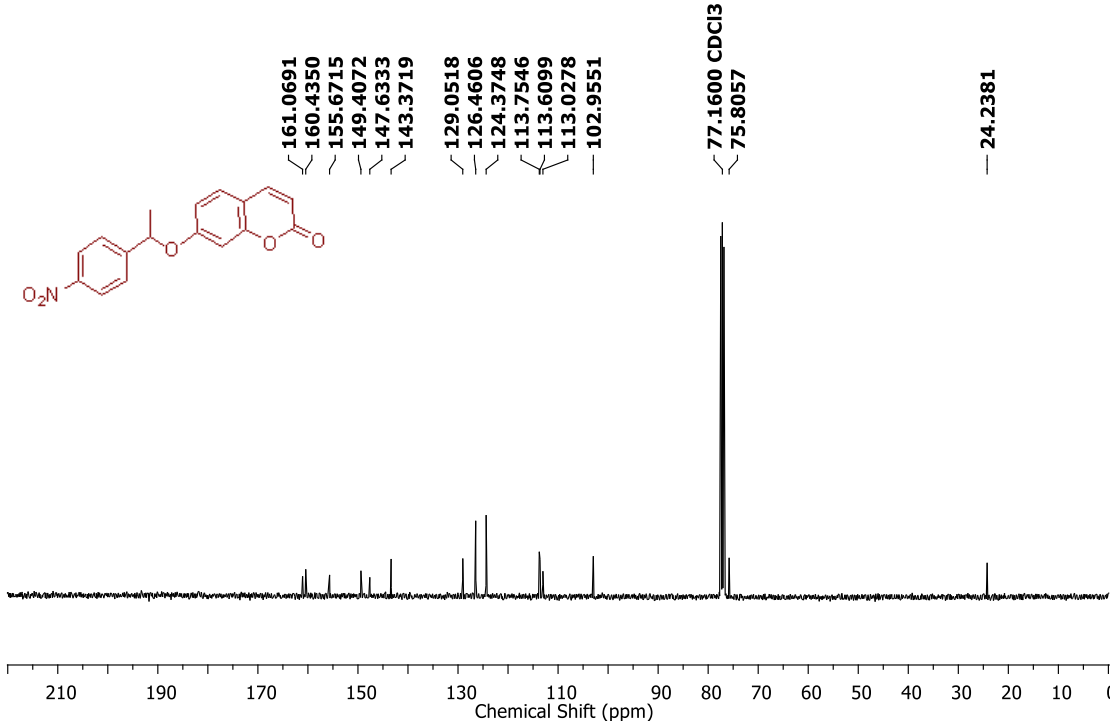

^{1}H NMR Spectrum (400 MHz, $CDCl_3$) of compound **29**

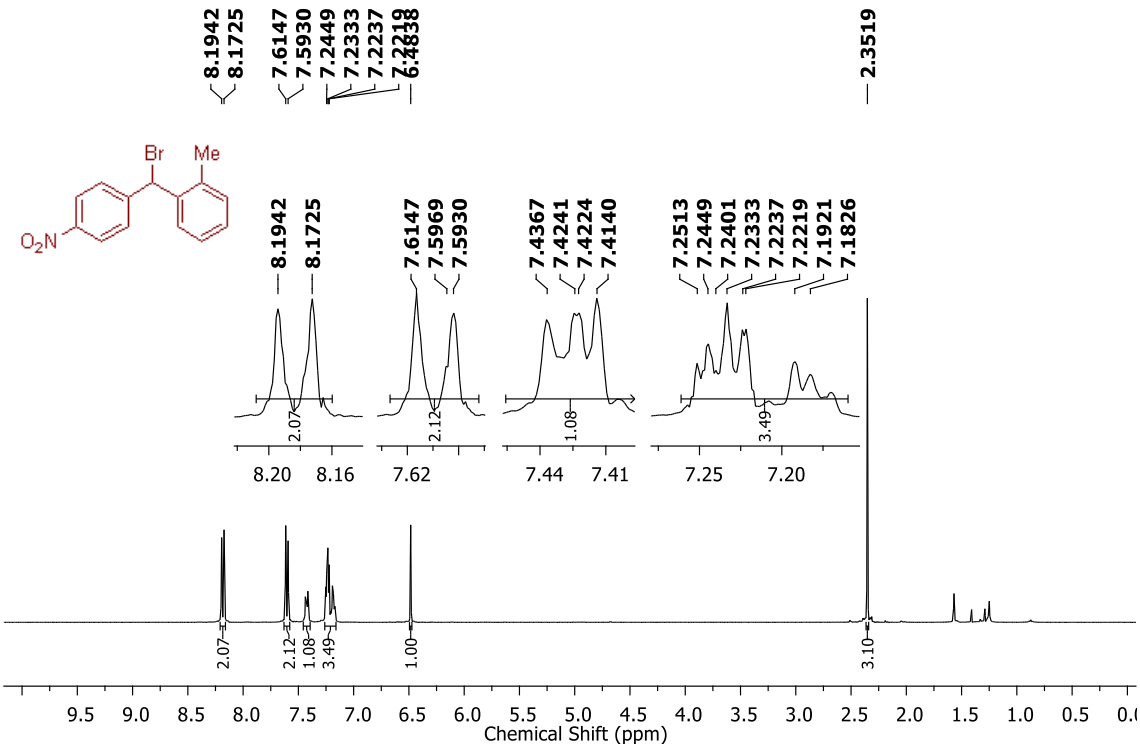

^{13}C NMR Spectrum (100 MHz, $CDCl_3$) of compound **29**

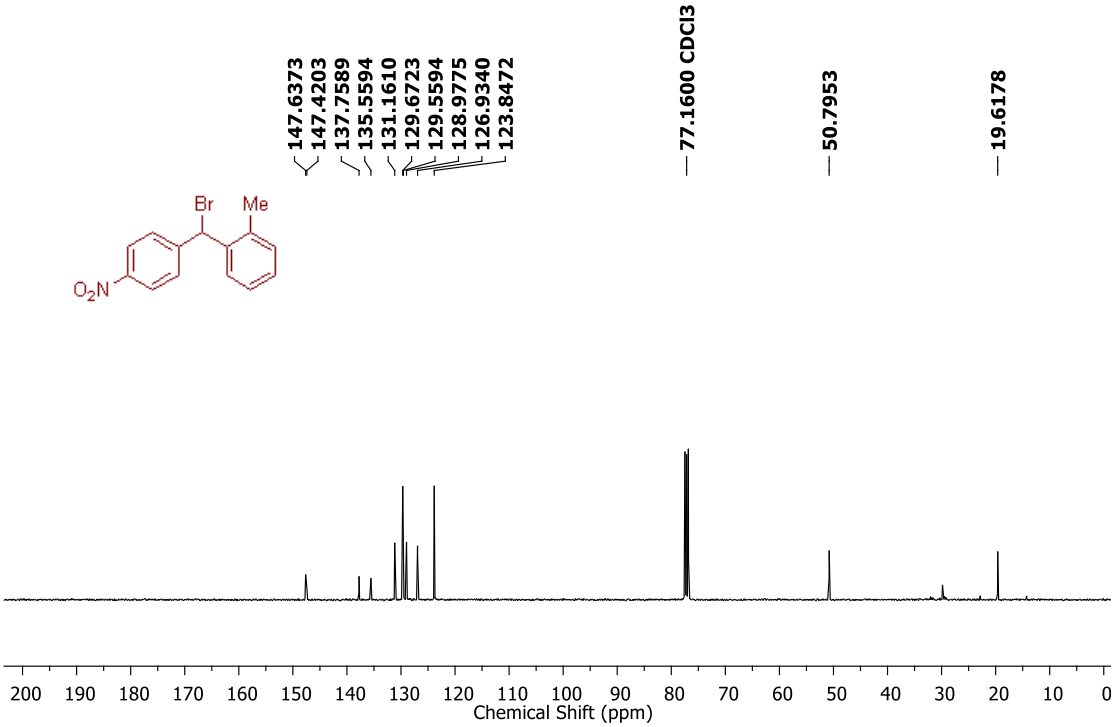

^{1}H NMR Spectrum (400 MHz, $CDCl_3$) of compound **30**

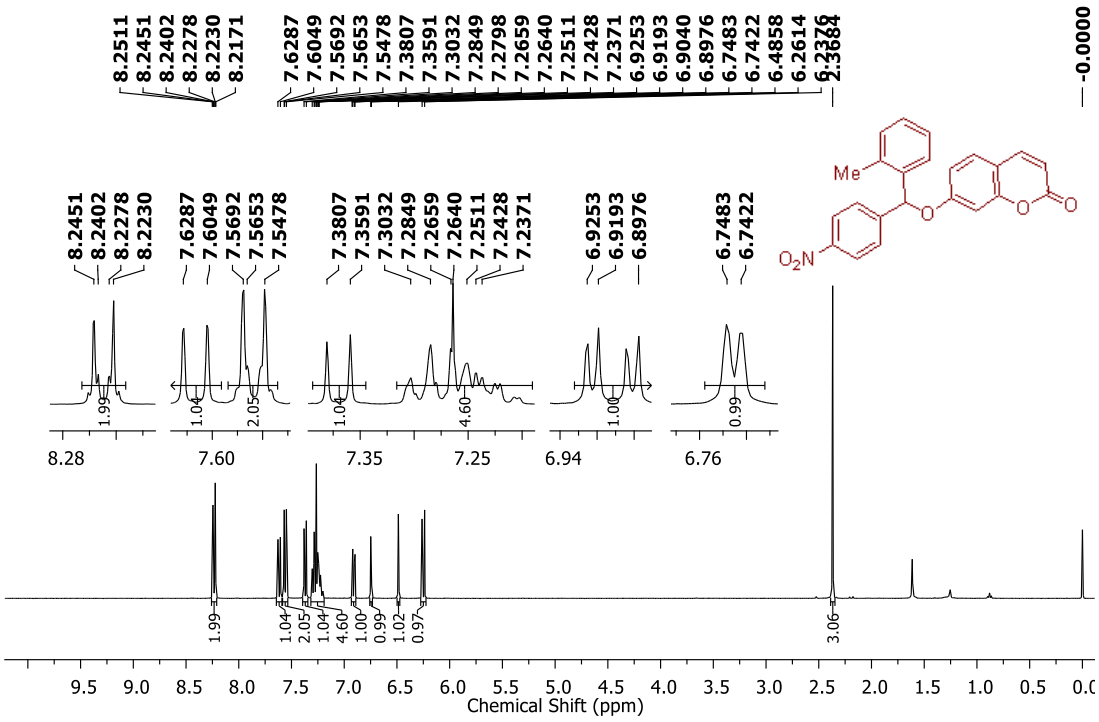

^{13}C NMR Spectrum (100 MHz, $CDCl_3$) of compound **30**

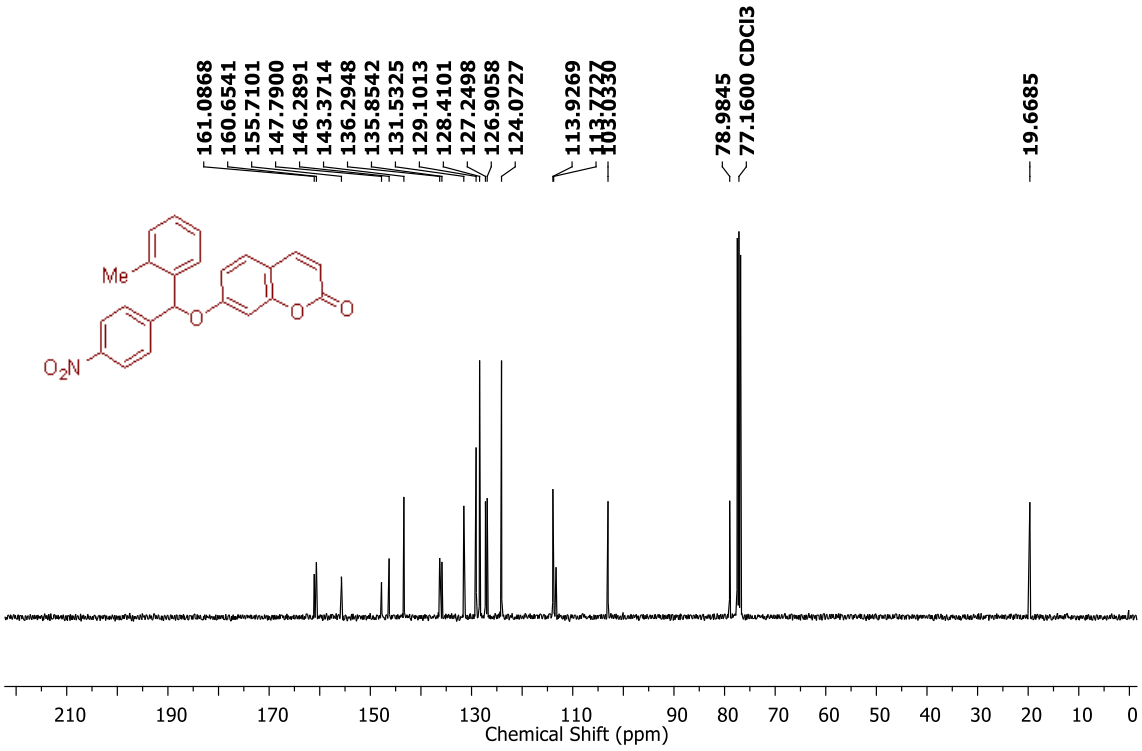

^{1}H NMR Spectrum (400 MHz, $CDCl_3$) of compound **32**

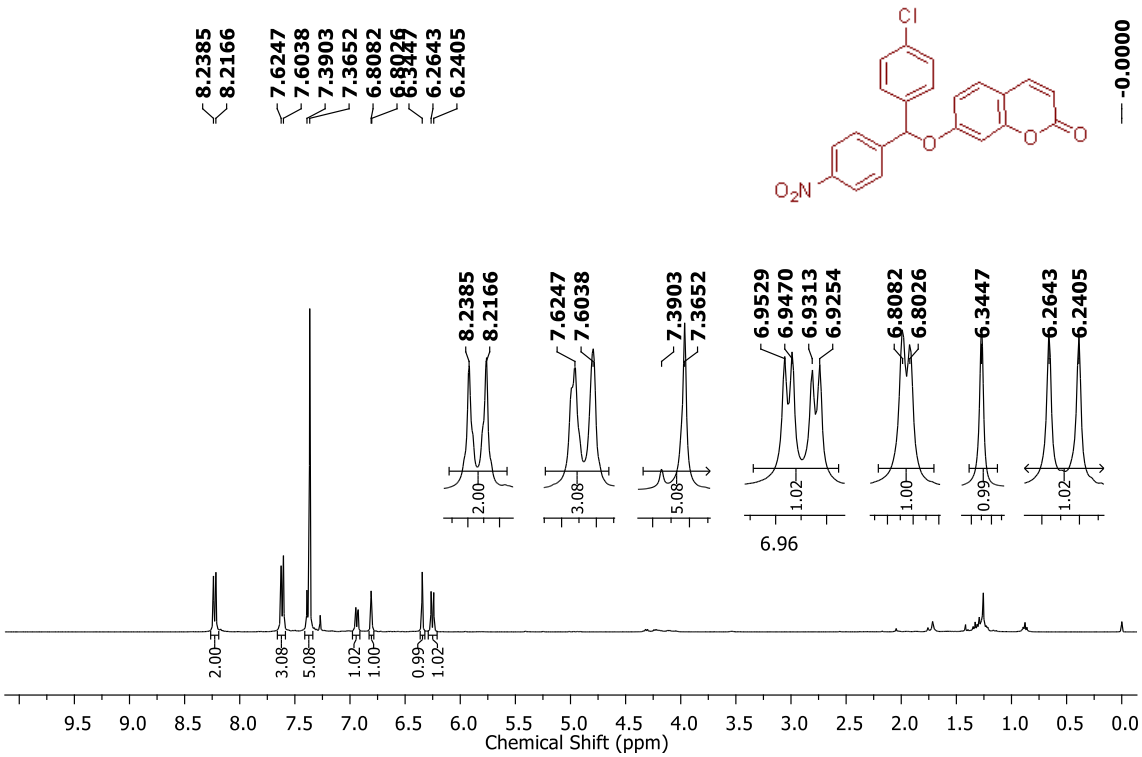

^{13}C NMR Spectrum (100 MHz, $CDCl_3$) of compound **32**

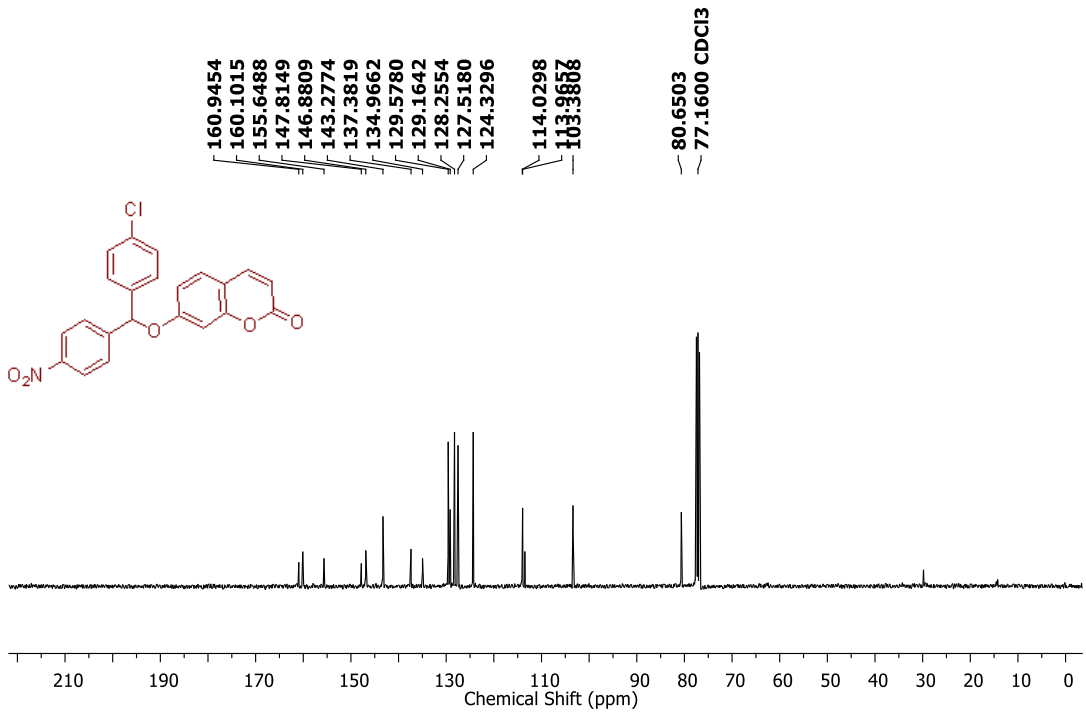

^{1}H NMR Spectrum (400 MHz, $CDCl_3$) of compound **34**

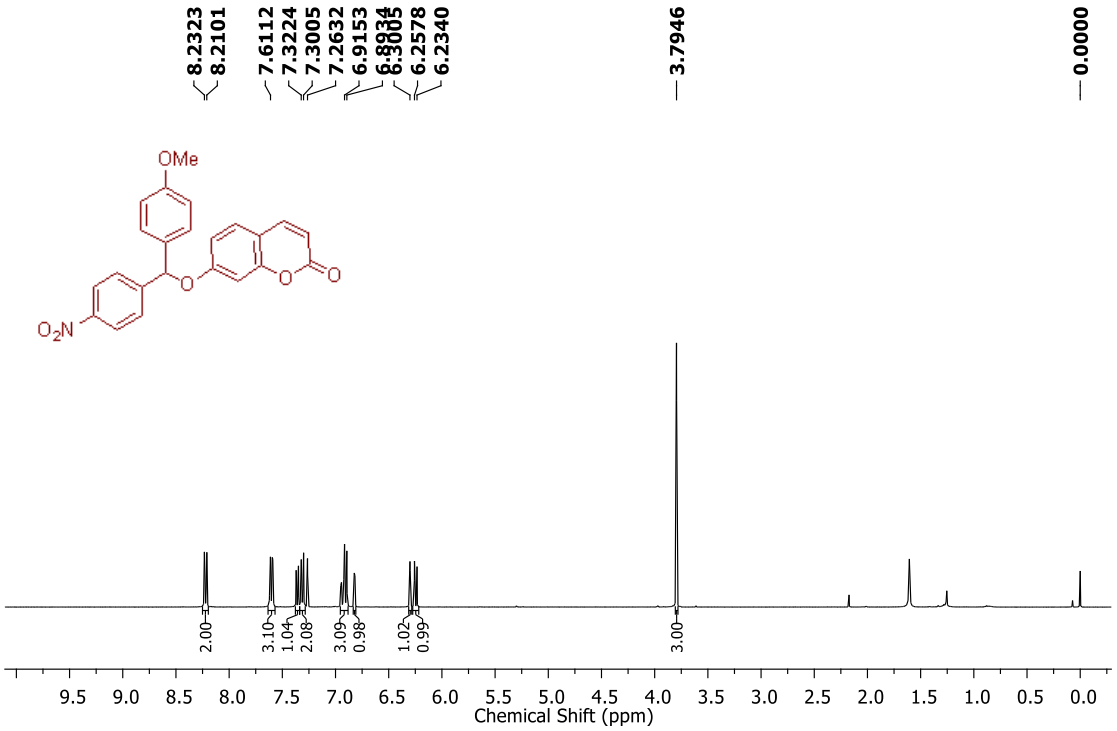

^{13}C NMR Spectrum (100 MHz, $CDCl_3$) of compound **34**

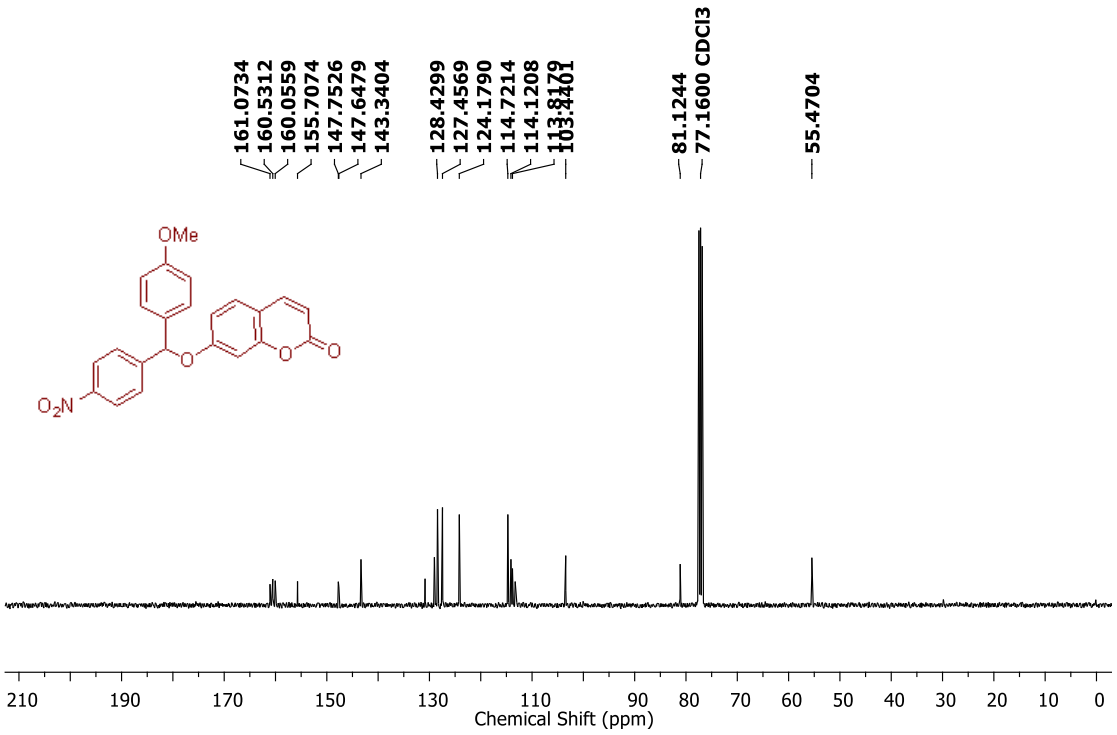

^{1}H NMR Spectrum (400 MHz, $CDCl_3$) of compound **35**

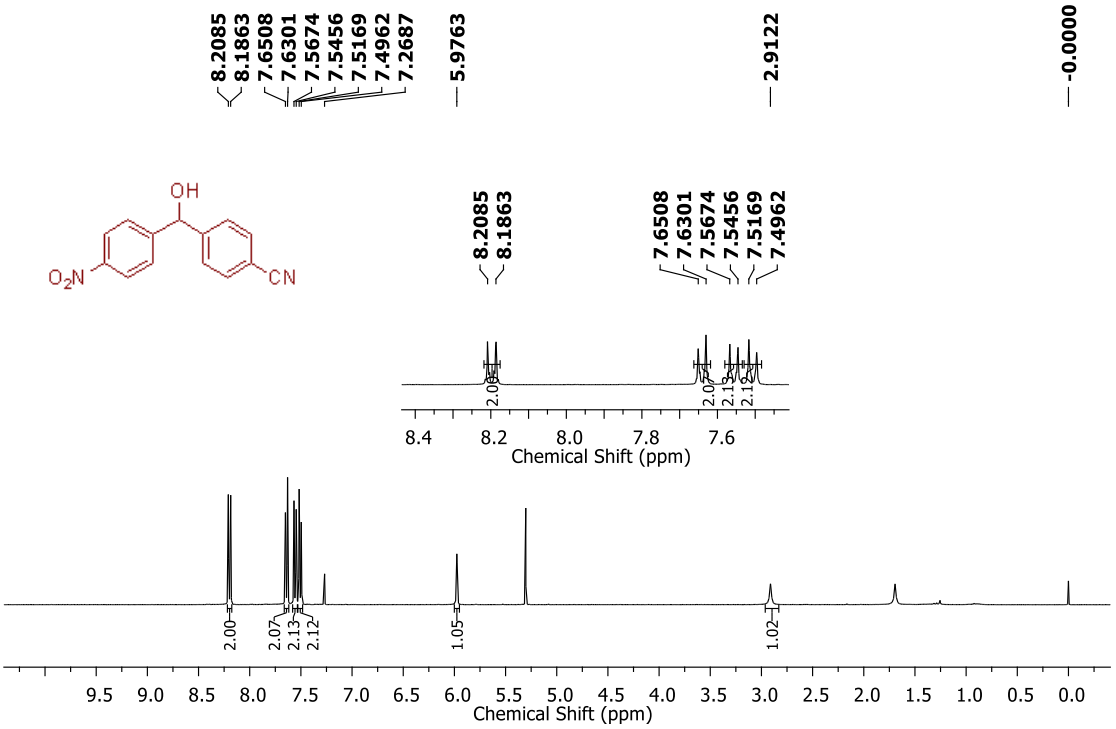

^{13}C NMR Spectrum (100 MHz, $CDCl_3$) of compound **35**

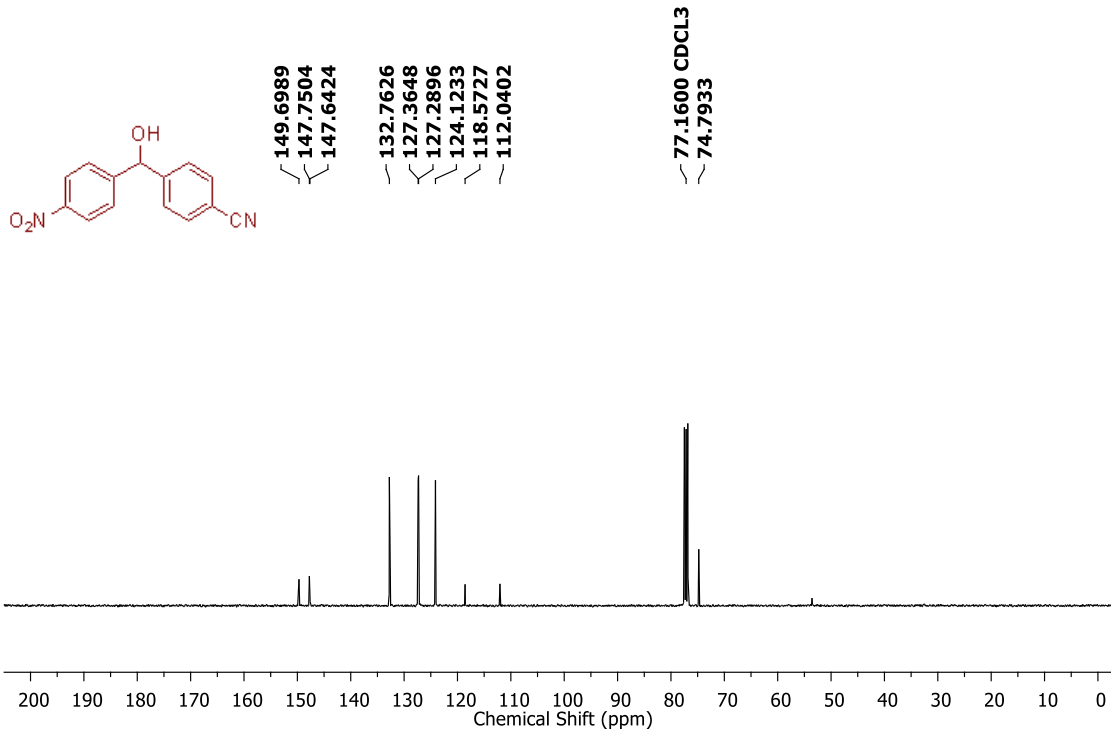

^{1}H NMR Spectrum (400 MHz, $CDCl_3$) of compound **36**

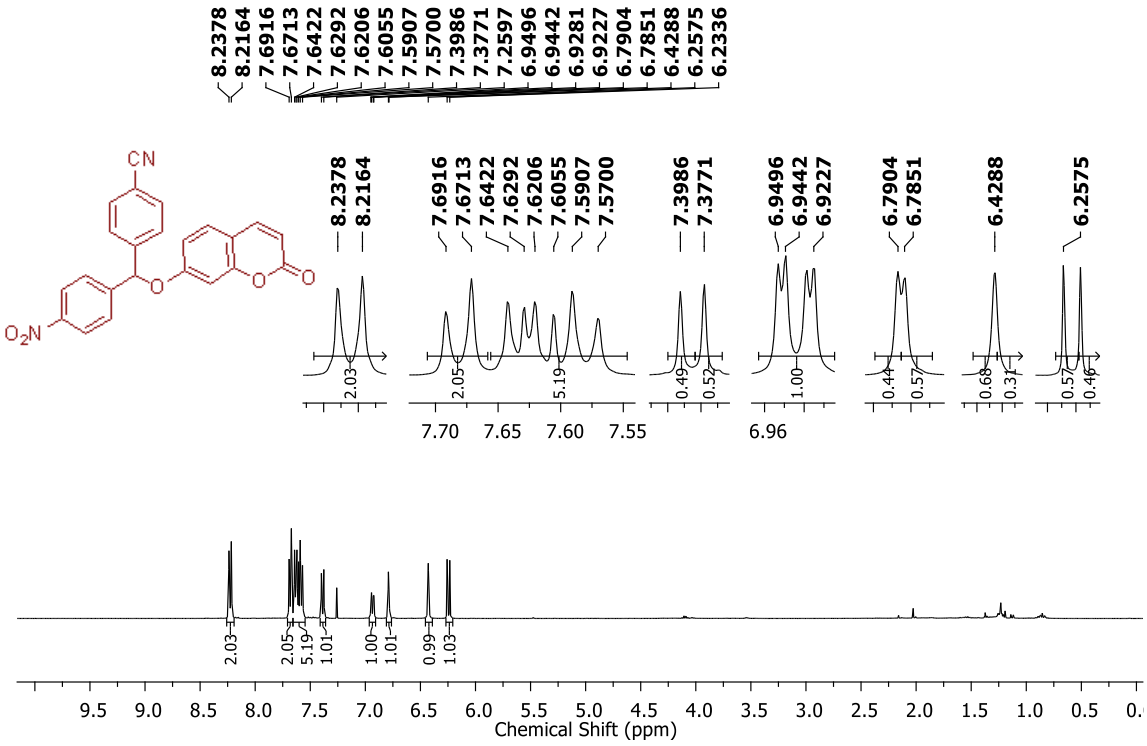

^{13}C NMR Spectrum (100 MHz, $CDCl_3$) of compound **36**

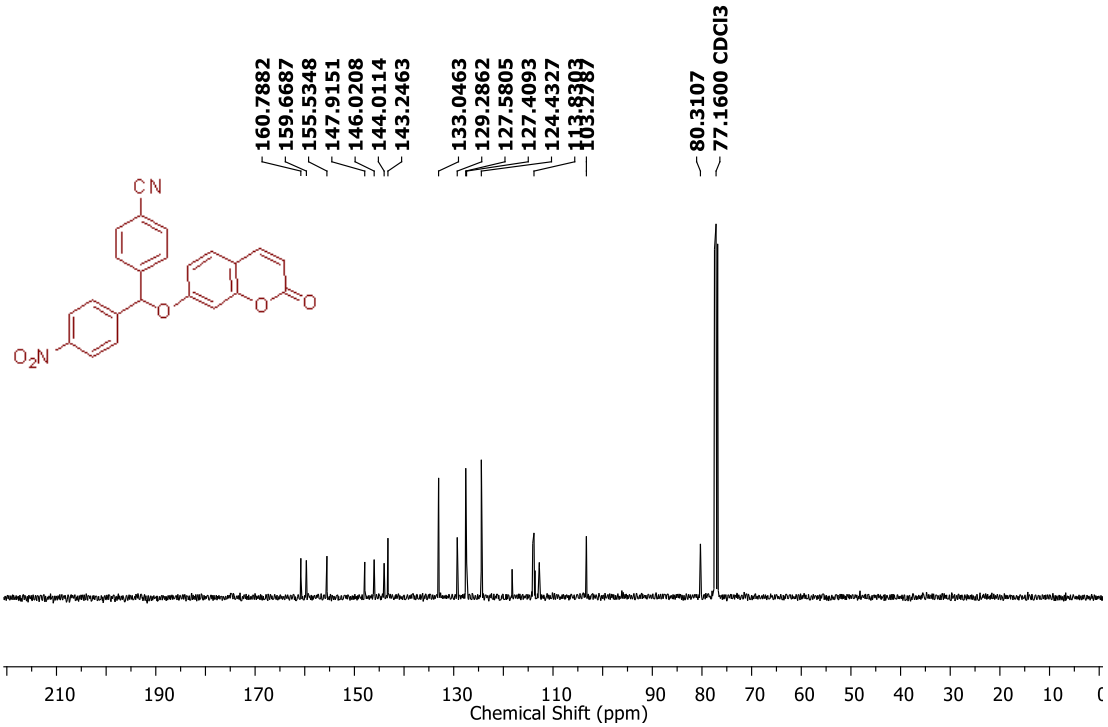

^{1}H NMR Spectrum (400 MHz, $CDCl_3$) of compound **38**

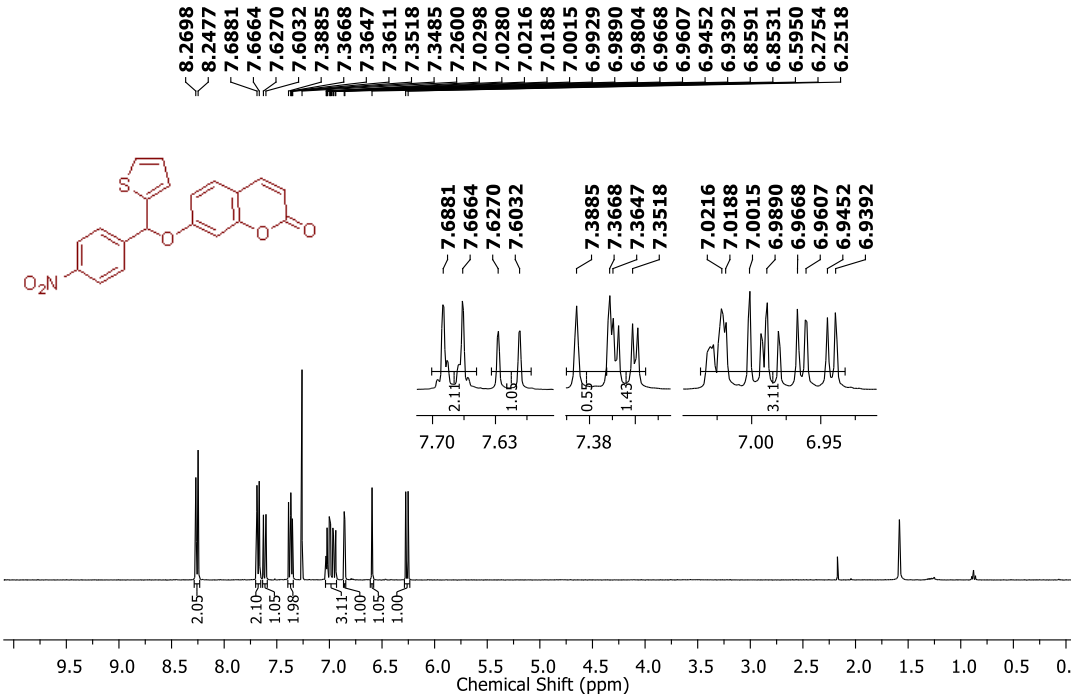

^{13}C NMR Spectrum (100 MHz, $CDCl_3$) of compound **38**

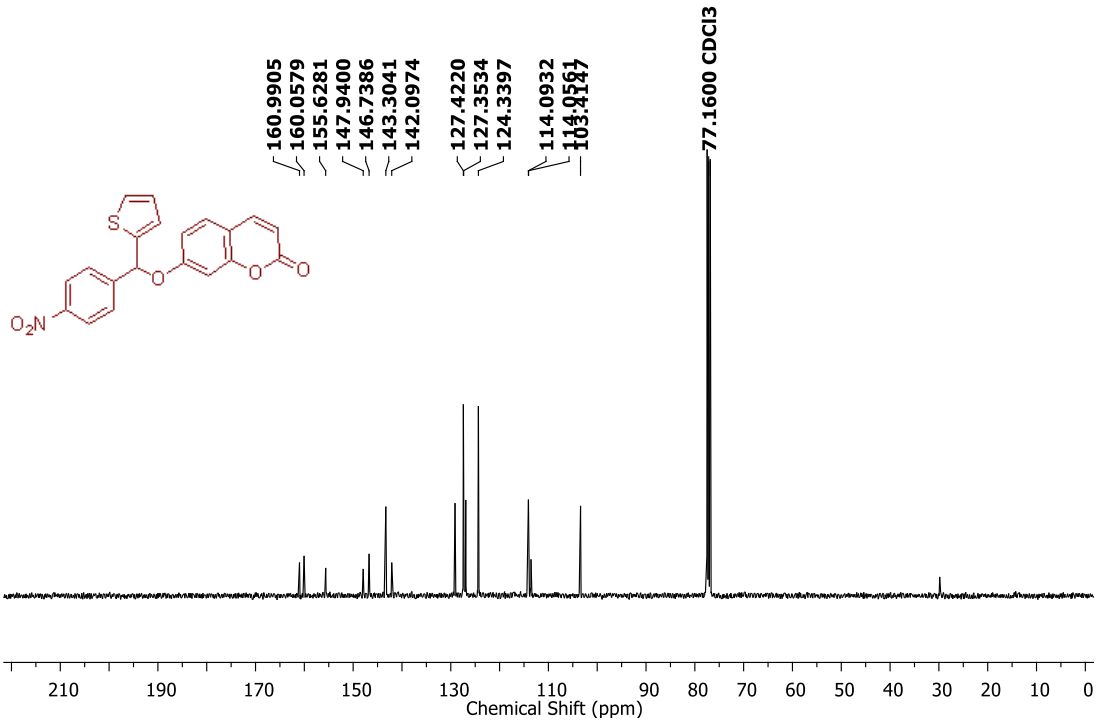

3.2.6. References

1. Hu, L.; Wu, X.; Han, J.; Chen, L.; Vass, S. O.; Browne, P.; Hall, B. S.; Bot, C.; Gobalakrishnapillai, V.; Searle, P. F.; Knox, R. J.; Wilkinson, S. R., Synthesis and structure–activity relationships of nitrobenzyl phosphoramide mustards as nitroreductase-activated prodrugs. *Bioorg. Med. Chem. Lett.* **2011,** *21* (13), 3986-3991.

2. (a) Tavares, A. F. N.; Nobre, L. S.; Melo, A. M. P.; Saraiva, L. M., A Novel Nitroreductase of Staphylococcus aureus with S-Nitrosoglutathione Reductase Activity. *J. Bacteriol.* **2009,** *191* (10), 3403-3406; (b) Bryant, D. W.; McCalla, D. R.; Leeksma, M.; Laneuville, P., Type I nitroreductases of Escherichia coli. *Can. J. Microbiol.* **1981,** *27* (1), 81-86; (c) Prosser, G. A.; Copp, J. N.; Syddall, S. P.; Williams, E. M.; Smaill, J. B.; Wilson, W. R.; Patterson, A. V.; Ackerley, D. F., Discovery and evaluation of Escherichia coli nitroreductases that activate the anti-cancer prodrug CB1954. *Biochem. Pharmacol.* **2010,** *79* (5), 678-687.

3. (a) Zou, T.; Pi, S.-S.; Li, J.-H., FeCl3-Catalyzed 1,2-Addition Reactions of Aryl Aldehydes with Arylboronic Acids. *Org. Lett.* **2009,** *11* (2), 453-456; (b) Lin, S.; Lu, X., Cationic Pd(II)/Bipyridine-Catalyzed Addition of Arylboronic Acids to Arylaldehydes. One-Pot Synthesis of Unsymmetrical Triarylmethanes. *J. Org. Chem.* **2007,** *72* (25), 9757-9760.

4. Maslak, P.; Guthrie, R. D., Electron apportionment in cleavage of radical anions. 1. Nitro-substituted benzyl phenyl ethers. *J. Am. Chem. Soc.* **1986,** *108* (10), 2628-2636.

5. Stein, A. R.; Dawe, R. D.; Sweet, J. R., Preparation of chiral 1-phenylethanols and bromides. *Can. J. Chem.* **1985,** (12), 3442-3448.

6. Row, E. C.; Brown, S. A.; Stachulski, A. V.; Lennard, M. S., Design, synthesis and evaluation of furanocoumarin monomers as inhibitors of CYP3A4. *Organic & Biomolecular Chemistry* **2006,** *4* (8), 1604-1610.

7. Zou, T.; Pi, S.-S.; Li, J.-H., FeCl3-Catalyzed 1,2-Addition Reactions of Aryl Aldehydes with Arylboronic Acids. *Organic Letters* **2008,***11* (2), 453-456.

8. Qin, C.; Wu, H.; Cheng, J.; Chen, X. a.; Liu, M.; Zhang, W.; Su, W.; Ding, J., The Palladium-Catalyzed Addition of Aryl- and Heteroarylboronic Acids to Aldehydes. *J. Org. Chem.* **2007,** *72* (11), 4102-4107.

CHAPTER 4: A bioreductively-activated NO donor with a fluorescence reporter

4.1. Introduction

NO forms an important constituent of our immune system.[1] The cytostatic or cytotoxic ability of host immune cells towards pathogens has been correlated to endogenous production of NO.[2] Furthermore, it has been demonstrated in various studies that NO when delivered from exogenous sources showed cytotoxicity to a wide spectrum of bacteria *in vitro*.[3] However, certain pathogens are capable of detoxifying or deactivating the damage induced by NO.[4] Also, endogenously produced NO in bacteria has been implicated with cytoprotective role in bacteria by attenuating the oxidative stress induced by class of antibiotics.[5] In order to address the exact role of NO inside bacteria, it is necessary to localise NO inside bacteria using appropriate NO donors and subsequently study the effects of NO. Having developed a method for releasing NO within bacteria in Chapter 3.1, we next wanted to study the possibility of incorporating a reporter in the NO delivery system. Activation of the trigger is expected to release NO and simultaneously a reporter molecule which may enable real-time monitoring of the NO release in a non-invasive manner.

Weinstein *et al*. reported real-time monitoring of drug release using a reporting drug delivery system where 7-hydroxycoumarin linker was attached to the peptidase substrate to one end and to the drug molecule on the other end (Scheme 4.1).[6]

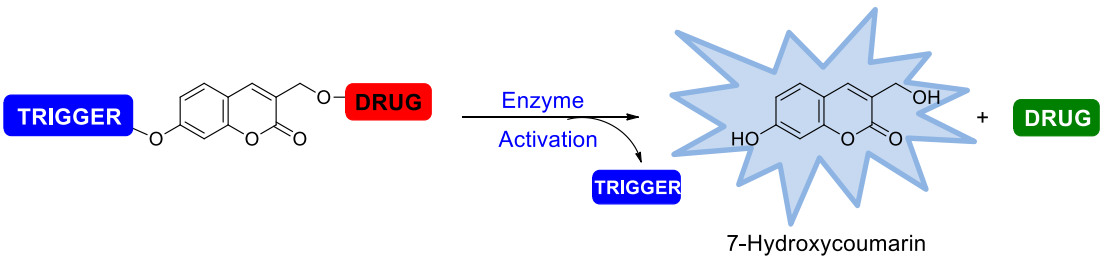

Scheme 4.1. Reporting drug delivery system by Weinstein *et al*. for real-time monitoring of drug release using 7-hydroxycoumarin as the reporter molecule.

Based on the above strategy of real-time monitoring of drug release, we propose to design a reporter linked NTR-activated NO donor for bacterial system. The design consists of 4-nitrobenzyl group as a trigger for bacterial enzyme, NTR and diazeniumdiolate, as the source of NO linked through the fluorescent reporter 7-hydroxycoumarin (Scheme 4.2). The proposed strategy is expected to facilitate

monitoring of NO donor localisation, its permeability and studying prodrug activation mechanism *in vivo*.

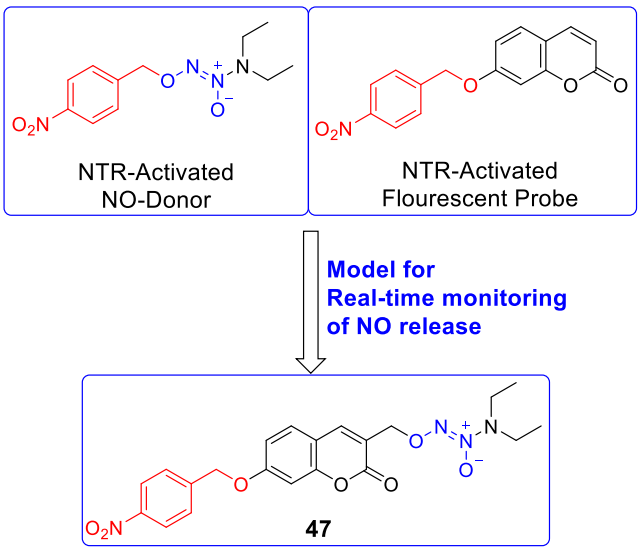

Scheme 4.2. Proposed design of model for the real-time monitoring of NO release.

The proposed mechanism of activation of the reporter probe, **47** is as follows. In the presence of NTR, the nitro group is reduced to the hydroxylamine or amine with an increased electron density on the phenyl group. Subsequently, the flow of electrons release the self-immolative phenolate linker, followed by 1,8 elimination to release the diazeniumdiolate that is hydrolysed to generate NO and fluorescent molecule, **44** (Scheme 4.3).

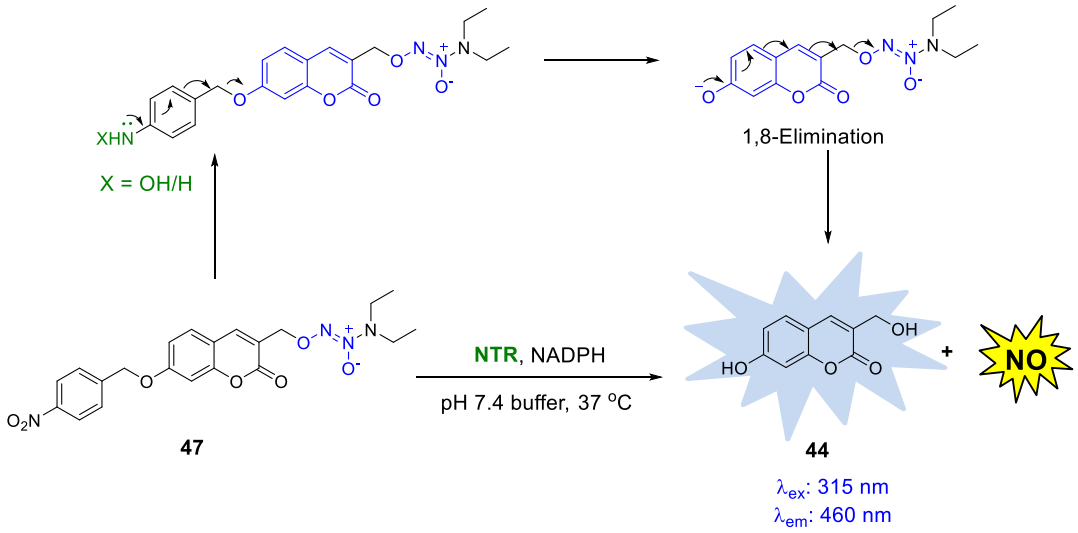

Scheme 4.3. Proposed mechanism of activation of the bioreductively activated reporter linked NO donor to release NO and the turn-on fluorescent probe **44**.

4.2. Results and discussion

4.2.1. Synthesis

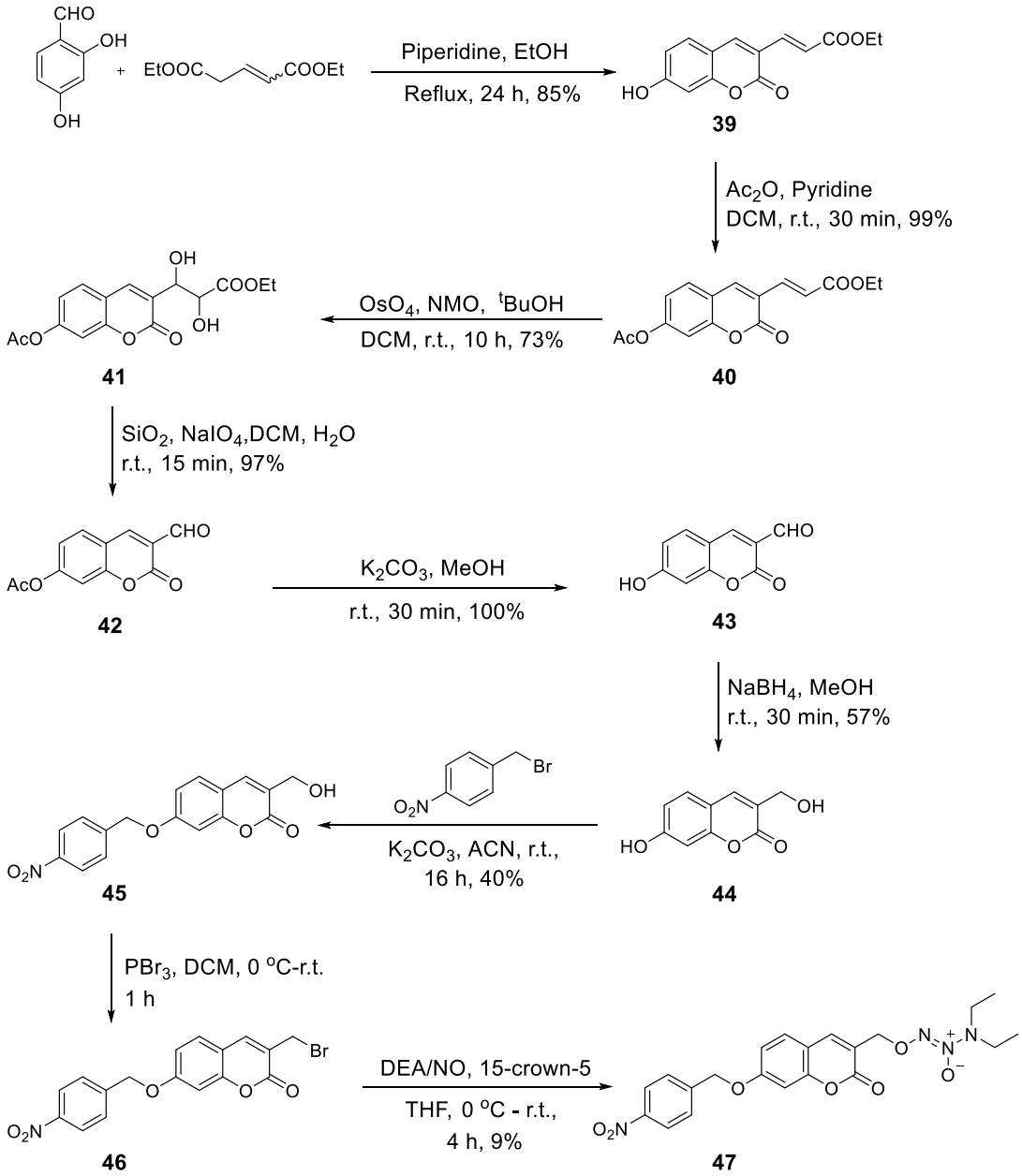

Scheme 4.4. Synthesis of **47**.

In order to test our hypothesis that compound **47** is a bioreductively activated reporter linked NO donor, we synthesized **47** in nine steps starting from 2, 4-dihydroxy benzaldehyde (Scheme 4.4). Briefly, 2, 4-dihydroxy benzaldehyde was reacted with diethyl glutaconate to form the coumarin **39** in 85% yield. It was acetylated using acetic anhydride in DCM-pyridine to form **40** in quantitative yield. Using osmium tetraoxide (OsO_4) and *N*-methyl morpholine *N*-oxide, olefin **40** was oxidised to diol

41 in 73% yield. The resulting diol was cleaved using sodium periodate and silica to obtain aldehyde **42**, in quantitative yield. Deacetylation of **42** was achieved using K_2CO_3 to get **43** in 100% yield. Fluorescent reporter compound **44** was obtained by reducing the aldehyde **43** with $NaBH_4$. Compound **44** was protected with 4-nitrobenzyl bromide to obtain **45** in 40% yield. The alcohol **45** was converted into the bromide **46** using PBr_3 in DCM which was further used without purification. The bromide was displaced by DEA/NO to afford **47** in 9% yield.

4.2.2. Evaluation of NTR reduction

In order to evaluate the suitability of compound **47** to undergo reduction by NTR to release NO, compound **47** was incubated in the presence and absence of NTR and the cofactor NADPH at 37 ^{o}C in pH 7.4 buffer and the amount of NO released was measured using chemiluminescence based NOA. Compound **47** (12.5 µM) in the presence of NTR was reduced to release approximately 3 µM NO after 30 min (Figure 4.1.A). However under similar reaction conditions, negligible amount of NO was estimated from **47** in the absence of NTR.

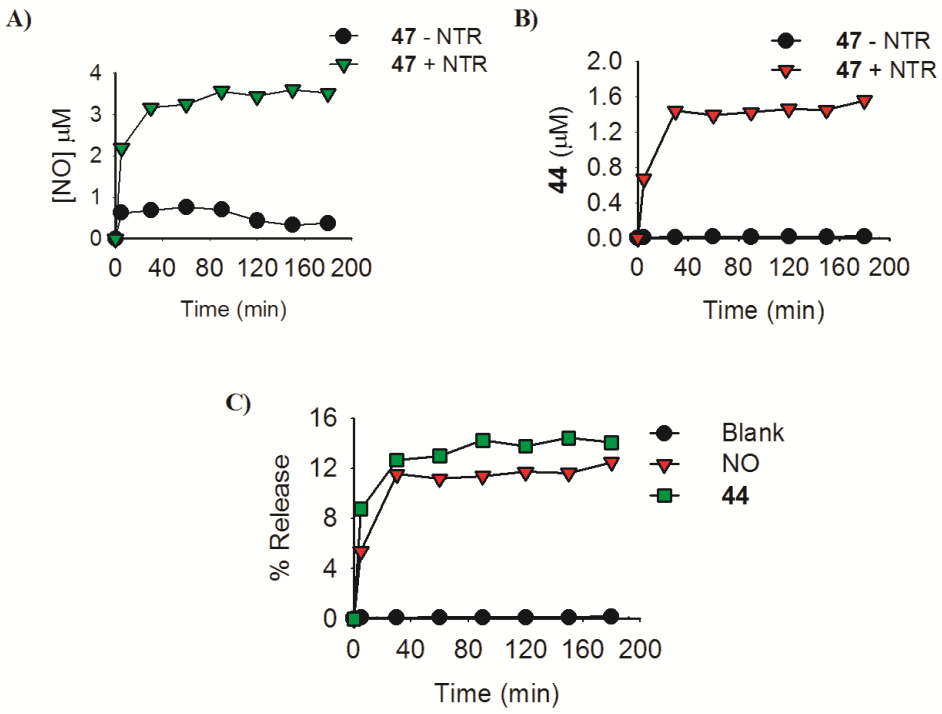

Figure 4.1. A) NO release from **47** in the presence and absence of NTR in pH 7.4 buffer detected using chemiluminesence based assay using NOA. **B)** Estimation of **44** release from **47** in the presence and absence of NTR in pH 7.4 buffer detected using increase in

flourescence at λ_{ex}: 315 nm and λ_{em}: 460 nm. **C)** Concomitant release of NO and **44**, products of reduction of **47** by NTR in pH 7.4 buffer at 37 ^{o}C.

As per the proposed mechanism, the release of NO should be accompanied by the release of fluorescent reporter compound, **44**. So an increase in fluorescence of **44** was measured using a microwell plate reader at λ_{ex}: 315 nm and λ_{em}: 460 nm. An increase in the fluorescence intensity was detected from **47** when incubated with NTR, which was estimated to be 1.5 µM of **44** after 30 min. On the contrary, no fluorescence was seen from **47** in the absence of NTR (Figure 4.1.B).

A direct comparison of release of NO and release of fluorescent reporter **44** was done to compare the % release of the products of NTR reduction. It was observed that the % release of both products were almost equivalent, approximately 12-13% over 3 h duration (Figure 4.1.C). Thus, the enzymatic reduction of **47** by NTR showed that **47** was substrate for NTR enzyme and gets reduced in the presence of NTR to release NO and fluorescent reporter compound, concomitantly.

4.3. Intracellular activation in bacteria

4.3.1. Bioreduction to release 44

In order to study the bioreduction of **47**, we selected *Escherichia coli* (*E. coli*), *Mycobacterium smegmatis* (*M. smeg*) and *Staphylococcus aureus* (SA).[7] A HPLC based experiment was performed to qualitatively assess the release of fluorescent reporter **44** in the bacterial supernatant from incubation of **47** in the bacteria after 12 h. Compound **47** was incubated in *E. coli* for 12 h and the supernatant was injected in the HPLC attached with a fluorescence detector. The release of fluorescent reporter **44** was monitored at λ_{ex}: 315 nm and λ_{em}: 460 nm (Figure 4.2.A). In *E. coli* supernatant, an increase in fluorescence corresponding to release of **44** was observed. However, negligible increase in fluorescence was observed in *E. coli* control which was not treated with **47**. Using same protocol, **47** was treated individually with *M. smeg* and SA and we found an increase in the fluorescence in the compound treated supernatants compared to untreated bacterial supernatants (Figure 4.2.B and Figure 4.2.C, respectively). Thus, the release of fluorescent reporter **44** in bacterial culture incubated with **47**, suggested that **47** was bioreductively activated to release fluorophore **44**.

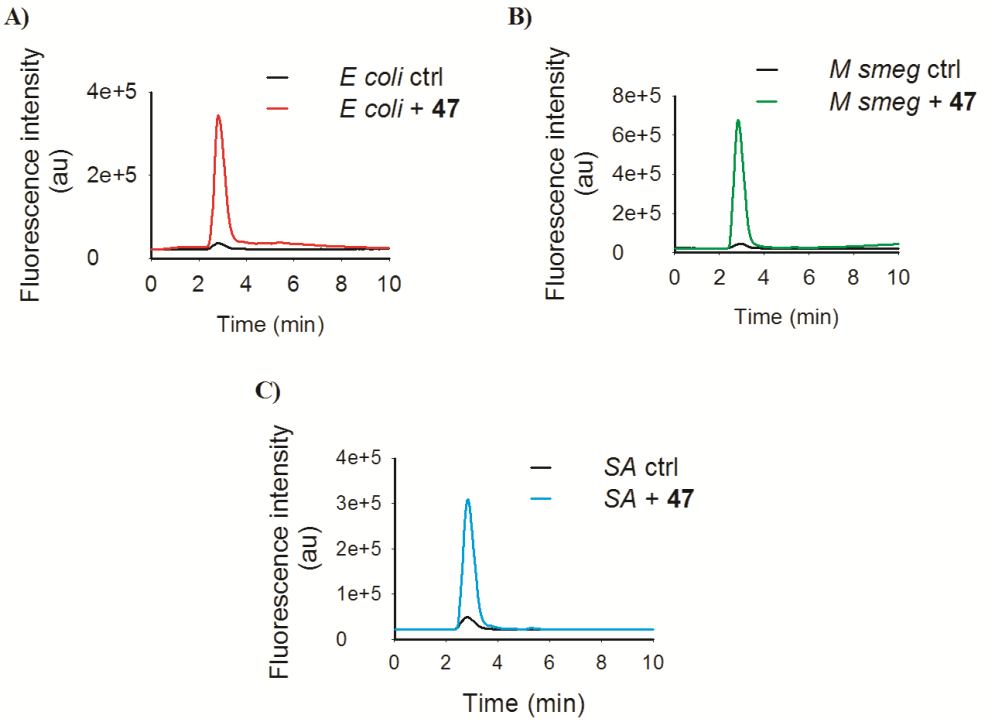

Figure 4.2. HPLC profiles of bacterial supernatants incubated with **47** at 37 ^{o}C for 12 h to monitor release of fluorescent reporter **44**. **A)** Incubation of **47** in *E. coli*. **B)** Incubation of **47** in *M. smeg*. **C)** Incubation of **47** in SA.

4.3.2. Intracelular NO release

As **47** was reduced in the bacterial cultures to release fluorescent reporter **44**, so next to demonstrate that NO is also released during bioreduction, a frequently used diaminofluorescein based secondary assay was used.[8] *M. smeg* was used as a model to study bioreduction of **47** to release NO. In this assay, a 4,5-diaminofluorescein diacetate (DAF-2DA) dye was treated with *M. smeg*. The dye permeate the cells and the diester is hydrolysed to form DAF. Bacteria was then treated with **47** which is bioreductively activated to release NO. In the presence of NO^{+}, DAF reacts with NO to form a flourescent dye DAF-2T. By measuring the fluorescence for DAF-2T at λ_{ex}: 495 nm and λ_{em}: 515 nm, intracellular NO release was monitored. Two different concentrations of compound **47** were independently incubated in DAF treated *M. smeg* for 12 h and the fluorescence for DAF-2T was then measured. A concentration dependent increase in fluorescence of DAF-2T in *M. smeg* was seen in **47** treated cells, indicating it was reduced by bacteria to generate NO intracellularly (Figure 4.3.A).

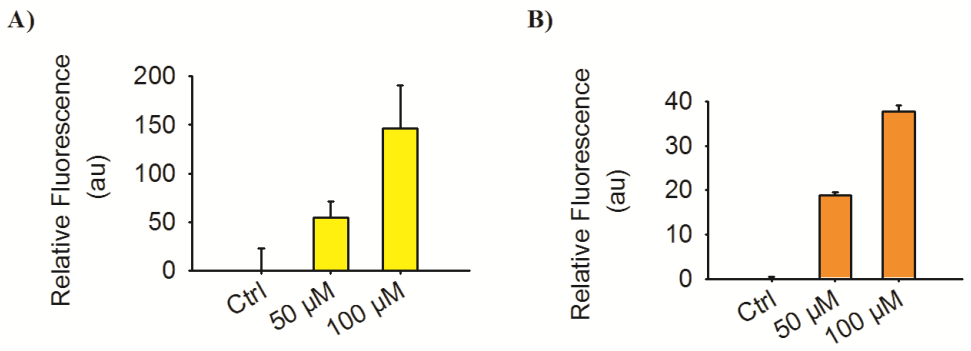

Figure 4.3. A) Levels of intracellular NO measured using fluorescence of DAF-2T in *M. smeg* upon incubation with 50 and 100 µM of **47** using DAF assay (λ_{ex}: 490 nm and λ_{em}: 530 nm). **B)** Fluorescence measurement for released **44** in *M. smeg* upon incubation with 50 and 100 µM of **47** at λ_{ex}: 315 nm and λ_{em}: 460 nm.

Furthermore, the release of fluorescent reporter **44** in the bacterial suspension of *M. smeg* was simultaneously examined under similar conditions. A concentration dependent increase in fluorescence of **44**, a pattern similar to intracellular NO release, was noticed (Figure 4.3.B). Therefore, from intracellular activation of **47** in *M. smeg* it was inferred, that **47** is capable to undergo bioreduction by bacterial nitroreductases to release NO within bacteria and simultaneously report the activation of NO donor to release NO, without performing any secondary assays for NO detection.

Next, to verify the activation of **47** occurs inside bacteria and not in the bacterial media, we used fluorescence-activated cell sorting (FACS) to track the release of **44** within the *M. smeg* at different time points using λ_{ex}: 405 nm and λ_{em}: 460 nm. We determined the release of **44** in *M. smeg* in aerated and standing cultures of *M. smeg*, which serves as a model for bacteria in oxic and hypoxic condition, respectively. The aerated and standing cultures were incubated with 100 µM of compound **47** and the release of **44** was pursued every 5 min using fluorescence. In case of *M. smeg*, the standing culture was found to be able to activate **44** release more potently than the aerated culture (Figure 4.4) probably due to the greater relative abundance of nitroreductases in the standing culture, as opposed to the aerated culture.(FACS data provided by Dr. Amit Singh, IISc, Bangalore.)

4.3.3. Study in Mycobacterium tuberculosis, H37Rv

PA-824, a cyclic nitroimidazole, has been reported to get reduced intracellulary by deazaflavin-dependent nitroreductase (Ddn) to release NO under anaerobic conditions

and has been implicated in killing *Mycobacterium tuberculosis* (*Mtb*) which is the causative agent of tuberculosis affecting a million each year.[8-9]

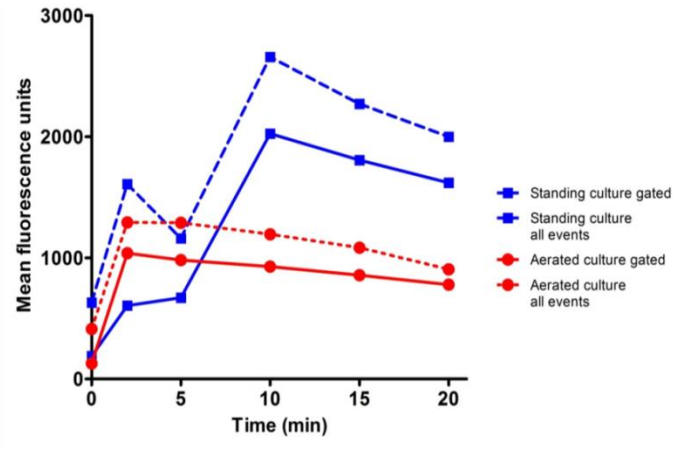

Figure 4.4. Time dependent activation of **47** in the aerated and standing cultures of *M. smeg* to release the flourescent probe **44** using FACS at λ_{ex}: 405 nm and λ_{em}: 460 nm. Data provided by Dr. Amit Singh, IISc Bangalore.

Since **47** produced NO inside *M. smeg*, the bioreduction of **47** was examined in *Mtb* H37Rv as well. The activation of reporter linked NO donor **47** releases NO intracellulary and is reported by the turn-on fluorescence of reporter **44**. So we monitored release of NO in H37Rv by means of increase in fluorescence of turn-on fluorescent reporter **44**. The bioreduction of **47** in H37Rv demonstrated that the activation of incubation of **47** occurred to release **44**, similar to *M. smeg*.

Next, **47** was tested for its ability to inhibit the growth of *Mtb*. Minimum inhibitory concentration (MIC) of **47**, the lowest compound concentration that prevents visible growth of bacteria, was found to be 1mM. Since the MIC value for **47** is very high, it reveals that intracellular nitric oxide does not kill H37Rv, unless very high doses of the NO donor is administered. Further studies on role of NO and cellular stress in *Mtb* are underway. (*Mtb* data provided by Dr. Amit Singh, IISc, Bangalore.)

4.4. Conclusion

In this chapter, we have designed a bioreductively activated real-time monitoring NO donor, **47** for bacterial system to understand the role of NO in bacteria. With help of bacterial nitroreductases, the compound is activated to release NO intracellularly and a turn-on fluorescent reporter **44**, concomitantly. Therefore, the release of turn-on probe **44** within cell reports the delivery of NO donor and also its activation inside cell to release NO without help of secondary assay for NO detection. Further, the

compound **47** was found to be bioreductively activated in *E. coli*, *M. smeg*, SA to release **44** and enhanced the intracellular levels of NO**.** Using FACS it was demonstrated that the activation of **47** to release **44** occurred within cells. In the cytotoxicity studied performed in H37Rv, we found that **47** was toxic to mycobacteria at a very high concentration. Together, we have developed a tool for bacterial system that enables monitoring the intracellular delivery of NO. As NO has been used as an adjuvant with antibiotics to increase cytotoxicity, it would be beneficial to study the roles of NO in adjuvant therapy as well.

4.5. Experimental and characterization data

4.5.1. Synthesis and characterization

Compounds **30–44**[6, 10] have been previously reported and analytical data that we collected were consistent with the reported values.

Synthesis of 3-(hydroxymethyl)-7-((4-nitrobenzyl)oxy)-2H-chromen-2-one, 45.

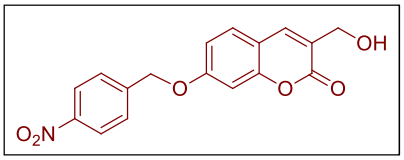

To a solution of compound **45** (0.10 g, 0.53 mmol) in dry acetonitrile (10 mL) under a nitrogen atmosphere, K_2CO_3 (0.22 g, 1.59 mmol) was added and the reaction mixture was stirred for 15 min. To this reaction mixture, 4-nitrobenzyl bromide (0.17 g, 0.79 mmol) was added and stirring was continued at room temperature for 18 h. The reaction mixture was diluted with ethyl acetate and washed with water. The organic layer was washed with brine, dried (Na_2SO_4), filtered and the filtrate was evaporated to give crude product. Purification was done using silica gel column chromatography using methanol to obtain pure product, **45** (0.15 g, 57%) as an off-white solid: m.p. 237-238 °C; FT-IR (ν_{max}, cm^{-1}): 3397, 2921, 2854, 1692, 1607, 1514, 1384, 1340, 1237,1155; ^{1}H NMR (400 MHz, DMSO-d_6): δ 8.27 (d, *J* = 8.7 Hz, 2H), 7.91 (s, 1H), 7.74 (d, *J* = 8.8 Hz, 2H), 7.70 (d, *J* = 8.6 Hz, 1H), 7.10 (d, *J* = 2.4 Hz, 1H), 7.04 (dd, *J* = 8.6, 2.3 Hz, 1H), 5.39 (s, 2H), 4.32 (d, *J* = 1.1 Hz, 2H); ^{13}C NMR (100 MHz, DMSO-d_6): δ 160.2, 159.9, 154.0, 147.1, 144.2, 137.4, 129.2, 128.4, 125.8, 123.7, 113.1, 112.9, 101.4, 68.5, 58.1; HRMS (ESI) for $C_{17}H_{13}NO_6$ $[M]^+$: Calcd., 327.0743, Found, 327.0792.

Synthesis of 3-(bromomethyl)-7-((4-nitrobenzyl)oxy)-2H-chromen-2-one, 46.

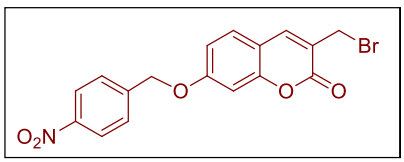

A solution of **46** (65 mg, 0.19 mmol) in dry DCM (10 mL) was cooled to 0 °C under a nitrogen atmosphere. To this solution, PBr_3 (0.04 mL, 0.39 mmol) was added and the reaction mixture was stirred at 0 °C and gradually warmed to room temperature for 1 h. The reaction mixture was quenched with saturated $NaHCO_3$ solution. The aqueous layer was extracted with ethyl acetate (3×10 mL). The combined organic layer was washed with brine, dried (Na_2SO_4), filtered and the filtrate was evaporated to give crude product. The crude product **47** obtained as a pale yellow solid was used without further purification (73 mg, 94%); FT-IR (ν_{max}, cm^{-1}): 2920, 2846, 1719, 1605, 1510, 1337,

1256; ^{1}H NMR (400 MHz, $(CD_3)_2CO$): δ 8.30 (d, *J* = 8.7 Hz, 2H), 8.14 (s, 1H), 7.82 (d, *J* = 8.8 Hz, 2H), 7.67 (d, *J* = 8.6 Hz, 1H), 7.09 (dd, *J* = 8.6, 2.4 Hz, 1H), 7.06 (d, *J* = 2.4 Hz, 1H), 5.47 (s, 2H), 4.51 (s, 2H).

Synthesis of (Z)-3,3-diethyl-1-((7-((4-nitrobenzyl)oxy)-2-oxo-2H-chromen-3-yl)methoxy)triaz-1-ene 2-oxide, 47.

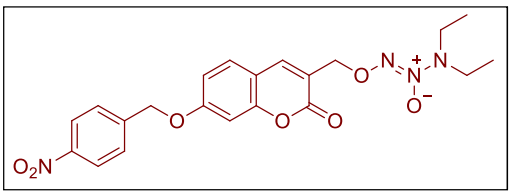

To an ice-cooled dry THF, DEA/NO (50 mg, 0.12 mmol) was added under a nitrogen atmosphere and the reaction mixture was stirred at 0 ^{o}C for 15 min followed by the addition of 15-crown-5 (50 µL). This reaction mixture was stirred at 0 ^{o}C for 15 min and then compound **46** (29 mg, 0.19 mmol) was added and reaction mixture was stirred at room temperature for 4 h. The reaction mixture was diluted with water and extracted with ethyl acetate (3×15 mL). The combined organic layer was washed with brine, dried (Na_2SO_4), filtered and the filtrate was evaporated to give crude product. The final product **47** was purified using column chromatography in 40-50% ethyl acetate: pet ether as a pale yellow solid (10 mg, 9%): m.p. 145-146 °C; FT-IR (ν_{max}, cm^{-1}): 2925, 2856, 2364, 1722, 1613, 1517, 1458, 1347, 1263, 1161, 1012; ^{1}H NMR (400 MHz, $CDCl_3$): δ 8.28 (d, *J* = 8.7 Hz, 2H), 7.71 (s, 1H), 7.62 (d, *J* = 8.7 Hz, 2H), 7.41 (d, *J* = 8.6 Hz, 1H), 6.93 (dd, *J* = 8.5, 2.4 Hz, 1H), 6.87 (d, *J* = 2.0 Hz, 1H), 5.23 (s, 2H), 5.22 (d, *J* = 1.1 Hz, 2H), 3.15 (q, *J* = 7.2 Hz, 4H), 1.09 (t, *J* = 7.0 Hz, 6H); ^{13}C NMR (100 MHz, $CDCl_3$): δ 161.2, 160.2, 155.2, 147.9, 143.1, 140.4, 129.3, 127.8, 124.1, 120.6, 113.4, 113.1, 101.8, 70.0, 69.2, 48.6, 11.6; HRMS (ESI) for $C_{21}H_{22}N_4O_7$ $[M+Na]^+$: Calcd., 465.1385, Found, 465.1388.

4.5.2. NTR mediated reduction

A 10 mM stock solution of **47** was prepared in DMSO and a 1 mM stock solution of NADPH was prepared in TRIS buffer pH 7.4. The NTR enzyme stock solution of 0.5 mg/mL was prepared in TRIS buffer pH 7.4. A 2 mL solution of compound **47** (final concentration of **47** = 12.5 µM in 2 mL) and NADPH (final concentration of NADPH = 125 µM in 2 mL) was prepared in TRIS buffer pH 7.4. This solution was divided into several portions of 200 µL in a 96-well plate. To the reaction mixture, 5 µL of NTR was added while to the blank, 5 µL TRIS buffer was added. This assay was conducted in quadruplicate. The 96-well plate was incubated at 37 ^{o}C in microwell

plate reader and fluorescence measurement was done at the mentioned time intervals, using λ_{ex}: 315 nm and λ_{em}: 460 nm.

4.5.3. Fluorescence detection

A 10 mM stock solution of **44** was prepared in DMSO. The standard calibration curve was obtained by using a concentration range varying from 0-100 µM solutions of **44** prepared in TRIS buffer pH 7.4. 200 µL of each concentration was aliquot in a 96-well plate and fluorescence was measured at λ_{ex}: 315 nm and λ_{em}: 460 nm (bandwidth ± 4nm). The assay was conducted in triplicate.

The amount of **44** released from enzymatic reduction of **47** was quantified as follows: the reaction solutions were prepared as mentioned in previous section 4.5.2 and 200 µL of the blank and reaction mixtures were aliquot in 96-well plate. Increase in fluorescence with respect to blank was measured using a microwell plate reader and amount of **44** released was quantified using the standard calibration curve for **44** (Figure 4.5.A; $y = 5.505x$; $R^2 = 0.984$).

4.5.4. Nitric oxide (NO) detection

A 10 mM stock solution of $NaNO_2$ was prepared in TRIS buffer pH 7.4. The standard calibration curve was obtained by using a concentration range varying from 0-25 µM solutions of $NaNO_2$ prepared in TRIS buffer pH 7.4. 10 µL of each varying concentrations were injected in NOA.

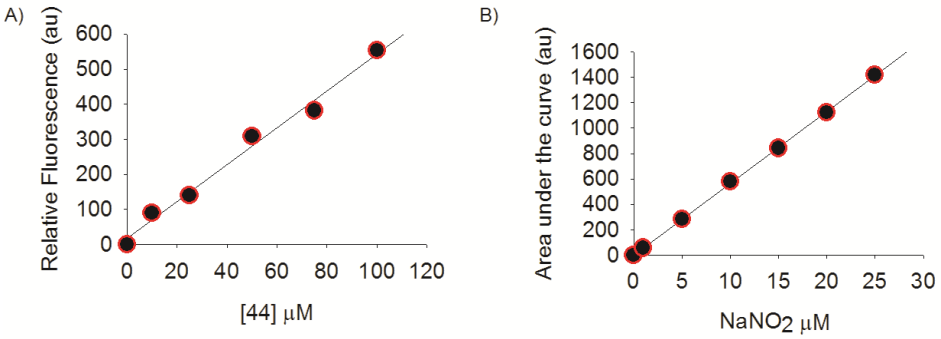

Figure 4.5. A) Calibration curve for **44** in TRIS buffer pH 7.4 using fluorescence. **B)** Calibration curve for $NaNO_2$ in TRIS buffer pH 7.4 using chemiluminescence based assay.

For quantifying amount of NO released from enzymatic reduction of **47**, the reaction solutions were prepared as mentioned in section 4.5.2 and 10 µL of the blank and reaction mixtures were analysed at the specified time points. The amount of NO

released was measured using the $NaNO_2$ standard calibration curve (Figure 4.5.B; y = 56.62x; R^2 = 0.999).

4.5.5. Intracellular activation in bacteria

Escherichia coli (EC2065) was cultured in 10 mL of Luria Bertani (LB) medium at 37 ºC for 16 h. *Mycobacterium smegmatis* (mc^2155) was inoculated in 10 mL middle brook M7H9 medium for 16 h. *Staphylococcus aureus* (SA5021) was cultured in 10 mL of Luria Bertani (LB) medium at 37 ºC for 16 h. The cultured bacteria were centrifuged to aspirate out the medium and resuspended in fresh medium to obtain O.D of 0.5. 1 mL of the bacterial suspension was aliquot in six falcon tubes. For control set, three falcons containing the bacterial suspension were untreated. In remaining three falcon tubes, 12.5 µL of **47** (final concentration of **47** = 125 µM in 1 mL) was added in each falcon. The treated and untreated bacterial solutions were incubated at 37 ^oC for 12 h. The bacterial suspension was then centrifuged, washed with fresh media and then lysed using acetonitrile. The cell lysate was filtered and injected into HPLC attached with a fluorescent detector (Phenomenex, 5 µm, 4.6 × 250 mm; flow rate: 1 mL/min; eluent 70% ACN: H_2O). The appearance of peak for **44** in fluorescence detection channel with λ_{ex}: 315 nm and λ_{em}: 460 nm was recorded.

4.5.6. DAF assay-Intracellular NO release in M. smeg

Using a reported protocol[8] with slight modification intracellular NO release was detected as follows: a 5 mM stock solution of diaminofluorescein 2 diacetate (DAF-2DA) was prepared in DMSO. Using a 10 mM DMSO stock solution of **47**, 2 mL solutions of concentration 100 and 200 µM were prepared in middle brook M7H9 medium. *M. smeg* (mc^2155) was inoculated in 10 mL M7H9 for 16 h. The bacterial culture was suspended to apsirate out the medium and then resuspended in fresh medium to make bacterial solution of O.D 1.0. To 2 mL of this bacterial culture, 4 µL of DAF-2DA solution was added so as to obtain a final concentration of 10 µM. The bacterial suspension was incubated at 37 ^oC for 2 h. The bacterial cells were suspended to aspirate media and washed with fresh media twice. The cell pellet was resuspended in 1 mL fresh media and again incubated at 37 ^oC for 1 h. A diluted bacterial suspension with O.D 0.5 was prepared. In a 96-well plate, 100 µL of bacterial suspension treated with DAF was added. For control set, 100 µL of bacterial suspension was diluted with 100 µL of medium. For obtaining 50 µM of **47**, the 100

µL of bacterial suspension was diluted with 100 µL of 100 µM solution of **47**. Likewise, for obtaining 100 µM of **47**, the 100 µL of bacterial suspension was diluted with 100 µL of 200 µM solution of **47**. The 96-well plate was incubated at 37 ^{o}C for 12 h. Fluorimetric reading was recorded in a microwell plate reader with excitation wavelength of 490 nm and emission wavelength of 530 nm. Reading for each concentration corresponds to average of three readings.

4.6. Spectral charts

^{1}H NMR Spectrum (400 MHz, DMSO-d_6) of compound **45**

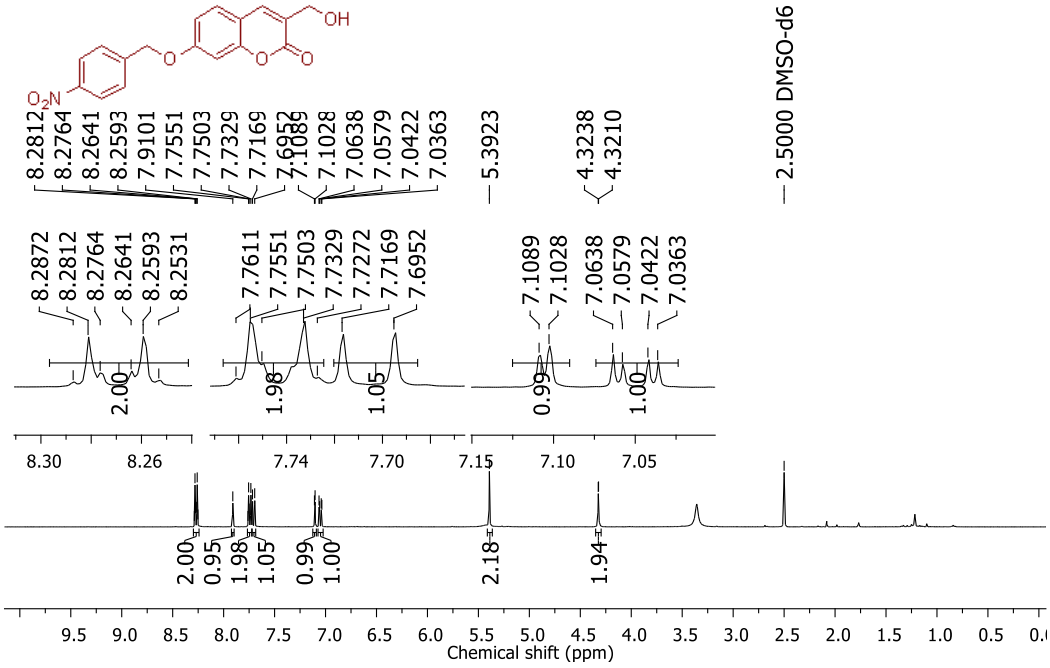

^{13}C NMR Spectrum (100 MHz, DMSO-d_6) of compound **45**

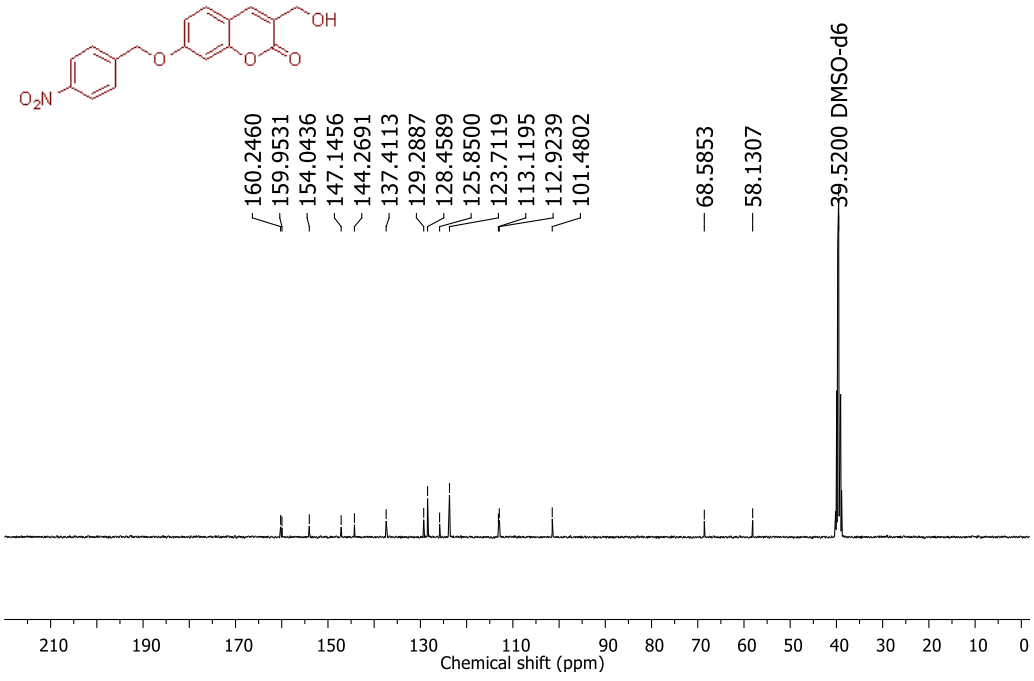

Crude ^{1}H NMR Spectrum (400 MHz, $(CD_3)_2CO$) of compound **46**

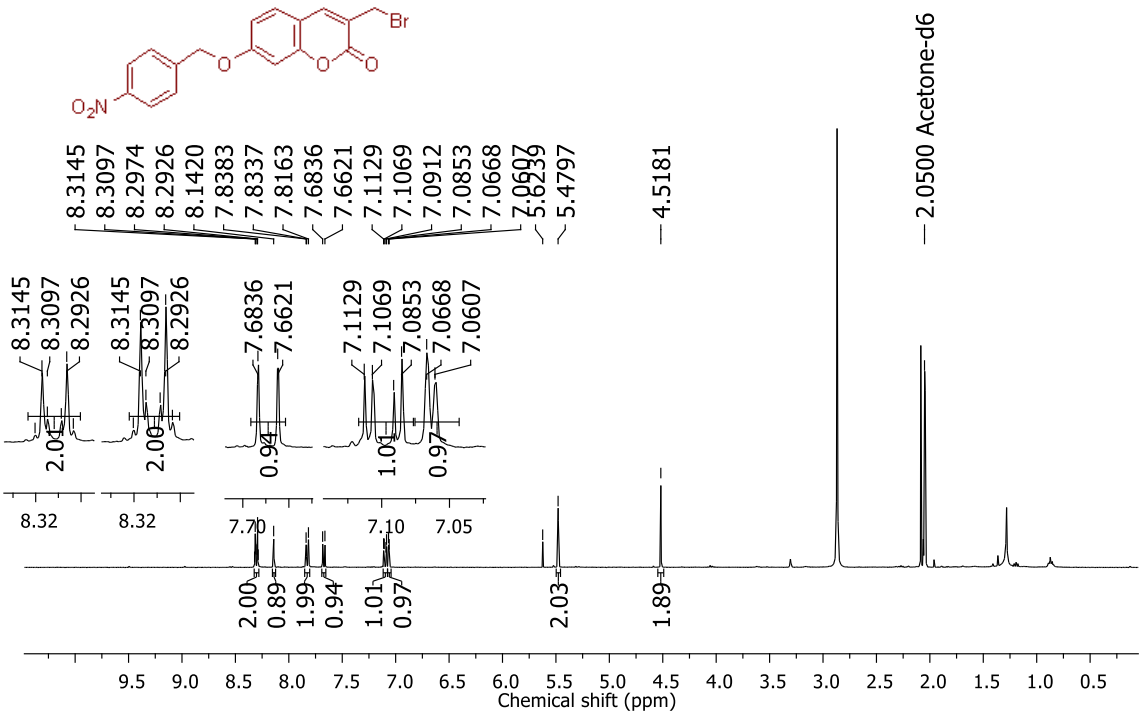

^{1}H NMR Spectrum (400 MHz, $CDCl_3$) of compound **47**

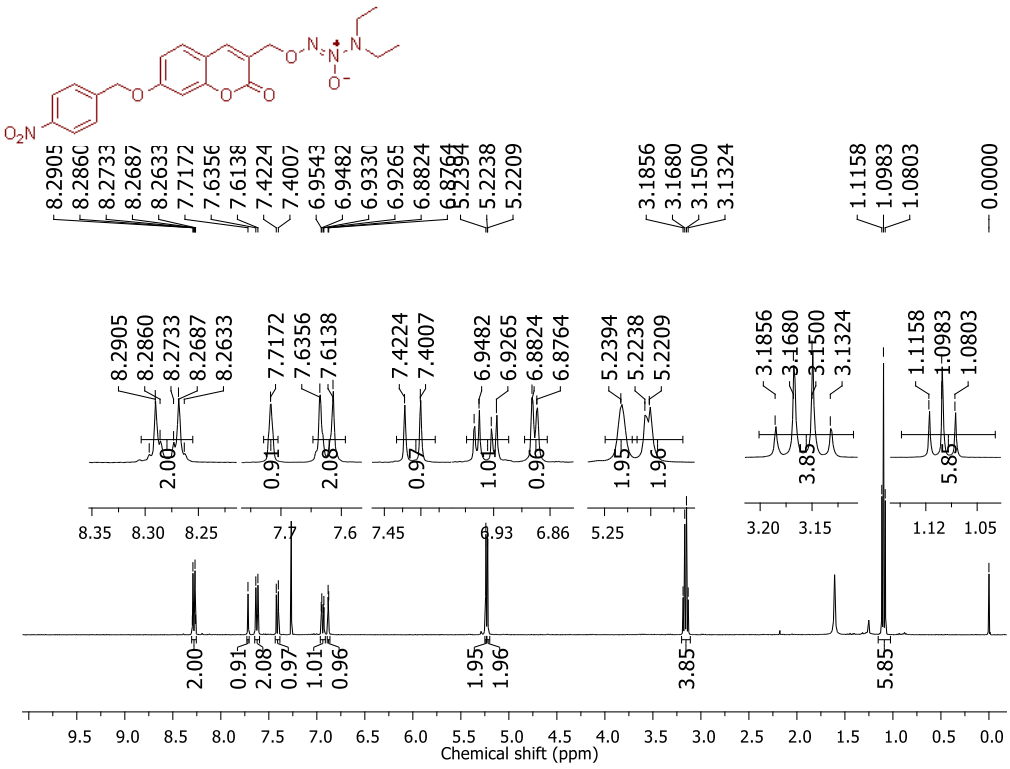

^{13}C NMR Spectrum (100 MHz, $CDCl_3$) of compound **47**

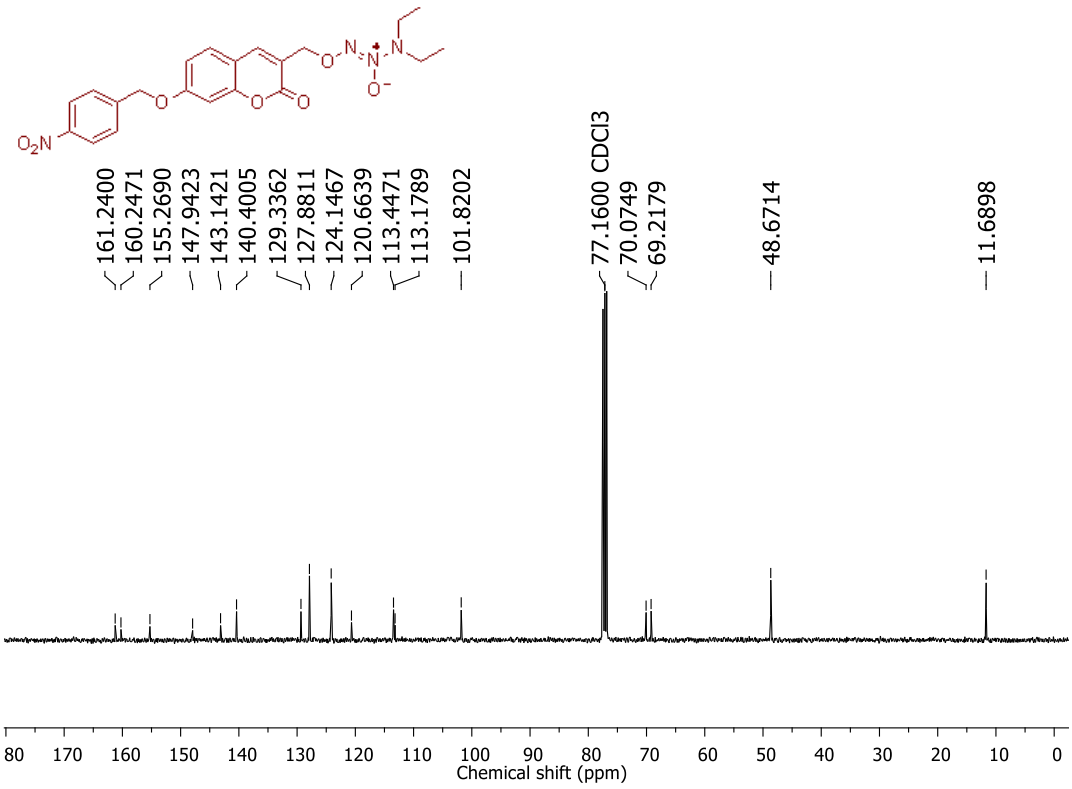

4.7. References

1. (a) Wink, D. A.; Hines, H. B.; Cheng, R. Y. S.; Switzer, C. H.; Flores-Santana, W.; Vitek, M. P.; Ridnour, L. A.; Colton, C. A., Nitric oxide and redox mechanisms in the immune response. *J. Leukoc. Biol.* **2011,** *89* (6), 873-891; (b) Bogdan, C., Nitric oxide and the immune response. *Nat Immunol* **2001,** *2* (10), 907-916.

2. MacMicking, J. D.; North, R. J.; LaCourse, R.; Mudgett, J. S.; Shah, S. K.; Nathan, C. F., Identification of nitric oxide synthase as a protective locus against tuberculosis. *Proc. Natl Acad. Sci.* **1997,** *94* (10), 5243-5248.

3. (a) McMullin, B. B.; Chittock, D. R.; Roscoe, D. L.; Garcha, H.; Wang, L.; Miller, C. C., The Antimicrobial Effect of Nitric Oxide on the Bacteria That Cause Nosocomial Pneumonia in Mechanically Ventilated Patients in the Intensive Care Unit. *Respir. Care* **2005,** *50* (11), 1451-1456; (b) Ghaffari, A.; Miller, C. C.; McMullin, B.; Ghahary, A., Potential application of gaseous nitric oxide as a topical antimicrobial agent. *Nitric Oxide* **2006,** *14* (1), 21-29.

4. (a) VALLANCE, P.; CHARLES , I., Nitric oxide as an antimicrobial agent: does NO always mean NO? *Gut* **1998,** *42* (3), 313-314; (b) Shatalin, K.; Gusarov, I.; Avetissova, E.; Shatalina, Y.; McQuade, L. E.; Lippard, S. J.; Nudler, E., Bacillus anthracis-derived nitric oxide is essential for pathogen virulence and survival in macrophages. *Proc. Natl. Acad. Sci.* **2008,** *105* (3), 1009-1013; (c) Gusarov, I.; Nudler, E., NO-mediated cytoprotection: Instant adaptation to oxidative stress in bacteria. *Proc. Natl. Acad. Sci.* **2005,** *102* (39), 13855-13860.

5. Gusarov, I.; Shatalin, K.; Starodubtseva, M.; Nudler, E., Endogenous Nitric Oxide Protects Bacteria Against a Wide Spectrum of Antibiotics. *Science* **2009,** *325* (5946), 1380-1384.

6. Weinstain, R.; Segal, E.; Satchi-Fainaro, R.; Shabat, D., Real-time monitoring of drug release. *Chem. Commun.* **2010,** *46* (4), 553-555.

7. (a) Tavares, A. F. N.; Nobre, L. S.; Melo, A. M. P.; Saraiva, L. M., A Novel Nitroreductase of Staphylococcus aureus with S-Nitrosoglutathione Reductase Activity. *J. Bacteriol.* **2009,** *191* (10), 3403-3406; (b) Bryant, D. W.; McCalla, D. R.; Leeksma, M.; Laneuville, P., Type I nitroreductases of Escherichia coli. *Can. J. Microbiol.* **1981,** *27* (1), 81-86; (c) Prosser, G. A.; Copp, J. N.; Syddall, S. P.; Williams, E. M.; Smaill, J. B.; Wilson, W. R.; Patterson, A. V.; Ackerley, D. F., Discovery and evaluation of Escherichia coli nitroreductases that activate the anti-cancer prodrug CB1954. *Biochem. Pharmacol.* **2010,** *79* (5), 678-687.

8. Singh, R.; Manjunatha, U.; Boshoff, H. I. M.; Ha, Y. H.; Niyomrattanakit, P.; Ledwidge, R.; Dowd, C. S.; Lee, I. Y.; Kim, P.; Zhang, L.; Kang, S.; Keller, T. H.; Jiricek, J.; Barry, C. E., PA-824 Kills Nonreplicating Mycobacterium tuberculosis by Intracellular NO Release. *Science* **2008,** *322* (5906), 1392-1395.

9. (a) Diacon, A. H.; Dawson, R.; du Bois, J.; Narunsky, K.; Venter, A.; Donald, P. R.; van Niekerk, C.; Erondu, N.; Ginsberg, A. M.; Becker, P.; Spigelman, M. K., Phase II Dose-Ranging Trial of the Early Bactericidal Activity of PA-824. *Antimicrob Agents Chemother.* **2012,** *56* (6), 3027-3031; (b) Manjunatha, U.; Boshoff, H. I. M.; Barry, C. E., The mechanism of action of PA-824: Novel insights from transcriptional profiling. *Commun. Integr Biol* **2009,** *2* (3), 215-218.

10. (a) Hettie, K. S.; Klockow, J. L.; Glass, T. E., Three-Input Logic Gates with Potential Applications for Neuronal Imaging. *J. Am. Chem. Soc.* **2014,** *136* (13), 4877-4880; (b) Lim, N. C.; Schuster, J. V.; Porto, M. C.; Tanudra, M. A.; Yao, L.; Freake, H. C.; Brückner, C., Coumarin-Based Chemosensors for Zinc(II): Toward the Determination of the Design Algorithm for CHEF-Type and Ratiometric Probes. *Inorg. Chem.* **2005,** *44* (6), 2018-2030.

CHAPTER 5: Indole based scaffold for tunable release rate

5.1. Introduction

An ideal delivery vehicle should provide a structural handle to tune the release of leaving group. In Chapter 2, our results indicated that NO release was retarded from indolequinone scaffold by substituting methyl group at the C-2 position. Next, in Chapter 3.2, we examined 4-nitrobenzyl scaffold for studying tunability by varying substituents at the benzylic position. However, due to inconclusive differences probably arising due to solubility issues, the 4-nitrobenzyl scaffold was not explored further for tunability. Although, indolequinone and 4-nitrobenzyl scaffolds used for delivery of NO are specific for DT-D[1] and NTR[2], respectively but they are limited due to their inefficiency for modulating release profile. Therefore, to explore the tunability aspect of a delivery system we need to have a more versatile scaffold with a) feasibility to modulate the scaffold synthetically; and b) potential to accommodate variety of protecting groups for designing delivery vehicle for different triggers.

In order to study the tunability aspect, we propose a new indole based scaffold. In this model the indole nitrogen is protected with palladium (Pd) sensitive allyloxy carbonyl (alloc) group. Additionally, the substituents present on the indole may affect the release of leaving group due to their electronic and steric effects.

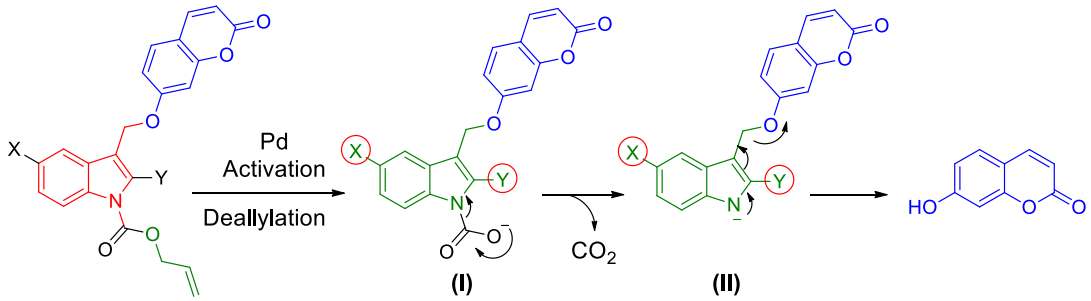

Scheme 5.1. A new indole based scaffold for studying the tunability of the release of umbelliferone from the scaffold. Alloc protected indole gets rapidly deprotected in the presence of a Pd catalyst and due to interplay of electronic and steric effects of the substituents X and Y, the release of umbelliferone may be modulated.

In order to study the indole scaffold, few indole based model compounds using umbelliferone as the leaving group and alloc as the protecting group on the indole nitrogen were synthesized. In the presence of a Pd catalyst, alloc gets rapidly cleaved[3] to release umbelliferone (Scheme 5.1) and the increased fluorescence upon activation

serves as a convenient signal to monitor the release profiles of the model compounds. The proposed mechanism is as follows: in the presence of a Pd catalyst, alloc group gets deprotected to form the intermediate **(I)**, followed by decarboxylation to generate the intermediate **(II)**. The electrons are relayed through the indole ring of the intermediate **(II)** to release the umbelliferone. The relay of electrons and release of leaving group may depend on the electron density on the indole ring, which in turn may depend on the substituents present on the indole. Furthermore, the substituents may affect the release of leaving group due to steric effects as well. To study the substituent's effect on the release profile we focused on a) the C-5 position of the indole that may regulate the release electronically; b) the C-2 position which may affect the release by virtue of its steric as well as the electronic effects.

5.2. Results and discussion

5.2.1. Synthesis

In order to evaluate the indole-based model, we synthesized a set of five alloc protected indole compounds with substituents varying at the C-5 and C-2 position of the indole ring (Figure 5.1).

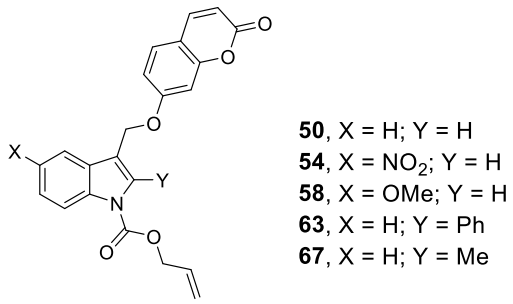

Figure 5.1. Palladium-activated indole based compounds.

We first synthesized the alloc protected indole compound **50** starting from indole-3-carbaldehyde. Briefly, the indole nitrogen of the indole-3-carbaldehyde was protected with the alloc group using allyl chloroformate in the presence of TEA in DCM to obtain **48** in 90% yield. The aldehyde **48** was reduced using $NaBH_4$ to obtain the indole-3-carbinol **49** in 65% yield. The alcohol **49** was subjected to Mitsunobu reaction with umbelliferone in the presence of PPh_3 and DIAD to obtain **50** in 72% yield (Scheme 5.2).

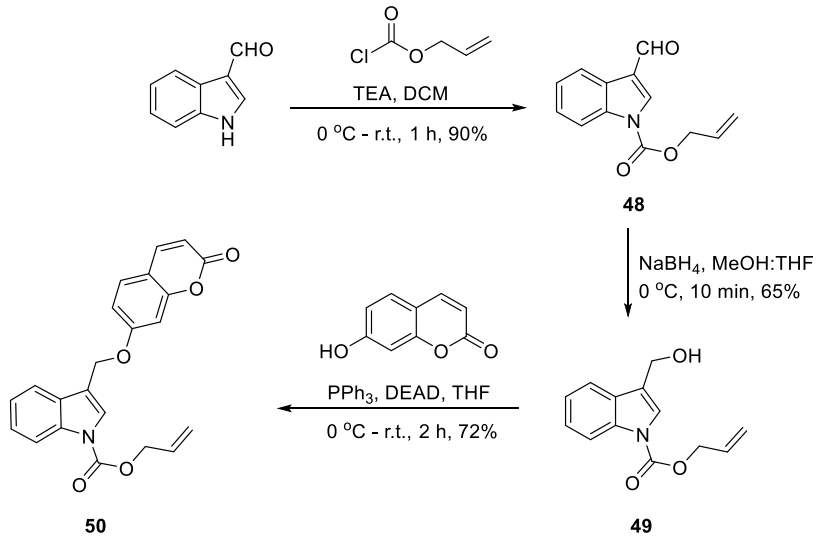

Scheme 5.2. Synthesis of **50**.

Next, the 5-NO_2 substituted indole compound, **54** and the 5-OMe substituted indole compound **58** were synthesized using a similar synthetic scheme (Scheme 5.3). The 5-substituted indole was first formylated using $POCl_3$ and DMF (Vilsmeiyer reagent) to obtain the indole-3-carbaldehyde which was reacted with allyl chloroformate to form alloc protected indole. The substituted indole-3-carbaldehyde was reduced by reacting it with $NaBH_4$ to obtain alcohol, which was then reacted with umbelliferone using Mitsunobu reaction to afford final compound.

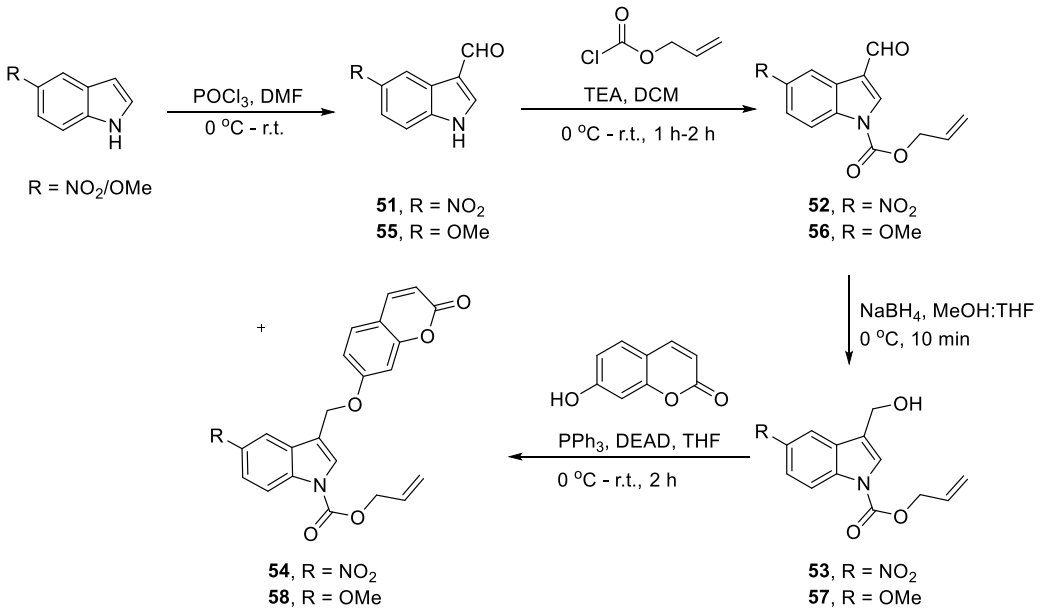

Scheme 5.3. Synthesis of **54** and **58**.

Further, we synthesized C-2 substituted indole compounds, **63** and **67**, in order to study effects of the C-2 substitutents. The synthesis of **63** was started with Pd catalysed C-2 arylation of indole to afford 2-phenyl indole **59** in 80% yield. Compound **59** was formylated using $POCl_3$ and DMF to obtain **60** in 63% yield. Using allyl chloroformate, the indole nitrogen was protected with the alloc group to get **61** in 37% yield. The aldehyde **61** was then reduced using $NaBH_4$ to obtain alcohol **62** in 97% yield. Finally, the alcohol was reacted with umbelliferone in the presence of PPh_3 and DIAD in THF to obtain the 2-phenyl substituted indole compound, **63** (Scheme 5.4).

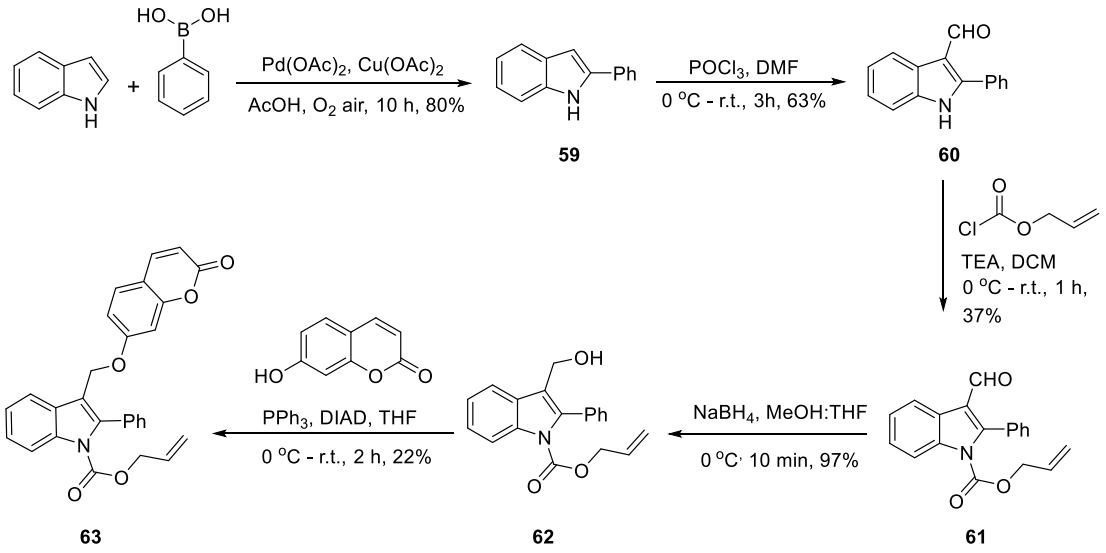

Scheme 5.4. Synthesis of **63**.

In order to synthesize the 2-Me substituted indole compound **67**, we started from 2-Me indole. It was formylated using Vilsmeiyer reagent to obtain **64** in 83% yield. The alloc protection on the indole nitrogen was achieved by reacting **64** with allyl chloroformate and TEA in DCM to obtain **65** in 71% yield. The aldehyde **65** was reduced using $NaBH_4$ to obtain alcohol **66**, which was then reacted with umbelliferone in the presence of PPh_3 and DIAD in THF to obtain 2-methyl substituted compound, **67** (Scheme 5.5).

To determine the suitability of the alloc protected indole scaffold for delivery of NO, we synthesized a Pd-activated NO donor using the alloc protected indole scaffold, **69** (Scheme 5.6). The indole-3-carbinol, **49** was converted into the bromide **68** by

treatment with PBr_3 in DCM. The bromide was displaced by PYRRO/NO to afford **69** in 4% yield.

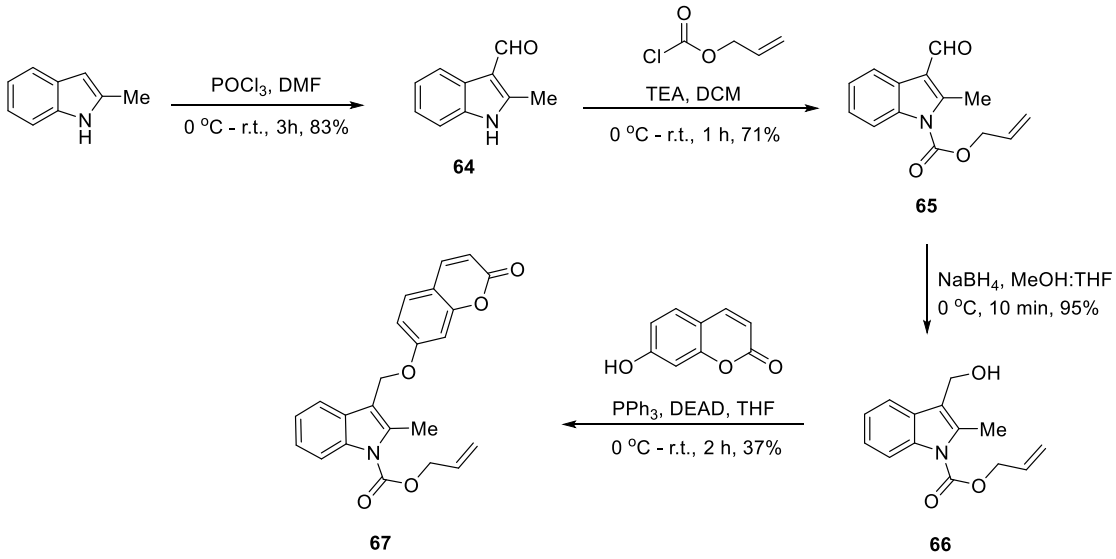

Scheme 5.5. Synthesis of **67**.

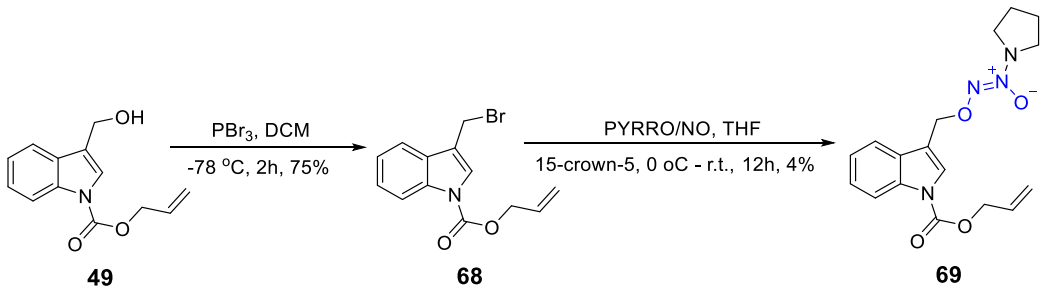

Scheme 5.6. Synthesis of **69**.

5.2.2. Palladium-catalysed deallylation and evaluation of umbelliferone release

The proposed alloc protected indole compounds undergo deallylation in the presence of Pd catalyst and releases umbelliferone. So, in order to evaluate the release of umbelliferone from indole scaffold using palladium-catalysed deallylation, we used a reported protocol.[3] We first reacted **50** with 10 mol% of $Pd(PPh_3)_4$, excess of Bu_3SnH and acetic acid in THF for 30 min. A 10 µL aliquot of the reaction mixture was removed at the specified time and diluted with 1:1 ACN-buffer solution and this solution was then analysed using HPLC for decomposition of **50** and the release of umbelliferone. From the HPLC profile data of the reaction mixture, it was found that the peak for compound **50** (Abs λ: 320 nm) disappeared in 5 min of catalyst addition, suggesting **50** was deprotected completely by Pd within 5 min (Figure 5.2.A). In

addition to the peak disappearance of **50**, emergence of a new peak was observed, which was identified as umbelliferone (Abs λ: 320 nm).

Next, we quantified the umbelliferone release from **50** using HPLC over 30 min. The aliquots from the reaction mixture were hydrolysed and then injected into HPLC at the specified time points. The amount of umbelliferone released was quantified using a standard calibration curve for umbelliferone obtained from HPLC (Abs λ: 320 nm). It was found that the Pd-activated indole scaffold **50** released nearly 80% of umbelliferone during 30 min (Figure 5.2.B). However, under similar conditions in absence of Pd, **50** was stable and did not release umbelliferone. Thus, **50** was found to be a substrate for activation by a chemical trigger to release a fluorophore.

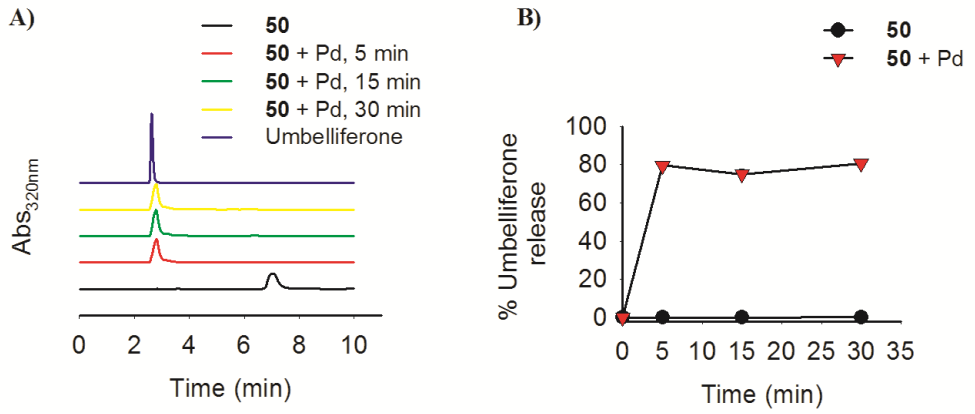

Figure 5.2. A) HPLC traces for monitoring decomposition of **50** in the presence of Pd catalyst over time (Abs λ: 320 nm). Umbelliferone was injected to identify the new emerging peak. **B)** Estimation of umbelliferone released from **50** in the presence and absence of Pd catalyst using HPLC (Abs λ: 320 nm).

In the tunable model for release of phenols by Schmid *et al.*, the methoxy substituted phenyl rings released phenols at a faster rate compared to unsubstituted analogue.[3] So next, in order to evaluate the release of umbelliferone from the C-5 substituted alloc protected indoles, we performed Pd-catalysed deallylation of **54** and **58**. It was found from the HPLC decomposition data that both 5-NO_2 and 5-OMe were deprotected in presence of Pd catalyst. However, a remarkable difference in the amount of umbelliferone released from the two compounds was noticed (Figure 5.3.A). The 5-NO_2 indole, **54** was found to release umbelliferone at a slow rate during 30 min with ~25% umbelliferone produced. The compound **54** was incubated with Pd catalyst for 180 min to efficiently produce umbelliferone (Figure 5.3.B). However, the 5-OMe substituted indole, **58** release profile of umbelliferone was comparable with **50**. Being

a strong electron withdrawing group, 5-NO_2 presumably delocalises the electron density being formed on the indole ring after the alloc deprotection. As a result of which the electrons are not free to flow in the direction that expels the leaving group.

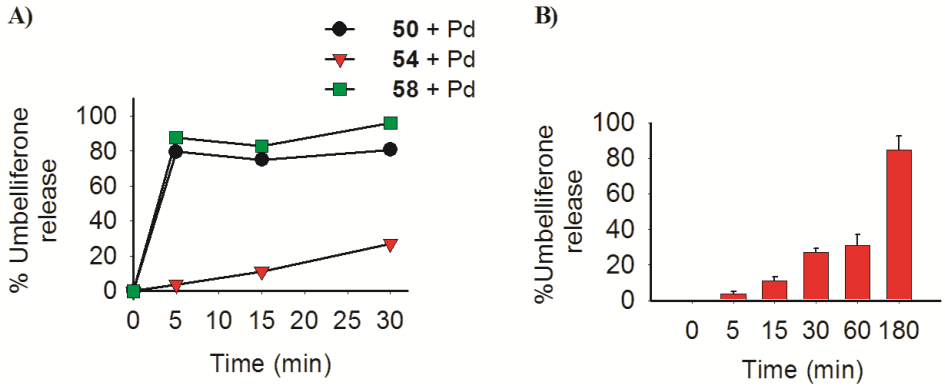

Figure 5.3. A) Estimation of umbelliferone released from **54** and **58** in the presence of Pd using HPLC (Abs λ: 320 nm), comparing umbelliferone release from **50** under similar condition. **B)** Time course release of umbelliferone from **54** during 3 h.

Next, in order to evaluate the release of umbelliferone from the C-2 substituted alloc protected indoles, we performed the Pd-catalysed deallylation of **63** and **67**. Under the similar reaction conditions as **50**, it was found that the release of umbelliferone was reduced to 60% after 30 min for both **63** and **67** (Figure 5.4). Probably due to an increase in the sterics at the C-2 position, the release of umbelliferone was decelerated.

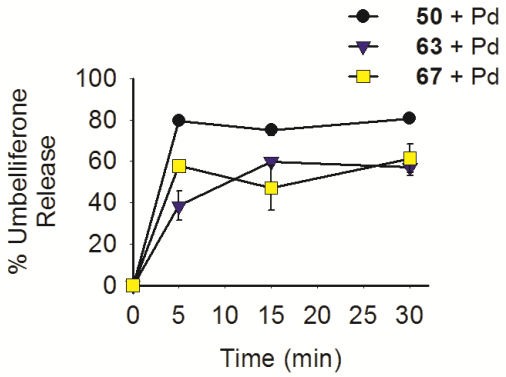

Figure 5.4. Estimation of umbelliferone released from **63** and **67** in the presence of Pd using HPLC (Abs λ: 320 nm), comparing umbelliferone release from **50** under similar condition.

The calculated half-lives of the five alloc protected indole compounds in the presence of Pd varied from 2 min to 1 h (calculated using $3\times t_{1/2}$ = 90% decomposition). Thus, using substituted indole scaffold, the release of umbelliferone was tuned by varying

the substituents on the indole ring. As alloc group is highly sensitive to the presence of Pd, we compared the release of umbelliferone after 5 min to comment on the differences in the release profile from indole scaffold. We found that **50** (unsubstituted indole) released ~80% umbelliferone; **54** (5-NO_2 substituted indole) released ~4% umbelliferone, **58** (5-OMe substituted indole) released ~90% umbelliferone, **63** (2-Ph substituted indole) released ~40% umbelliferone and **67** (2-Me substituted indole) released ~60% umbelliferone (Figure 5.5).

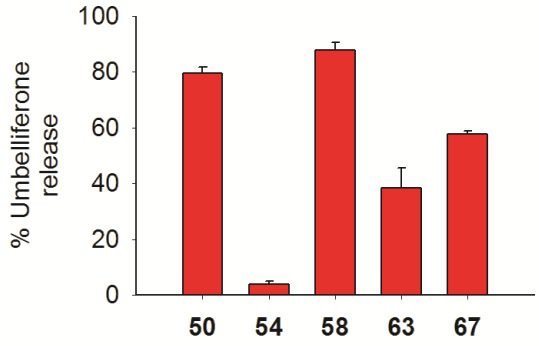

Figure 5.5. Estimation of umbelliferone released using HPLC during deallylation of the alloc protected indoles in the presence of Pd catalyst after 5 min.

We observed a distinct difference in the release profile of umbelliferone from indole scaffold after 5 min. The presence of strong electron withdrawing 5-NO_2 group on indole decelerates the release of umbelliferone from the indole ring. However, due to high electron density for 5-OMe indole **58**, release of umbelliferone was marginally better than **50**. We observed 2-Me indole **67** was better in releasing umbelliferone as compared to **63**, due less steric bulk of 2-Me group. As a result of bulky phenyl group at the C-2 position, it becomes difficult for the molecule to achieve planarity for smooth flow of electrons and to release umbelliferone.

Furthermore, the increase in fluorescence of umbelliferone was simultaneously measured using microwell plate reader (λ_{ex}: 320 nm; λ_{em}: 460 nm). A similar release profile as HPLC data was observed. 5-OMe indole compound **58** released comparable amount of umbelliferone as **50**. The C-2 substituted indole compounds, **63** and **67**, however released umbelliferone at a slower rate. Compound **54**, 5-NO_2 substituted indole compound was releasing umbelliferone sluggishly (Figure 5.6).

Thus using the palladium deprotection strategy, we demonstrated that the subsitutents on the indole ring were capable of modulating the release of leaving by means of electronic and steric effects.

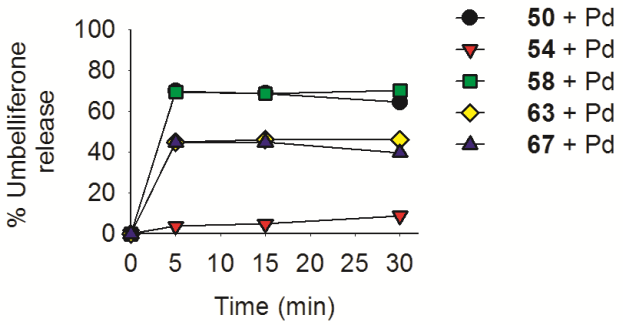

Figure 5.6. Estimation of umbelliferone released from alloc protected indole compounds in the presence of Pd by fluorescence using microwell plate reader (λ_{ex}: 320 nm; λ_{em}: 460 nm).

5.2.3. Evaluation of palladium-catalysed NO release

In order to check the suitability of the indole scaffold to deliver NO, compound **69** was synthesized (Scheme 5.6). It was reacted with 10 mol% of $Pd(PPh_3)_4$ in the presence of Bu_3SnH and AcOH in THF. 10 µL of the reaction mixture was hydrolysed in 1:1 ACN: buffer solution and the decomposition of **69** was monitored by HPLC and release of NO was quantified using Sievers NOA (280i) in the reaction mixture. HPLC analysis (Abs λ: 250 nm) of the reaction mixture showed that peak corresponding to **69** reduced within 5 min indicating Pd mediated deallylation of indole scaffold (Figure 5.7.A).

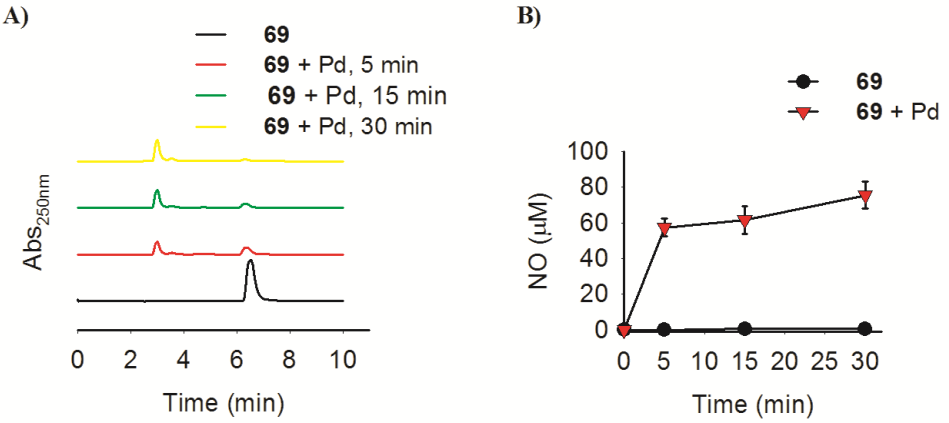

Figure 5.7. A) HPLC traces for monitoring decomposition of **69** in the presence of Pd catalyst over time (Abs λ: 250 nm). **B)** NO release from **69** in the presence and absence of Pd detected using a chemiluminesence-based assay.

Simultaneously, the amount of NO released in the reaction mixture was measured and it was found that nearly 80% of NO was detected in the reaction mixture after 30 min (Figure 5.7.B).

When NO release and the umbelliferone release were compared, we found similar release profiles (Figure 5.8). Thus, based on the tunability on the umbelliferone release by varying substituents on the indole ring, we suggest suitability of the indole scaffold to tune NO releases rate as well.

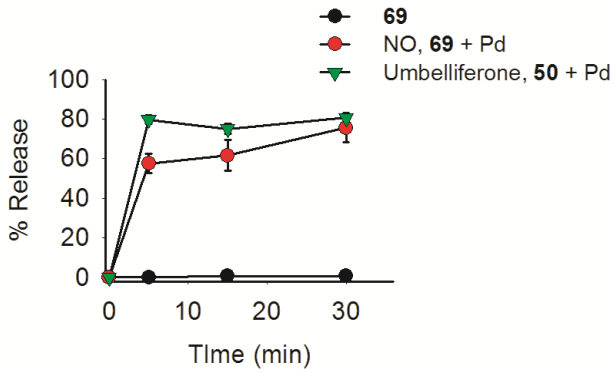

Figure 5.8. Comparison of NO release from **69** and umbelliferone release from **50** after Pd activation during 30 min.

5.3. Conclusion

Two important features of a drug delivery vehicle are i) targeted delivery of the drug; and ii) controlled release of the drug at the desired site. A scaffold capable of tethering to variety of triggers and also offering synthetic handle to tune release of drug molecule would be preferred as an appropriate drug delivery vehicle. In this chapter, we presented a new indole scaffold which can be synthetically modified to tune the release rate of leaving group. We used indole as a scaffold, alloc as a cleavable protecting group and umbelliferone as the fluorescent readout for monitoring release profile. We observed comparable umbelliferone release profile from indole compound with an electron donating group at C-5 with unsubstituted indole. However, an electron withdrawing group on the C-5 of indole, decelerated the release of umbelliferone. By increasing steric bulk at the C-2 position, we found that the umbelliferone release rate was reduced. Also, we found the indole–alloc scaffold was suitable for delivery of NO using Pd as chemical trigger. When the release of umbelliferone and NO as leaving group from same scaffold were analysed, we found similar release profile. Thus, taken together we provide evidence that by using indole

scaffold, the release profile of the leaving group can be predictably tuned by varying the aromatic substituents on the indole ring.

5.4. Experimental and characterization data

Compounds **48**,[4] **51**,[5] **55**,[6] **59**[4] and **60**[7] were synthesized by using previously reported procedures and analytical data that we collected were consistent with the reported values.

5.4.1. General procedure for alloc protection

To an ice cold stirred solution of sodium hydride (0.67 mmol, 1.5 eq.) in DMF (5 mL) under nitrogen atmosphere, indole-3-carbaldehyde (0.45 mmol, 1 eq.) was added and the reaction mixture was stirred at 0 ^{o}C for 15 min. To the reaction mixture allyl chloroformate (0.45 mmol, 2 eq.) was added and the reaction mixture was gradually warmed to room temperature and stirred for 3 h. The reaction mixture was quenched with ice cold water (100 mL) and extracted in ethyl acetate (3×20 mL). The combined organic layer was washed with brine, dried (Na_2SO_4) and filtered. The filtrate was evaporated to get crude product which was purified by column chromatography.

Synthesis of allyl 3-formyl-1H-indole-1-carboxylate, 48.

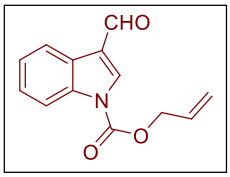

The crude product was purified by column chromatography using 5% ethyl acetate: pet ether as eluent to obtain **48** as a white solid (2.82 g, 89%): m.p. 38-39 °C; FT-IR (ν_{max}, cm^{-1}): 1749, 1675, 1451, 1224, 1093; ^{1}H NMR ($CDCl_3$, 400 MHz): δ 9.99 (s, 1H), 8.20–8.22 (m, 1H), 8.11 (s, 1H), 8.08 (d, *J* = 7.68 Hz, 1H), 7.29–7.38 (m, 2H), 6.01–6.10 (m, 1H), 5.45–5.50 (m, 1H), 5.37–5.40 (m, 1H), 4.90–4.92 (m, 2H); ^{13}C NMR ($CDCl_3$, 100 MHz): δ 185.5, 149.7, 135.8, 130.7, 126.2, 125.9, 124.7, 122.0, 120.2, 115.0, 68.4; HRMS (ESI) for $C_{13}H_{11}NO_3$ $[M+H]^+$: Calcd., 230.0817, Found, 230.0827.

Synthesis of allyl3-formyl-5-nitro-1H-indole-1-carboxylate, 52.

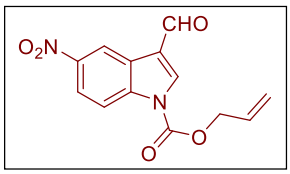

The crude product was purified by column chromatography using dichloromethane as eluent to obtain **52** as a white solid (0.23 g, 53%): m.p. 145-146 °C; FT-IR (ν_{max}, cm^{-1}): 1755, 1687, 1517, 1454, 1339, 1267, 1090; ^{1}H NMR ($CDCl_3$, 400 MHz): δ 10.13 (s, 1H), 9.17 (m, 1H), 8.42 (s, 1H), 8.32-8.32 (m, 2H), 6.05-6.15 (m, 1H), 5.52-5.57 (m, 1H), 5.45-5.48 (m, 1H), 5.01-5.03 (m, 2H); ^{13}C NMR ($CDCl_3$, 100 MHz): δ 184.9, 149.4, 145.4, 138.9, 137.8, 130.2, 126.2, 122.3, 121.8, 121.5, 118.7,

115.7, 69.5; HRMS (ESI) for $C_{13}H_{10}N_2O_5$ $[M+H]^+$: Calcd., 275.0668, Found, 275.0681.

Synthesis of allyl 3-formyl-5-methoxy-1H-indole-1-carboxylate, 56.

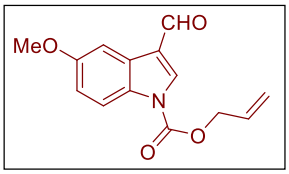

The crude product was purified using 10% ethyl acetate: pet ether as eluent to obtain **56** as a white solid (0.25 g, 56%): m.p. 74-75 °C; FT-IR (ν_{max}, cm^{-1}): 1746, 1672, 1398, 1245, 1084; ^1H NMR ($CDCl_3$, 400 MHz): δ 10.07 (s, 1H), 8.23 (s, 1H), 8.04 (d, *J* = 9.0 Hz, 1H), 7.76 (d, *J* = 2.6 Hz, 1H), 7.02 (dd, *J* = 9.0, 2.6 Hz, 1H), 6.03-6.13 (m, 1H), 5.47-5.53 (m, 1H), 5.39-5.43 (m, 1H), 4.95-4.97 (m, 2H), 3.89 (s, 3H); ^{13}C NMR ($CDCl_3$, 100 MHz): δ 185.9, 157.7, 150.1, 136.4, 130.9, 130.6, 127.1, 122.2, 120.5, 116.0, 116.0, 104.1, 68.6, 55.9; HRMS (ESI) for $C_{14}H_{13}NO_4$ $[M+H]^+$: Calcd., 275.0668, Found, 275.0678.

Synthesis of allyl 3-formyl-2-phenyl-1H-indole-1-carboxylate, 61.

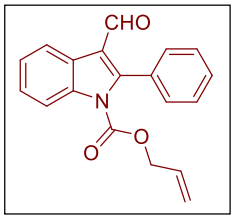

The crude product was purified using 5% ethyl acetate: pet ether as eluent to obtain **61** as a white solid (0.26 g, 37%): m.p. 60 -61 °C; FT-IR (ν_{max}, cm^{-1}): 1744, 1662, 1481, 1306, 1079; ^1H NMR ($CDCl_3$, 400 MHz): δ 9.73 (s, 1H), 8.39-8.41 (m, 1H), 8.17-8.19 (m, 1H), 7.39-7.51 (m, 7H), 5.58-5.68 (m, 1H), 5.13-5.20 (m, 2H), 4.66-4.68 (m, 2H); ^{13}C NMR ($CDCl_3$, 100 MHz): δ 188.2, 150.8, 150.1, 136.1, 130.3, 130.2, 129.5, 128.1, 126.3, 125.8, 125.1, 122.2, 120.5, 120.1, 115.2, 68.4; HRMS (ESI) for $C_{19}H_{15}NO_3$ $[M+H]^+$: Calcd., 306.1130, Found, 306.1137.

Synthesis of allyl 3-formyl-2-methyl-1H-indole-1-carboxylate, 65.

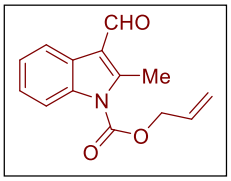

The crude product was purified using 10-15% ethyl acetate: pet ether as eluent to obtain **65** as a white solid (0.54 g, 71%): m.p. 88-89 °C; FT-IR (ν_{max}, cm^{-1}): 1744, 1658, 1455, 1321, 1218; ^1H NMR ($CDCl_3$, 400 MHz): δ 10.33 (s, 1H), 8.28-8.32 (m, 1H), 8.04-8.09 (m, 1H), 7.32-7.36 (m, 2H), 6.06-6.16 (m, 1H), 5.49-5.54 (m, 1H), 5.41-5.44 (m, 1H), 4.98-5.00 (m, 2 H), 2.94 (s, 3H); ^{13}C NMR ($CDCl_3$, 100 MHz): δ 186.0, 151.4, 148.8, 135.5, 130.8, 126.3, 125.3, 124.8, 121.2, 120.7, 119.0, 115.3, 68.6, 13.8; HRMS (ESI) for $C_{14}H_{13}NO_3$ $[M+H]^+$: Calcd., 244.0973, Found, 244.0973.

5.4.2. General procedure for aldehyde reduction

The alloc protected aldehyde (1 eq.) was dissolved in 1: 2 solution of THF and MeOH cooled to 0 ^{o}C under a nitrogen atmosphere. To this ice cooled solution, sodium borohydride (0.6 eq.) was added and the reaction mixture was stirred at 0 ^{o}C for 15 min to 30 min (till reactant was completely consumed). The reaction mixture was quenched using saturated NH_4Cl solution and then extracted using ethyl acetate (3 × 10 mL). The combined organic layer was washed with brine, dried (Na_2SO_4) and filtered. The filtrate was evaporated to get crude product which was purified by column chromatography.

Synthesis of allyl 3-(hydroxymethyl)-1H-indole-1-carboxylate, 49.

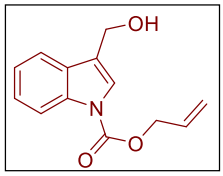

The crude product was purified using 20-25% ethyl acetate: pet ether as eluent to obtain **49** as a brown liquid (1.8 g, 64 %): FT-IR (ν_{max}, cm^{-1}): 1730, 1452, 1392, 1244, 1087; ^{1}H NMR ($CDCl_3$, 400 MHz): δ 8.17 (d, *J* = 7.8 Hz, 1H), 7.63-7.66 (m, 1H), 7.60 (s, 1H), 7.33-7.37 (m, 1H), 7.26-7.30 (m, 1H), 6.01-6.11 (m, 1H), 5.43-5.48 (m, 1H), 5.33-5.37 (m, 1H), 4.89-4.91 (m, 2H), 4.83 (s, 2H), 1.71 (s, 1H); ^{13}C NMR ($CDCl_3$, 100 MHz): δ 150.8, 136.0, 131.5, 129.3, 125.1, 123.3, 123.2, 121.5, 119.5, 115.5, 67.7, 57.3; HRMS (ESI) for $C_{13}H_{13}NO_3$ $[M+Na]^+$: Calcd., 254.0792, Found, 254.0799.

Synthesis of allyl 3-(hydroxymethyl)-5-nitro-1H-indole-1-carboxylate, 53.

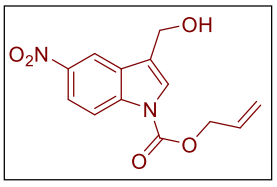

The crude product was purified using 50% ethyl acetate: pet ether as eluent to obtain **53** as a white solid (0.182 g, 94 %): m.p. 128-129 °C; FT-IR (ν_{max}, cm^{-1}): 3286, 1737, 1518, 1453, 1395, 1339, 1247; ^{1}H NMR ($CDCl_3$, 400 MHz): δ 8.54 (d, *J* = 2.1 Hz, 1H), 8.18-8.25 (m, 2H), 7.74 (s, 1H), 6.02-6.12 (m, 1H), 5.46-5.52 (m, 1H), 5.39-5.42 (m, 1H), 4.93-4.95 (m, 2H), 4.88 (s, 2H), 2.17 (s, 1H); ^{13}C NMR ($CDCl_3$, 100 MHz): δ 150.1, 143.9, 138.9, 130.9, 129.2, 125.9, 122.0, 120.4, 120.2, 116.1, 115.5, 68.4, 56.8; HRMS (ESI) for $C_{13}H_{12}N_2O_5$ $[M+H]^+$: Calcd., 277.0824, Found, 277.0832.

Synthesis of allyl3-(hydroxymethyl)-5-methoxy-1H-indole-1-carboxylate, 57.

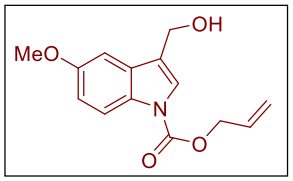

The crude product was purified using 50% ethyl acetate: pet ether as eluent to obtain **57** as a white solid (0.23 g, 99%): m.p. 68-69 °C; FT-IR (ν_{max}, cm^{-1}): 3442, 1731, 1457, 1397, 1257, 1081, 1247; ^{1}H NMR ($CDCl_3$, 400 MHz): δ 8.05 (d, *J* = 6.7 Hz, 1H), 7.59 (s, 1H), 7.11 (d, *J* = 2.5 Hz, 1H), 6.96 (dd, *J* = 9.0, 2.5 Hz, 1H), 6.01-6.11 (m, 1H), 5.43-5.48 (m, 1H), 5.33-5.36 (m, 1H), 4.89 (d, *J* = 5.8 Hz, 2H), 4.81 (s, 2H), 3.87 (s, 3H); ^{13}C NMR ($CDCl_3$, 100 MHz): δ 156.2, 150.6, 131.5, 130.4, 130.1, 123.8, 121.2, 119.4, 116.1, 113.7, 102.1, 67.5, 57.1, 55.7; HRMS (ESI) for $C_{14}H_{15}NO_4$ $[M+Na]^+$: Calcd., 284.0898, Found, 284.0905.

Synthesis of allyl 3-(hydroxymethyl)-2-phenyl-1H-indole-1-carboxylate, 62.

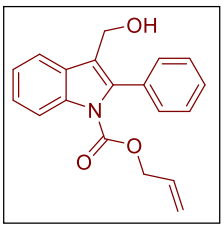

The crude product was purified using 20-25% ethyl acetate: pet ether as eluent to obtain **62** as a brown liquid (0.14 g, 97%): FT-IR (ν_{max}, cm^{-1}): 3369, 1729, 1452, 1318, 1076; ^{1}H NMR ($CDCl_3$, 400 MHz): δ 8.19–8.21 (m, 1H), 7.72-7.75 (m, 1H), 7.29-7.42 (m, 7H), 5.57-5.67 (m, 1H), 5.07-5.14 (m, 2H), 4.60-4.62 (m, 4H), 1.65 (bs, 1H); ^{13}C NMR ($CDCl_3$, 100 MHz): δ 151.4, 137.8, 136.4, 132.6, 131.0, 129.9, 129.0, 128.3, 127.9, 125.1, 123.5, 120.4, 119.4, 119.1, 115.6, 67.5, 55.9; HRMS (ESI) for $C_{19}H_{17}NO_3$ $[M+Na]^+$: Calcd., 330.1105, Found, 330.1104.

Synthesis of allyl3-(hydroxymethyl)-2-methyl-1H-indole-1-carboxylate, 66.

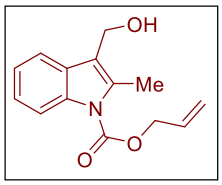

The crude product was purified using 50% ethyl acetate: pet ether as eluent to obtain **66** as a white solid (0.23 g, 95%): m.p. 93-94 °C; FT-IR (ν_{max}, cm^{-1}): 3352, 1733, 1459, 1320, 1142; ^{1}H NMR ($CDCl_3$, 400 MHz): δ 8.08-8.12 (m, 1H), 7.59-7.63 (m, 1H), 7.23-7.30 (m, 2H), 6.04-6.14 (m, 1H), 5.45-5.50 (m, 1H), 5.35-5.38 (m, 1H), 4.92-4.94 (m, 2H), 4.80 (s, 2H), 2.63 (s, 3H), 1.45 (bs, 1H); ^{13}C NMR ($CDCl_3$, 100 MHz): δ 152.0, 135.8, 135.7, 131.5, 129.3, 124.1, 123.2, 119.7, 118.3, 118.3, 115.7, 67.7, 55.6, 13.8; HRMS (ESI) for $C_{14}H_{15}NO_3$ $[M+Na]^+$: Calcd., 268.0949, Found, 268.0920.

5.4.3. General procedure for Mitsunobu coupling

A solution of alloc protected alcohol (1 eq.), umbelliferone (1 eq.) and PPh_3 (2 eq.) in dry THF was cooled to 0 ^oC under a nitrogen atmosphere. After 5 min, DIAD (2 eq.) was added to the reaction mixture and warmed to room temperature. The reaction mixture was stirred at room temperature for 2-4 h (reaction progress was monitored by TLC). The reaction mixture was then diluted with water and the aqueous layer was extracted using ethyl acetate (3 × 10 mL). The combined organic layer was washed with brine, dried (Na_2SO_4) and filtered. The filtrate was evaporated to get crude product which was purified by column chromatography.

Synthesis of allyl 3-(((2-oxo-2H-chromen-7-yl)oxy)methyl)-1H-indole-1-carboxylate, 50.

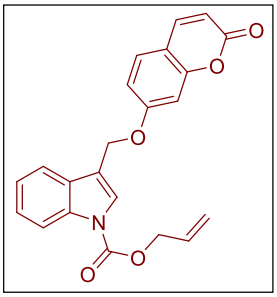

The crude product was purified using 10-15% ethyl acetate: pet ether as eluent to obtain **50** as a white solid (0.14 g, 87%): m.p. 117-118 °C; FT-IR (ν_{max}, cm^{-1}): 1733, 1612, 1455, 1369, 1228, 1901; ^1H NMR (DMSO-d_6, 400 MHz): δ 8.10 (d, *J* = 8.2 Hz, 1H), 7.95-7.97 (m, 2H), 7.70-7.72 (m, 1H), 7.61 (d, *J* = 8.6 Hz, 1H), 7.36-7.40 (m, 1H), 7.28-7.32 (m, 1H), 7.18 (d, *J* = 2.3 Hz, 1H), 7.04 (dd, *J* = 8.6, 2.4 Hz, 1H), 6.27 (d, *J* = 9.4 Hz, 1H), 6.06-6.15 (m, 1H), 5.45-5.51 (m, 1H), 5.41 (s, 2H), 5.32-5.36 (m, 1H), 4.92-4.94 (m, 2H); ^{13}C NMR (DMSO-d_6, 100 MHz): δ 161.2, 160.1, 155.2, 149.9, 144.2, 134.9, 131.9, 129.4, 128.9, 125.3, 124.9, 123.1, 119.8, 118.8, 116.4, 114.7, 113.0, 112.5, 112.4, 101.5, 67.3, 62.2; HRMS (ESI) for $C_{22}H_{17}NO_5$ $[M+H]^+$: Calcd., 376.1185, Found, 376.1189.

Synthesis of allyl 5-nitro-3-(((2-oxo-2H-chromen-7-yl)oxy)methyl)-1H-indole-1-carboxylate, 54.

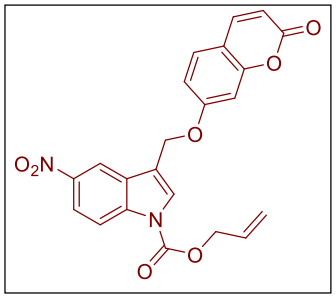

The crude product was purified using 10-15% ethyl acetate: pet ether as eluent to obtain **54** as a light green solid (0.07 g, 35%): m.p. 230-231 °C; FT-IR (ν_{max}, cm^{-1}): 1713, 1618, 1517, 1395, 1342, 1239; ^1H NMR (DMSO-d_6, 400 MHz): δ 8.66-8.67 (m, 1H), 8.29 (m, 2H), 8.21 (s, 1H), 7.99 (d, *J* = 9.4 Hz, 1H), 7.65 (d, *J* = 8.6 Hz, 1H), 7.22 (d, *J* = 2.3 Hz, 1H), 7.07 (dd, *J* = 8.6, 2.4 Hz, 1H), 6.30 (d, *J* = 9.4 Hz, 1H), 6.07-6.16 (m, 1H), 5.48-5.54 (m, 3H), 5.35-5.38 (m, 1H), 4.97-4.99 (m, 2H); due to poor

solubility of the compound in DMSO-d_6 ^{13}C NMR could not obtained; HRMS (ESI) for $C_{22}H_{16}N_2O_7$ $[M+H]^+$: Calcd., 421.1036, Found, 421.1039.

Synthesis of allyl 5-methoxy-3-(((2-oxo-2H-chromen-7-yl)oxy)methyl)-1H-indole-1-carboxylate, 58.

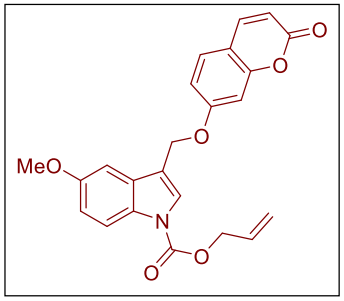

The crude product was purified using 25-30% ethyl acetate: pet ether as eluent to obtain **58** as a white solid (0.09 g, 38%): m.p. 162-163 °C; FT-IR (ν_{max}, cm^{-1}): 1732, 1612, 1477, 1260, 1083; ^{1}H NMR ($CDCl_3$, 400 MHz): δ 8.07 (d, *J* = 7.4 Hz, 1H), 7.71 (s, 1H), 7.63 (d, *J* = 9.48 Hz, 1H), 7.38 (d, *J* = 8.4 Hz, 1H), 6.99 (d, *J* = 2.5 Hz, 1H), 6.92-7.00 (m, 3H), 6.26 (d, *J* = 9.4 Hz, 1H), 6.02-6.12 (m, 1H), 5.44-5.49 (m, 1H), 5.35-5.38 (m, 1H), 5.24 (s, 2H), 4.90-4.92 (m, 2H), 3.85 (s, 3H); ^{13}C NMR ($CDCl_3$, 100 MHz): δ 161.8, 161.2, 156.5, 155.9, 150.4, 143.4, 131.5, 130.5, 129.9, 128.9, 125.3, 119.7, 116.3, 116.2, 113.9, 113.4, 113.3, 113.0, 102.3, 101.9, 67.8, 63.1, 55.9; HRMS (ESI) for $C_{23}H_{19}NO_6$ $[M+Na]^+$: Calcd., 428.1109, Found, 428.1111.

Synthesis of allyl3-(((2-oxo-2H-chromen-7-yl)oxy)methyl)-2-phenyl-1H-indole-1-carboxylate, 63.

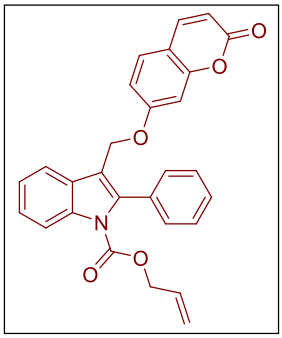

The crude product was purified using 25% ethyl acetate: pet ether as eluent to obtain **63** as a white solid (0.56 g, 22%): m.p. 110-111 °C; FT-IR (ν_{max}, cm^{-1}): 1722, 1611, 1455, 1224, 1116; ^{1}H NMR ($CDCl_3$, 400 MHz): δ 8.21-8.24 (m, 1H), 7.68-7.70 (m, 1H), 7.60 (d, *J* = 9.4 Hz, 1H) 7.30-7.46 (m, 8H), 6.80 (dd, *J* = 8.5, 2.4 Hz, 1H), 6.75 (d, *J* = 2.4 Hz, 1H), 6.23 (d, *J* = 9.4 Hz, 1H), 5.59-5.69 (m, 1H), 5.10-5.16 (m, 2H), 5.06 (s, 2H), 4.63-4.66 (m, 2H); ^{13}C NMR ($CDCl_3$, 100 MHz): δ 161.8, 161.2, 155.9, 151.3, 143.4, 139.1, 136.4, 132.2, 130.9, 129.9, 128.8, 128.8, 128.7, 128.2, 125.4, 123.7, 119.5, 119.4, 115.8, 115.8, 113.4, 113.3, 112.8, 102.1, 67.7, 62.4; HRMS (ESI) for $C_{28}H_{21}NO_5$ $[M+Na]^+$: Calcd., 474.1317, Found, 474.1317.

Synthesis of allyl 3-(((2-oxo-2H-chromen-7-yl)oxy)methyl)-1H-indole-1-carboxylate, 67.

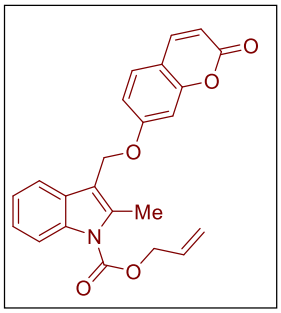

The crude product was purified using 10-15% ethyl acetate: pet ether as eluent to obtain **67** as a white solid (0.03 g, 37 %): m.p. 134-135 °C; FT-IR (ν_{max}, cm^{-1}): 1732, 1611, 1461, 1320, 1122; ^{1}H NMR ($CDCl_3$, 400 MHz): δ 8.11-8.13 (m, 1H), 7.63 (d, *J* = 9.4 Hz, 1H), 7.54-7.56 (m, 1H), 7.37 (d, *J* = 8.5 Hz, 1H), 7.23-7.31 (m, 2H), 6.94 (d, *J* = 2.2 Hz, 1H), 6.90 (dd, *J* = 8.4 Hz, 1H), 6.25 (d, *J* = 9.4 Hz, 1H), 6.05-6.15 (m, 1H), 5.46-5.51 (m, 1H), 5.36-5.39 (m, 1H), 5.22 (s, 2H), 4.94-4.95 (m, 2H), 2.68 (s, 3H); ^{13}C NMR ($CDCl_3$, 100 MHz): δ 162.0, 161.2, 155.9, 151.8, 143.4, 136.9, 135.8, 131.4, 129.1, 128.9, 124.3, 123.4, 119.9, 118.3, 115.8, 113.6, 113.4, 113.3, 112.9, 101.9, 67.8, 61.9, 14.1; HRMS (ESI) for $C_{23}H_{19}NO_5$ $[M+Na]^+$: Calcd., 412.1161, Found, 412.1167.

Synthesis of allyl 3-(bromomethyl)-1H-indole-1-carboxylate, 68.

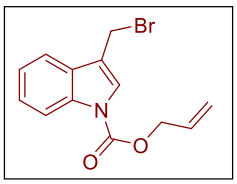

A solution of compound **49** (1.78 g, 7.69 mmol) was dissolved in dry DCM under a nitrogen atmosphere and was cooled to -78 ^{o}C. To the reaction mixture, PBr_3 (0.87 mL, 11.54 mmol) was added and the reaction mixture was stirred at -78 ^{o}C for 2 h. The reaction was quenched with saturated $NaHCO_3$ solution. The aqueous layer was extracted with ethyl acetate (3×20 mL). The combined organic layer was washed with brine, dried (Na_2SO_4), filtered and the filtrate was evaporated to obtain crude product **68** as a brown solid (1.70 g, 75%). Due to its sensitivity to decomposition this compound was not isolated and the crude data is presented as follows: ^{1}H NMR (400 MHz, $CDCl_3$): δ 8.19 (d, *J* = 5.8 Hz, 1H), 7.68-7.72 (m, 2H),7.32-7.41 (m, 2H), 6.01–6.10 (m, 1H), 5.44-5.50 (m, 1H), 5.35-5.38 (m, 1H), 4.91-4.92 (m, 2H), 4.67 (d, *J* = 0.6 Hz, 2H).

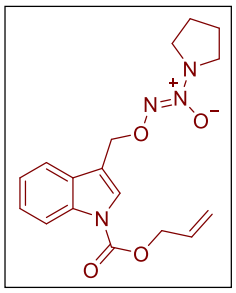

Synthesis of (Z)-2-((1-((allyloxy)carbonyl)-1H-indol-3-yl)methoxy)-1-(pyrrolidin-1-yl)diazene oxide, 69.

To an ice cold solution of the PYRRO/NO (0.62 g, 4.07mmol) in THF (30 mL), 15-crown-5 (0.10 mL) was added under a nitrogen atmosphere and the reaction mixture was stirred at 0 ^{o}C for 15

min. To this reaction mixture a solution of compound **68** in dry THF was added. The reaction mixture was stirred at room temperature for 12 h. The reaction mixture was then diluted with water and was extracted using ethyl acetate (3×20 mL). The combined organic layer was washed with brine, dried (Na_2SO_4) and filtered. The filtrate was evaporated to get crude product which was purified by column chromatography using 20% ethyl acetate: pet ether as eluent. The product was further purified using semi-preparative HPLC to obtain **69** as a light yellow solid (0.044 g, 4%): m.p. 90-91 °C; FT-IR (ν_{max}, cm^{-1}): 1738, 1483, 1394, 1294; ^1H NMR ($CDCl_3$, 400 MHz): δ 8.17 (d, *J* = 7.8 Hz, 1H), 7.70-7.72 (m, 2H), 7.33-7.37 (m, 1H), 7.26-7.30 (m, 1H), 6.02-6.11 (m, 1H), 5.44-5.49 (m, 1H), 5.34-5.38 (m, 1H), 5.31 (d, *J* = 0.6 Hz, 2H), 4.91-4.93 (m, 2H), 3.47-3.51 (m, 4H), 1.88-1.92 (m, 4H); ^{13}C NMR ($CDCl_3$, 100 MHz): δ 150.6, 135.7, 131.5, 129.6, 125.7, 125.1, 123.3, 119.8, 119.6, 116.9, 115.3, 67.7, 66.6, 51.0, 22.9; HRMS (ESI) for $C_{17}H_{20}N_4O_4$ $[M+Na]^+$: Calcd., 367.1382, Found, 367.1386.

5.4.4. Estimation of palladium catalysed umbelliferone release

A 10 mM stock solution of umbelliferone was prepared in acetonitrile. The standard calibration curve was obtained by using a concentration range varying from 0-150μM of umbelliferone prepared in 1:1 solution of acetonitrile and TRIS buffer pH 7.0. 50 μL of each concentration was injected in HPLC attached with a diode-array detector (DAD) and fluorescence detector (FLD).

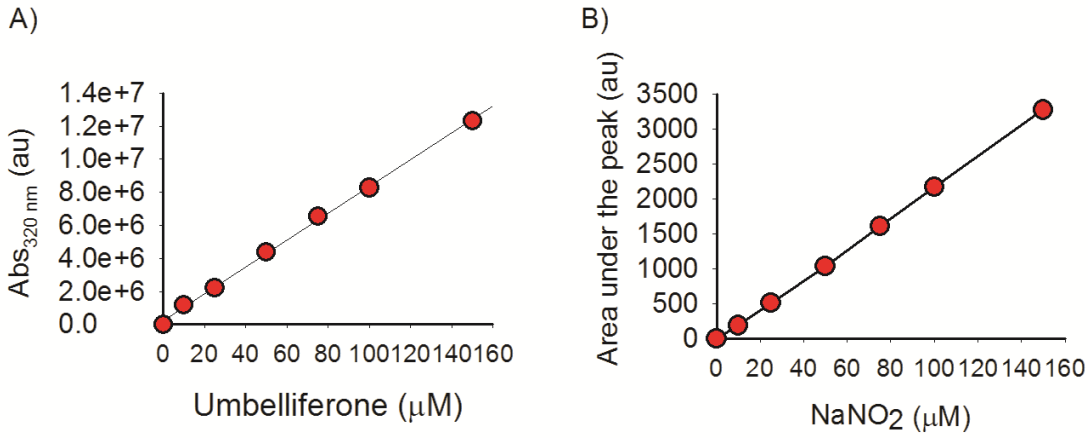

Figure 5.9. A) Calibration curve for umbelliferone in 1:1 ACN and TRIS buffer pH 7.0 water solution using HPLC (absorbance 320 nm). **B)** Calibration curve for $NaNO_2$ in 1:1 ACN and TRIS buffer pH 7.0 solution using chemiluminescence based assay.

A 70% acetonitrile: TRIS buffer pH 7.0 system was used as eluent with flow rate of 1 mL/min. Analysis was performed by measuring peak area detected using diode array detector, absorbance λ: 320 nm. The standard calibration curve was obtained by measuring area under the peak for various concentration (Figure 5.9.A; y = 83324x and R^2 = 0.997). Each concentration represents average of two values.

A 10 mM stock solution of test compound was prepared in THF and a 1 mM stock solution of tetrakis(triphenylphosphine)palladium (0) [$Pd(PPh_3)_4$] was prepared in THF. To 50 µL of test compound (10 mM stock) in a vial, 50 µL of [$Pd(PPh_3)_4$] solution (1 mM stock) was added. To this vial, 0.25 µL of tributyl tin hydride and 0.075 µL of acetic acid were added. In control set, the 50 µL of test compound was diluted with 50 µL of THF and then 0.25 µL of tributyl tin hydride and 0.075 µL of acetic acid were added. Both control and reaction mixture vials were stirred at room temperature. At specified time points, 10 µL of control and reaction mixtures were aliquot, diluted with 490 µL of 1:1 ACN and TRIS buffer pH 7.0 solution (final concentration of test compound: 100 µM). This solution was filtered and then injected into HPLC attached with DAD and FLD. The decomposition of test compound and release of umbelliferone was monitored by using HPLC.

5.4.5. Estimation of palladium-catalysed umbelliferone release

A 10 mM stock solution of $NaNO_2$ was prepared in TRIS buffer pH 7.0. The standard calibration curve was obtained by using a concentration range varying from 0-150µM of $NaNO_2$ prepared in 1:1 ACN and TRIS buffer pH 7.0 solution.10 µL of each varying concentrations were injected in NOA and the standard calibration curve was obtained by measuring area under the peaks for each concentration. (Figure 5.9.B; y = 41.68x, R^2 = 0.996). Each concentration represents average of three values.

A stock solution of **69** was prepared in THF. The control and reaction vials were prepared as mention in previous section 5.4.4 for estimation of release of NO from **69**. 10 µL of the blank and reaction mixtures were aliquot at specified time points and diluted to 1 mL to make a solution with final concentration of 50 µM. 10 µL of the diluted reaction mixture was injected into NOA. The amount of NO released was measured using the $NaNO_2$ standard calibration curve.

5.5. Spectral charts

^{1}H NMR Spectrum (400 MHz, $CDCl_3$) of compound **48**

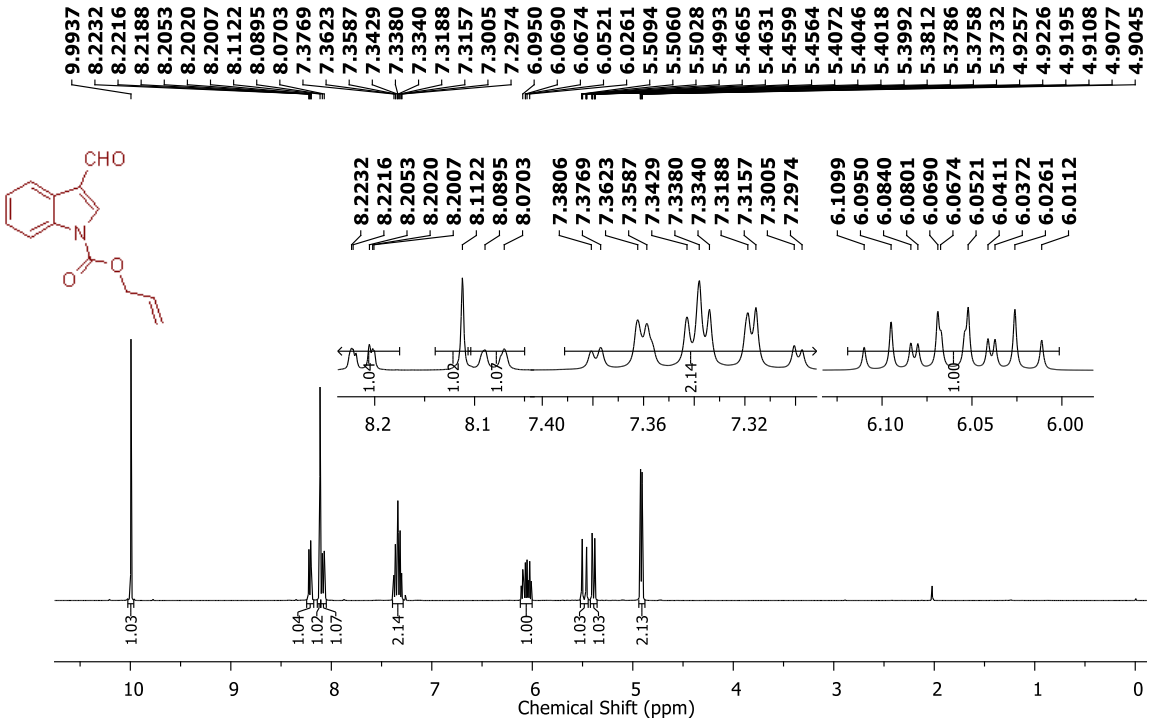

^{13}C NMR Spectrum (100 MHz, $CDCl_3$) of compound **48**

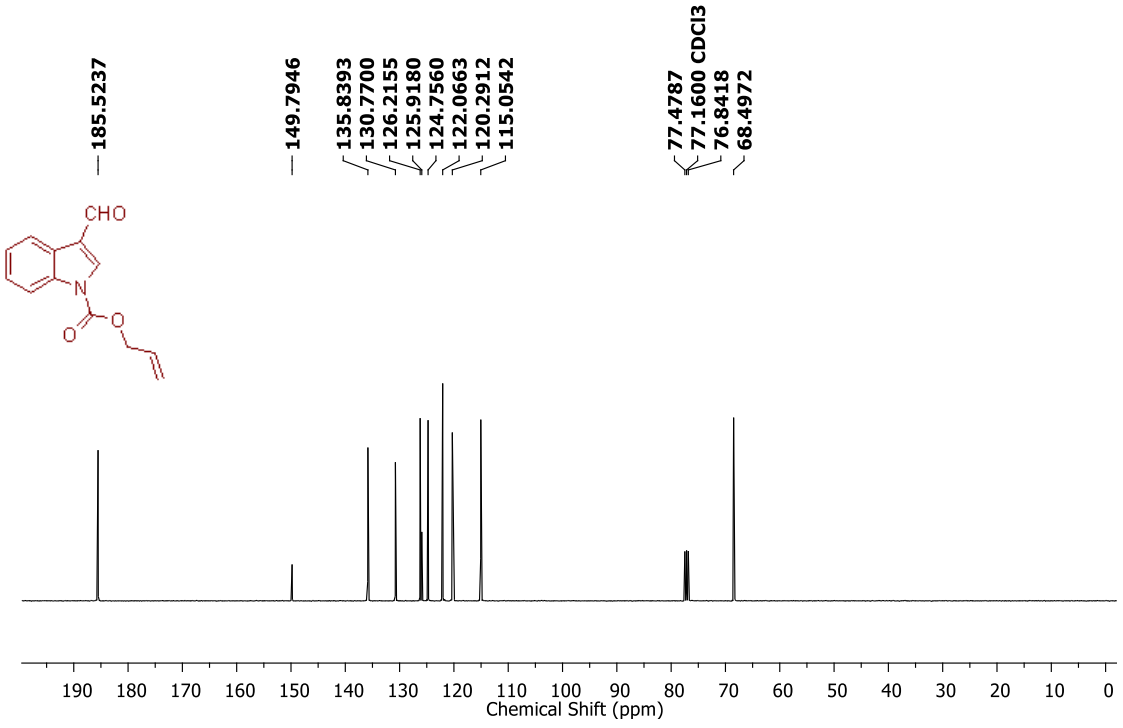

^{1}H NMR Spectrum (400 MHz, $CDCl_3$) of compound **49**

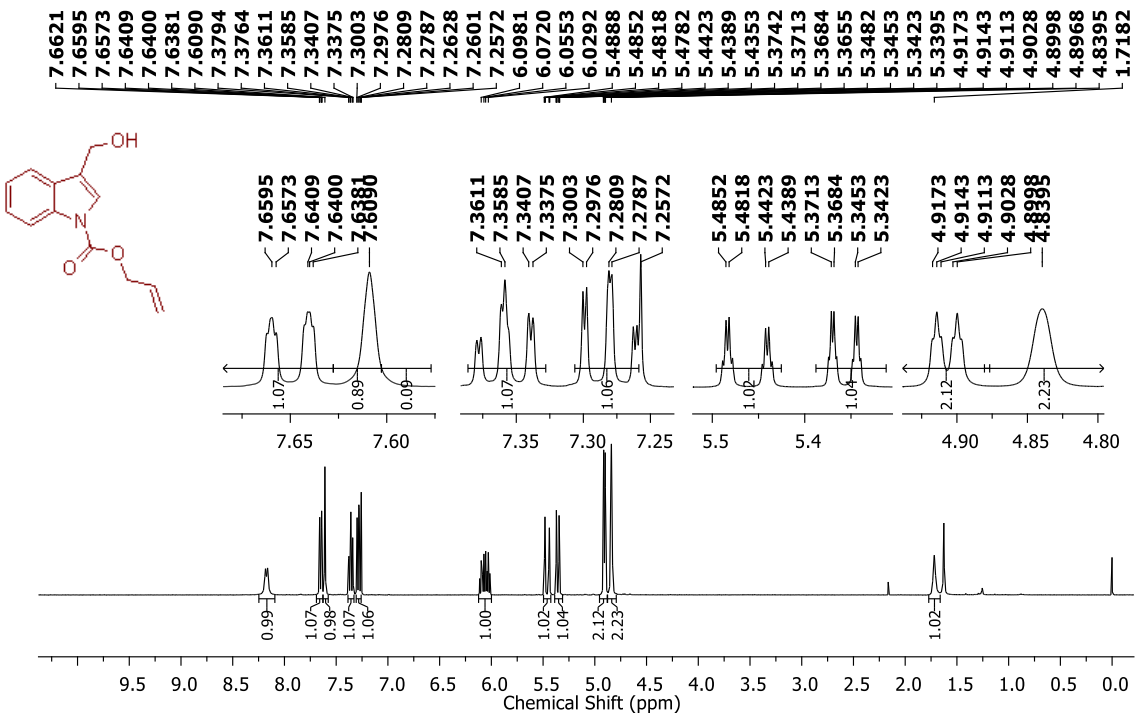

^{13}C NMR Spectrum (100 MHz, $CDCl_3$) of compound **49**

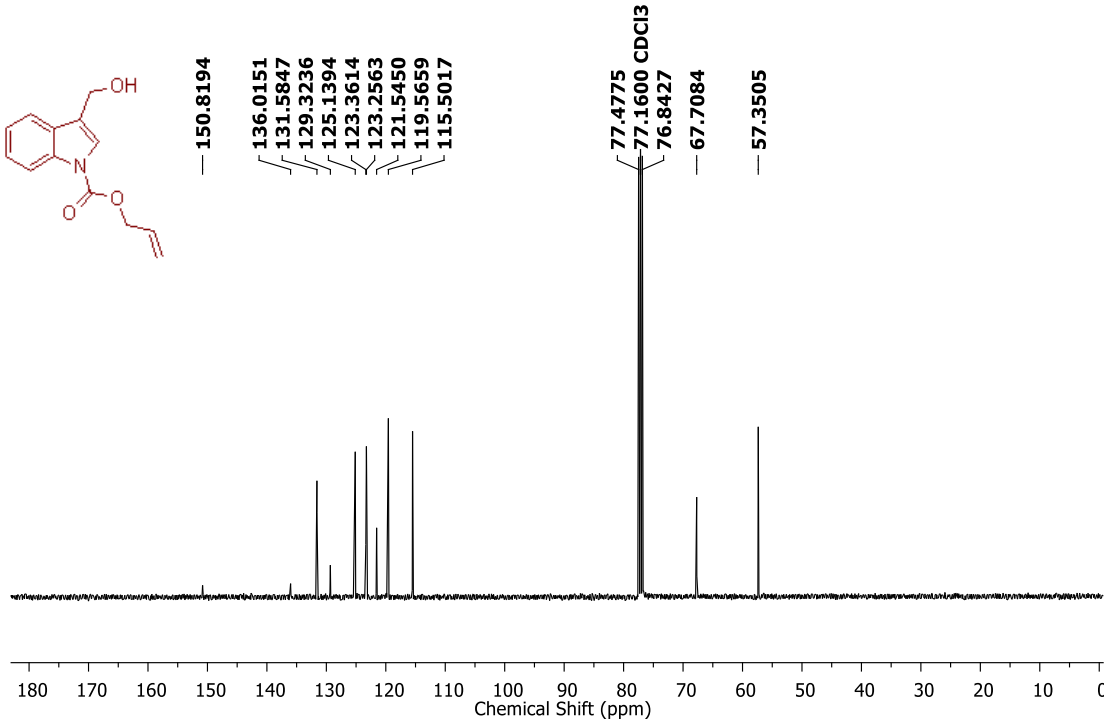

^{1}H NMR Spectrum (400 MHz, DMSO-d_6) of compound **50**

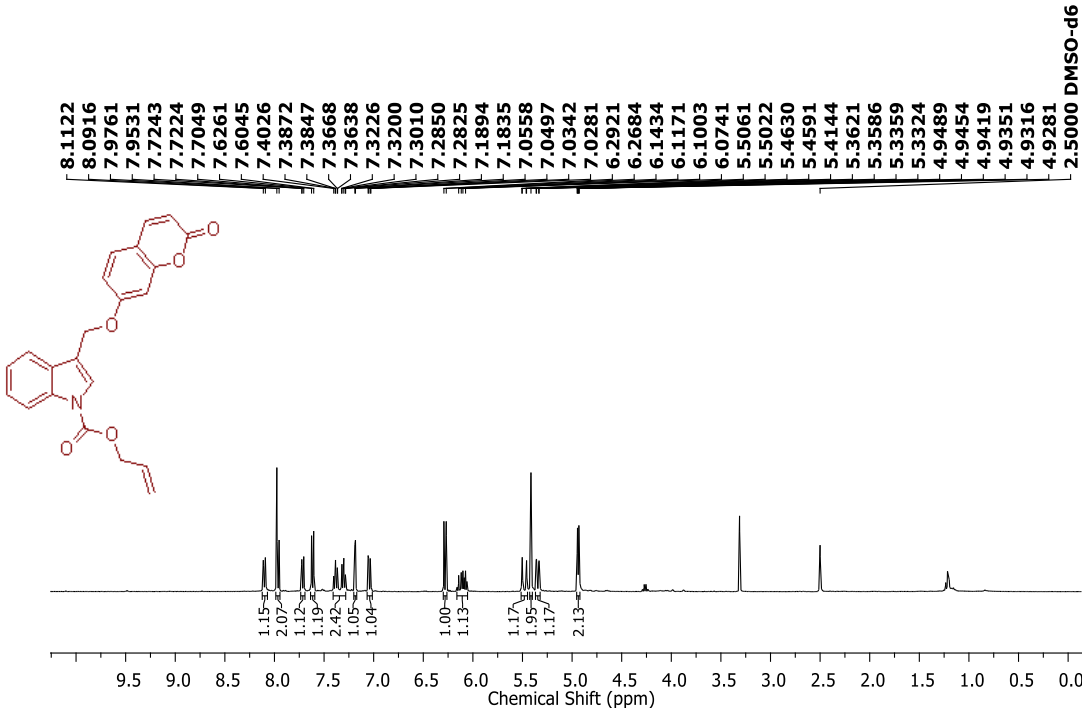

^{13}C NMR Spectrum (100 MHz, DMSO-d_6) of compound **50**

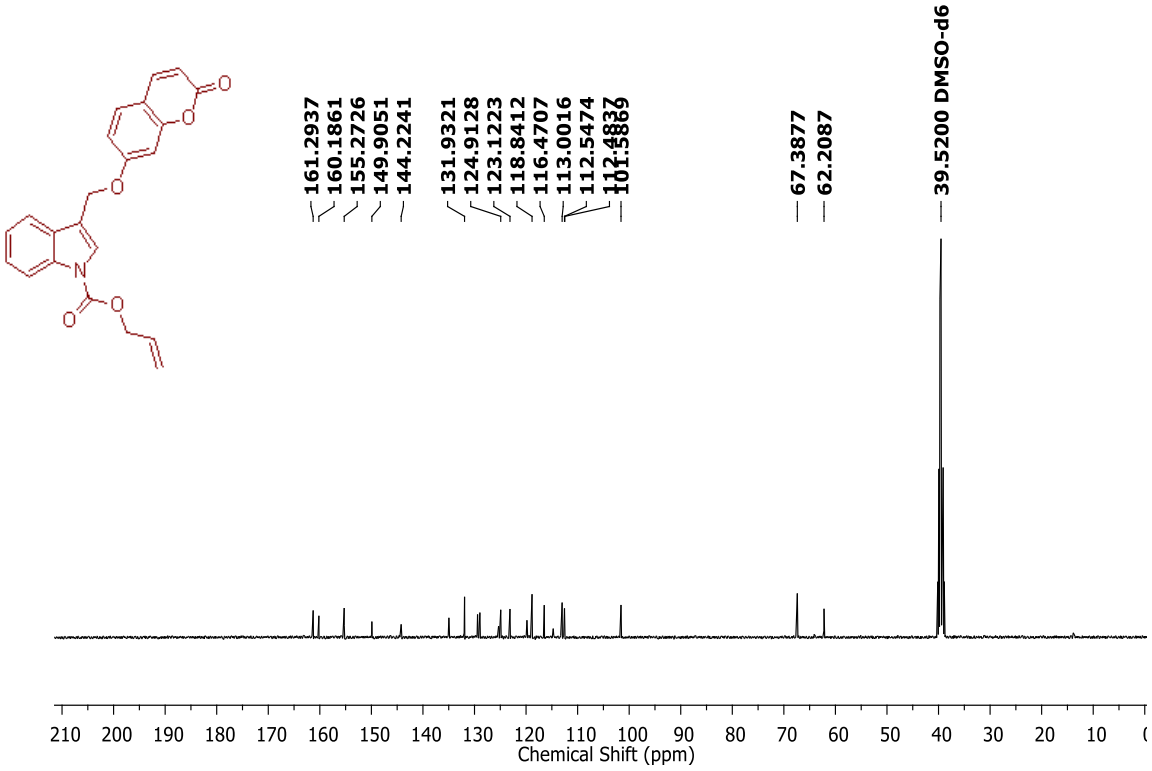

^{1}H NMR Spectrum (400 MHz, $CDCl_3$) of compound **52**

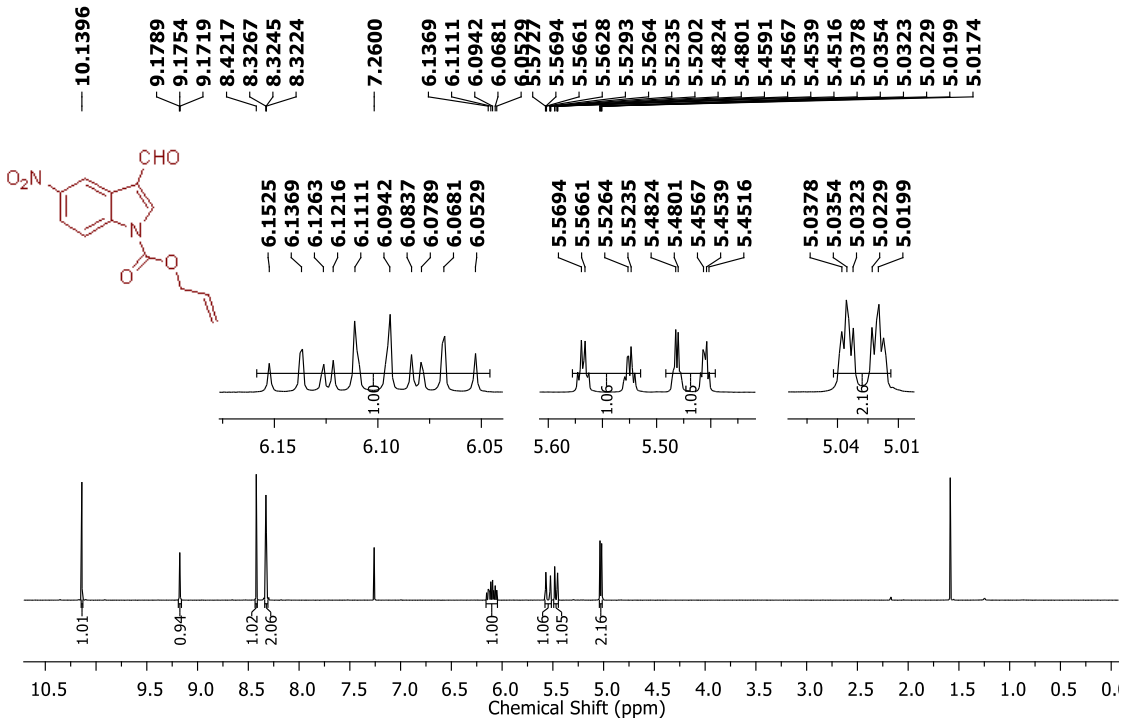

^{13}C NMR Spectrum (100 MHz, $CDCl_3$) of compound **52**

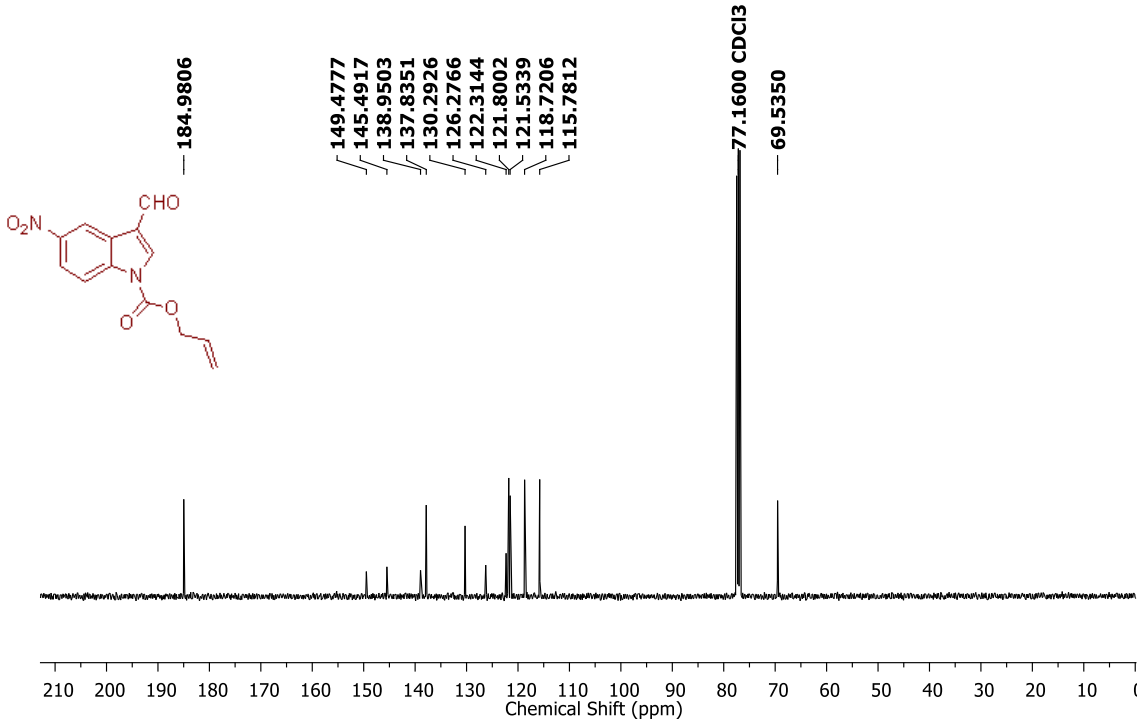

^{1}H NMR Spectrum (400 MHz, $CDCl_3$) of compound **53**

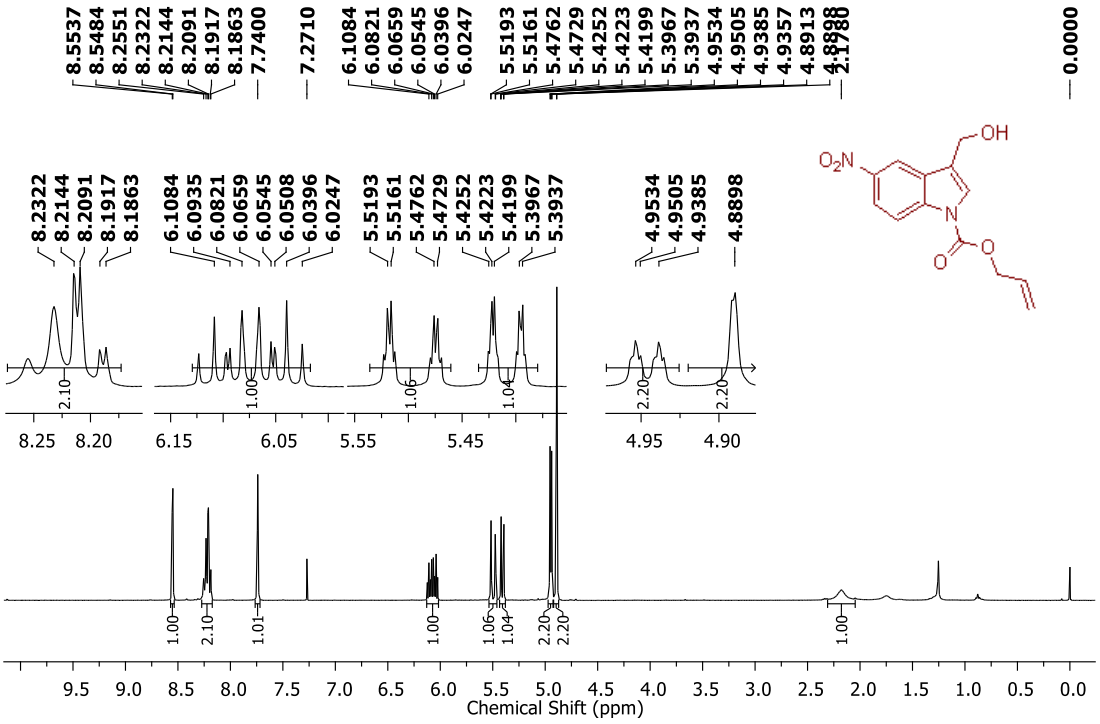

^{13}C NMR Spectrum (100 MHz, $CDCl_3$) of compound **53**

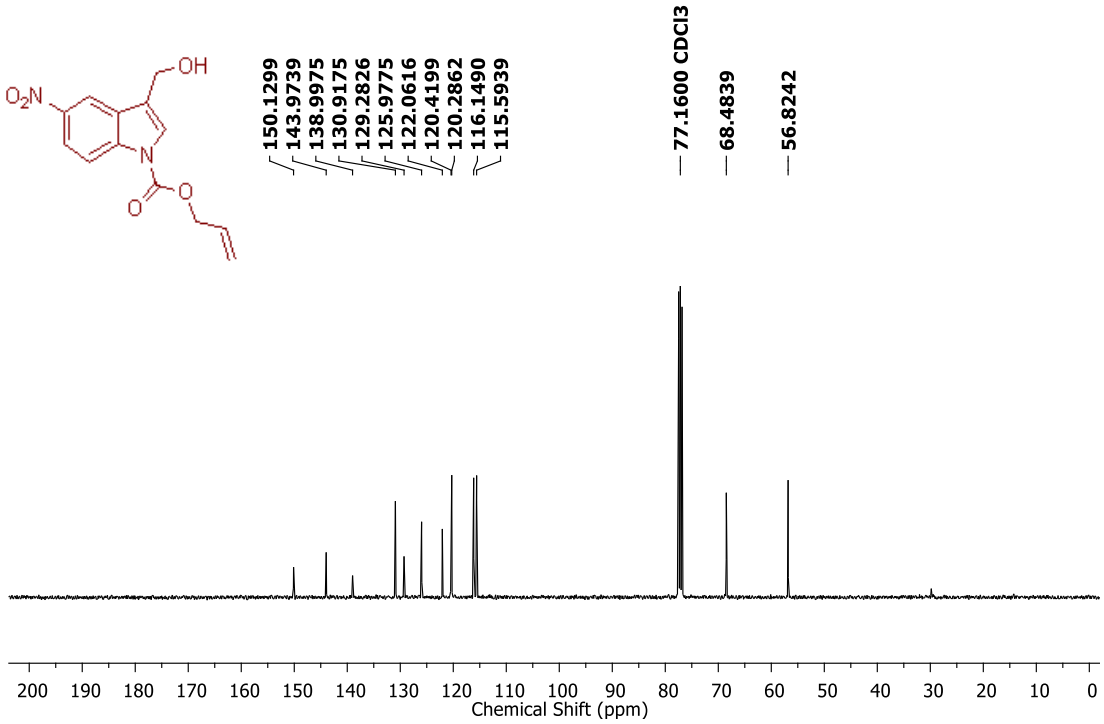

^{1}H NMR Spectrum (400 MHz, $CDCl_3$) of compound **56**

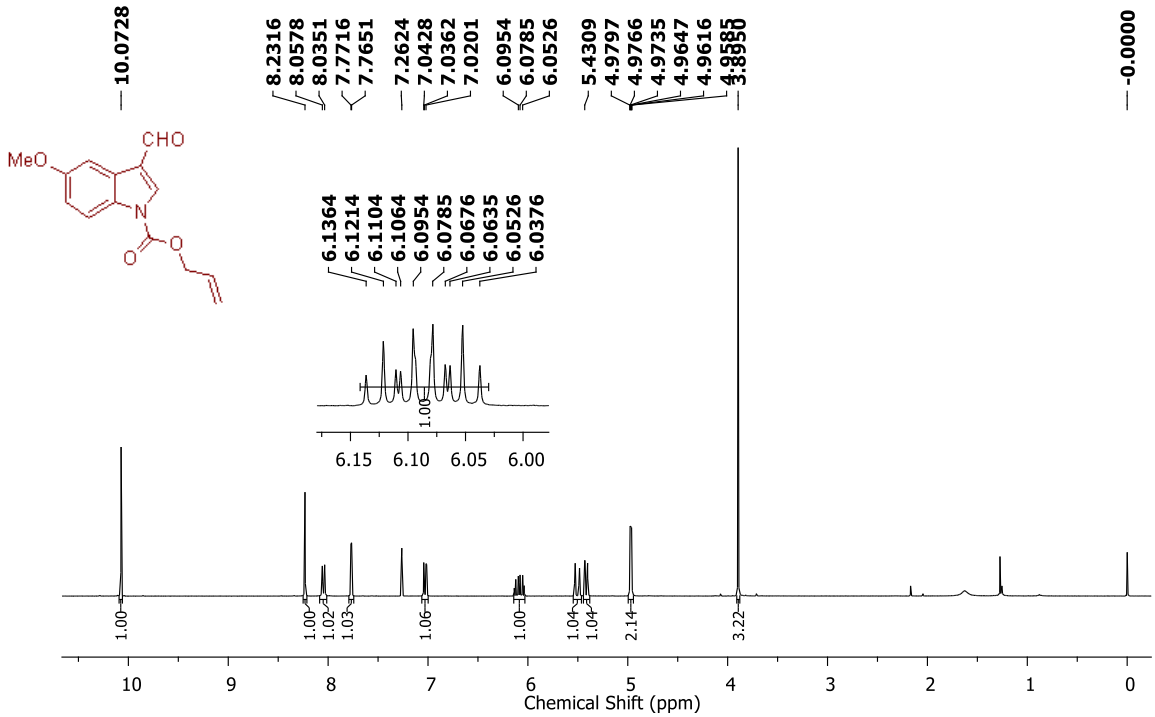

^{13}C NMR Spectrum (100 MHz, $CDCl_3$) of compound **56**

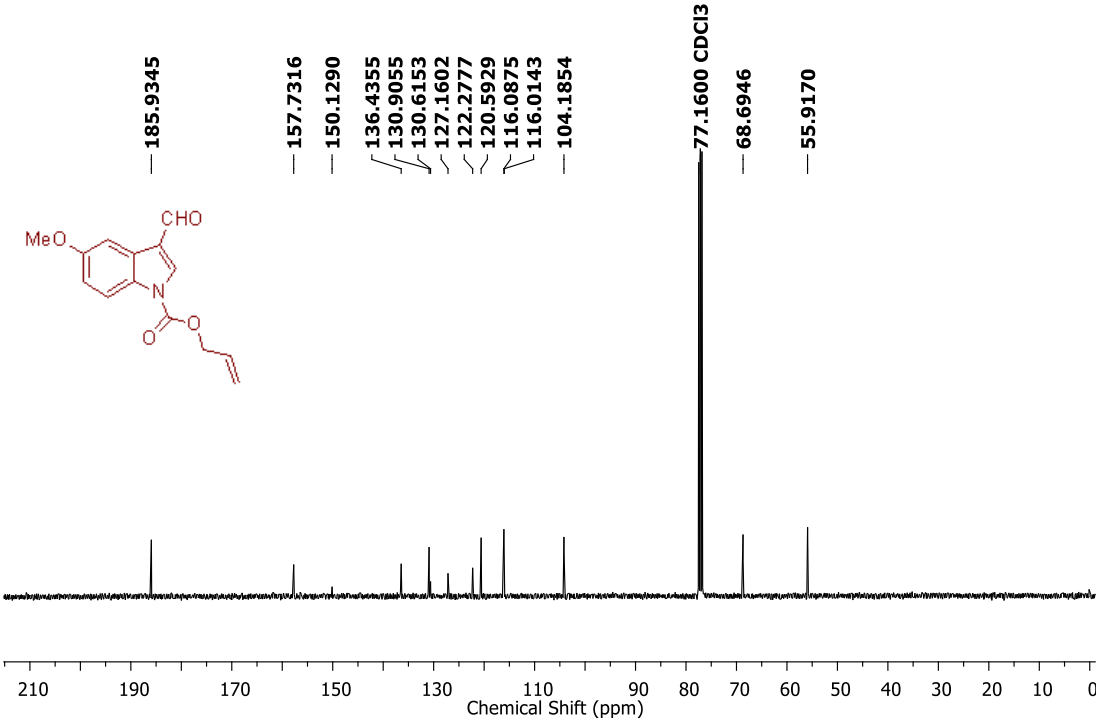

^{1}H NMR Spectrum (400 MHz, $CDCl_3$) of compound **57**

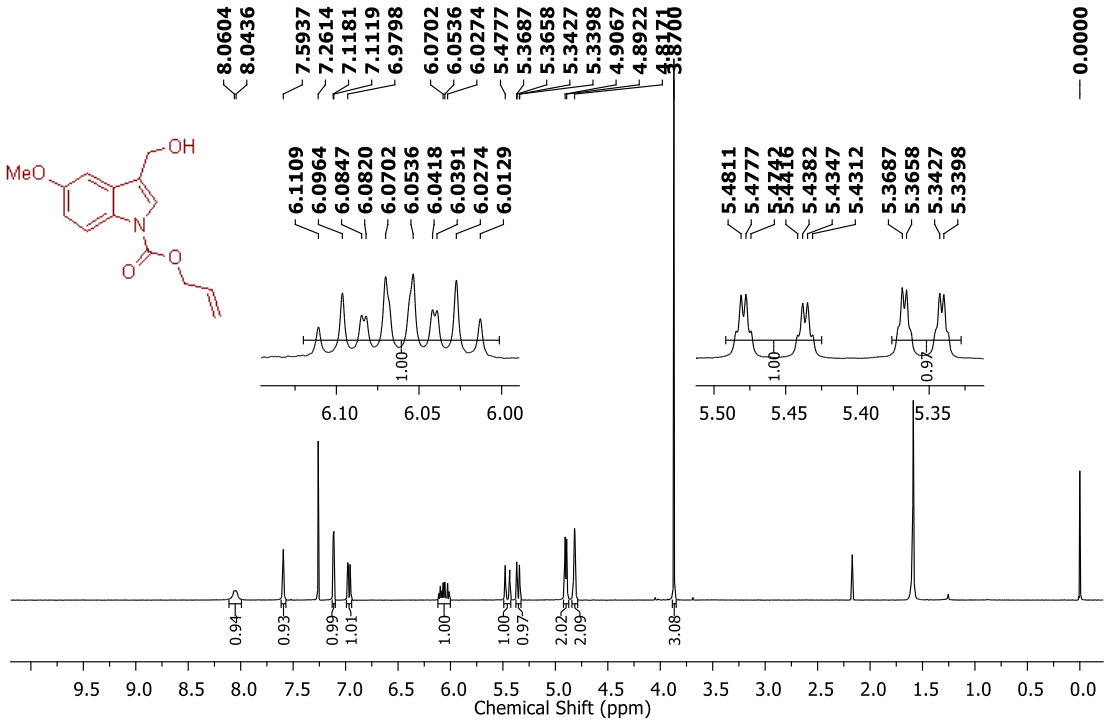

^{13}C NMR Spectrum (100 MHz, $CDCl_3$) of compound **57**

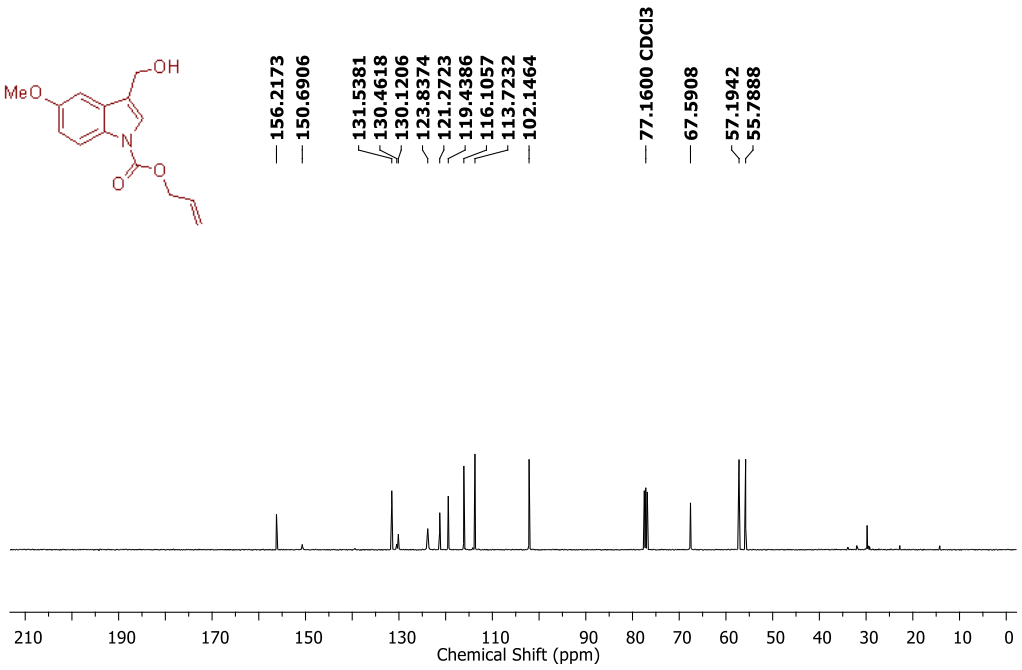

^{1}H NMR Spectrum (400 MHz, $CDCl_3$) of compound **58**

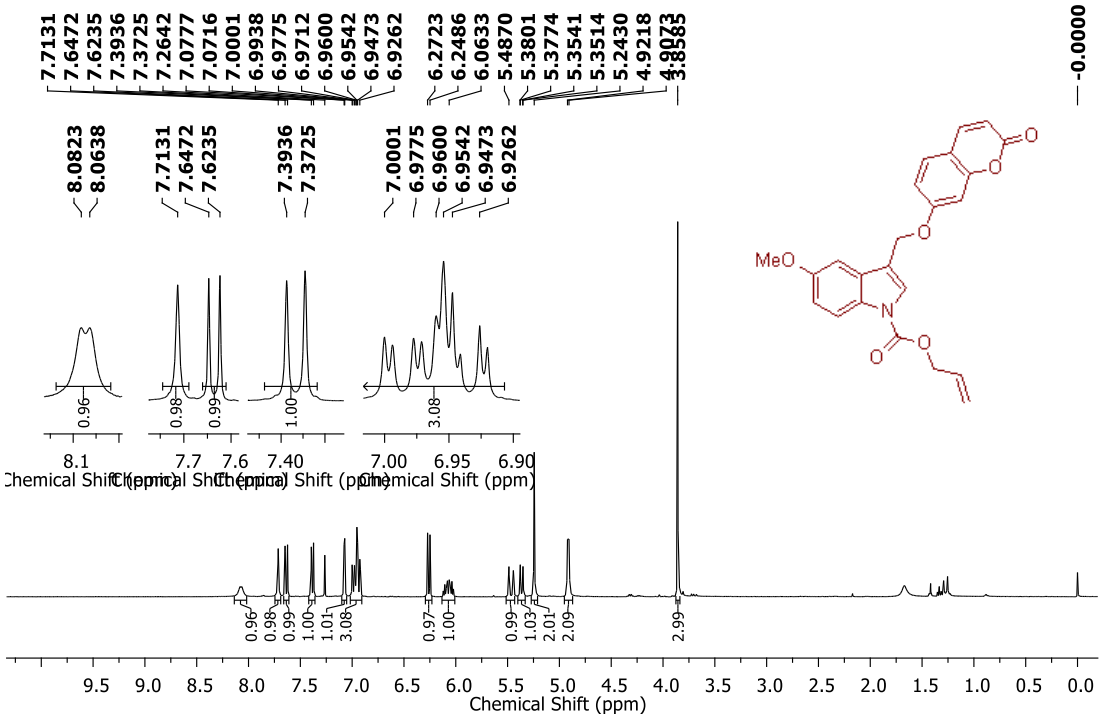

^{13}C NMR Spectrum (100 MHz, $CDCl_3$) of compound **58**

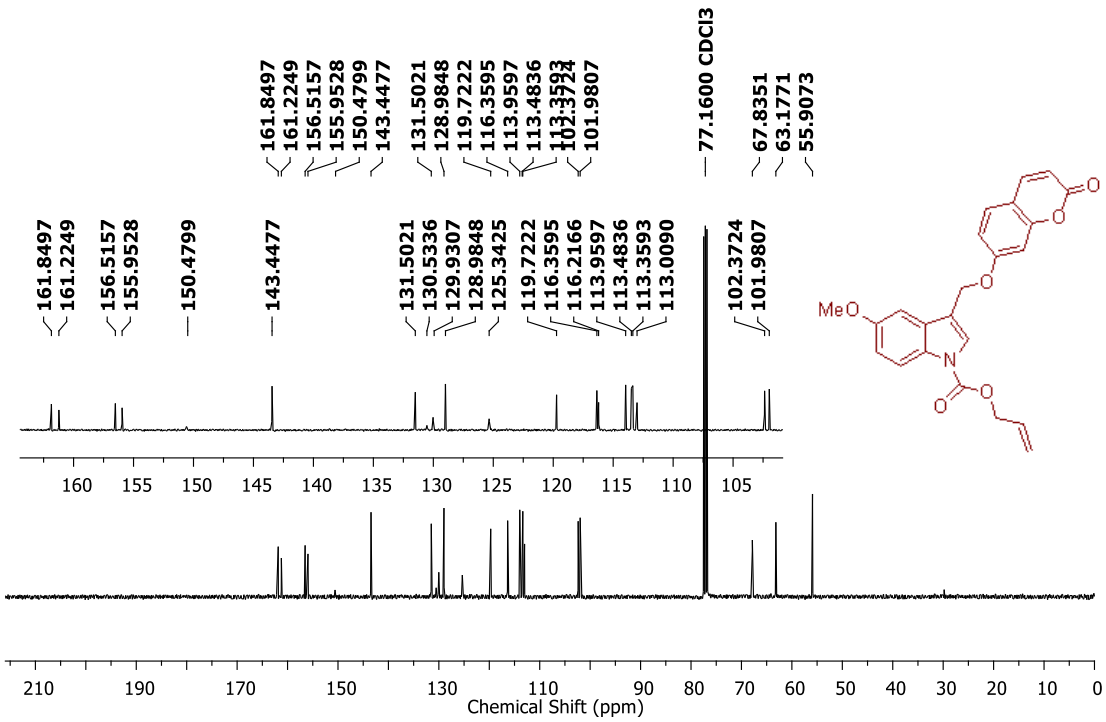

^{1}H NMR Spectrum (400 MHz, $CDCl_3$) of compound **61**

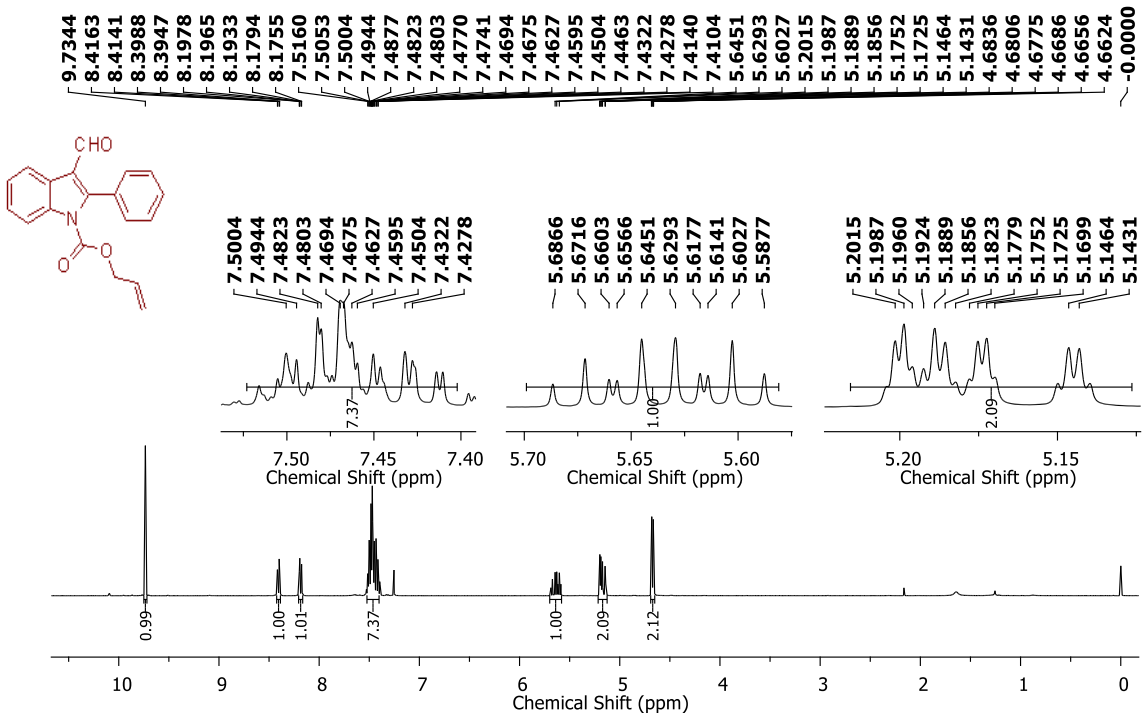

^{13}C NMR Spectrum (100 MHz, $CDCl_3$) of compound **61**

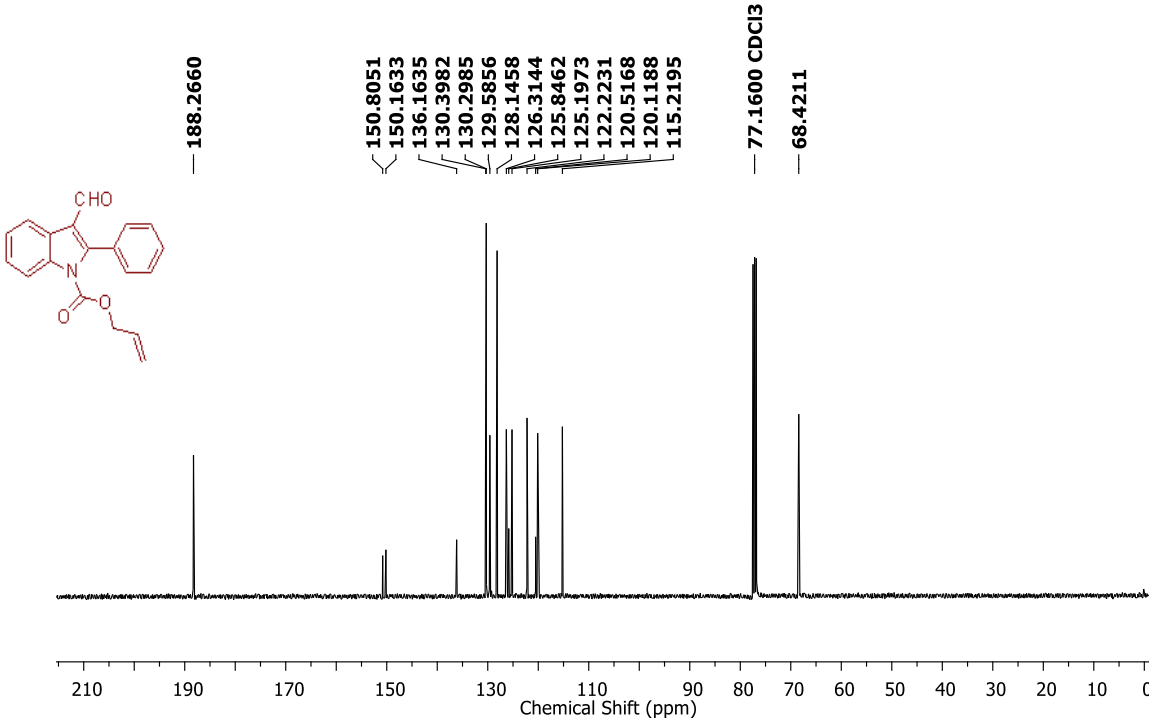

^{1}H NMR Spectrum (400 MHz, $CDCl_3$) of compound **62**

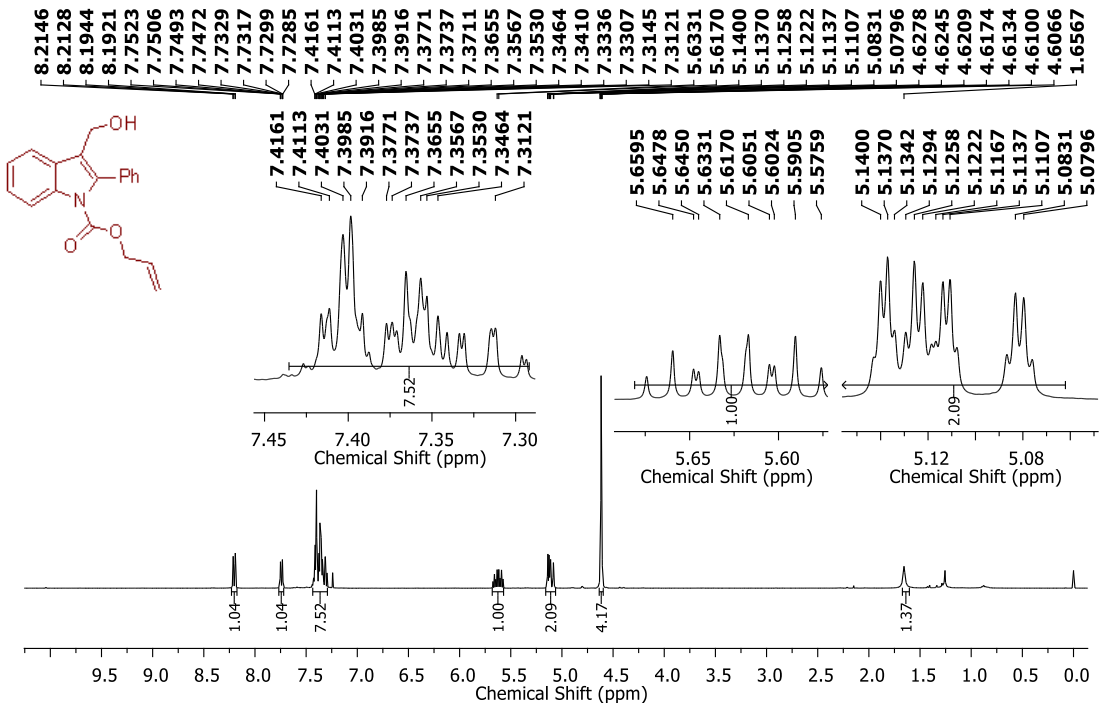

^{13}C NMR Spectrum (100 MHz, $CDCl_3$) of compound **62**

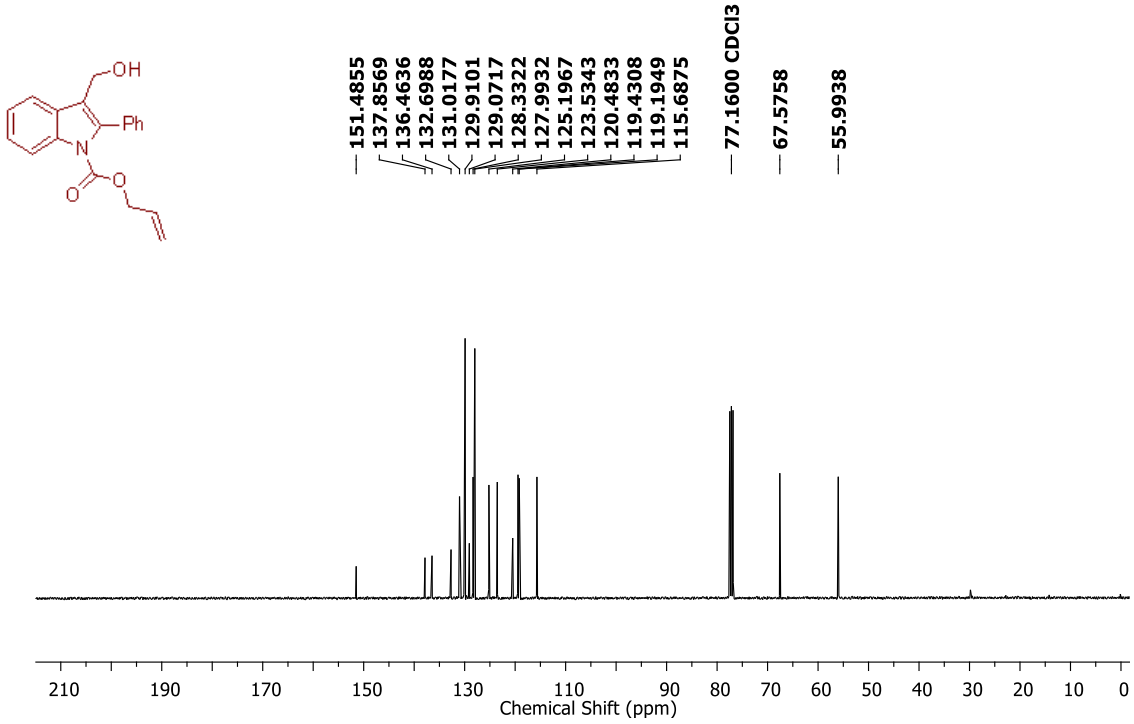

^{1}H NMR Spectrum (400 MHz, $CDCl_3$) of compound **63**

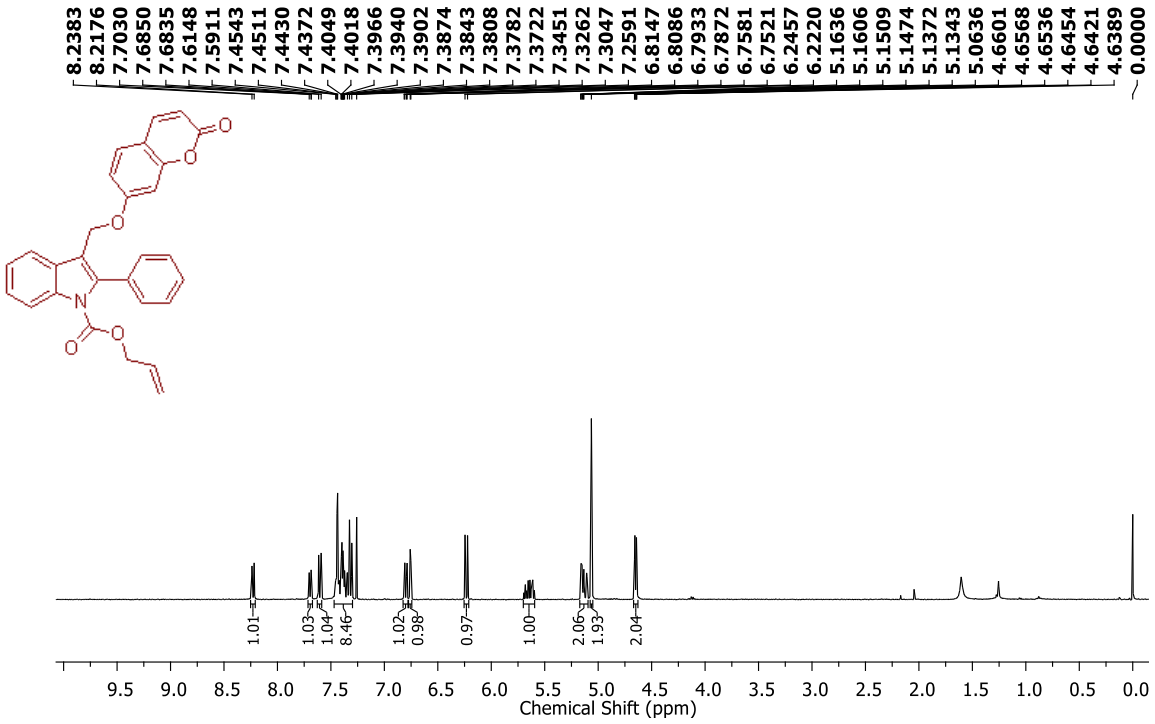

^{13}C NMR Spectrum (100 MHz, $CDCl_3$) of compound **63**

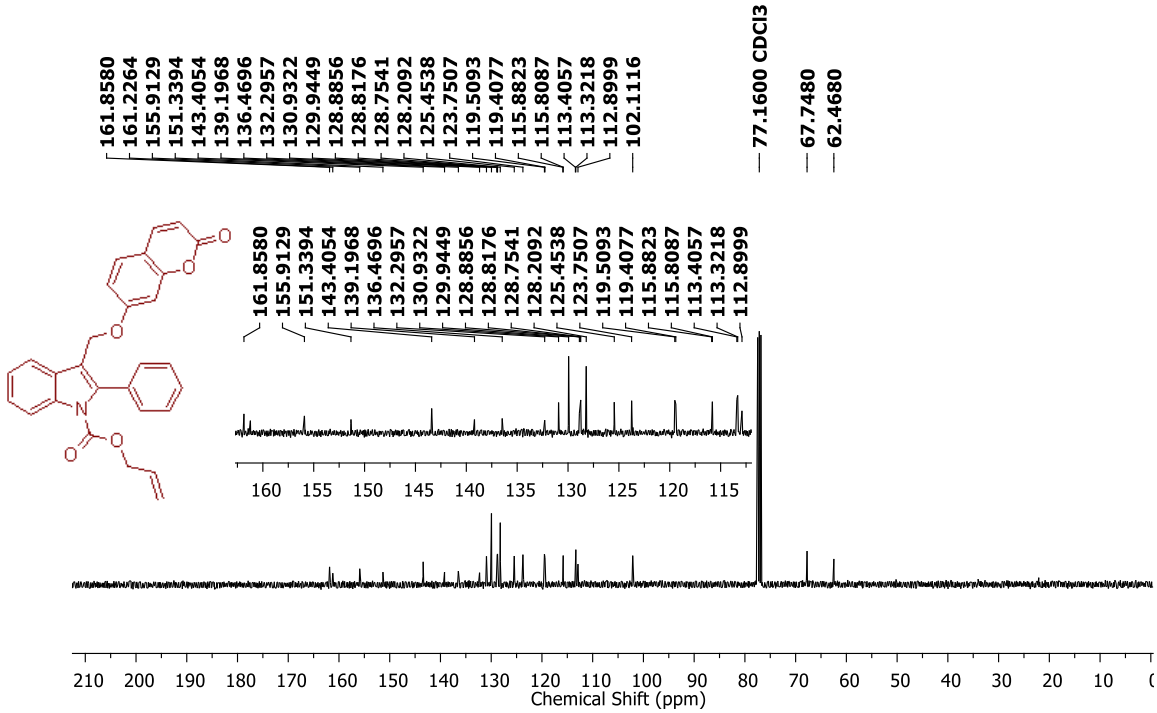

^{1}H NMR Spectrum (400 MHz, $CDCl_3$) of compound **65**

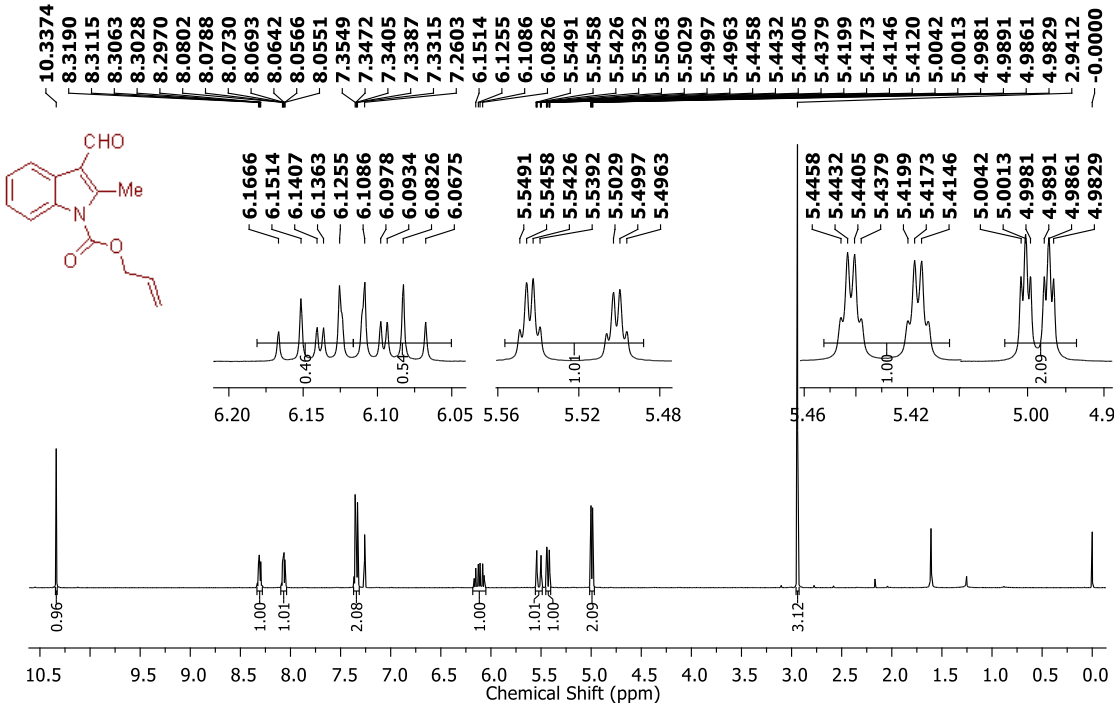

^{13}C NMR Spectrum (100 MHz, $CDCl_3$) of compound **65**

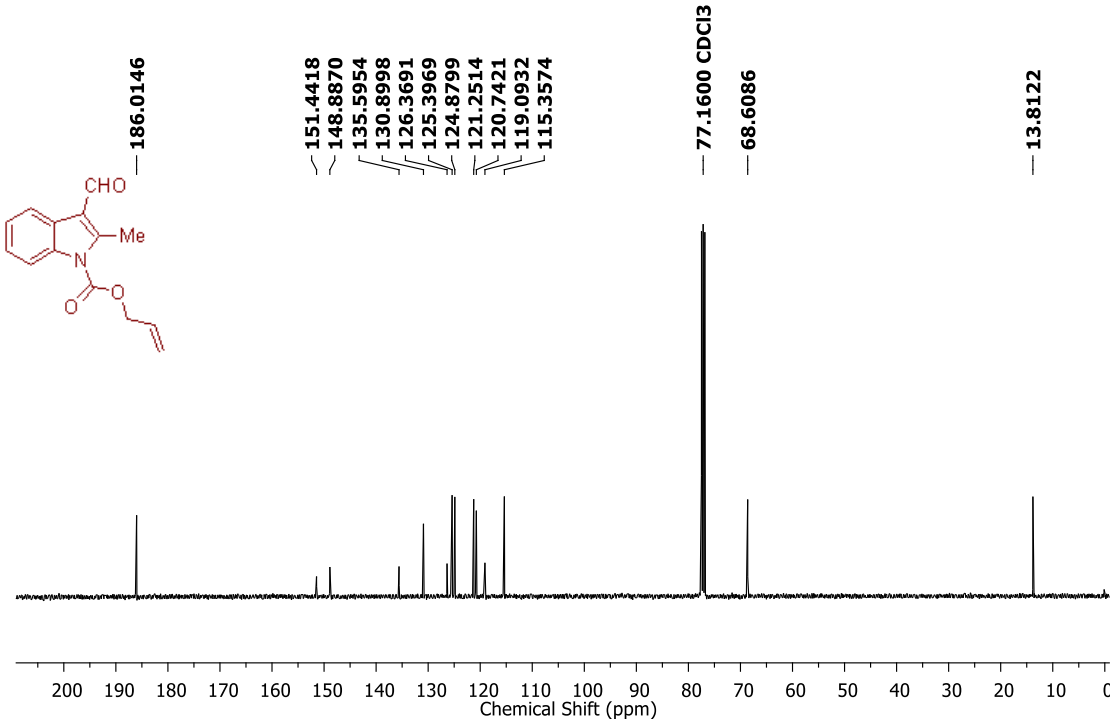

^{1}H NMR Spectrum (400 MHz, $CDCl_3$) of compound **66**

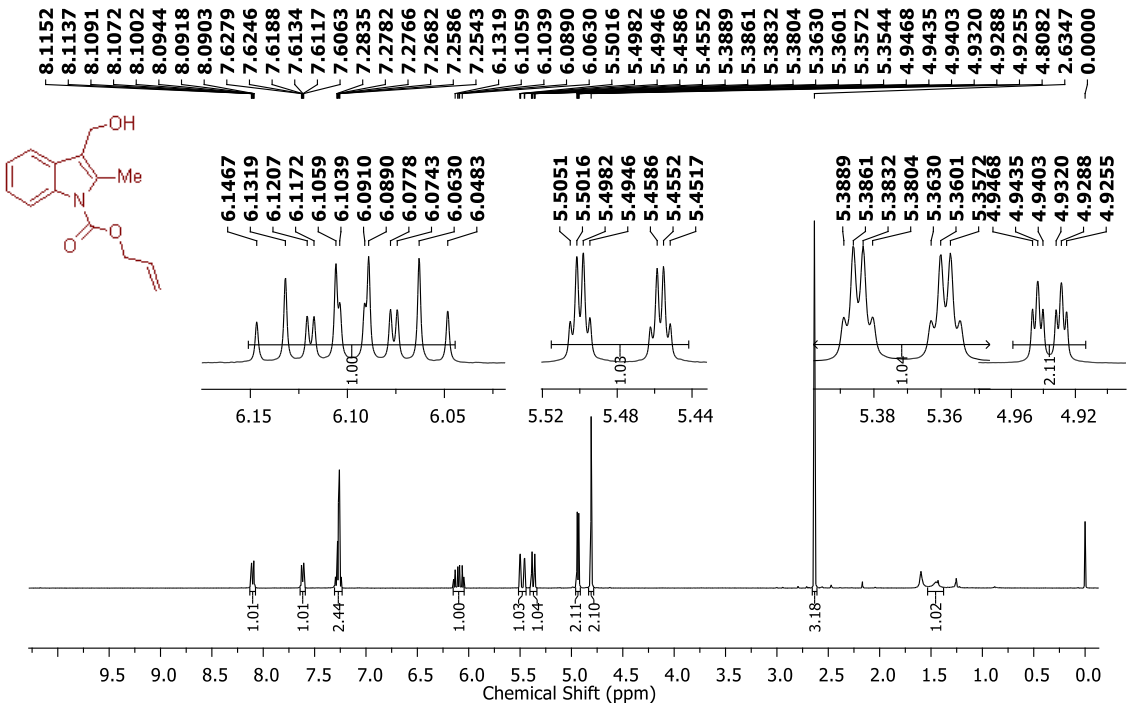

^{13}C NMR Spectrum (100 MHz, $CDCl_3$) of compound **66**

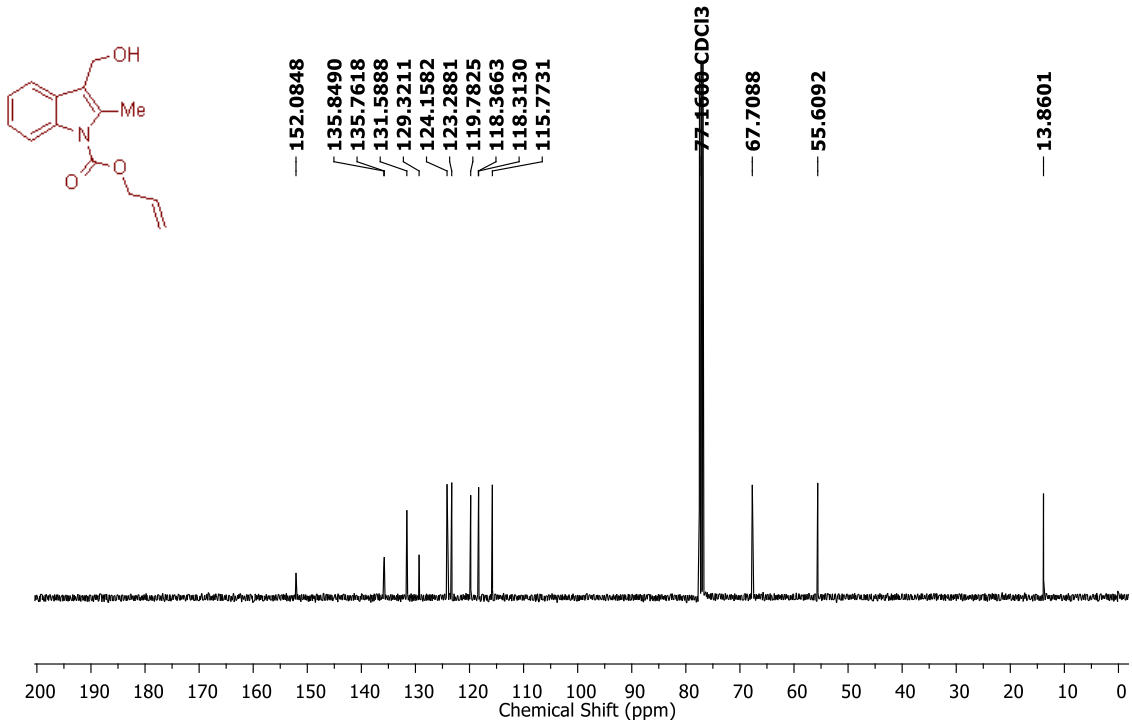

^{1}H NMR Spectrum (400 MHz, $CDCl_3$) of compound **67**

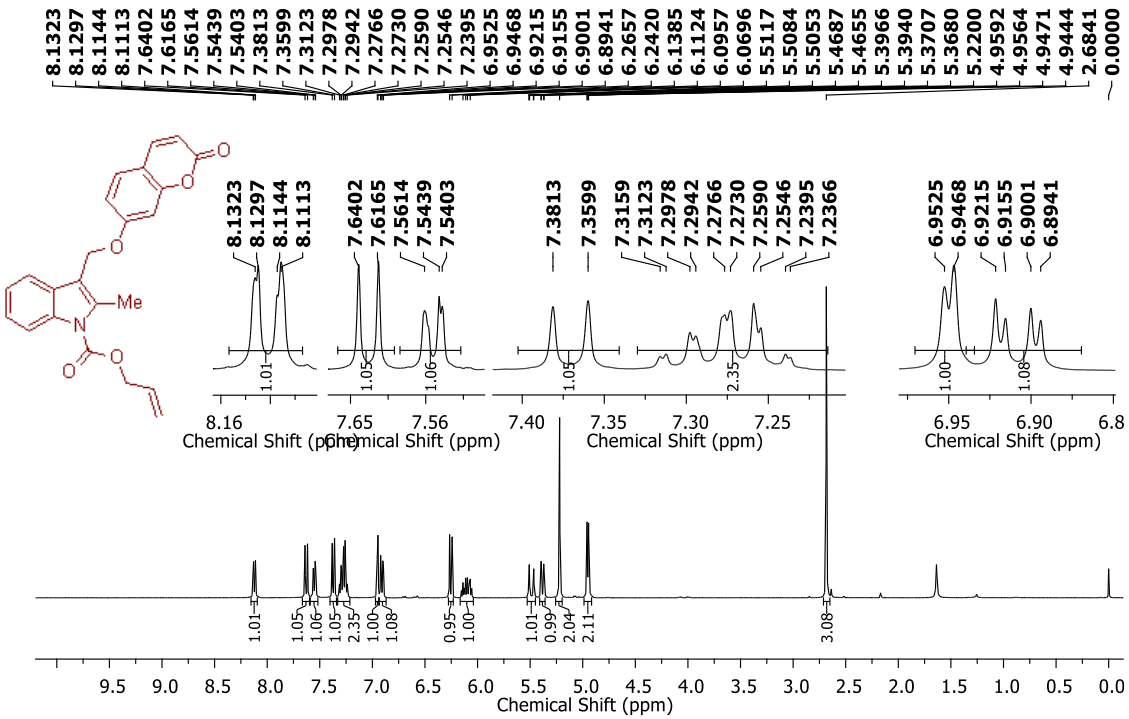

^{13}C NMR Spectrum (100 MHz, $CDCl_3$) of compound **67**

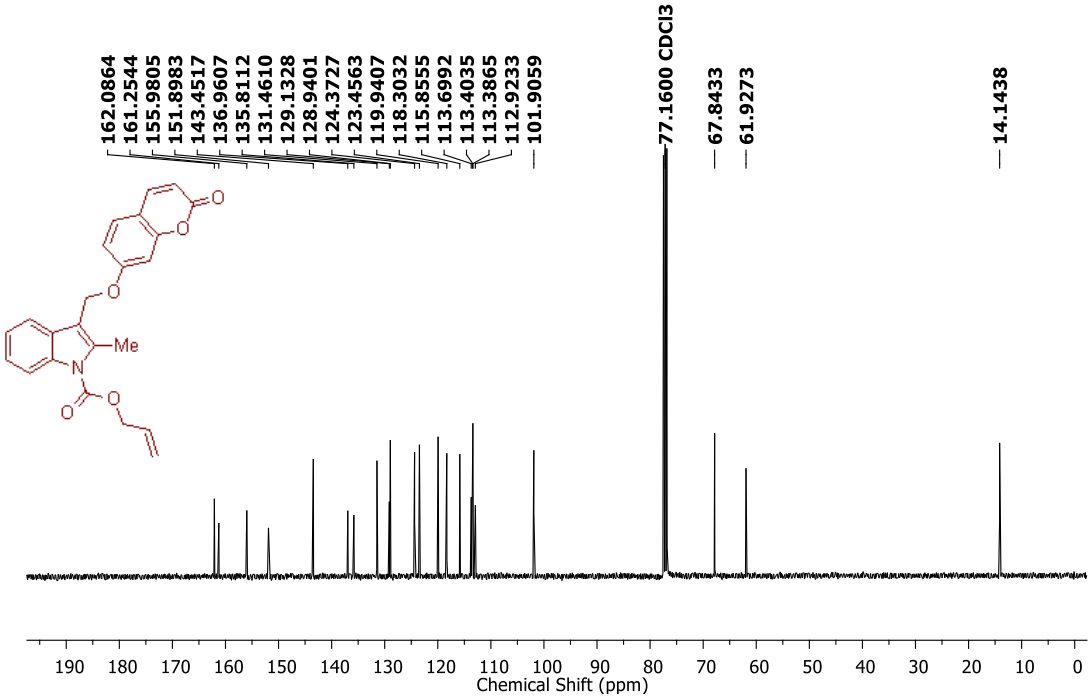

^{1}H NMR Spectrum (400 MHz, DMSO-d_6) of compound **54**

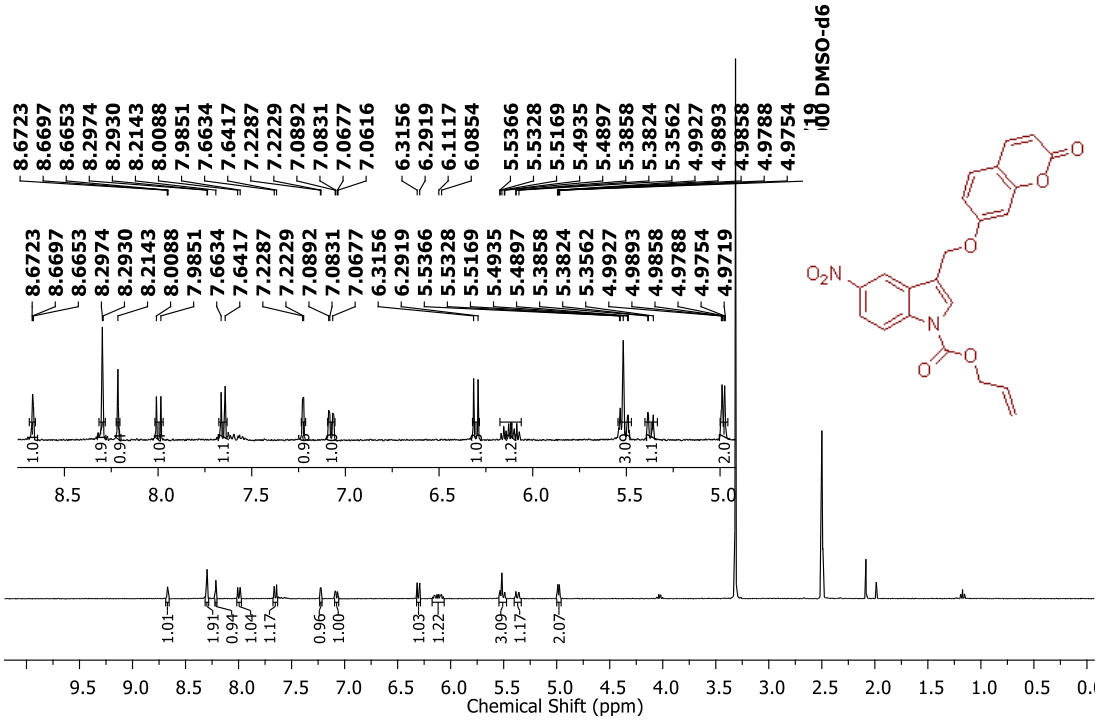

Crude ^{1}H NMR Spectrum (400 MHz, $CDCl_3$) of compound **68**

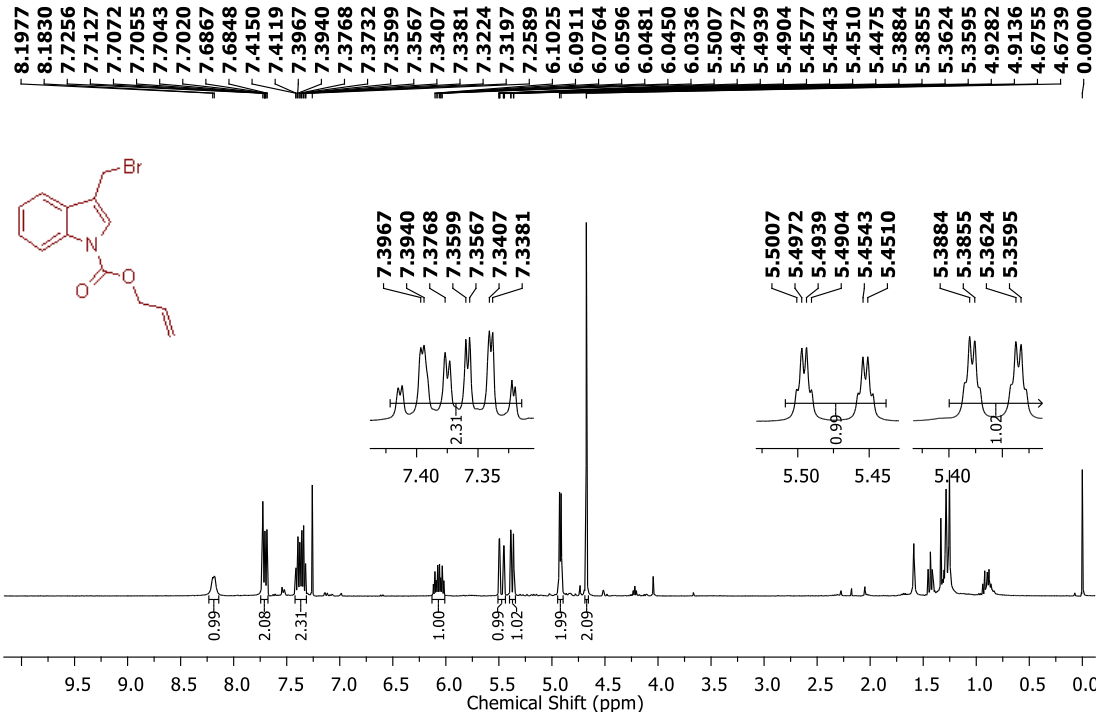

^{1}H NMR Spectrum (400 MHz, $CDCl_3$) of compound **69**

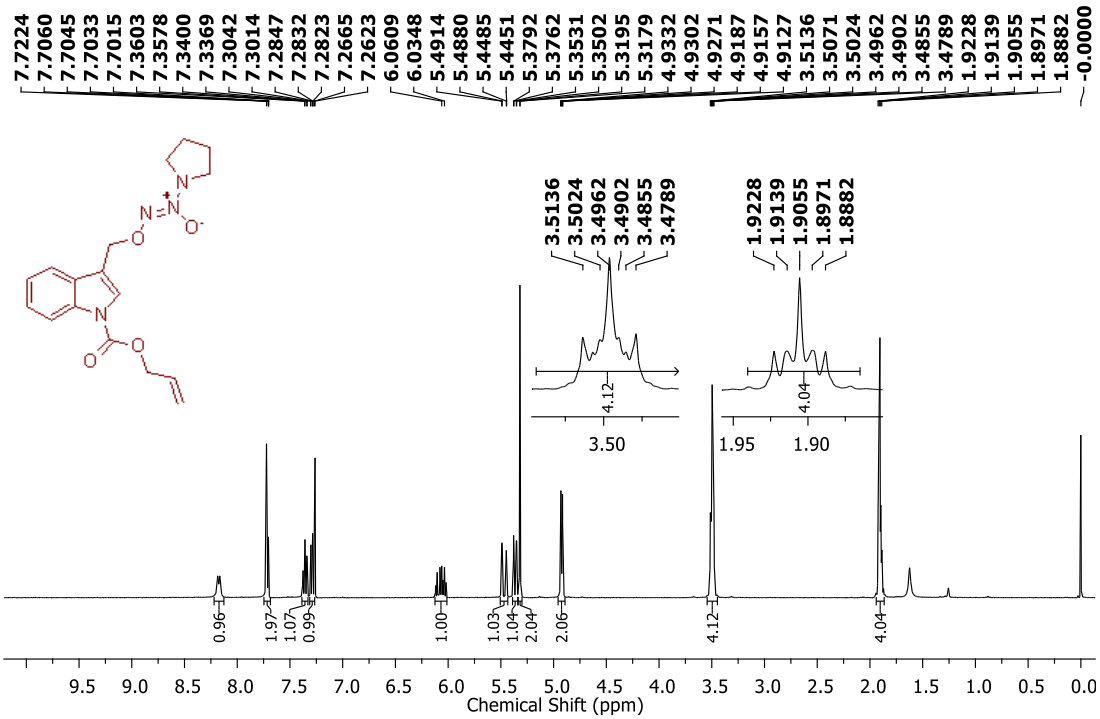

^{13}C NMR Spectrum (100 MHz, $CDCl_3$) of compound **69**

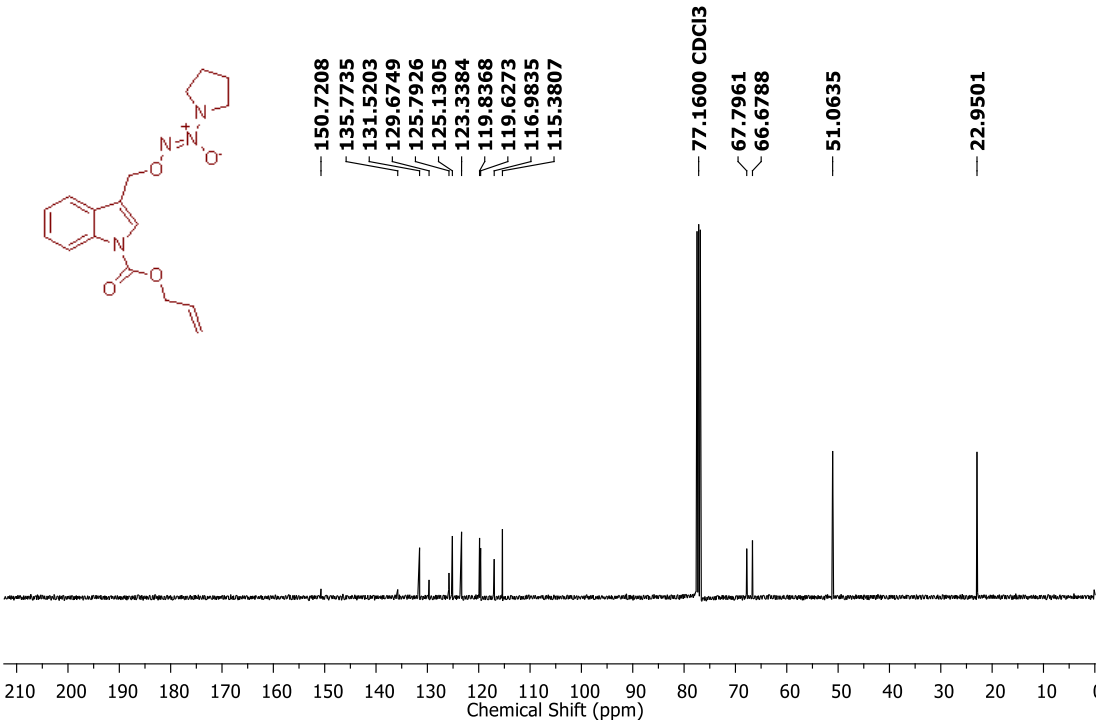

5.6. References

1. (a) Hernick, M.; Borch, R. F., Studies on the Mechanisms of Activation of Indolequinone Phosphoramidate Prodrugs. *J. Med. Chem.* **2003,** *46* (1), 148-154; (b) Huang, B.; Desai, A.; Tang, S.; Thomas, T. P.; Baker, J. R., The Synthesis of a c(RGDyK) Targeted SN38 Prodrug with an Indolequinone Structure for Bioreductive Drug Release. *Org. Lett.* **2010,** *12* (7), 1384-1387; (c) Phillips, R. M.; Naylor, M. A.; Jaffar, M.; Doughty, S. W.; Everett, S. A.; Breen, A. G.; Choudry, G. A.; Stratford, I. J., Bioreductive Activation of a Series of Indolequinones by Human DT-Diaphorase: Structure−Activity Relationships. *J. Med. Chem.* **1999,** *42* (20), 4071-4080; (d) Siegel, D.; Beall, H.; Senekowitsch, C.; Kasai, M.; Arai, H.; Gibson, N. W.; Ross, D., Bioreductive activation of mitomycin C by DT-diaphorase. *Biochemistry* **1992,** *31* (34), 7879-7885; (e) Zhang, Z.; Tanabe, K.; Hatta, H.; Nishimoto, S.-i., Bioreduction activated prodrugs of camptothecin: molecular design, synthesis, activation mechanism and hypoxia selective cytotoxicity. *Org. Biomol. Chem.* **2005,** *3* (10), 1905-1910; (f) Hernick, M.; Flader, C.; Borch, R. F., Design, Synthesis, and Biological Evaluation of Indolequinone Phosphoramidate Prodrugs Targeted to DT-diaphorase. *J. Med. Chem.* **2002,** *45* (16), 3540-3548.

2. (a) Friedlos, F.; Denny, W. A.; Palmer, B. D.; Springer, C. J., Mustard Prodrugs for Activation by Escherichia coli Nitroreductase in Gene-Directed Enzyme Prodrug Therapy. *J. Med. Chem.* **1997,** *40* (8), 1270-1275; (b) Hay, M. P.; Atwell, G. J.; Wilson, W. R.; Pullen, S. M.; Denny, W. A., Structure−Activity Relationships for 4-Nitrobenzyl Carbamates of 5-Aminobenz[e]indoline Minor Groove Alkylating Agents as Prodrugs for GDEPT in Conjunction with E. coli Nitroreductase. *J. Med. Chem.* **2003,** *46* (12), 2456-2466; (c) Hay, M. P.; Wilson, W. R.; Denny, W. A., Nitrobenzyl carbamate prodrugs of enediynes for nitroreductase gene-directed enzyme prodrug therapy (GDEPT). *Bioorg. Med. Chem. Lett.* **1999,** *9* (24), 3417-3422; (d) Hu, L.; Wu, X.; Han, J.; Chen, L.; Vass, S. O.; Browne, P.; Hall, B. S.; Bot, C.; Gobalakrishnapillai, V.; Searle, P. F.; Knox, R. J.; Wilkinson, S. R., Synthesis and structure–activity relationships of nitrobenzyl phosphoramide mustards as nitroreductase-activated prodrugs. *Bioorg. Med. Chem. Lett.* **2011,** *21* (13), 3986-3991; (e) Hu, L.; Yu, C.; Jiang, Y.; Han, J.; Li, Z.; Browne, P.; Race, P. R.; Knox, R. J.; Searle, P. F.; Hyde, E. I., Nitroaryl Phosphoramides as Novel Prodrugs for E. coli Nitroreductase Activation in Enzyme Prodrug Therapy. *J. Med. Chem.* **2003,** *46* (23), 4818-4821.

3. Schmid, K. M.; Jensen, L.; Phillips, S. T., A Self-Immolative Spacer That Enables Tunable Controlled Release of Phenols under Neutral Conditions. *J. Org. Chem.* **2012,** *77* (9), 4363-4374.

4. Yang, S.-D.; Sun, C.-L.; Fang, Z.; Li, B.-J.; Li, Y.-Z.; Shi, Z.-J., Palladium-Catalyzed Direct Arylation of (Hetero)Arenes with Aryl Boronic Acids. *Angew. Chem. Int. Ed.* **2008,** *47* (8), 1473-1476.

5. Nishimura, T.; Yamada, K.; Takebe, T.; Yokoshima, S.; Fukuyama, T., (1-Nosyl-5-nitroindol-3-yl)methyl Ester: A Novel Protective Group for Carboxylic Acids. *Org. Lett.* **2008,** *10* (12), 2601-2604.

6. Diana, P.; Carbone, A.; Barraja, P.; Montalbano, A.; Martorana, A.; Dattolo, G.; Gia, O.; Via, L. D.; Cirrincione, G., Synthesis and antitumor properties of 2,5-bis(3′-indolyl)thiophenes: Analogues of marine alkaloid nortopsentin. *Bioorg. Med. Chem. Lett.* **2007,** *17* (8), 2342-2346.

7. Moody, C. J.; Ward, J. G., [2,3] Fused indoles. Synthesis of [small beta]-carbolines and azepino[4,5-b]indoles from 3-(2-alkylindol-3-yl)-2-azidoacrylates1. *J. Chem. Soc., Perkin Trans. 1* **1984,** (0), 2895-2901.

Summary and future perspective

Nitric oxide (NO) has multifaceted roles in biological system including neurotransmission, respiration, regulation of blood pressure, platelet aggregation, cardiac functioning, signal transduction, regulating multiple functions in reproductive systems, antimicrobial defence, altering cellular redox status and anti-proliferative activity. The biological roles of NO depend on its concentration, dosage, duration and its location of release. NO is known to exhibit either pro- or anti-apoptotic effects in cells depending on concentration of NO and cell type. When NO is produced in low concentration, it rapidly diffuses and stimulates angiogenesis that leads to tumor progression. However, at elevated concentrations NO inhibits proliferation of cancer cells. Similarly, the role of NO as an antimicrobial agent is uncertain. NO and reactive oxygen species (ROS) generated by the immune cells induce oxidative and nitrosative stress and shows cytotoxicity to pathogens. On the other hand, there have been reports demonstrating NO protecting bacteria from oxidative and nitrosative stress induced by immune cells and antibiotics. NO being a key weapon of immune system against invading cells, it is thus important to precisely understand role of NO. Also, it is necessary to understand the complexity in the behaviour of NO, *i.e.*, why NO shows contradictory effects in condition of cancer and infection. Therefore, developing methodologies for delivery of NO in a controlled manner at the desired site is important.

Resistance to drugs is a major concern in the field of medicine which puts burden of inventing new drugs over period of time. It would be better to make resistant cells more vulnerable to existing drugs using adjuvant therapy rather than designing new drug molecules. The role of NO as an adjuvant in drug treatment can be studied. Solid tumors with improper vascularization have regions of low partial oxygen pressure. As a result of hypoxia, these cells are resistant to both chemotherapy and radiation therapy. Over expression of efflux pumps or multiple drug resistance-associated proteins (MRP) are observed in drug resistant tumors. It has been found that NO inhibited the MRP-3 efflux pump by nitrating the tyrosine and thereby led to reversal of drug resistance. Furthermore, NO also acts as a hypoxic radiosensitizer and can accentuate radiation-induced DNA damage thus causing increased cell death. We

have developed two methodologies for selectively delivering NO within cancer cells: a) DT-Diaphorase activated indolequinone based NO donor, INDQ/NO for delivering NO in cancer cells over-expressing the enzyme, in Chapter 2; and b) Nitroreductase activated NO donors for delivering NO in cancer cells which can be a candidate for directed enzyme prodrug therapy, in Chapter 3.1. Therefore, our NO donors can be used in conjunction with other clinical agents to overcome drug resistance and sensitize cancers to other cytotoxic agents. The adjuvant therapy of NO with clinical drugs might lower the effective dosage of the clinical drug as well.

In case of infection assault, NO is generated by the immune cells. In the presence of superoxide in the vicinity of NO, formation of reactive nitrogen species (RNS) potentiates the cytotoxic effects against pathogen. Nitrosative stress and oxidative stress are induced by RNS and ROS which leads to alteration in the redox potential of the bacterial cell, as a result of which bacteriostasis or bacterial killing is observed. However, NO from macrophage or produced within bacteria has been reported to mediate cytoprotective behaviour in bacteria against immunogenic response and antibiotics. Generally, pathways or genes that potentially deactivate the toxic effects of NO are activated in bacteria. However, the exact role of NO in cellular stress condition induced in bacteria upon antibiotic treatment or within macrophages is not fully understood. The NTR activated NO donors capable of delivering NO within bacteria can be used in future to study the effects of NO on the redox potential of bacteria in macrophages or treatment with antibiotics. Also, NTR activated NO donors can also be used as an adjuvant with known antibiotics and enhancement in toxicity profile can be examined.

Another area of interest is to develop methodologies that actively visualize NO released in cells and study responses in cells with increased NO. With the current methods for detecting NO in cells, simultaneous enhancement of NO and detection is cumbersome. So, in Chapter 4 we developed, a NTR activated reporter linked NO donor which released NO and reporter probe concomitantly. The molecule can be used in cells to monitor the permeability and localisation of the NO donor and its activation to release NO by visualizing the reporter. Also, the mechanism of NO donor activation can be studied *in vivo*. The bacterial studies to understand the role of NO on the redox potential in mycobacteria are presently underway.

Another important aspect in development of NO based donors is use of delivery vehicle capable of tuning NO release. The indole scaffold-based model compounds, synthesized in Chapter 5, need to be further studied for substituents effect. Based on the results obtained, next we would like to study the scaffold with incorporation of bioactivable trigger in place of chemically activated trigger. A bioactivable indole based prodrug design would suitable for studying the release profiles and cytotoxicity of drugs/cytotoxic species in cell based systems.

Therefore, the present strategies for delivering NO focus only on designing and optimizing NO delivery systems in *in vitro* and in animal models. However, further investigations are required on safety, site-specificity and suitability to use in animal models.

Synopsis

Synthesis and Evaluation of Bioactivable Nitric Oxide (NO) Donors

Chapter 1: Introduction

Nitric oxide (NO), a highly reactive gaseous molecule, is produced in nearly all living cells. The major enzymatic pathway for NO production is during turnover of L-arginine to L-citrulline by nitric oxide synthases, NOS (Scheme 1).[1] NO mediates various physiological processes that include vasodilation, immune regulation, neurotransmission and respiration. Depending on the location, concentration and duration of NO production, the effects of NO can vary from cytoprotective to cytotoxic.[2] NO, when produced in submicromolar concentration, mediates cell protective and regulatory processes. These cytoprotective effects are mainly due to improved blood flow to local areas and inhibition of platelet aggregation or cell adhesion, inhibition of key enzymes involved in cell destruction.[3] However, elevated levels of NO are often associated with cytotoxicity and form a vital part of immunogenic response.[3a] NO reacts with oxygen or reactive oxygen species (ROS) such as the superoxide radical ($O_2^{\bullet -}$) to form reactive nitrogen species (RNS). ROS and RNS are often deployed during infection or cancer and the synergy between the two leads to enhanced cytotoxicity.[4] RNS can directly react with a spectrum of molecules in cells such as transition metals, thiols and aromatic groups present in proteins and nucleobases in DNA/RNA leading to impaired functioning (Figure 1).

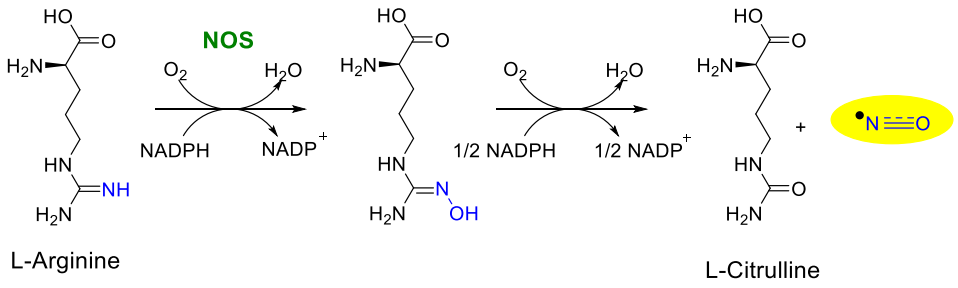

Scheme1. Biosynthesis of NO catalysed by NOS.

NO has been reported to play dichotomous role in the pathophysiological conditions of cancer and pathogen attack.[3a, 4-5] On the one hand, NO shows cytotoxicity towards cancer cells[2, 6] and pathogens,[4-5, 7] whereas on the other hand, NO is also known to stimulate cancer growth[3a, 6b] and protect bacteria[8] from phagocytes. In order to

understand the precise roles of NO in a cellular environment, it is necessary that an appropriate amount of NO is released at the desired site in a controlled manner.

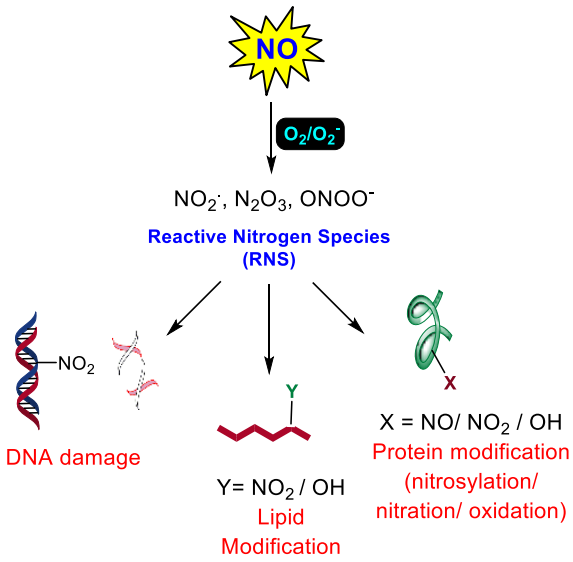

Figure 1. Damage caused to cellular components by RNS derived from NO.

The effects of NO have been studied using different classes of NO donors, which are organic or inorganic compounds capable of releasing NO upon activation.[3b] These include organic nitrates and nitrites, metal-NO complexes, nitrosothiols and diazeniumdiolates. Diazeniumdiolates are a highly efficient, reliable and versatile class of NO donors. These organic salts undergo hydrolysis in aqueous solution to release upto two moles of NO (Scheme 2). The half-lives of diazeniumdiolates range from 2 s to 20 h depending on the groups present on the amine nitrogen.[3b, 9]

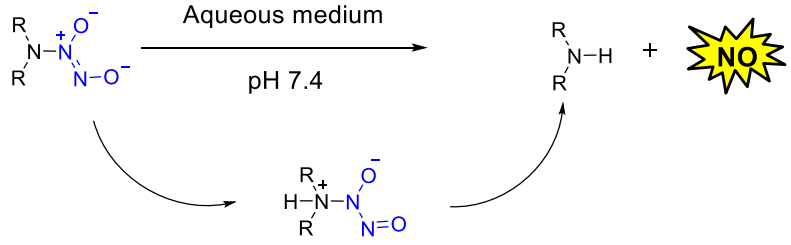

Scheme 2. Hydrolysis of a diazeniumdiolate anion in the aqueous solution to release an amine and two molecules of NO.

Another major advantage of using diazeniumdiolates as a surrogate for NO is that they can be synthetically modified to afford protected diazeniumdiolates. The protecting groups generally incorporated for derivatizing diazeniumdiolates are substrates for cellular enzymes. The protected diazeniumdiolates are then metabolized

into an active NO-donor by specific enzymes/biological triggers and thus ensure release of NO inside the cell (Scheme 3).

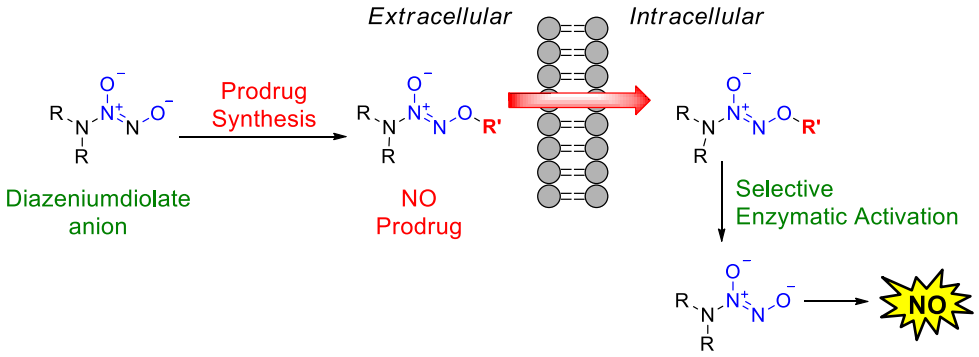

Scheme 3. Protected diazeniumdiolates as stable donors of NO.

So far, the reported bioactivated diazeniumdiolates are designed as substrates for esterases, glycosidases and cellular thiols.[10] However, aforementioned methodologies have the following limitations: a) the triggers that have been used for activation are present in normal cells as well thus possibly compromising directed delivery; b) enzymes such as glycosidase do not efficiently catalyse activation to release NO; c) no scope for tunability of NO release; and d) no reporter for monitoring intracellular NO release. Therefore, an ideal NO-delivery vehicle should: a) be easily localized inside the desired target cell; b) be selectively activated by a specific trigger; c) have a provision for tuning NO release rates; and d) have a mechanism to report NO release within cells.

Delivery of NO inside the cell requires a three-pronged strategy for effectively studying its role intracellularly (Figure 2). First, the specificity for NO delivery to target cells can be achieved by selecting trigger that have high expression levels in the target cells and/or is not present in normal cells. Next, as the biological effects of NO mainly depend on its concentration, it would be beneficial to have a scaffold where the release of NO can be tuned. Lastly, there should be easy ways of monitoring released NO inside the cells. The existing methods for detecting NO lack specificity and are dependent on secondary assays. These assays are typically destructive in nature and further cellular experiments are typically not possible. In other words, enhancement of NO within cells as well as simultaneous detection is cumbersome. A reporter linked NO donor would report NO release immediately without the need for secondary assays for detection.

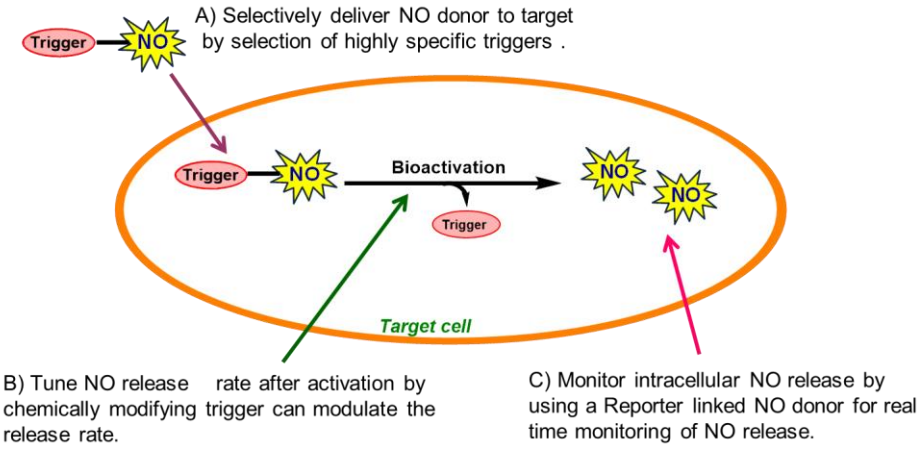

Figure 2. Strategies to study the effects of NO intracellularly. **A)** Selectively delivering NO in the desired cell or tissue. **B)** Modulation of NO release from the scaffold. **C)** Monitoring NO inside cell, once released from the NO donor.

This thesis contains five chapters. An overview of NO and NO delivery methods is presented in Chapter 1. In Chapter 2, a new indolequinone based NO donor, **INDQ/NO** which is a substrate for bioreductive enzyme DT-Diaphorase (DT-D) is presented. In Chapter 3.1, nitroreductase (NTR), a bacterial enzyme is considered for selective activation and the utility of O^2-(4-nitrobenzyl) diazeniumdiolates as substrates for NTR is demonstrated. In Chapter 3.2, a model for understanding release rates was constructed and the effects of substitution at the benzylic position of 4-nitrobenzyl on release profile was studied. In Chapter 4, in order to eliminate the need of secondary assays for detecting NO, a NTR-activated NO donor with a fluorescence reporter was developed. Lastly, in Chapter 5, a new indole-based scaffold where the release of leaving group is modulated by varying the substituent on the indole scaffold was developed. Altogether, the results presented in this thesis address important problems associated with site-specific delivery of NO and may find use for directed and tuneable drug delivery as well. Also, these approaches may be used as tools to study mechanisms of NO in cellular stress responses.

Chapter 2: INDQ/NO, a DT-Diaphorase Activated NO Donor

DT-Diaphorase (DT-D) is a two electron reductase enzyme involved in detoxification of quinone containing compounds.[11] The enzyme uses the cofactors NADPH and FAD for bioreduction of quinones. DT-D is over-expressed in certain types of cancers and has been exploited for activation of many quinone containing prodrugs in chemotherapy.[12] Due to diminished expression of DT-D expression in normal cells,

considerably reduced activation to release cytotoxic species is expected. Indolequinone is a suitable substrate for DT-D and several prodrugs have been reported with indolequinone as the enzyme trigger.[13]

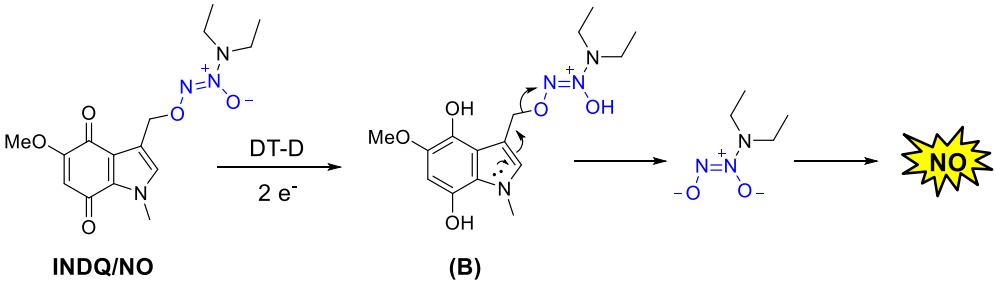

Scheme 4. Proposed mechanism of activation of **INDQ/NO** by two electron reduction by DT-Diaphorase.

Using indolequinone as a DT-D substrate and diazeniumdiolates as the NO donor, compound **INDQ/NO** was synthesized (Scheme 4). In the presence of DT-D, **INDQ/NO** is expected to undergo two electron reduction in the presence of cofactors NADPH and FAD to form the dihydroxyindole intermediate **B**. The electronic rearrangement releases the diazeniumdiolate, which is hydrolysed to release NO.

In order to study enzymatic activation, **INDQ/NO** was incubated with DT-D in presence of NADPH and FAD in pH 7.4 buffer at 37 ^{o}C. The decomposition of **INDQ/NO** and release of NO were independently monitored. It was found that **INDQ/NO** was reduced by DT-D to release NO in physiological solution (Figure 3.A and 3.B).

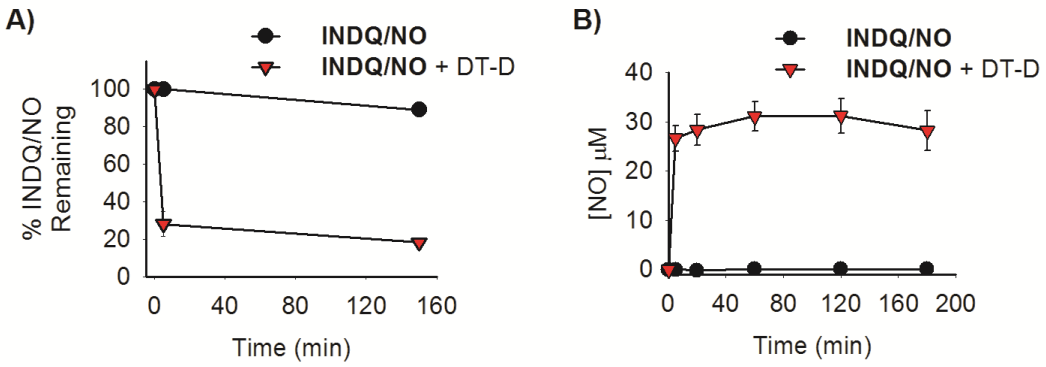

Figure 3. A) HPLC decompostion profiles of **INDQ/NO** in pH 7.4 buffer in the presence and absence of DT-D. **B)** NO release from **INDQ/NO** in the presence and absence of DT-D in pH 7.4 buffer detected using a chemiluminesence-based assay.

Next, to study metabolism of this NO donor in cells, DLD-1 human colorectal adenocarcinoma cells were incubated with **INDQ/NO**. Increased nitrite release in extracellular media for cells treated with **INDQ/NO** in comparison with untreated cells supported the ability of this compound to enhance NO in cells (Figure 4).

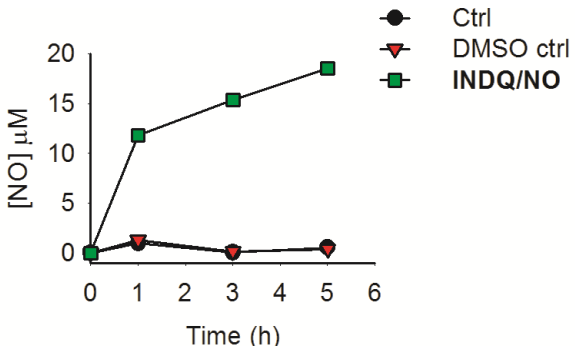

Figure 4. NO released during incubation of **INDQ/NO** with DLD-1 human colorectal adenocarcinoma cells for 5 h was estimated by analysis of an aliquot of extracellular medium using a chemiluminescence-based assay.

RNS-induced modifications are nitration and nitrosylation DNA, deamination of DNA leading to mutations possibly causing loss in functions and triggering induction of necrosis and/or apoptosis. RNS are known to induce DNA double strand breaks.[14] So, in order to determine whether **INDQ/NO** induces DNA damage or not, HeLa cells were exposed to **INDQ/NO**. By using an immunofluorescence assay for detecting γ-H2AX, the levels of DNA damage induced were detected.

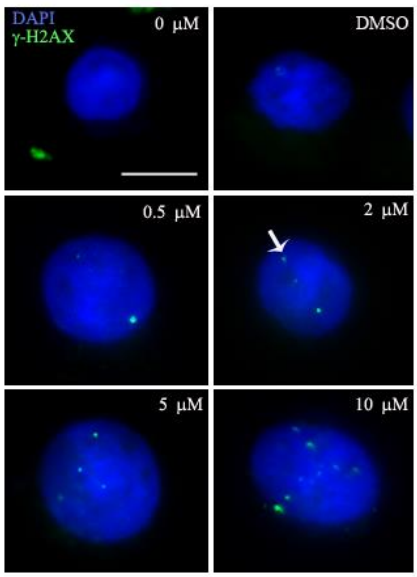

Figure 5. Representative images of HeLa cells labelled with anti-γ-H2AX antibody in immunofluorescence assay after treatment with 10 µM **INDQ/NO** for 1.5 h. Nuclei were counterstained with DAPI. Arrow indicates γ-H2AX foci (Scale bar: ~5 µm).

A dose dependent increase in DNA damage was observed (Figure 5), which indicated that **INDQ/NO** induced DNA double strand breaks presumably as a result of released NO.

Further, **2-Me INDQ/NO** was prepared in order to study the effects of C-2 substitution on the release of NO. Diminished metabolism of **2-Me INDQ/NO** by DT-D as well as low NO yields were observed, consistent with previous reports.[14]

Chapter 3.1: Nitroreductase-Activated NO Donors

Another methodology to selectively enhance cytotoxic species within cells is directed prodrug therapy. *Escherichia coli* nitroreductase (NTR) is an enzyme that is frequently used as a metabolic trigger for "directed" prodrugs including antibody directed enzyme prodrug therapy (ADEPT) and gene directed enzyme prodrug therapy (GDEPT).[15] As NTR is not usually found in human cells, this enzyme is introduced either by transfection methodologies (for GDEPT) or by conjugating the enzyme to an antibody specific for tumour-antigen (for ADEPT). Upon exposure to the exogenous enzyme, the inactive prodrug, which is a substrate for the enzyme is metabolized to produce the cytotoxic species either intracellularly or in the proximity of tumours. As normal cells do not express this enzyme, potential deleterious side-effects can be minimized. A typical NTR-activated prodrug contains a 4-nitrobenzyl group which forms a substrate for NTR.[16]

Based on this, O^2-(4-nitrobenzyl) diazeniumdiolates were synthesized as NTR activated NO donors. It is proposed that NTR reduces the 4-nitrobenzyl group by two or four electron reduction using NADPH as the cofactor (Scheme 5). Due to reduction, the electron withdrawing nitro group is converted into an electron donating hydroxylamine or amine group that pushes electron into the phenyl ring. As a result of this electronic rearrangement, the diazeniumdiolate is freed from the benzylic position and gets hydrolysed to release upto 2 moles of NO.

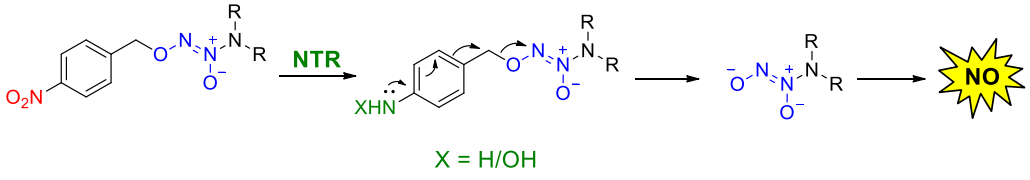

Scheme 5. Proposed design and activation of NTR-activated NO donor.

In order to study NTR-activated NO release, four different O^2-(4-nitrobenzyl) diazeniumdiolates were synthesized (Figure 6).

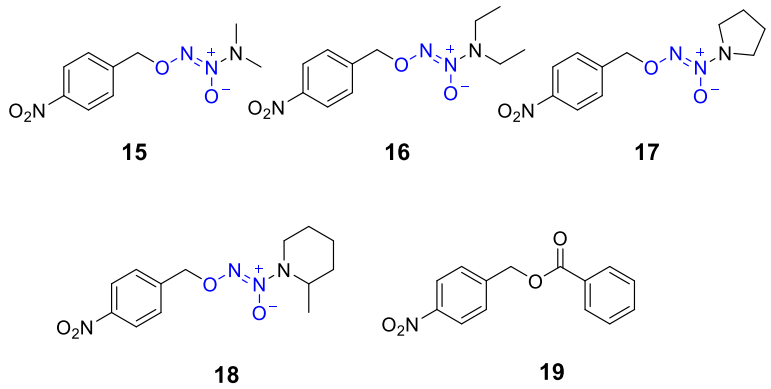

Figure 6. O^2-(4-Nitrobenzyl) diazeniumdiolates **15**-**18** and compound **19** synthesized as substrates for NTR.

A negative control **19**, which is a substrate for NTR but not a source of NO, was synthesized. To evaluate the NTR activation and NO release, the compounds were independently incubated with NTR in the presence of NADPH in pH 7.4 buffer at 37 ^{o}C. O^2-(4-Nitrobenzyl) diazeniumdiolates were found to be reduced by NTR to release NO. However, under similar incubation condition, **19** did not generate NO, but was found to be reduced by NTR (Figure 7.A and 7.B).

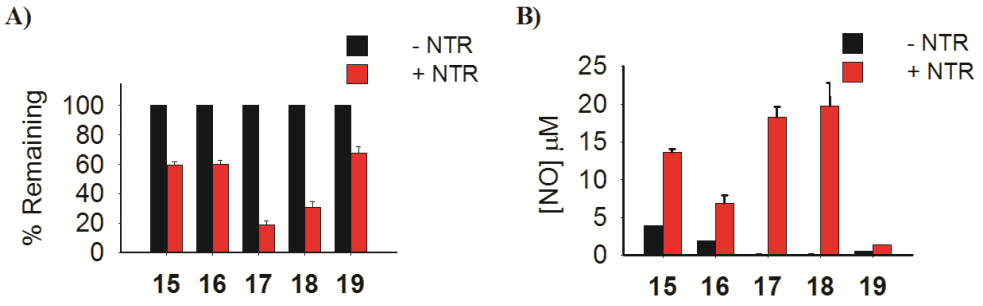

Figure 7. A) HPLC decompostion profiles of O^2-(4-nitrobenzyl) diazeniumdiolates and **19** (50 µM) in pH 7.4 buffer in the presence and absence of NTR after 1 h. **B)** NO release from O^2-(4-nitrobenzyl) diazeniumdiolates in the presence and absence of NTR in pH 7.4 buffer after 1 h, detected using a chemiluminesence based assay.

Next, the cytotoxicity assay was performed in DLD-1 cells using **15** to **19** and it was found that the compounds showed moderate inhibitory activity at 75 µM, however the cytotoxicity was increased in the presence of NTR (Figure 8). Compound **19** did not exhibit significant cytotoxicity even in the presence of NTR, demonstrating minimal cytotoxicity due to by-products of NTR reduction.

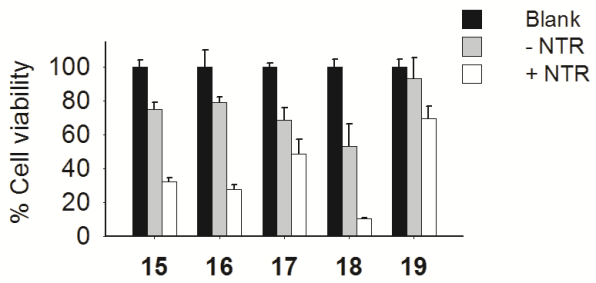

Figure 8. Percent viability of DLD-1 cells upon 72 h incubation with 75 µM of **15-19** in the presence and absence of NTR.

As compound **18** was found to be a better substrate for NTR, a concentration-dependent cell viablity assay was performed in DLD-1 cells and an enhancement in the cytotoxicity of compound **18** in the presence of NTR was observed. The cell viability assay performed in HeLa cells also showed similar enhanced cytotoxic effects of **18** in the presence of NTR.

As NTR is a bacterial enzyme, release of NO from O^2-(4-nitrobenzyl) diazeniumdiolate, **17**, in *Mycobacterium smegmatis* (*M. smeg*) was monitored. The incubation of *M. smeg* with **17** resulted in intracellular release of NO suggesting that O^2-(4-nitrobenzyl) diazeniumdiolates are capable of enhancing NO in bacterial cells as well.

Chapter 3.2: Investigation into modulation of release rate

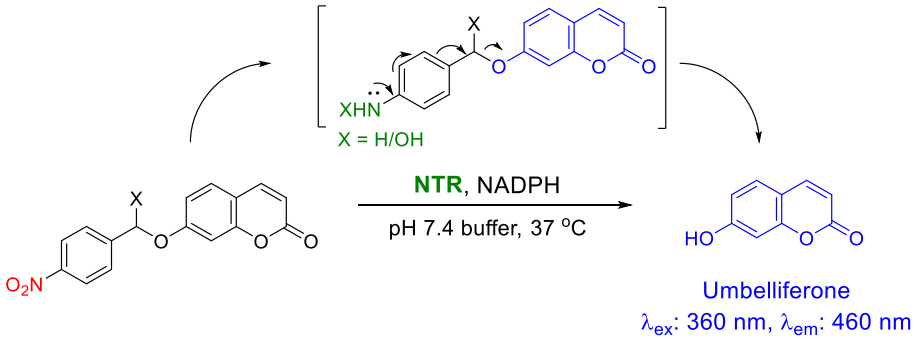

Scheme 6. NTR-activated model to study the effects of substituents at the benzylic position on the release of leaving group.

The release of NO from O^2-(4-nitrobenzyl) diazeniumdiolates takes place after reduction of the nitro group to an hydroxyl amino or amino group which undergoes electronic rearrangement to expel the diazeniumdiolate. As the flow of electrons dictate the release of leaving group, we hypothesized that the substituents on the

benzylic position of 4-nitrobenzyl group may affect the release of NO or any other leaving group (Scheme 6). In order to investigate the effects of substituent variation on the release of leaving group, several 4-nitrobenzyl umbelliferone ethers were synthesized as model compounds (Figure 9). The increased fluorescence upon activation of the latent fluorophore serves as a convenient signal to monitor.

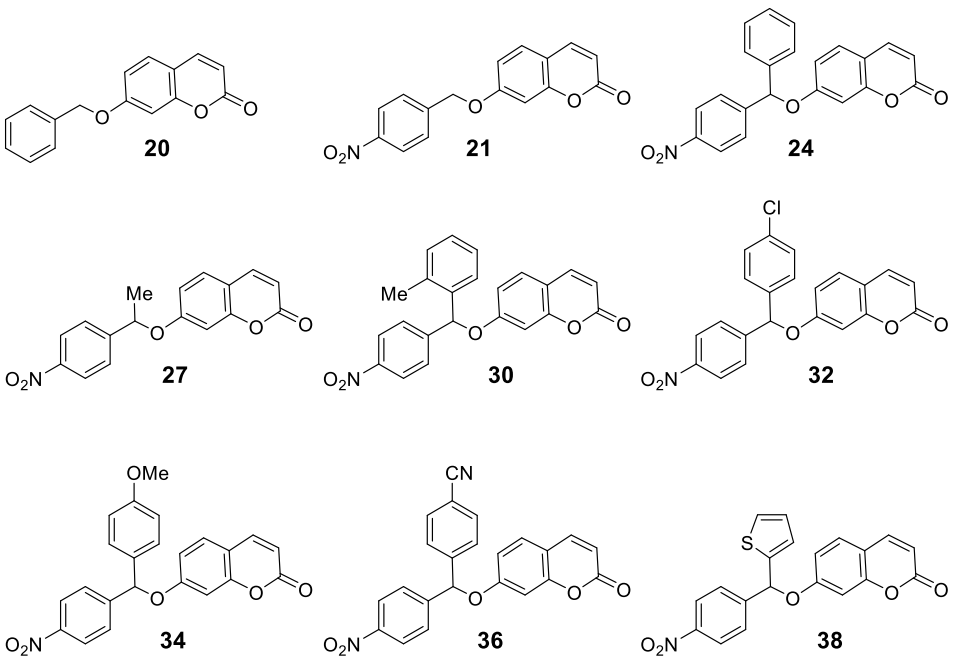

Figure 9. Substituted 4-nitrobenzyl umbelliferone ethers synthesized to study the modulation on release of umbelliferone from 4-nitrobenzyl group.

In order to verify the activation of the test compounds by NTR, **21** was first incubated with NTR and it was found that umbelliferone was released upon NTR reduction. Next, the negative control **20** was incubated with NTR under similar conditions and an increase in fluorescence was not observed suggesting that **20** was not a substrate for NTR (Figure 10).

Next, compounds **24**, **27**, **30**, **32**, **34**, **36** and **38** were independently incubated with NTR and the release of umbelliferone over 3 h was monitored. Although these compounds were reduced by NTR to release umbelliferone, no major effect on the rate of release of umbelliferone with changing substituent at the benzylic position was observed. In addition, due to solubility issues the compounds were not further pursued for studying the tunability aspect of 4-nitrobenzyl scaffold.

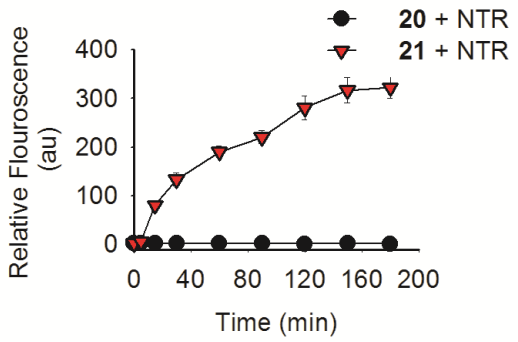

Figure 10. Fluorescence measurement due to umbelliferone release upon NTR reduction of **20** and **21** (50 µM) using NADPH as cofactor (λ_{ex}: 360 nm; λ_{em}: 460 nm).

Chapter 4: A Bioreductively-Activated NO Donor with a Fluorescence Reporter

Having developed a method for releasing NO within bacteria, we next examined the possibility of incorporating a reporter in the NO delivery system. Using a reported self-immolative fluorescent coumarin linker,[17] a NTR-activated reporter linked NO donor, **47** was synthesized. Inside bacteria, **47** is expected to undergo activation by NTR and subsequently release NO and fluorescent coumarin reporter molecule **44**, simultaneously upon self-immolation (Scheme 7).

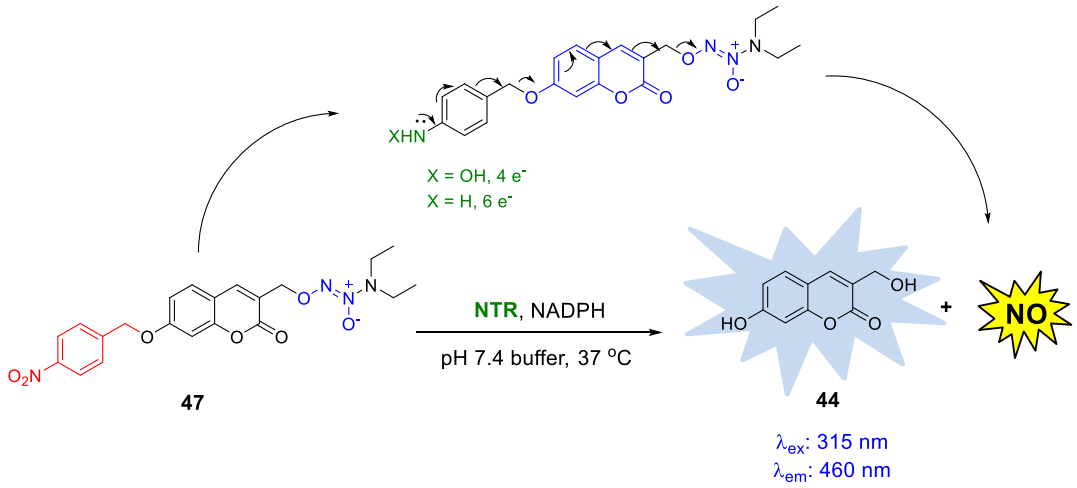

Scheme 7. Bioreductively activated NO donor with a fluorescence reporter: the turn-off reporter molecule inside bacteria gets reduced by NTR to form electron rich intermediate that spontaneously rearranges the electron and releases the turn-on fluorescent coumarin reporter molecule, **44** and NO.

In order to evaluate the reduction of **47** by NTR, **47** was incubated with NTR and NADPH in pH 7.4 buffer at 37 °C and the release of reduction products: NO and **44**, were monitored. Concomitant release of both NO and **44** was observed (Figure 11).

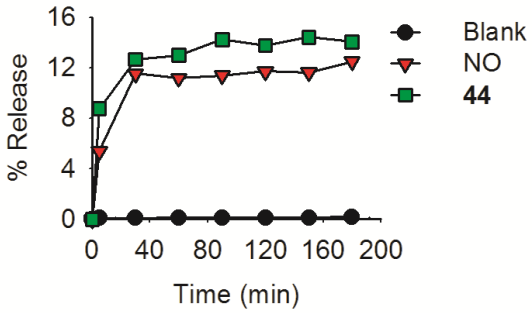

Figure 11. Percent release of NO and **44** from reduction of **47** in the presence of NTR and cofactor NADPH at 37 ^{o}C over 3 h.

The cell permeability of the compound was studied using *Escherichia coli* (*E. coli*), *Staphylococcus aureus* (SA) and *M. smeg*. Compound **47** was incubated in the bacterial suspension of *M. smeg* for 12 h and release of **44** was monitored. Comound **47** was bioreductively activated to release **44** (Figure 12.A). In order to monitor intracellular NO, fluorescence based DAF assay was used.[18] Based on fluorescence measurement, the intracellular NO measured in *M. smeg* was similar to the release of **44** (Figure 12.B).

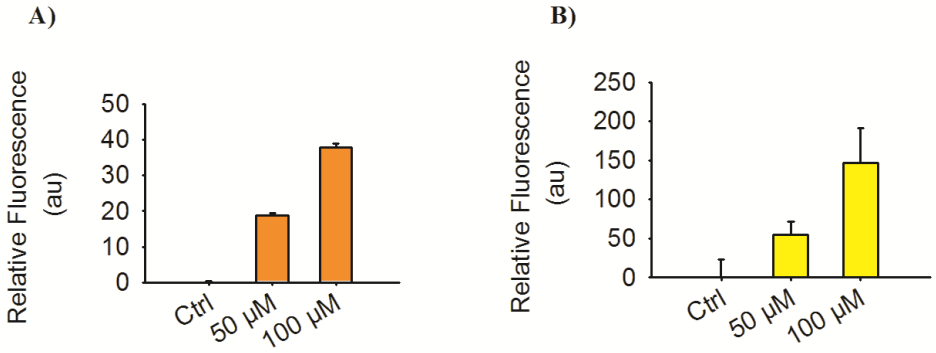

Figure 12. A) A concentration dependent increase in fluorescence for **44** was observed when **47** was incubated in *M. smeg* for 12 h (λ_{ex}: 315nm; λ_{em}: 460 nm). **B)** Using DAF assay, intracellular NO generated by bioreduction of **47** in *M. smeg* was monitored. Increase in the fluorescence (λ_{ex}: 490 nm; λ_{em}: 530 nm) corresponding to the formation of fluorescent triazole DAF-2T was measured.

In order to demonstrate that the activation of **47** occurs intracellularly and not in the media fluorescence assisted cell sorting (FACS) was used. Various strains of *M. smeg* were incubated with **47** and the cells were analysed for intracellular release of **44**. The FACS data indicated **47** was bioreductively activated inside *M. smeg* to release fluorescent molecule **44**.

Chapter 5: Indole-Based Scaffold for Tunable Release Rate

One of the ideal characteristics of a delivery vehicle is its capability to tune the release of leaving group by structural modification. In order to study the tunability aspect, a new indole based scaffold is presented. The substituents present on the indole may be expected to affect the release of leaving group due to their electronic or steric effects. To study the tunability of indole scaffold, we focused on a) the C-5 position of indole that may electronically regulate the release and b) the C-2 position, which may sterically and electronically affect the release. In order to study the indole scaffold, few indole based compounds using umbelliferone as the leaving group and allyloxy carbonyl (alloc) as protecting group on the indole nitrogen were synthesized. In the presence of a palladium catalyst, alloc is rapidly cleaved[19] to release umbelliferone (Scheme 8).

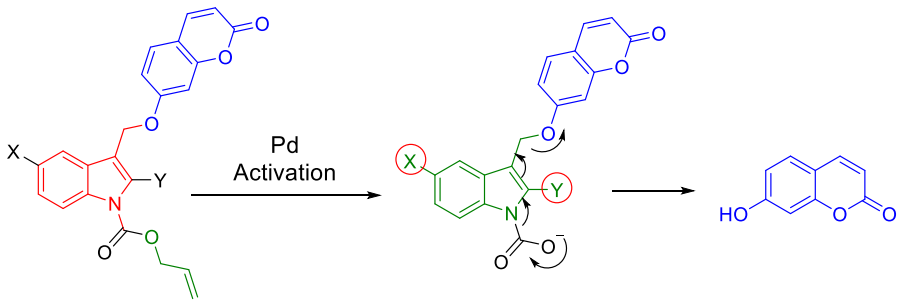

Scheme 8. A new indole based scaffold to study the tunability of the release of leaving group. Alloc protected indole gets rapidly deprotected in the presence of Pd catalyst and due to interplay of electronic or/and steric effects of substituents: X and Y, the release of umbelliferone may be modulated.

In order to investigate the effects of substituent variation on the release of leaving group, alloc protected indoles were synthesized as model compounds (Figure 13). In order to study palladium mediated alloc deprotection, the compounds were independently treated with *tetrakis*(triphenylphosphine)palladium(0) and umbelliferone release was measured using HPLC. A significant difference in the release of umbelliferone from the compounds over 30 min was observed. 5-OMe substituted indole compound **58** was better in releasing umbelliferone whereas 5-NO_2 substituted indole compound **54** slowly released umbelliferone (Figure 14.A).

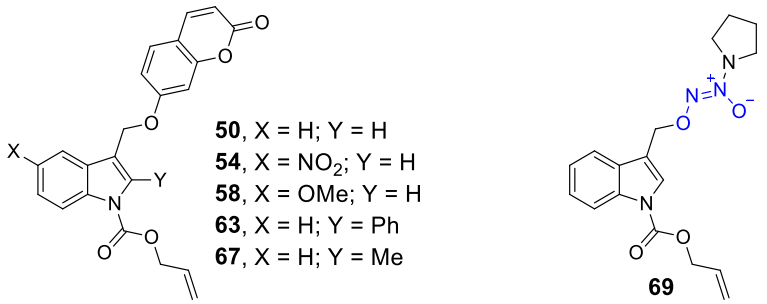

Figure 13. Palladium activated indole based compounds.

Under similar conditions, in the absence of palladium no umbelliferone release were observed from these compounds. It was found that **54** released upto 90% umbelliferone over 3 h (Figure 14.B). Thus, the calculated half-lives of these compounds in the presence of palladium varied from 2 min to 1 h.

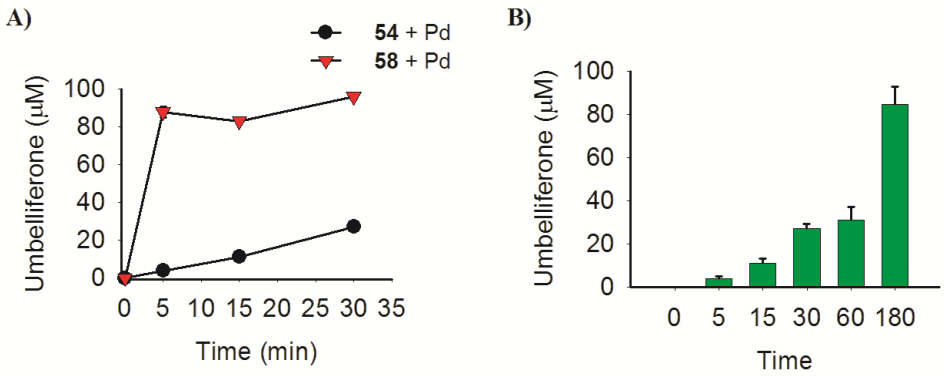

Figure 14. A) Representative data for release of umbelliferone after alloc deprotection using palladium. **B)** Time course release of umbelliferone from **54** over 3 h.

In order to determine the suitability of the indole scaffold to deliver NO, an NO donor **69** was synthesized (Figure 13). Compound **69** was treated with palladium catalyst and the amount of NO released was measured. When NO release from **69** and umbelliferone release from **50** were compared, it was found that the release profiles were similar (Figure 15). Thus, in principle, indole-based scaffold can be used for tunable release of leaving group.

Taken together, we attempted to solve the three major aspects of NO delivery inside living cells. Two new strategies for selective NO delivery using DT-D and NTR as enzyme triggers were developed. For monitoring NO release in cells, a NTR-activated NO donor linked with reporter molecule was presented. Finally, the new indole-based scaffold was synthesized that offers a handle to tune the release profile of the leaving

group. These strategies may help in accurately studying the roles of NO inside living cells.

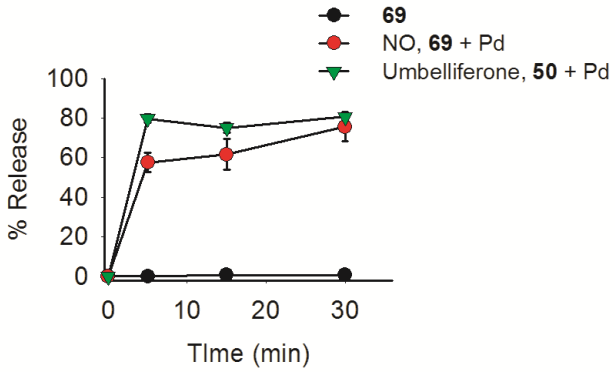

Figure 15. Comparison of NO release from **69** and umbelliferone release from **50** after Pd activation.

References

1. (a) Andrew, P. J.; Mayer, B., Enzymatic function of nitric oxide synthases. *Cardiovasc. Res.* **1999,***43* (3), 521-531;(b) Knowles, R. G.; Moncada, S., Nitric oxide synthases in mammals. *Biochem. J.* **1994,***298* (Pt 2), 249-258.

2. Heinrich, T. A.; da Silva, R. S.; Miranda, K. M.; Switzer, C. H.; Wink, D. A.; Fukuto, J. M., Biological nitric oxide signalling: chemistry and terminology. *Br. J. Pharmacol.* **2013,***169* (7), 1417-1429.

3. (a) Burke, A. J.; Sullivan, F. J.; Giles, F. J.; Glynn, S. A., The yin and yang of nitric oxide in cancer progression. *Carcinogenesis* **2013,***34* (3), 503-512;(b) Wang, P. G.; Xian, M.; Tang, X.; Wu, X.; Wen, Z.; Cai, T.; Janczuk, A. J., Nitric Oxide Donors: Chemical Activities and Biological Applications. *Chem.Rev.* **2002,***102* (4), 1091-1134;(c) Wink, D. A.; Mitchell, J. B., Chemical biology of nitric oxide: insights into regulatory, cytotoxic, and cytoprotective mechanisms of nitric oxide. *Free Radical Bio. Med.* **1998,***25* (4–5), 434-456.

4. Fang, F. C., Perspectives series: host/pathogen interactions. Mechanisms of nitric oxide-related antimicrobial activity. *J. Clin. Invest.* **1997,***99* (12), 2818-2825.

5. Bogdan, C., Nitric oxide and the immune response. *Nat Immunol* **2001,***2* (10), 907-916.

6. (a) Maciag, A. E.; Chakrapani, H.; Saavedra, J. E.; Morris, N. L.; Holland, R. J.; Kosak, K. M.; Shami, P. J.; Anderson, L. M.; Keefer, L. K., The Nitric Oxide Prodrug JS-K Is Effective against Non–Small-Cell Lung Cancer Cells In Vitro and In Vivo: Involvement of Reactive Oxygen Species. *J. Pharmacol. Exp. Ther.* **2011,***336* (2), 313-320;(b) Wink, D. A.; Vodovotz, Y.; Laval, J.; Laval, F.; Dewhirst, M. W.; Mitchell, J. B., The multifaceted roles of nitric oxide in cancer. *Carcinogenesis* **1998,***19* (5), 711-721.

7. (a) De Groote, M. A.; Fang, F. C., NO Inhibitions: Antimicrobial Properties of Nitric Oxide. *Clin. Infect. Dis.* **1995,***21* (Supplement 2), S162-S165;(b) Wink, D. A.; Hines, H. B.; Cheng, R. Y. S.; Switzer, C. H.; Flores-Santana, W.; Vitek, M. P.; Ridnour, L. A.; Colton, C. A., Nitric oxide and redox mechanisms in the immune response. *J. Leukoc. Biol.* **2011,***89* (6), 873-891.

8. (a) Gusarov, I.; Nudler, E., NO-mediated cytoprotection: Instant adaptation to oxidative stress in bacteria. *Proc. Natl. Acad. Sci.* **2005,***102* (39), 13855-13860;(b) Gusarov, I.; Shatalin, K.; Starodubtseva, M.; Nudler, E., Endogenous Nitric Oxide

Protects Bacteria Against a Wide Spectrum of Antibiotics. *Science* **2009,***325* (5946), 1380-1384;(c) van Sorge, N. M.; Beasley, F. C.; Gusarov, I.; Gonzalez, D. J.; von Köckritz-Blickwede, M.; Anik, S.; Borkowski, A. W.; Dorrestein, P. C.; Nudler, E.; Nizet, V., Methicillin-resistant Staphylococcus aureus Bacterial Nitric-oxide Synthase Affects Antibiotic Sensitivity and Skin Abscess Development. *J. Biol. Chem.* **2013,***288* (9), 6417-6426.

9. Chakrapani, H.; Showalter, B. M.; Citro, M. L.; Keefer, L. K.; Saavedra, J. E., Nitric Oxide Prodrugs: Diazeniumdiolate Anions of Hindered Secondary Amines. *Org. Lett.* **2007,***9* (22), 4551-4554.

10. (a) Saavedra, J. E.; Shami, P. J.; Wang, L. Y.; Davies, K. M.; Booth, M. N.; Citro, M. L.; Keefer, L. K., Esterase-Sensitive Nitric Oxide Donors of the Diazeniumdiolate Family: In Vitro Antileukemic Activity. *J. Med. Chem.* **2000,***43* (2), 261-269; (b) Wu, X.; Tang, X.; Xian, M.; Wang, P. G., Glycosylated diazeniumdiolates: a novel class of enzyme-activated nitric oxide donors. *Tetrahedron Lett.* **2001,***42* (23), 3779-3782; (c) Shami, P. J.; Saavedra, J. E.; Wang, L. Y.; Bonifant, C. L.; Diwan, B. A.; Singh, S. V.; Gu, Y.; Fox, S. D.; Buzard, G. S.; Citro, M. L.; Waterhouse, D. J.; Davies, K. M.; Ji, X.; Keefer, L. K., JS-K, a Glutathione/Glutathione S-Transferase-activated Nitric Oxide Donor of the Diazeniumdiolate Class with Potent Antineoplastic Activity1. *Mol. Cancer Ther.* **2003,***2* (4), 409-417.

11. Bello, R. I.; Gómez-Díaz, C.; Navarro, F.; Alcaín, F. J.; Villalba, J. M., Expression of NAD(P)H:Quinone Oxidoreductase 1 in HeLa Cells: Role of Hydrogen Peroxide and Growth phase. *J. Biol. Chem.* **2001,***276* (48), 44379-44384.

12. Kelland, L. R.; Sharp, S. Y.; Rogers, P. M.; Myers, T. G.; Workman, P., DT-Diaphorase Expression and Tumor Cell Sensitivity to 17-Allylamino,17-demethoxygeldanamycin, an Inhibitor of Heat Shock Protein 90. *J. Natl. Cancer Inst.* **1999,***91* (22), 1940-1949.

13. Zhang, Z.; Tanabe, K.; Hatta, H.; Nishimoto, S.-i., Bioreduction activated prodrugs of camptothecin: molecular design, synthesis, activation mechanism and hypoxia selective cytotoxicity. *Org. Biomol. Chem.* **2005,***3* (10), 1905-1910.

14. Colucci, M. A.; Reigan, P.; Siegel, D.; Chilloux, A.; Ross, D.; Moody, C. J., Synthesis and Evaluation of 3-Aryloxymethyl-1,2-dimethylindole-4,7-diones as Mechanism-Based Inhibitors of NAD(P)H:Quinone Oxidoreductase 1 (NQO1) Activity. *J. Med. Chem.* **2007,***50* (23), 5780-5789.

15. (a) Tietze, L. F.; Schuster, H. J.; Krewer, B.; Schuberth, I., Synthesis and Biological Studies of Different Duocarmycin Based Glycosidic Prodrugs for Their Use in the Antibody-Directed Enzyme Prodrug Therapy. *J. Med. Chem.* **2009,***52* (2), 537-543; (b) Mauger, A. B.; Burke, P. J.; Somani, H. H.; Friedlos, F.; Knox, R. J., Self-Immolative Prodrugs: Candidates for Antibody-Directed Enzyme Prodrug Therapy in Conjunction with a Nitroreductase Enzyme. *J. Med. Chem.* **1994,***37* (21), 3452-3458; (c) Xu, G.; McLeod, H. L., Strategies for Enzyme/Prodrug Cancer Therapy. *Clin. Cancer Res.* **2001,***7* (11), 3314-3324; (d) Greco, O.; Dachs, G. U., Gene directed enzyme/prodrug therapy of cancer: Historical appraisal and future prospectives. *J. Cell. Physiol.* **2001,***187* (1), 22-36.

16. Hu, L.; Yu, C.; Jiang, Y.; Han, J.; Li, Z.; Browne, P.; Race, P. R.; Knox, R. J.; Searle, P. F.; Hyde, E. I., Nitroaryl Phosphoramides as Novel Prodrugs for E. coli Nitroreductase Activation in Enzyme Prodrug Therapy. *J. Med. Chem.* **2003,***46* (23), 4818-4821.

17. Weinstain, R.; Segal, E.; Satchi-Fainaro, R.; Shabat, D., Real-time monitoring of drug release. *Chem. Commun.* **2010,***46* (4), 553-555.

18. Singh, R.; Manjunatha, U.; Boshoff, H. I. M.; Ha, Y. H.; Niyomrattanakit, P.; Ledwidge, R.; Dowd, C. S.; Lee, I. Y.; Kim, P.; Zhang, L.; Kang, S.; Keller, T. H.; Jiricek, J.; Barry, C. E., PA-824 Kills Nonreplicating Mycobacterium tuberculosis by Intracellular NO Release. *Science* **2008,***322* (5906), 1392-1395.

19. Schmid, K. M.; Jensen, L.; Phillips, S. T., A Self-Immolative Spacer That Enables Tunable Controlled Release of Phenols under Neutral Conditions. *J. Org. Chem.* **2012,***77* (9), 4363-4374.

List of Figures

List of Schemes

List of Tables

List of Publications

1. **Sharma, K.**, Iyer, A., Sengupta, K., Chakrapani, H., "INDQ/NO, a Bioreductively Activated Nitric Oxide Prodrug" *Org. Lett*., **2013**, *15*, 2636-2639.
2. **Sharma, K.**, Sengupta, K., Chakrapani, H., "Nitroreductase-activated nitric oxide (NO) prodrugs" *Bioorg. Med. Chem .Lett.*, **2013**, *23*, 5964-5967.
3. **Sharma, K.**, Chakrapani, H., "Site-Directed Delivery of Nitric oxide to Cancers" *Nitric Oxide*, **2014**, *43*, 8-6.
4. Surnar, B., **Sharma, K.**, Jayakannan, M., "Core-Shell Polymer Nanoparticles for Prevention of GSH Drug Detoxification and Cisplatin Delivery to Breast Cancer Cells" *Nanoscale*, **2015**, *7*, 17964-17979.

Manuscripts in Preparation

1. Ravikumar, G., **Sharma, K.**, Chakrapani, H., "FLUORO/NO, A Small Molecule with a Turn-ON Nitric Oxide and Fluorescence Switch".
2. **Sharma, K.**, Chauhan, P., Chakrapani, H., "An indole-based scaffold for tunable release"